UNIVERSITY OF CALGARY

Lithic Raw Material Characterisation at Olduvai Gorge, Tanzania

by

Julien Favreau

A THESIS
SUBMITTED TO THE FACULTY OF GRADUATE STUDIES
IN PARTIAL FULFILMENT OF THE REQUIREMENTS FOR THE
DEGREE OF MASTER OF ARTS

GRADUATE PROGRAM IN ARCHAEOLOGY

CALGARY, ALBERTA

APRIL, 2019

Abstract

Olduvai Gorge is located within the Ngorongoro Conservation Area, a UNESCO World Heritage Site in northern Tanzania along the western margin of the East African Rift System. Olduvai's sedimentary record exhibits a complex sequence of inter-stratified lithic technologies including Oldowan, Acheulean, Middle Stone Age, and Later Stone Age assemblages. While diachronic technological change is perceptible, one aspect that remained largely unchanged through time was the totality of locally available rock types. This study constitutes Olduvai Gorge's first systematic survey and characterisation of source lithologies using thin section petrography. The primary objectives of this thesis were to establish the range of available lithic raw materials, petrographically characterise these, and determine if there were unique inter-outcrop petrographic signatures to determine if it is feasible to source lithic artifacts at the mineralogical level. Geological samples were collected in primary and secondary positions within the greater Olduvai Gorge region. A total of seventy-four thin sections of sixty-two geological samples from nineteen sources were analysed. By way of comparative analyses, it is shown that four quartzitic outcrops have unique mineral compositions, four meta-granite varieties are unique to individual outcrops, Engelosin phonolite samples are texturally and mineralogically unique, and magmatic samples recovered in secondary position may be sourced to their volcanic centre. The results of this thesis demonstrate it is feasible to differentiate between source material by way of optical mineralogy which implies that sourcing lithic artifacts from Olduvai is possible. Altogether, these revelatory insights will allow future researchers to glean new understandings of hominin raw material transport, as well as ecological and social behaviour within the Olduvai paleobasin.

Keywords: Lithic; mineralogy; petrography; sourcing; provenance; Olduvai Gorge.

Acknowledgements

First and foremost, I want to express my gratitude and appreciation to my supervisor and friend, Dr. Julio Mercader. His incredible vision within the field of paleoanthropology helped channel my passion for lithic technology and get me to where I am today. The entire SDS team has been instrumental to my success which includes Drs. Julio Mercader, Pastory Bushozi, Tristan Carter, Paul Durkin, Stephen Hubbard, Jamie Inwood, María Soto along with Tope Akeju, Siobhán Clarke, David Isilebo, Makarius Itambu, Fergus Larter, Patrick Lee, Aloyce Mwambwiga, Reuben Ngwali, Robert Patalano, Lisa Tillotson, and Laura Tucker. I am especially grateful to María Soto whose expertise in lithic raw material characterisation was key to my success. I would like to express my sincere appreciation to Dr. Rajeev Nair who introduced me to the world of mineralogy and Mickey Horvath who's open (lab) door policy allowed me to quickly solve issues that arose during my lab work. I would like to thank Drs. Damien Delvaux, Harald Fritz, Richard Leakey, Godwin Mollel, Duncan Macgregor, and Jay Reti who promptly replied my emails to answer any and all questions and generously shared geospatial data with me. I am deeply indebted to the entire Maasai community whose help and support with fieldwork was indispensable to this study. I would especially like to thank Lucas Elirehema, Meshack Kidiri, Lekaai Kisota, Samson Koromo, Sumat Olenjorio, and Lucas Zebedayo who so graciously shared their knowledge of the landscape and local place names. I wish to formally thank the Tanzania Commission for Science and Technology, the Division of Antiquities, and the Ngorongoro Conservation Area for allocating research permits that made this work possible. I am grateful for the funding and support provided by the Social Sciences and Humanities Research Council and the Department of Anthropology and Archaeology. Last but not least, I am especially appreciative of my family and friends who have supported my studies all along the way. Thank you.

Dedication

To my grand-mother Yvette, my parents Sylvie and Jean, my sister Virginie, my brother Olivier, Adriana, and my dog Whisky.

Table of Contents

List of Tables

List of Figures

List of Abbreviations

2*V* = acute angle between optic axes of a biaxial mineral
Aeg = aegirine
Afs = alkali feldspar
BP = before present
Bt = biotite
Cal = calcite
Chl = chlorite
CODI = Comprehensive Olduvai Database Initiative
EARS = East African Rift System
ESA = Early Stone Age
Fu = fuchsite
g = gram
Hbl = hornblende
Hem = hematite
Ka = Kilo-annum
kg = kilogram
km = kilometre
LSA = Later Stone Age
m = metre
Ma = Mega-annum
Mag = magnetite
m.a.s.l. = metres above sea level
mL = millilitre
mm = millimetre
Ms = muscovite
MSA = Middle Stone Age
na = not applicable
NCA = Ngorongoro Conservation Area
nd = no data
NTDZ = North Tanzania Divergence Zone
NVH = Ngorongoro Volcanic Highlands
OGAP = Olduvai Geochronology and Archaeology Project
OLAPP = Olduvai Landscape Paleoanthropology Project
Op = opaque mineral
OVPP = Olduvai Vertebrate Paleontology Project
Pl = plagioclase
PPL = plane-polarised light
Qtz = quartz
Rt = rutile
SDS = Stone Tools, Diet, and Sociality at the Dawn of Humanity
TOPPP = The Olduvai Paleoanthropology and Paleoecology Project
Ttn = titanite
μm = micrometre
x = magnification
XP = cross-polarised light

Chapter 1

Introduction

Olduvai Gorge is located in northern Tanzania along the western margin of the EARS and is widely considered as Africa's most iconic paleoanthropological complex. During the Early Pleistocene, Olduvai was an endorheic basin that hosted a saline alkaline lake fed by stream networks from the NVH, and characterised by abruptly rising metamorphic inselbergs (Hay 1976). While diachronic alterations in sedimentary infill and drainage patterns altered Olduvai's paleoecology, the latter formed the backdrop upon which a host of hominin species subsisted and manufactured stone tools for a variety of daily tasks (Diez-Martín et al. 2010, 2015; Leakey 1971; Mora and de la Torre 2005; Yravedra et al. 2017).

Preserved in Olduvai's sedimentary sequence spanning from the Early Pleistocene to the Holocene are inter-stratified lithic industries including Oldowan, Acheulean, MSA, and LSA assemblages (Eren et al. 2014; Leakey 1971; Leakey et al. 1972; Leakey and Roe 1994; Mabulla 1990). These assemblages are often found in the same context as faunal remains, and occasionally, hominin fossils that are together representative of evolutionary processes. While diachronic hominin technological change is perceptible, one aspect that remained largely unchanged through time was the totality of locally available rock types minus two key exceptions: 1) chert petrogenesis during saline alkaline lake conditions and subsequent disentombment at lowstands (Hay 1968, 1976; O'Neil and Hay 1973; Stiles et al. 1974); and 2) the Olduvai paleobasin being continually fed by paleoconglomerates from the NVH (Hay 1976). With such a vast array of exploitable rock types, this along with other factors allowed hominins to impose choice on their usage of lithic raw materials.

Rocks used in artifact production are alternatively known as lithic raw materials and naturally occur as mineral aggregates of igneous, metamorphic, and sedimentary origin that are non-renewable and spatially exhaustible (Kyara 1996) over a non-geological timeframe. Their mineral constituents are natural, inorganic, and have both a crystalline structure and a well-defined chemical composition (Jones 1987). In fact, minerals form the basis of most, if not all, anthropogenic technologies (Perkins 1998) including the earliest one reported from the archaeological record (Harmand et al. 2015). With the development of optical mineralogy and thin section petrography in the 1800s, these have emerged as foundational techniques in the field of petrology (Nesse 2013). Thin section analyses have been commonly used in archaeological contexts to source artifacts, and characterise materials and manufacturing processes. Lithic raw material characterisation and sourcing can provide insights into selection and procurement strategies (Stout et al. 2005), transportation costs (Kyara 1999), technological façonnage (Mason and Aigner 1987), functional suitability (Ebright 1987), landuse behaviour (Tactikos 2005), population movements (Reimer 2018), and social networks of trade and exchange (Lebo and Johnson 2007). By extension, inferences may be drawn concerning prehistoric technological, economic, ritual, and political organisations in a variety of archaeological contexts (e.g. Flannery 1976; Renfrew 1975; Sidrys 1976).

Previous studies on Olduvai's rock types have relied on macroscopic, petrographic, and geochemical techniques but have not systematically sampled and characterised sources (e.g. Blumenschine et al. 2008; Hay 1976; Jones 1994; Kyara 1999; Leakey 1971; McHenry and de la Torre 2018; Santonja et al. 2014; Stiles 1991, 1998; Stiles et al. 1974; Tactikos 2005), particularly those of metamorphic lithologies, presumably grounded on the assumptions that they are homogenous and undistinguishable. This is despite the fact that they were likely heavily exploited

during the Pleistocene (Leakey 1971; Leakey and Roe 1994), are of assumed importance in artifact production based on experimental studies (e.g. Byrne et al. 2016; de la Torre et al. 2013; Diez-Martín et al. 2011; Gurtov and Eren 2014; Yustos et al. 2015), and their central role in discussions about hominin behaviour in the Olduvai paleobasin (e.g. Blumenschine et al. 2008; Hay 1976; Leakey 1971; Tactikos 2005). Geological studies in the NVH (e.g. Dawson 2008; Greenwood 2014; Kervyn et al. 2008; Mana et al. 2012; Manega 1993; McHenry et al. 2008; Mollel 2002, 2007; Mollel and Swisher 2012; Mollel et al. 2008, 2009; Zaitsev et al. 2012) have made it possible to determine from which volcanic centre stone tools ultimately came from, but not from where they were precisely sourced by early hominins. Considering that research at Olduvai has been ongoing for over a century along with ubiquity of stone tools recovered from its sedimentary units, it is surprising that only limited studies have sought to characterise lithic raw materials, let alone to unravel the sources from which these were obtained by early hominins.

This study represents Olduvai's first systematic survey and characterisation of source materials using thin section petrography. The primary objectives of this thesis were to establish the range and variability of available lithic raw materials, petrographically characterise these, and determine if there were unique inter-outcrop petrographic signatures to determine if it is feasible to source lithic artifacts at the mineralogical level. Geological samples were collected in primary and secondary positions within the greater Olduvai Gorge region over the course of several years as part of the SDS project. Thus far, this has resulted in the largest reported reference collection for the region, totalling >270 samples. For this study, seventy-four thin sections of sixty-two geological samples from nineteen sources were analysed. Comparative analyses show that four quartzitic outcrops have unique mineral compositions, and four meta-granite varieties are unique to individual outcrops. Engelosin phonolite is mineralogically and texturally unique, and magmatic

samples recovered in secondary position may be sourced to their volcanic centre. The results of this thesis demonstrate it is feasible to differentiate between source material by way of optical mineralogy. This implies that sourcing lithic artifacts from Olduvai using thin section petrography is possible, irrespective of archaeological context. These results not only establish the merit of conducting future studies with archaeological applications scaffolded upon additional characterisation efforts, but also contribute to the growing body of work which shows that quartzitic outcrops can be differentiated from each other despite their assumed homogeneity on a regional scale (e.g. Blomme et al. 2012; Cnudde et al. 2013; Dalpra and Pitblado 2016; Pitblado et al. 2008, 2013; Soto et al. forthcoming; Veldeman et al. 2012). Overall, these findings will serve as an important stepping-stone to allow future researchers to gain new insights into hominin raw material transport, as well as ecological and social behaviour at one of Africa's most important paleoanthropological complexes.

Chapter 1.1

Thesis Organisation

Chapter 2 covers provenance studies in archaeology by retracing this sub-discipline's history and development, and describing its key principles. This chapter serves to explicitly identify the methodological and theoretical scaffolding upon which this study is based.

Sub-divided into six sub-chapters, Chapter 3 reviews key sourcing studies on the African Stone Age ranging in archaeological context from the earliest occurrence of the Oldowan to the MSA-LSA transition. This literature review is prefaced by hominin biological and technological evolutionary syntheses for the ESA and MSA. As a whole, this chapter serves to identify what is known about hominin raw material procurement and behaviour, and the strengths and weaknesses

of previous studies, particularly those dealing with Olduvai Gorge which justify the work done herein.

Chapter 4's first two sub-chapters cover Olduvai Gorge's toponym and etymology, geography, history of research, sedimentary sequence, paleoecology, and geochronology. These are followed by an additional two sub-chapters on Olduvai's geological setting, and on sampled outcrops which includes descriptions of their structural geology and previously recorded mineral assemblages in given rock types.

Chapter 5 discusses the materials and methods used for this study. This includes three sub-chapters dealing with field sampling, thin sectioning, and analytical techniques, respectively.

Chapter 6 presents detailed descriptions of the seventy-four thin sections analysed for this study and includes geological interpretations. The first ten sub-chapters are organised alphabetically according to outcrop and source area. The final two sub-chapters comprise of comparative analyses dealing exclusively with quartzites and meta-granites, respectively, to identify if metamorphic outcrops have unique mineral assemblages.

Sub-divided into four sub-chapters, Chapter 7 summarises the results of this thesis, discusses the strengths and weaknesses of the methods employed in this study, and introduces a multi-scalar approach that may best allow future studies to differentiate between source material. The third sub-chapter features inferences about hominin raw material transport based on the results of this thesis in combination with published data. The last sub-chapter identifies future research opportunities that build upon the work done herein as well as outstanding questions.

Chapter 8 recapitulates the work that was done for this study, its main goals, how these were accomplished, and the manner in which this thesis contributes to the discipline of archaeology as a whole.

Chapter 2

Provenance Studies in Archaeology

Since the invention of the petrographic microscope by William Nichol in 1828 and the pioneering thin section studies by Henry Clifton Sorby in 1851 (Garrison 2003), thin section petrography has emerged as a foundational technique in igneous, metamorphic, and sedimentary petrology (Nesse 2013). However, well before the development of the petrographic microscope and archaeology as a formal discipline have prehistorians been resolute in breathing life into the static behavioural residues of the past by sourcing artifactual materials which extend beyond stone tools to include ceramics, metals, glassware, amber, and even asphaltum, only to name a few. It is worth noting that some of the earliest "sourcing" studies dealt not with materials *per se*, but rather with the diffusion of ideas, artifact styles, practices, manufacturing techniques, and occasionally by assumption, of different groups from one locality to another (Trigger 2006). Since diffusionism has a well-chronicled developmental history (Clark and Lindly 1991; Trigger 2006) and lies beyond the scope of this thesis, it will not be dealt with in this chapter. The objectives of this chapter are to retrace the history and development of provenance studies in archaeology, list and describe their theoretical and methodological underpinnings, and conclude with an explanation of four key concepts that guide sourcing studies.

One of the earliest known publications dealing with material sourcing dates to 1656 in which Sir William Dugdale inspected a polished Neolithic stone axe from a site in southern England and discerned it was not made of local flint to imply that it must have been imported from elsewhere (Shotton and Hendry 1979). In 1740, William Stukeley analysed a rock sample obtained from one of the monoliths at Stonehenge. However, it was not until 1923 when Herbert Henry Thomas (1923) identified the Preseli Mountains as the likely source of some of Stonehenge's

monoliths that archaeological petrography by way of optical mineralogy is said to have been established (Shotton and Hendry 1979). By the 1930s, researchers in England began to establish lithic raw material groups based on the macroscopic identification and thin sectioning of Neolithic and Bronze age artifacts in reference to geological collections (Keiller et al. 1941). Upon careful examination, it was realised that not all artifacts from English sites were represented in reference collections meaning that they must have been imported from continental Europe. This led to a formal collaboration between English and French researchers working in Brittany whose studies revealed that prehistoric European societies quarried and manufactured stone tools at nearly industrial levels that were sometimes exported to faraway regions (Cogné and Giot 1952). At around this period in Sub-Saharan Africa, geologist Geoffrey Bond (1948) published Zimbabwe's first macroscopic study of lithic raw materials from Stone Age sites to reconstruct hominin procurement patterns. Bond's expertise on the country's geology and knowledge of exposed outcrops allowed him to infer transport distances for certain rock types. According to Bond (1948), Acheulean tool-making hominins transported and utilised a greater variety of rocks than later hominins who were more selective and tended to utilise finer-grained materials to manufacture smaller implements.

As for the use of thin section petrography in ceramic-aged archaeological contexts, Anna Shepard's (1936) study based in the American Southwest is considered as the earliest use of this analytical technique on ceramics to understand manufacturing processes and the provenance of raw materials (Stoltman 1989; Vince 2005). Perhaps better-known are David Peacock's later studies (e.g. Peacock 1967) which revealed that Romano-British coarse-wares, long assumed to have been manufactured using local raw materials, contained igneous and metamorphic mineral additives sourced to distant regions.

At the beginning of the twentieth century prior to the use of thin section petrography as a technique to source artifacts, Wilhelm Röntgen discovered X-rays which are a form of high-energy electromagnetic radiation with short wavelengths. Ensuing studies on this form of radiation by Charles Barkla and Henry Moseley laid the foundation of X-ray spectroscopy to characterise the elemental composition of a sample (Shackley 2011). This analytical technique uses X-ray photons to displace the inner shell electrons of an atom's nucleus which forces outer shell electrons to occupy lower energy levels and emit excess energy as fluorescence that is characteristic of an element (Shackley 2011). By the 1950s, X-ray spectroscopy began to be utilised in the commercial sector and several years later, Edward Hall (1960) published the earliest study using this technique to characterise Roman coinage which highlighted the technical difficulties to analyse patinated metals. Later, independent testing on obsidian sources from northern California using X-ray spectroscopy revealed that the ratio between strontium and rubidium could be used to distinguish between regional sources (Parks and Tieh 1966). From the 1960s onwards, the collaborative work between archaeologists and geoscientists at the University of California, Berkeley, played a critical role in the development of X-ray spectroscopy in archaeological contexts (Shackley 2011; Weisler 1993) which resulted in many of the earliest publications concerned with obsidian sourcing (e.g. Heizer et al. 1965; Jack and Heizer 1968; Weaver and Stross 1965).

Starting in the 1950s with the construction of nuclear reactors and the gradual refinement of instrumentation for neutron activation analysis made possible by the seminal work of George de Hevesy and Hilde Levi, this allowed for the accurate and precise elemental characterisation of materials (Glascock and Neff 2003). This analytical technique uses neutrons to irradiate a sample which causes radioactive nuclei to decay into daughter nuclei that emit gamma rays which can be calculated to determine a sample's elemental abundances (Glascock and Neff 2003). This

technique's potential for sourcing artifacts was first realised by Robert Oppenheimer (Glascock and Neff 2003; Sayre and Dodson 1957). By 1964, Cann and Renfrew (1964) published the first archaeological study using neutron activation analysis to characterise and source obsidian artifacts in the Mediterranean region which allowed them to reconstruct social networks of trade and exchange. However, it is worth noting that the earliest archaeological application using neutron activation analysis came seven years earlier with Sayre and Dodson's (1957) analysis of pottery, also dealing with material from the Mediterranean region. In another key publication several years later, Stross et al. (1988) implemented neutron activation analysis in combination with petrography to determine the provenance of Pharaonic Egyptian quartzite monoliths. They determined that two quarry sites were geochemically and petrographically distinguishable, yet the quarry furthest from where the monoliths were erected was ultimately the source of the quartzitic raw material, thereby casting doubt on distance-decay models for this study's archaeological context.

With the gradual decommissioning of nuclear reactors available for neutron activation analysis (Speakman and Glascock 2007), inductively coupled plasma mass spectrometry has largely succeeded the former technique due to its comparable detection capabilities. This analytical technique requires that a sample is first converted into an aerosol either by aspiration of a liquid or a dissolved solid, or through laser ablation of a solid sample. The aerosol is desolvated which results in the conversion of atoms into a gaseous state that are then ionised. The resulting ions are separated according to their mass-to-charge ratio, and the number of atoms for each element is detected by a mass spectrometer (Neff 2017). Inductively coupled plasma mass spectrometry first became available to the commercial sector in the early 1980s and was first utilised for archaeological provenance analyses in the following decade. One of the earliest studies using this technique is Redmount and Morgenstein's (1996) geochemical characterisation and petrographic

analysis of modern traditional Egyptian ceramic wares. This study showed that inductively coupled plasma mass spectrometry can successfully discriminate between present-day sedimentary sources in the Nile valley that were exploited for ceramic manufacture thereby offering promise to sourcing Egyptian archaeological ceramics (Redmount and Morgenstein 1996). Two years later, Mallory-Greenough et al. (1998) analysed Egyptian pottery dating to different periods from two sites using inductively coupled plasma mass spectrometry to obtain trace element compositions. This study further showed the utility of this analytical technique, particularly in comparison with neutron activation analysis, and its ability to identify ceramic sub-groups based on elemental variations. More recently, Pitblado et al. (2008) have utilised two forms of inductively coupled plasma mass spectrometry in combination with ultraviolet fluorescence, X-ray fluorescence spectroscopy, neutron activation analysis, and thin section petrography to characterise quartzite sources in southwestern Colorado. Of critical importance, this study shows that thin section petrography together with inductively coupled plasma mass spectrometry allows one to differentiate between quartzites (Pitblado et al. 2008) thereby dispelling the assumption/s that this rock type is not amenable to provenance studies (see also Dalpra and Pitblado 2016; Pitblado et al. 2013).

Thin section petrography along with X-ray spectroscopy, neutron activation analysis, and inductively coupled plasma mass spectrometry continue to dominate the methodological components of provenance studies (Shackley 2008). Although other techniques have also been applied, both past and present, which includes but is not limited to, electron microprobe analysis (e.g. Merrick and Brown 1984), proton-induced X-ray and gamma ray emission analysis (e.g. Agha-Aligol et al. 2015; Bird et al. 1981), cold neutron prompt gamma activation analysis (e.g. Kasztovszky et al. 2008), Fourier transform infrared reflectance microspectroscopy (e.g. Parish et al. 2013), and $^{87}Sr/^{86}Sr$ isotopic data (e.g. Curran et al. 2001). Based on this history and

development of provenance studies, we may conclude that for nearly a century, archaeologists have successfully implemented analytical techniques developed in other fields to more accurately and precisely reconstruct the past (Caley 1948), or as a means to an end (Carter 2014). Whether it be thin section petrography or neutron activation analysis, all techniques used in material sourcing are based on the provenance postulate which states that mineralogical, textural, and/or geochemical inter-source variation must be greater than intra-source variation (Shotton and Hendry 1979; Weigand et al. 1977). In addition to this foundational postulate, theoretical and methodological variables are listed below and recommended for implementation in provenance studies, particularly as it relates to lithic raw material sourcing (Diez-Martín et al. 2009; Glascock et al. 1998; Glascock and Neff 2003; Henderson 2000; Jones 1994; Kooyman 2000; Pollard et al. 2014; Shackley 2008; Shotton and Hendry 1979; Sunyer et al. 2017; Weigand et al. 1977):

1. It is recommended to establish a modern reference collection which contains complete intra- and inter-source variation prior to attempting to provenance artifacts;
    a. This assumes that sources have not been lost to natural and/or anthropogenic processes;
2. It is recommended to sample both the primary and secondary extent of a source which refers to an outcrop or a geological formation and the natural geographic extent of its rock types, respectively;
3. It is recommended to establish the spatial and temporal availability of a source since past geological and anthropogenic processes were spatially and temporally variable and may have been temporally constraint;

a. The earlier a source became available, the greater the possibility that geological and/or anthropogenic processes dispersed its raw materials on a wider geographic range and/or exhausted source material;

4. Sedimentary exposures may not attest to the presence of a source;
    a. Modern outcrops may have had greater paleogeographic extents. Therefore, only the most prominent and/or geologically recent sources are accessible on the modern landscape which raises the possibility that there may exist unexposed sources. Such hypothetical sources could be problematic if they were exploited and unaccounted for in modern reference collections. In which case, it would be recommended to use both geological samples and artifacts to establish macroscopic, petrographic, and/or geochemical inter- and intra-source variation;
5. There may be sequential differences in source material at the macroscopic, mineralogical, and/or geochemical level that would render modern reference collections to yield different macroscopic, petrographic, and/or geochemical data than artifactual materials;
6. Samples may have macroscopic, mineralogical and/or geochemical concentrations that may result in intra-sample variation;
    a. Resource-bearing, samples should be analysed and tested more than once on different surfaces;
7. Diagenetic processes may have impacted the characteristics of source material and/or artifacts thereby confounding their macroscopic, petrographic, and/or geochemical signatures;

8. Finally, it is recommended to include a time dimension to determine how long it took for an artifact to travel a given distance from its source to its final point of discard.

These aforementioned variables fundamentally hinge on four interrelated concepts, namely precision, accuracy, reliability, and validity (Frahm 2012). The former two concepts do not bear defining, while reliability is synonymous with two other terms, namely reproducibility and repeatability, that are both subsumed under precision. Validity involves the suitability of a technique to answer an archaeological question and the degree to which a unit of analysis is valid to provenance an artifact to its source. In conclusion, it is recommended that all characterisation and sourcing studies are diligently designed based on the principles outlined in the second half of this chapter.

Chapter 3

Provenance Studies in African Stone Age Archaeology

African Stone Age lithics have been traditionally classified in five technological modes (Clark 1969) that fall within three techno-temporal sub-divisions, namely the ESA, MSA, and LSA (Goodwin and Van Riet Lowe 1929). The ESA includes the Oldowan (Mode I) and Acheulean (Mode II) industries, the MSA includes prepared core (Mode III), blade (Mode IV), flake, and point industries, and the LSA is characterised by microlithic (Mode V) industries. Upending this long-held classificatory framework are reported stone tools from Lomekwi 3 which are dated to approximately 3.3 Ma and may therefore pre-date the advent of Oldowan technology by 700 Ka (Harmand et al. 2015). Over 95% of the Lomekwian artifacts were made from igneous rocks available in pene-contemporary paleochannels which would imply that its makers (e.g. *Kenyanthropus platyops* (Leakey et al. 2001); *Australopithecus afarensis* (Johanson et al. 1978)) may have ventured as little as <100 m from the site for raw materials (Harmand et al. 2015). If indeed artifactual (Domínguez-Rodrigo and Alcalá 2016), the Lomekwi 3 discovery forces paleoanthropologists to reconsider the origins of stone tool use and classification schemes. Pending more exceptional discoveries of this age, the objectives of the following sub-chapters are to recapitulate and review material sourcing and selection studies within the two earliest techno-temporal sub-divisions of the African Stone Age, with a strong emphasis on the ESA at Olduvai Gorge. This literature review will serve to contextualise this thesis by establishing what is known from Early and Middle Pleistocene complexes, hominin techno-temporal behavioural trends, and evaluate previous studies undertaken in the Olduvai paleobasin that, in part, contributed to the need to conduct this study.

Chapter 3.1

Early Stone Age

The Oldowan industry dates from approximately 2.6-1.4 Ma and is characterised by hammerstones, cores, flakes, debris, and unmodified stones (Leakey 1971; Semaw et al. 1997, 2003). African Oldowan sites are found in Northern, Eastern, and Southern Africa, and sites in the latter two regions chronologically overlap with as many as nine hominin species from three genera including *Australopithecus africanus*, *A. garhi*, *A. sediba*, *Paranthropus aethiopicus*, *P. boisei*, *P. robustus*, *Homo sp.*, *H. habilis*, *H. rudolfensis*, and *H. erectus*/*ergaster* (Toth and Schick 2018). The earliest appearance of the Acheulean industry is reported from Eastern Africa dating to approximately 1.7 Ma and is characterised by large cutting tools such as handaxes, cleavers, and picks (Beyene et al. 2013; Diez-Martín et al. 2015; Lepre et al. 2011). This lithic technology persisted in Africa until approximately 250 Ka. The African Acheulean is generally attributed to *Homo erectus*/*ergaster* and *H. heidelbergensis*/*rhodesiensis*. With this biological and technological evolutionary preface in mind, the following sub-chapters will recapitulate key studies dealing with raw material sourcing and selection in the ESA, note the behavioural implications these entail, and include discussions centred on Olduvai Gorge.

Chapter 3.1.1

Oldowan

Stout et al. (2005) compare the qualities of Oldowan lithic raw materials with clasts from pene-contemporary conglomerates at Gona, Ethiopia. Totalling nearly 900 pieces, the studied lithics were recovered from six localities dating from 2.6-2.27 Ma and constitute as some of the earliest known Oldowan sites on the African continent. In comparison to >600 reference samples, Stout et al. (2005) utilised a hand lens to determine artifact rock types, as well as their phenocryst

percentages, average phenocryst sizes, and groundmass textures. The results show that hominins preferentially exploited fine-grained felsic igneous raw materials with small phenocrysts which together may have been ideal tool-making properties. Importantly, the results of this study demonstrate that even at the earliest recorded occurrence of Oldowan lithic technology were its makers preferentially selecting raw materials based on certain qualitative traits (Stout et al. 2005).

Goldman-Neuman and Hovers (2012) study patterns of Oldowan raw material selection and transport in the Makaamitalu Basin, Ethiopia, by semi-quantitatively comparing stone tools from two sites dating to >2.36 Ma with clasts from a large pene-contemporary conglomerate. Goldman-Neuman and Hovers (2012) found that hominins at one site did not preferentially select specific morphometric raw materials whereas at the second site, hominins sourced certain high-quality raw materials that may have been rarely available in the sampled conglomerate or obtained from more distant, unknown sources. In closing, Goldman-Neuman and Hovers (2012) suggest that hominins responsible for both assemblages employed a least-effort strategy with minor selective criteria for lithic raw materials.

Braun et al. (2008) reconstruct Oldowan raw material procurement strategies in the Kanjera South Formation near Lake Victoria's Winam Gulf, Kenya. Systematic excavations undertaken at one site revealed three successive units dating from 2.3-1.95 Ma that yielded 4,474 lithics. The entire assemblage was macroscopically identified, geochemically characterised primarily using non-destructive energy dispersive X-ray spectroscopy, and compared with an extensive reference collection of primary and secondary source material. Braun et al. (2008) show that early hominins preferentially utilised certain raw materials, with approximately one-third of lithics manufactured on rock types that were only available >10 km distant. Importantly, these results put into question

the assumption that Oldowan raw material utilisation and transport behaviour was simplistic and opportunistic (Braun et al. 2008).

In the second chapter to Mary Leakey's (1971) seminal volume on the archaeological and paleontological collections from Olduvai Gorge, Richard Hay (1971) describes the array of lithic raw materials that were utilised by hominins in Bed I and II based on their macroscopic and microscopic traits. For geochronological context, Bed I dates from >2.038-1.803 Ma and the earliest known archaeological site is DK whose artifact-bearing horizons are bracketed between 1.877-1.848 Ma while the overlying Bed II is bracketed between <1.803-1.338 Ma (Deino et al. 2012; Habermann et al. 2016). Hay (1971) states that most lithics of igneous raw materials were on non-porphyritic basalts of similar rock type to conglomerates draining Lemagrut, while also acknowledging the use of andesite, trachyte, phonolite, nephelinite, and occasionally, of tuffaceous rocks. Phonolite and nephelinite lithics resemble materials from Sadiman, a volcanic centre southeast of Lemagrut. Highly vesicular basaltic outcroppings at the base of the Olduvai paleobasin appear to have been sporadically utilised as well. Exploited raw materials of basement origin includes quartzite, granite gneiss, pegmatite, and pink feldspar. Hay (1971) expounds the resemblance of quartzitic artifacts to material available at Naibor Soit, a large inselberg >2 km northwest of the confluence between Olduvai's two branches. Two varieties of granite gneiss were exploited by hominins, including one that is shown to be mineralogically similar to the granite gneiss inselbergs west of the Side Gorge. A temporally restricted use of chert is also evidenced from Olduvai's Bed II when fluctuations in lake levels exposed chert-bearing deposits. Hay's (1971) synthesis demonstrates that hominins preferentially exploited igneous rocks, likely sourced from nearby paleoconglomerates, along with quartzite from nearby inselbergs.

In the concluding chapter of her volume, Mary Leakey (1971) outlines behavioural trends of hominin lithic raw material usage at Olduvai Gorge during the Early Pleistocene. In Bed I and II, fine-grained igneous rocks and quartzites were the most heavily exploited raw materials while at times of lower lake levels in Early Bed II, chert was occasionally exploited. According to Mary Leakey's (1971) typology, there exists temporal trends between lithic raw materials and artifact types. In Bed I and Lower Bed II, heavy-duty tools (mean diameter >50 mm) and utilised material were manufactured on fine-grained igneous rocks, while light-duty tools (mean diameter <50 mm) and debitage tended to be made on quartzite. The only exception being the lithic assemblage from DK where hominins produced an appreciable amount of igneous debitage whereas at most pene-contemporary sites, it appears as though hominins frequently carried out initial flaking of igneous materials off-site prior to on-site reduction, utilisation, and discard (Leakey 1971). During the deposition of Middle and Upper Bed II, hominins preferentially relied on quartzite to produce heavy- and light-duty tools as well as utilised material. This diachronic modification in hominin raw material exploitation together with the presence, absence, and ratios between artifact types allowed Mary Leakey (1971) to define the Oldowan, Developed Oldowan A and B, and Acheulean industries. According to Leakey's (1971) typology, choppers are defined as the "index fossil" of the Oldowan, varying proportions of bifaces, flake tools, and spheroids are indexical of the Developed Oldowan A and B, and a site containing >40-50% of bifaces is considered Acheulean. As for the differentiation between the Developed Oldowan and Acheulean industries, Leakey (1971) specifies that bifaces classed in the former show greater variation in morphometry and reduction technique than the Acheulean.

In the concluding chapter of Richard Hay's (1976) seminal volume on the geology of Olduvai Gorge, he discusses hominin ecology from a paleogeographic and raw material

procurement perspective. Based on his macroscopic and mineralogical analyses of available rock types and artifact assemblages excavated by Mary Leakey, Hay (1976) suggests three factors dictated hominin raw material use, namely morphometry, mechanical properties, and distance to source. At Oldowan sites, there was a clear preference for mid-sized rounded cobbles while at Acheulean sites, large cutting tools tended to be manufactured on larger blanks than what could have been extracted from typical Oldowan cores. Throughout Bed I and Lower Bed II, hominins preferentially utilised nephelinite for artifact manufacture whose dense homogenous texture may have been a selective factor and would have been available in riverbeds, ultimately sourced to Sadiman. While higher in the sedimentary sequence at sites such as FC and SHK, hominins drastically reduced their use of nephelinite for unknown reasons despite this material being available nearby. Interestingly, phonolite from Engelosin has not been reported from any Bed I site, its earliest archaeological occurrence is at the base of Bed II and progressively becomes a highly exploited raw material, particularly in Bed III and IV. Lower in the sequence, Hay (1976) states that phonolite artifacts have not been recovered from any Bed II site above the Lower Augitic Sandstone which may have to do with diachronic changes in regional drainage patterns. Centrally located to many archaeological sites in the eastern Main Gorge, the Naibor Soit inselberg is reported to yield coarse-grained quartzite of colourless, brown, and green varieties that were intensively utilised throughout the Olduvai sequence perhaps due to this material's hardness and edge durability (Hay 1976). Medium-grained varieties of quartzite outcrop at Naisiusiu, and have been reported from sites >10 km distant in the eastern Main Gorge. The saline alkaline environment of the Olduvai paleolake allowed for the petrogenesis of chert nodules in Bed I and II, although the lowermost chert horizon in Bed I is stratigraphically below any known archaeological site (Hay 1976). By Bed II, hominins sporadically but intensively utilised chert for

artifact manufacture (see Stiles et al. 1974). According to both Mary Leakey (1971) and Richard Hay (1976), several grey to brown chert artifacts have been recovered from Bed I and II sites although its source is unknown. A single gabbro artifact was also uncovered in Lower Bed II and its suspected source is the Tanzania Craton several tens of kilometres west. Based on Hay's (1976) synthesis of hominin lithic raw material usage, it is suggested that most artifacts in Bed I and II were produced on materials naturally available in nearby paleoconglomerates of volcanic origin or from outcrops as far as 10 km distant. In closing, Hay (1976) concludes that early hominins were moderately selective of raw material traits and distance to source was a major factor influencing material choice.

Based on the re-appraisal of Olduvai Gorge's Bed I lithic assemblages from FLK Zinj and FLK N together with observations gleaned from analogous low-energy lacustrine settings, de la Torre and Mora (2005) argue that most unmodified igneous stones, or manuports, found in the same context as Oldowan lithics are not artifactual, but rather geofactual. Grounded in a literature review, de la Torre and Mora (2005) first assess the epistemological underpinnings of what constitutes a manuport which is defined as an unmodified lithic transported and discarded by hominin agency within a sedimentary setting disbelieved to have motioned large clasts. As alluded to by de la Torre and Mora (2005), the manuport artifact type has been hypothesised as a prime variable in hominin behavioural models, namely the stone cache model which posits that hominins systematically provisioned key localities on a paleolandscape with unmodified stones with the forethought of future re-occupation (Potts 1988). For both assemblages, there was a high quantity of purported manuports when compared with artifactual pieces, and nearly all unmodified stones were of igneous material whereas both large and small lithics were mostly on quartzite. Morphometric comparisons between large artifacts and unmodified stones with poor flaking

qualities in the FLK Zinj assemblage revealed that both categories had similar weights which suggests that the latter were not provisioned stones for future reduction. As for the FLK N assemblage, unmodified stones are similar in morphometry and texture to hammerstones. Therefore, de la Torre and Mora (2005) do not preclude the possibility that some natural stones at this site were amassed by anthropogenic means. In lake margin environments (Manyara, Natron, Eyasi, and Ndutu) analogous to the Olduvai paleobasin, de la Torre and Mora (2005) also observed that sedimentary processes can lead to the deposition and accumulation of large clasts in low-energy environments. Altogether, this study presents an alternative explanation for the co-occurrence of unmodified stones and lithics in paleolacustrine settings (de la Torre and Mora 2005).

Tactikos (2005) studies Oldowan technological organisation at Olduvai Gorge using a techno-typological approach complemented by macroscopic raw material identification and functional experiments. Based on the analysis of 4,334 individual artifacts excavated from several sites in Bed I and Lower Bed II across the Olduvai paleobasin, Tactikos (2005) tests three behavioural ecological models based on site paleogeography, artifact attributes, distance to raw material sources, and raw material characteristics for functional needs. Tactikos (2005) macroscopically identified lithic raw materials and recorded specific traits, namely colour, mineral composition, and groundmass using a reference collection based on material collected from Naibor Soit, Naisiusiu, and present-day secondary igneous and metamorphic sources. Quartzite from Naibor Soit is differentiated from that of Naisiusiu based on grain size, the former is generally coarse-grained while the latter is medium-grained. Tactikos (2005) suggests that depending on the studied sites' paleogeographic locations, hominins expediently, optimally, and opportunistically procured raw materials usually from sources <10 km distant. However, these aforementioned

behavioural trends do not fully account for intra-assemblage diversity which suggests that Oldowan technological organisation was not strictly simplistic but rather ecologically integrated and inter-dependent on other variables (Tactikos 2005).

From a behavioural ecological perspective, Blumenschine et al. (2008) test distance-decay models for Oldowan quartzite assemblages from thirteen different localities positioned along the Eastern Lake Margin and Alluvial Fan of Lower Bed II. From west to east, the sites include MNK, FLK, VEK, HWK W, HWK E, HWK EE, KK, MCK, Long K, WK-PDK, JK-DK, and the THC Complex which are all located at different distances to the assumed raw material source known as Naibor Soit. Theoretically, Blumenschine et al. (2008) expect that proximity to raw material source in addition to scavenging opportunities and access to arboreal refuge were major ecological determinants of hominin landuse and the nature of lithic assemblages. By studying the assemblages using a techno-typological approach, Blumenschine et al. (2008) determined there were high levels of correlation between distance to outcrop and artifact weight density, while artifact size and reduction attributes did not correlate. Therefore, Blumenschine et al. (2008) conclude by stating that several other ecological variables beyond two-dimensional distances to Naibor Soit likely impacted the composition and attributes of Oldowan quartzite assemblages in the Olduvai paleobasin.

Since the Olduvai paleobasin hosted a saline alkaline lake in the Early Pleistocene (Hay 1976), these conditions allowed for the petrogenesis of authigenic chert nodules by way of sodium-silicate precipitation (O'Neil and Hay 1973). Therefore, at lowstands, chert deposits became exposed and available for exploitation by early hominins. Stiles et al. (1974) base their study on the guiding principle that chert's ^{18}O isotopic values are indicative of having been formed in high or low salinity environments. By obtaining $^{18}O/^{16}O$ values and X-ray spectroscopic data on chert

nodules from different localities in the Side Gorge compared with Lower Bed II Oldowan lithics from MNK-CFS and HWK E, Stiles et al. (1974) were able to retrace chert procurement distances in the Olduvai paleobasin. Interestingly, many of MNK-CFS's chert lithics had lower isotopic values compared with the locality's *in situ* pene-contemporarily exposed chert-bearing horizon. Therefore, it is believed that hominins transported chert for <1 km to the site where it was intensively knapped (but see Kimura 1997). Isotopic values of chert lithics from HWK E were similar to those from MNK-CFS which suggests that hominins responsible for both assemblages may have either exploited the same chert-bearing horizons or those with similar petrogenesis conditions (Stiles et al. 1974).

Using a combination of thin section petrography, X-ray spectroscopy, electron microprobe analysis, and inductively coupled plasma mass spectrometry, Mollel (2002) determines the provenance of igneous cobbles from Lower Bed II sites at Olduvai Gorge, namely HWK, MCK, and PEK. At the time of study, the geology of the NVH was poorly understood despite its known contribution to sedimentary infill of the Olduvai paleobasin, particularly in the form of paleoconglomerates that were likely important sources of lithic raw materials. Mollel (2002) collected a total of thirty-four geological samples from Olmoti, Ngorongoro, Lemagrut, and Sadiman compared with thirteen cobbles from the aforementioned sites. Samples from Olmoti were identified as basalt and trachyandesite, samples from Ngorongoro were identified as olivine basalt, trachyandesite, and trachyte, samples from Sadiman were identified as phonolite and phonolitic nephelinites, and samples from Lemagrut were identified as olivine basalt, hawaiite, trachybasalt, trachyte, and benmorite (Mollel 2002). Using this comparative data set, Mollel (2002) determined that of the thirteen igneous cobbles from Olduvai, seven were from Sadiman, three were from Lemagrut, two were from Ngorongoro, and one basalt cobble from HWK was

from an unknown source. Importantly, this study demonstrates that igneous rocks deposited in the Olduvai paleobasin may be sourced to a volcanic centre based on mineralogical and/or geochemical similarities (Mollel 2002). Nevertheless, it presently remains unachievable to determine the exact locality where igneous materials were obtained although it is hypothesised that hominins did not venture overly long distances to obtain such rock types considering their local availability in secondary deposits.

Chapter 3.1.2

Acheulean

In a re-appraisal of inter-stratified Bed II industries from Olduvai Gorge, Kyara (1999) identifies relationships between artifact types, lithic raw materials, and paleogeography. The author studied artifact assemblages from BK, EF-HR, FC, FLK N, HWK E, MNK, SHK, and TK by way of techno-typology, and macroscopically identified lithic raw materials. The latter were compared with reference material obtained from an extensive survey of local outcrops. According to Kyara's (1999) analysis, Oldowan assemblages from HWK E and MNK were predominately manufactured on igneous raw materials while lithics from FLK N were primarily on quartzite. Developed Oldowan A assemblages from FLK N and HWK E were primarily on quartzite while lithics from MNK were predominantly manufactured on chert. Developed Oldowan B assemblages from BK, FC, HWK E, SHK, and TK were dominated by quartzite. However, bifaces from sites lower in the stratigraphic sequence were made on igneous materials while the overlying bifaces assigned to the Developed Oldowan B were predominantly made on quartzite. The lithic assemblage from EF-HR was assigned to the Acheulean industry whose raw materials were predominately igneous-based. Based on his re-appraisal, Kyara (1999) maintains that most raw materials exploited during Olduvai's ESA were locally available. By comparing Oldowan and

Acheulean artifact types, Kyara (1999) found the latter to be primarily manufactured on large igneous clasts, and whose sites were located further inland from Olduvai's paleolake closer to stream channels where such raw materials would have been in greater abundance. In this seminal study, Kyara (1999) effectively demonstrates the short-comings of a traditional techno-typological approach to the study of ESA lithic assemblages by identifying how raw material source, rock type morphometry and mechanical properties, and paleogeography are integral components to be considered for Oldowan and Acheulean assemblages. As such, Kyara (1999) furthers our understanding of industrial variability which has been traditionally hypothesised as a by-product of different site activities, taxa authorship, and/or cultural traditions.

McHenry and de la Torre (2018) combine macroscopic, petrographic, and geochemical techniques to assess Oldowan and Acheulean lithic raw material exploitation from Olduvai's Bed II dating between approximately 1.7-1.4 Ma. The authors describe the nature and availability of lithic raw materials with igneous rocks primarily of Lemagrut, Sadiman, Ngorongoro, Olmoti, and Engelosin origin, quartzite from Naibor Soit and Naisiusiu, gneiss from Kelogi, and chert that was intermittently available at some localities during lowstands. McHenry and de la Torre (2018) macroscopically classified lithic raw materials from several sites at Olduvai, most notably HWK EE and EF-HR, which was their primary means to establish a reference collection. Both lithics and unmodified stones from HWK EE and EF-HR were subject to a comprehensive techno-typological analysis in order to identify selective traits and complement provenance determination. Representative samples from certain raw material groups were subject to destructive analytical techniques for rock type identification, namely thin section petrography, X-ray diffraction, loss on ignition, and wavelength dispersive X-ray spectroscopy. Based on their results, McHenry and de la Torre (2018) determined that Oldowan tool-makers at HWK EE appear to have preferentially

selected phonolite over fine-grained basalt from a known pene-contemporary secondary source, and exploited tabular quartzite that may have been transported from the Naibor Soit inselberg and was intensively knapped on-site. On the other hand, Acheulean tool-making hominins at EF-HR primarily exploited currently unknown secondary sources to obtain large, high-quality basaltic and trachytic clasts to manufacture large cutting tools. Based on these results, the major difference in raw material selection between the Oldowan and Acheulean lies on clast size although at both sites were igneous materials sourced from stream channels and quartzite from primary sources at local inselbergs (McHenry and de la Torre 2018).

Using non-destructive energy dispersive X-ray spectroscopy, Negash et al. (2006) determine the source of Oldowan and Acheulean obsidian lithics from the paleoanthropological complex of Melka Konture, Ethiopia. This complex is located near Ethiopia's capital, Addis Ababa, along the Awash River and its sedimentary deposits have yielded a wealth of ESA, MSA, and LSA artifact assemblages. Negash et al. (2006) geochemically characterised ten obsidian lithics from three ESA sites, two of which are described as Oldowan while the third is Middle Acheulean. Interestingly, one site in particular (Garba IV) yielded nearly twice as many artifacts on obsidian as other raw materials combined, and contained evidence of obsidian retouch. In comparison with a reference collection, Negash et al. (2006) found that all artifacts were procured from the Pliocene source of Balchit located approximately 10 km away despite there being atleast one source closer to the sites. The results of this study demonstrate that ESA hominins did not obtain their lithic raw materials from overly long distances and may be indexical of small foraging ranges (Negash et al. 2006).

Féblot-Augustins (1990) synthesises provenance of raw materials from twenty African Acheulean sites. Since the Acheulean industry is usually attributed to *Homo erectus/ergaster*, we

can gather that based on Féblot-Augustins's (1990) literature review, this species exploited raw materials over 95% of the time from sources <26 km distant. The Ethiopian site of Gadeb 8E has yielded four obsidian bifaces sourced 100 km away which constitutes the furthest recorded distance for raw material procurement during the Acheulean. Féblot-Augustins (1990) also effectively demonstrates that hominins transported unworked, partially worked, and finished pieces from sources <10 km away, and only transported finished pieces over distances >10 km.

Santonja et al. (2014) employ the chaîne opératoire technique on an Upper Bed II Acheulean assemblage from TK at Olduvai Gorge using a techno-typological approach complemented by the macroscopic identification of raw materials. A single quartzite slab fragment was subject to destructive wavelength dispersive X-ray spectroscopy to determine its elemental composition and confirm macroscopic identifications. Most of the quartzite artifacts are assumed to have been sourced from Naibor Soit Ndogo whose pene-contemporary outcroppings to the site may have been as close as 750 m away (Santonja et al. 2014). A small number of quartzite artifacts preserved rounded cortical surfaces which suggests that hominins sourced some quartzite from nearby conglomerates as opposed to the tabular shapes typical of Naibor Soit Ndogo. The assemblage's quartzite lithics have all reduction stages represented which suggests that this raw material was transported to the site where it was intensively knapped, utilised, and discarded. Santonja et al. (2014) found that phonolite, nephelinite, trachyte, and basalt artifacts represented latter reduction phases, which suggests that partially worked pieces were transported from nearby conglomerates where they may have been tested for suitability prior to on-site knapping, utilisation, and discard. A small number of lithics were also manufactured on gneiss and flint which may imply more distant procurement of raw materials. In closing, Santonja et al. (2014) state that

TK was an intensive knapping workshop and possibly a consumption locale evidenced by broken biface tips.

In Mary Leakey's (1994) introductory chapter to her second of two major volumes on Olduvai Gorge (Leakey and Roe 1994), she prefaces her studies of lithic assemblages from Bed III, IV, and the Masek Beds by stating that raw materials were macroscopically identified with the aid of a reference collection. The following three paragraphs describe the raw material assignment of certain artifact types from three sites excavated by Mary Leakey between 1969 and 1971, namely JK W, HEB, and HEB W.

The JK site was first discovered by Louis Leakey in 1931 and its western portion was excavated by Mary Leakey in the early 1970s. At JK W, Leakey (1994a) describes four artifact-bearing units in Bed III, with the two lowermost horizons being the subject of the following description. Most artifacts from the lowermost assemblage were primarily on tabular quartzite which may have been procured from the nearby Naibor Soit inselbergs whose closest actual outcroppings are approximately 1.5 km away. Rarer instances of rounded cortical quartzites were also flaked which implies a fluvial origin. Leakey (1994a) notes the presence of a bifacial roughout manufactured on granite gneiss that resembles material at Kelogi, a series of inselbergs >10 km southwest which could imply direct procurement. Alternatively, granite gneiss, along with some quartzite and igneous raw materials with rounded cortical surfaces may have been procured from nearby conglomerates (Leakey 1994a).

The HEB and HEB W sites were first excavated by John Waechter in 1962 and between 1969-1971, Mary Leakey re-opened both sites. At HEB, Leakey (1994b) describes two artifact-bearing horizons in Lower Bed IV with the uppermost horizon yielding an unusually high amount of phonolite artifacts (n=289) as opposed to the underlying unit which yielded only twenty-two

pieces. The upper unit's phonolite lithics consisted of fifty-two heavy- and light-duty tools such as bifaces and cores, and 237 knapping products which together suggests that hominins conducted intensive on-site knapping. Leakey (1994b) suggests that the phonolite was procured from Engelosin, a volcanic neck <10 km northeast of the site. The upper unit also yielded over ten large quartzite blocks that do not appear to have a fluvial origin meaning that they may have been transported to the site, with the closest known source being the Naibor Soit inselbergs >2.5 km north (Leakey 1994b).

At HEB W, Leakey (1994b) describes one stratigraphic unit that yielded a high number of sharp bifacial tools manufactured on trachyandesite and basalt with little to no debitage of the same material. According to Leakey (1994b), this raw material is macroscopically identical to that of Lemagrut which suggests that hominins may have obtained igneous clasts from a nearby secondary sources where they these artifacts were flaked and trimmed prior to on-site transport. Furthermore, this unit also yielded two large cutting tools with extensive scarring on an unrecognised igneous rock type which suggests that hominins procured some raw materials from an unknown and possibly distant source (Leakey 1994b).

Jones (1979) studies the characteristics of lithic raw materials at Olduvai Gorge to determine its effects on retouch and finished forms of Acheulean bifaces. The author collected quartzite, basalt, trachyandesite, and phonolite from local sources to experimentally manufacture bifaces and test their utilisation efficiency. Quartzite from Naibor Soit naturally occurs in a tabular form and can either be shaped into a biface or struck to obtain a large blank for trimming. Basalt and trachyandesite cobbles and slabs are present in conglomerates from Lemagrut. These materials are dense and most efficiently turned into bifaces by obtaining large blanks for trimming. Phonolite from Engelosin naturally occurs as slabs and large blocks which can either be shaped into a biface

or struck to obtain a large blank for trimming. Based on utilisation experiments, Jones (1979) determined that quartzite bifaces have the highest edge durability, while the primary edges of basalt and trachyandesite bifaces are sharper than retouched edges but both become easily blunted, and phonolite bifaces have sharp edges but become easily blunted. Considering these raw material characteristics, Jones (1979) studied bifaces from HEB (Lower Bed IV) and WK (Upper Bed IV). Bifaces from HEB were manufactured on large phonolite blanks, had straight edges, and were extensively trimmed while bifaces from WK were manufactured on basalt, trachyandesite, quartzite, and phonolite blanks, had irregular edges, and were minimally trimmed. Despite the majority of WK bifaces having a crude appearance, Jones (1979) suggests that its knappers more efficiently obtained working edges by doing less than the knappers of phonolite bifaces at HEB. In closing, Jones (1979) argues it is necessary to characterise the nature of lithic raw materials prior to assessing hominin technical skills.

In the tenth chapter of Mary Leakey's second seminal volume on Olduvai Gorge (Leakey and Roe 1994), Peter Jones (1994) synthesises the results of his experimental studies conducted between 1976-1983 which sought to understand the factors that influenced the nature and composition of Acheulean assemblages from Olduvai's Bed III and IV. These factors included reduction strategies, time involved in artifact production, and raw material characteristics. Jones (1994) describes lithic raw materials from nearby sources, including their natural morphometric occurrences and mechanical qualities which do not bear repeating apart from the raw material sources. The two presumed sources of artifactual quartzite are Naibor Soit and Naisiusiu, two inselbergs whose raw materials were almost continuously available apart from highstands that may have made the former inaccessible at times. The presumed phonolite source is Engelosin, a volcanic neck several kilometres north of the confluence between the Main and Side Gorge. Jones

(1994) notes that Engelosin phonolite was not exploited by hominins until after the deposition of Bed I (see Hay 1976), and when it was presumably utilised, some its non-flow-banded lithologies may have been fully exhausted thereby creating a discordant geological reference collection. Paleoconglomerates draining the Lemagrut volcanic centre supplied the Olduvai paleobasin with basalt and trachyandesite. Nephelinite is believed to have been naturally available in much the same fashion as the former and can ultimately be sourced to the Sadiman volcanic centre southeast of Lemagrut. Jones (1994) also states that trachytic rock types were naturally available in the eastern sector of Olduvai during the deposition of Bed II. During Bed II, chert-rich horizons became exposed at lowstands and were subsequently exploited.

In an important study on prehistoric obsidian use in Kenya and northern Tanzania, Merrick et al. (1994) use of X-ray spectroscopy and electron microprobe analysis to characterise eighty individual sources in an attempt to provenance obsidian artifacts from five Acheulean sites in central Kenya. The eleven studied artifacts from the 700 Ka site of Kariandusi revealed that hominins obtained obsidian from three sources between 15-30 km away, with the majority of obsidian stemming from the closest of the three sources. According to Merrick et al. (1994), Kariandusi's lithic assemblage is comprised of approximately 15% of obsidian but since the lithics are relatively large and appear to be re-worked, it is not possible to determine in what format obsidian was brought to the site, whether it be as partially worked or finished pieces (see Féblot-Augustins 1990). One obsidian artifact from the Later Acheulean site of Kaptabuya revealed that hominins sourced material between 10-30 km away depending on which outcrop they may have frequented considering the volcaniclastic origin of this particular obsidian (Merrick et al. 1994). The undated Isenya site revealed that one flake fragment was obtained approximately 60 km away to the nearest known outcrop. Two artifacts, one from Kilombe and the second from Kapthurin A,

did not match any source material meaning that hominins exploited currently unknown and uncharacterised obsidian outcrops. Overall, this study shows that during the Acheulean, hominins infrequently exploited obsidian which may be a matter of proximity to source or lack thereof, a preference for non-obsidian raw material, plentiful local raw material availability, or perhaps limited long-range mobility (Merrick et al. 1994).

Using geometric morphometrics in combination with experimental replication, Archer and Braun (2010) study shape variation of Acheulean large cutting tools recovered from Elandsfontein, South Africa, dating from 1-0.6 Ma. According to Archer and Braun (2010), Elandsfontein's large cutting tools are well-suited to undertake this study since there is recognisable variation in blank morphologies, and their makers utilised a wide range of raw materials whose primary extents were several kilometres away from the site. Archer and Braun (2010) hypothesise and effectively demonstrate by way of three-dimensional shape variables that raw material characteristics in conjunction with blank morphology, as well as reduction strategy and intensity best account for shape variation of large cutting tools rather than two-dimensional measures of shape.

Chapter 3.1.3

Discussion

Based on this literature review and over-looking the short-comings of certain studies, one can gather that during the ESA, Oldowan and Acheulean tool-making hominins jointly considered morphometry and mechanical properties together with distance to source for raw material exploitation. During the Oldowan, hominins were moderately selective of raw material characteristics and adopted a variety of procurement strategies ranging from local, opportunistic, and least-effort strategies to obtain raw materials sometimes >10 km distant (Braun et al. 2008; Goldman-Neuman and Hovers 2012; Hay 1976; Stout et al. 2005). Although most raw materials

were obtained from sources <10 km distant (Braun et al. 2008; Hay 1976; Negash et al. 2006). During the Acheulean, raw material procurement strategies became increasingly complex and transport distances reached a maximum of 100 km (Merrick et al. 1994), although most material was usually sourced from less than a few tens of kilometres away (Féblot-Augustins 1990).

At Olduvai Gorge specifically, Oldowan cores were typically manufactured on mid-sized rocks (Hay 1976). Despite only being available at further distances than rounded clasts in paleoconglomerates, angular quartzite was highly utilised in artifact production (Leakey 1971), and was sometimes prioritised for its knappability (McHenry and de la Torre 2018). Nevertheless, igneous paleoconglomerates remained an important secondary source for raw materials, and synchronic and diachronic differences in regional drainage patterns appear to have impacted whether such material was available for exploitation (Hay 1976). Considering that many Oldowan sites were located near river channels in low-energy lacustrine settings (Hay 1976), it is likely that some unmodified stones naturally accumulated alongside artifact assemblages and should not be *a priori* considered artifactual (de la Torre and Mora 2005). Based on predominantly incomplete Oldowan reduction sequences on igneous material, it appears as though hominins frequently knapped fluvially-derived stones off-site prior to on-site transport (Leakey 1971). Intermittently available chert deposits were intensively exploited, and such artifacts were both transported on- and off-site (Stiles et al. 1974). Not only were there diachronic alterations in raw material utilisation, but there appears to have been synchronic variations in technological organisation that were likely embedded with an array of behavioural and ecological variables (Blumenschine et al. 2008; Tactikos 2005).

At Olduvai, there are minor differences in raw material use between the Oldowan and Acheulean industries. The principal difference for igneous materials lies in clast size which is

attributed to the fact that the production of large cutting tools generally required larger clasts than those required for Oldowan cores (Hay 1976; Kyara 1999; McHenry and de la Torre 2018). This selective criterion may imply that igneous rocks were transported to sites from sources closer to volcanic centres. In line with this trend is the uppermost artifact horizon at HEB which revealed that large phonolite rocks from Engelosin <10 km away were transported to the site where these were intensively knapped. However, like most Oldowan sites at Olduvai, Acheulean artifacts on igneous rock types at HEB W, JK W, and TK are of latter reduction phases which implies that hominins initially knapped such material off-site, at nearby conglomerates and/or closer to volcanic centres (Leakey 1994a, b; Santonja et al. 2014). Certain Acheulean sites contain bifacial implements manufactured on thin tabular quartzitic rocks whose locations were proximal to outcrops where such material was available (Leakey 1994a, b; Santonja et al. 2014). Considering that quartzitic rocks in the Olduvai region preserve their cutting edges better than igneous rock types (Jones 1979, 1994), this implies that hominins may not have felt the need to obtain alternative material from potentially more distant sources. Artifactual quartzite with rounded cortical surfaces that imply a fluvial origin were also procured from nearby conglomerates and occasionally knapped which may attest to quartzite's diverse functional qualities (Jones 1994). These trends for the Acheulean at Olduvai are in accordance with the African record that suggests that unworked, partially worked, and finished pieces were procured <10 km away (Féblot-Augustins 1990).

Overall, the number of metamorphic outcrops adjacent to Olduvai and the paleoconglomerates that drained the volcanic highlands in the Pleistocene supplied the paleobasin with dispensable raw materials with ideal tool-making properties. For both the Oldowan and Acheulean industries at Olduvai, this appears to have made long-distance transport of exotic raw materials unnecessary. This fact makes lithic raw material studies all the more important to

understand hominin ecology within a resource-rich paleoenvironment that was Olduvai. However, what currently hampers our ability to understand hominin behaviour from a technological perspective is two-fold. First, it is well-documented that raw material morphometry and mechanical properties at and beyond Olduvai affect the classification of artifact assemblages (Archer and Braun 2010; Kyara 1999; Leakey 1971), and the behavioural interpretations gleaned from them such as the technical abilities of their makers (Jones 1979, 1994). Second, previous studies on Olduvai's lithic raw materials have relied on macroscopic, petrographic, and geochemical techniques (e.g. Blumenschine et al. 2008; Hay 1976; Jones 1994; Kyara 1999; Leakey 1971; Leakey and Roe 1994; McHenry and de la Torre 2018; Mollel 2002; Santonja et al. 2014; Stiles 1991, 1998; Stiles et al. 1974; Tactikos 2005). However, these studies have not comprehensively characterised metamorphic outcrops, particularly those of quartzitic lithology presumably based on the assumption that they are undistinguishable from one another. This lack of characterisation studies is unwarranted for several reasons. Most notable include the fact that research at Olduvai has been ongoing for over a century, stone tools are a ubiquitous artifact type, quartzite was heavily utilised in artifact production during the Olduvai's ESA (Leakey 1971; Leakey and Roe 1994) and thereupon, quartzite is of assumed importance based on experimental studies (e.g. Byrne et al. 2016; de la Torre et al. 2013; Diez-Martín et al. 2011; Gurtov and Eren 2014; Yustos et al. 2015), and certain quartzitic outcrops have played a central role in discussions about hominin behaviour in the Olduvai paleobasin (e.g. Blumenschine et al. 2008; Hay 1976; Leakey 1971; Tactikos 2005). Therefore, characterisation studies of metamorphic outcrops in the Olduvai paleobasin are in need and may yield a pathway to shed light on lithic provenance and hominin ecology. Altogether, this discussion based on a comprehensive literature review has

outlined ESA techno-temporal trends at and beyond Olduvai, and identified a significant gap in scientific knowledge that justifies the need to undertake this characterisation study.

Chapter 3.2

Middle Stone Age

The MSA began >300 Ka (Brooks et al. 2018; Richter et al. 2017) throughout different regions in Africa and persisted until <30 Ka (e.g. Mercader et al. 2012; Wadley 2001). The MSA is defined by the presence of prepared core technologies together with varying instances of blades (Johnson and McBrearty 2010; Wilkins and Chazan 2012) and points (McBrearty and Tryon 2006) that show regional and temporal standardisation alongside other innovative behaviours (McBrearty and Brooks 2000). MSA sites are generally attributed to *Homo sapiens* with the earliest direct association between the two dating to approximately 300 Ka (Hublin et al. 2017; Richter et al. 2017). It is worth noting that the MSA chronologically overlaps with two other species, namely *H. heidelbergensis/rhodesiensis* (Balzeau et al. 2017) and *H. naledi* (Berger et al. 2015; Dirks et al. 2017). Together with the earliest MSA sites antecedent to the earliest evidence for *H. sapiens* (Deino et al. 2018), this raises the possibility that MSA sites may be the by-products of three individual species. With this biological and technological evolutionary preface in mind, the following sub-chapter will recapitulate key studies dealing with raw material sourcing and selection in the MSA, and conclude with a sub-chapter that synthesises the behavioural implications these entail to highlight the profound differences between the ESA and the MSA.

Brooks et al. (2018) employ a multi-analytical approach to interpret archaeological material from five early MSA sites in the Olorgesailie paleobasin dating between approximately 320-295 Ka. Their findings indicate that hominins predominately used locally available basalt from Mount Olorgesailie, chert of unknown provenance, and obsidian obtained from sources between 25-50

km away (Brooks et al. 2018). Despite relying on distant obsidian sources for tool-making, their makers appear to have knapped obsidian on-site rather than importing finished pieces evidenced by refits, variable morphometric distributions, and other artifactual features. Faunal remains found in association with the lithics show that these hominins relied on a wide variety of taxa which suggests they had skilled yet flexible predatory behaviour. Manganese oxide and ochre mineral pigments, some with clear anthropogenic markings, were also found in association with the artifacts and may imply functional and/or symbolic usage. Unlike the preceding Acheulean in the Olorgesailie paleobasin, MSA hominins had developed innovative raw material procurement strategies, lithic technologies, and predatory hunting abilities (Brooks et al. 2018).

Blegen (2017) presents the earliest evidence of long-distance obsidian transport from the Sibilo School Road Site dated to approximately 200 Ka. In this article, Blegen (2017) reviews the Pleistocene archaeological of East Africa to suggest that known lithic assemblages usually consist of small amounts of obsidian, a material that was very rarely sourced >60 km away, and that there are few well-dated Middle Pleistocene sites. Using electron probe microanalysis, Blegen (2017) identified three compositionally distinct sources for the site's obsidian artifacts which account for approximately 43% of the total lithic assemblage. The obsidian was obtained from sources 25 km, 140 km, and 166 km away from the site, with the majority stemming from the furthest source. The implications of this distant ecological connection may be interpreted as evidence of high mobility, inter-group exchange networks, and/or territorial resource control (Blegen 2017).

Adelsberger et al. (2011) provenance MSA basalt lithics from Laetoli's Ngaloba Beds dating to approximately 200 Ka. Using a combination of thin section petrography, X-ray spectroscopy, and inductively coupled plasma mass spectrometry, Adelsberger et al. (2011) determined that all seventy-one lithics could be classed into three sub-groups which were

compared with reference samples. The nearby Ogol Lava outcroppings were the sources for some of the lithic raw materials while petrographic and geochemical data for a second sub-group overlapped with reference samples from the Ogol Lava outcroppings, as well as from Lemagrut and Olmoti. The third sub-group did not overlap with any sample from their reference collection (Adelsberger et al. 2011). Considering that the analysed lithics were found alongside others on phonolite, quartzite, and chert, this suggests that hominins may have obtained raw materials from varied and relatively distant sources, with the latter three materials being most typical of lithic assemblages from the Olduvai paleobasin tens of kilometres away.

Negash et al. (2011) provenance ninety-seven obsidian lithics from Aduma, Aladi Springs, Halibee, Herto, and Porc Epic, all located in Ethiopia and dating from approximately 160 Ka to the Late Pleistocene. Using a combination of non-destructive X-ray spectroscopy and electron microprobe analysis in reference to geological samples, Negash et al. (2011) found that obsidian from these sites were obtained from known sources between 15-405 km distant. At Aduma, Halibee, and Herto, twenty-six compositionally distinct obsidian sources were exploited of which only seven are known. Despite not having an exhaustive reference collection, Negash et al. (2011) suggest that some form of trade was likely involved in the procurement of distant obsidian varieties.

Nash et al. (2013) determine the provenance of MSA silcrete lithics from the site of White Paintings Shelter in Botswana's Kalahari Desert. This site is well-known as its archaeological sequence reaches a maximum depth of 9 m which constitutes as the deepest known site in the Kalahari. Throughout the site's MSA occupation between approximately 94-54 Ka, the majority of lithics were manufactured on chert and silcrete despite the area being naturally provisioned with abundant quartz and quartzite. In order to compile a reference collection, Nash et al. (2013)

sampled all known outcrops while acknowledging the possibility that some have since been exhausted by anthropogenic means or buried as a result of sedimentary processes. Using a combination of inductively coupled plasma mass spectrometry and atomic emission spectrometry, fourteen flakes were subject to destructive analysis and statistically compared with reference material. Five lithics were sourced to Lake Ngami 220 km distant, five others were obtained from the Boteti River nearly 300 km away, while the remaining four artifacts did not cluster with any sampled outcrop (Nash et al. 2013). The results of this study demonstrate that the site's MSA occupants obtained silcrete over great distances and consistently exploited the same outcrops over time, and that sourcing this material is feasible despite the fact that silcretes tend to be compositionally homogenous on a regional scale (Nash et al. 2013).

Using energy and wavelength dispersive X-ray spectroscopy, Negash and Shackley (2006) provenance MSA obsidian artifacts from Porc Epic, Ethiopia. A total of thirty-one obsidian lithics from a chert-dominated assemblage dating between 77.5-61 Ka was geochemically characterised and compared with a reference collection. Negash and Shackley (2006) identified at least three obsidian sources that were exploited, two of which are approximately 150 km away from the site while the third source is some 250 km away. Several artifacts did not geochemically cluster with their reference material meaning that additional, unknown sources were also exploited. Interestingly, none of the studied lithics were obtained from significantly closer sources, namely Meiso and Sodoma Misra Goro, both of which bear high-quality obsidian ideally suited for knapping. Negash and Shackley (2006) further contextualise their findings by eluding to previously noted technological and stylistic similarities between lithics from Porc Epic and Kone. The latter being the furthest of the three known sources from which obsidian at Porc Epic was obtained which may suggest that both sites were frequented by the same occupants or alternatively,

that obsidian was traded for at Porc Epic and may have led to artifactual similarities (Negash and Shackley 2006).

Mehlman (1977) studies the archaeological material recovered from the rockshelter at Soit Nasera, a large quartz-feldspathic monolith situated in northern Tanzania's Gol Mountains. Based on a 75 m^2 excavation grid reaching a maximum depth of 9 m, Mehlman (1977) recovered approximately 300,000 lithics, 200,000 faunal remains, and over 500 ceramic sherds. As it relates to lithic raw material sourcing, the uppermost LSA deposits yielded high numbers of obsidian artifacts of variable sizes that may have been obtained from sources hundreds of kilometres away in Kenya. The underlying lithic assemblage yielded high frequencies of quartzite which was locally available at nearby inselbergs. A second underlying lithic assemblage yielded several backed pieces on chert whose raw material source is unknown. According to Mehlman (1977), a purported transitional MSA-LSA industry was manufactured primarily on quartzite which was locally available. Some of the site's lowermost MSA lithics were manufactured on chert with reticulate cortical surfaces that is macroscopically similar to Olduvai's chert-bearing horizons >25 km away (Mehlman 1977). Based on Mehlman's (1977) preliminary studies, we may conclude that the makers of the earliest lithic assemblages at Nasera did not consistently exploit exotic raw materials in contrast to the site's LSA inhabitants.

Based on previously published data from Lukenya Hill and Soit Nasera, Barut (1994) studies diachronic changes in lithic raw material procurement strategies during the MSA and LSA as it relates to hunter-gatherer settlement and mobility patterns. Lukenya Hill is a gneissic inselberg located in southern Kenya within an ecotonal zone and hosts open-air sites and a rockshelter while Soit Nasera is quartz-feldspathic monolith in northern Tanzania overlooking the Serengeti Plains. According to Barut (1994), MSA inhabitants at Lukenya Hill were relatively more sedentary than

those at Soit Nasera based on a more expedient technology and a heavier reliance on local raw materials. During the LSA, inhabitants at Lukenya Hill had developed increasingly efficient technologies to hunt mobile game and heavily relied on non-local raw materials which suggests they had large territorial ranges. On the other hand, LSA occupants at Soit Nasera appear to have been more sedentary potentially as a result of being tethered to a purported semi-permanent water source although their use of non-local raw materials may have been embedded within planned resource forays similarly to the occupants at Lukenya Hill (Barut 1994).

Merrick and Brown (1984) characterise fifty-four obsidian sources in Kenya and Tanzania to successfully provenance approximately 1,400 obsidian lithics from thirty-two localities. Artifacts from five MSA sites were analysed, namely Cartwright, Wetherall, Lukenya Hill, Muguruk, and Songhor. To this day, these sites have not been radiometrically dated but are relatively dated to the MSA and MSA-LSA transition by techno-typology (Tryon and Faith 2013). Using a combination of X-ray spectroscopy for geological material and electron microprobe analysis for artifacts, Merrick and Brown (1984) found that fifty lithics from Cartwright were obtained from sources 5-35 km away, with most of the obsidian stemming from an outcrop 16 km away. Astonishingly, forty-seven lithics from Wetherall were obtained from nine individual sources between 12-45 km away. Lithic artifacts from two stratigraphic horizons at Lukenya Hill revealed that obsidian was obtained from individual sources between 6-130 km, with thirty pieces sourced >100 km away. Two artifacts from Muguruk revealed that obsidian was obtained from two outcrops between 185-190 km while one artifact from Songhor was sourced 145 km away. Overall, Merrick and Brown (1984) demonstrate that by the MSA, hominins began to obtain a small component of their lithic raw materials from increasingly distant sources up to 190 km away.

In the second half of their study on obsidian sourcing in Kenya and northern Tanzania, Merrick et al. (1994) present their results for MSA sites. Of particular interest are the results from Soit Nasera and Mumba, two key MSA-LSA sites in Tanzania. Nine obsidian pieces from the former were subject to microprobe analysis and compared with a refence collection which revealed that these were obtained from three individual sources between 230-240 km away. Analysis on fourteen obsidian artifacts from the 130-100 Ka facies at Mumba revealed that hominins obtained these raw materials from a single source 305 km away. These results reinforce the conclusions drawn by the authors in their previous study (Merrick and Brown 1984) that by the MSA, hominins began to procure small amounts of raw materials from increasingly distant sources in comparison with the ESA (Merrick et al. 1994).

Chapter 3.2.1

Discussion

Based on this literature review, the MSA record indicates that the emergence of innovative lithic technologies was approximately coeval with distant raw material procurement, and an increased reliance on diverse raw materials, particularly obsidian. Unlike the African Acheulean in which artifactual material procured from sources >10 km away was usually transported as finished pieces (Féblot-Augustins 1990), MSA obsidian artifacts in the Olorgesailie paleobasin suggests that this material was knapped on-site (Brooks et al. 2018). By approximately 200 Ka, hominins increased their exploitation of distant obsidian raw material, to an extent unseen among earlier MSA and ESA assemblages (Blegen 2017). The preponderance of obsidian exploitation in the MSA may be explained by a variety of reasons, including this material's mechanical qualities ideally suited for the manufacture of smaller, retouched implements atypical of the ESA, albeit with less durable edges, and the technical skills of hominins (Wadley and Kempson 2011).

Chapter 3.2's focus on kilometric distances between site and source, and the focus on exotic raw materials often comprising a low percentage of a lithic assemblage, is meant to highlight the fact that by the MSA, hominins became increasingly reliant on non-local resources. This is perhaps best exemplified by the archaeology at White Paintings Shelter in present-day Botswana where its occupants diachronically exploited the same outcrops between 220-300 km away for raw materials (Nash et al. 2013). Considering the challenging environment of the Kalahari Desert, continuous distant raw material procurement by the site's occupants suggests that there may have been a high continuity in ecological knowledge, as well as a greater hinge on faraway ecological resources and wider social networks. Analogous to the former point are the regional similarities in artifact types between Kone and Porc Epic and evidence for obsidian circulation from the former to the latter (Negash and Shackley 2006). This may indicate that Porc Epic was frequented by hominins who occupied Kone, or at the very least, an ecological connection and a reliance on distant resources. Likewise, hominins at Laetoli, Lukenya Hill, Soit Nasera, and Mumba relied on both local and non-local raw materials which is suggestive of a diversified economic supply (Adelsberger et al. 2011; Mehlman 1977; Merrick and Brown 1984; Merrick et al. 1994).

Altogether, the MSA record signals a profound shift in hominin behaviour which may have been characterised by higher mobility, inter-group exchange networks, and/or territorial resource control. From an evolutionary perspective, it may be that sheer distance to resources and/or peoples was a critical factor that heightened the pace of evolutionary forces, and systems of genetic, phenotypic, ecological, cultural, and material inheritance. As one example from a recent study, Roberts (2016) outlines Material Engagement Theory and brain metaplasticity to contend that among other behavioural residues, long-distance raw material procurement impacted the development of human cognition in the Late Pleistocene. Roberts (2016) argues that hominin

minds, particularly from 100 Ka onwards, became increasingly “engaged” with the properties of distant lithic raw materials, their spatial affinity, and their ornamental significance. Clearly, the prospects of raw material provenance studies are great. Such studies not only possess the ability to extend our understanding for the transport distances of stone between source and site, but also the paleoecological and social connections that are most evident in the MSA but may have been active on a finer-scale in the Olduvai paleobasin where there was an immediate quantity and quality of lithic raw materials. In this sense, characterisation and provenance studies at Olduvai withhold a tremendous opportunity to nuance our understanding of early hominin ecological and social behaviour.

Chapter 4

Olduvai Gorge, Tanzania

Olduvai Gorge is a paleoanthropological complex in northern Tanzania within the NCA. Since 1979, the NCA has been recognised as a UNESCO World Heritage Site and is acclaimed for its iconic wildlife, stunning geotourism, and sedimentary deposits that encase evidence of hominin biological and technological evolution (Leakey 1971). Lesser-known is that the NCA is inhabited by resilient Maasai pastoral communities that have occupied the area since historical times (Hodgson 2011). Despite their long-term residence in the area, the Maasai have not been actively engaged with paleoanthropological research in the Olduvai region for a variety of reasons (Lee 2018; Lee et al. 2019). This relationship's legacy is perhaps best epitomised by the fact that *Oldoway* or *Olduwai* or *Olduvai* (see Leakey et al. 1933; Leakey 1959a, b) is a misspelling of *Oldupai*, the Maasai toponym given after the burgeoning growth of the *Sansevieria ehrenbergii* plant. Despite *Olduvai* not being the correct spelling, it has and will continue to be used throughout this thesis since it has prevailed in scientific literature.

Chapter 4.1

History of Archaeological and Geological Research

The German entomologist Wilhelm Kattwinkel "discovered" Olduvai Gorge in 1911, and two years later, Hans Reck visited the paleoanthropological complex where he established the stratigraphic nomenclature and excavated a human burial (Hay 1990; Leakey 1978). In 1931, accompanied by Louis Leakey, Arthur Hopwood, Donald MacInnes, and Vivian Evelyn Fuchs, Reck returned to Olduvai to confirm its paleoanthropological potential which led to the discovery of Acheulean handaxes near Geolocality 6 and 7. In November 1931, the same team along with Edmund Teale visited the site where Reck had excavated a burial and subsequently published a

report to support the initial claim that it was of Bed II age (Leakey et al. 1931) but it was later shown to be of Late Pleistocene age (Boswell 1932; Leakey et al. 1933; Leakey 1974; Matu et al. 2017; Protsch 1974).

In 1932, Leakey visited Olduvai with Edward Wayland who mapped the stratigraphy which correlated with later studies (Leakey 1978). Three years later, accompanied by Peter Bell, Peter Kent, then Mary Nicol, and Stanhope White, Leakey led Olduvai's first paleoanthropological survey in the Side Gorge and excavations were undertaken at Geolocality 92 (Leakey 1984). In 1941, Louis Leakey and Anthony Arkell excavated a site informally known as "Black Rock" near the Second Fault where they discovered chert and obsidian artifacts (Leakey 1974). In 1947, Louis Leakey organised and directed the first Pan-African Congress of Prehistory, a watershed event in the history of African paleoanthropology. Afterwards, Leakey led congress participants on a tour of regional sites which included a visit to Olduvai (Leakey 1974; Leakey 1984). In late 1950, Louis and Mary Leakey established a camp on the south side of the Main Gorge and conducted surveys and excavations in the Side Gorge (Leakey 1974). In 1951, the Leakeys together with Charles Boise visited Olduvai and established a programme of excavations that were to begin the following year (Leakey 1974). In both 1956 and 1957, Ray Pickering mapped Olduvai's stratigraphy and regional geology (Pickering 1958, 1960).

On July 17th 1959, Mary Leakey discovered hominin fossils at Geolocality 45 that were eponymously named after Charles Boise ((*Paranthropus*) *Zinjanthropus boisei*) (Leakey 1959b). Official excavations at the site were temporarily halted until film producers, Armand and Michaela Denis, and their cameraman, Des Bartlett, arrived to capture the scenes. The original plan was to have the incoming film-crew record excavations at an entirely different site but prior to their arrival, Mary Leakey made the momentous discovery (Leakey 1984). In August 1959, Ray

Pickering dug a test pit at Geolocality 45a where he discovered stone tools and what were later believed to be butchered faunal remains of anthropogenic origin (Leakey 1971, 1979). In nearby excavations, the Leakeys discovered hominin remains of a new species, *Homo habilis*, that was bipedal and had a functional anatomical ability to manufacture stone tools (Leakey et al. 1964; Wood 2014). From 1958 to 1961, Jack Evernden, Garniss Curtis, and Louis Leakey collected samples from Geolocality 45 to conduct pioneering K-Ar radiometric dating. The resulting date of 1.75 Ma provided a *terminus ante quem* for the hominin and faunal remains found alongside stone tools (Leakey et al. 1961; Leakey 1984). From 1960 onwards, the National Geographic Society funded the Leakeys which increased Olduvai's media coverage and touristic attraction. As a result, three years later, Mary Leakey set out to build protective sheds that were later replaced by stone buildings to serve as viewing halls for tourists to witness *in situ* artifacts (Leakey 1979). Between 1961 and 1962, Maxine Kleindienst conducted excavations at the site known as JK where she excavated an important number of stone tools and faunal remains in Bed III (Hay 1990; Kleindienst 1964, 1973). In 1962, John Waechter conducted excavations at HEB where he discovered Acheulean handaxes, some of which were manufactured on phonolite believed to have been sourced directly from Engelosin (Leakey 1984).

By 1968, the Leakeys shifted their research programme at Olduvai to the uppermost sedimentary units (Leakey and Roe 1994). Within this framework, Mary Leakey conducted new excavations at JK where she unearthed stone tools and faunal remains pene-contemporary with *Homo erectus* remains, as well as pits and channels that were believed to be of anthropogenic nature (Day and Molleson 1976; Leakey 1979, 1984, 1994a; Morell 1995) but may alternatively be interpreted as aquatic craniate nests. In collaboration with Tanzania's Division of Antiquities,

Mary Leakey erected a museum to preserve these features for permanent display (Richard Leakey, personnel communication 2018) which eventually fell into disuse and is now largely dismantled.

Throughout their years of research at Olduvai, the Leakeys collaborated with other researchers resulting in a large corpus of published material (CODI 2017). Most notable are Gentry's (1966, 1967) studies on mammalian fossils, Gentry and Gentry's (1969, 1978a, 1978b) studies on fossil camelids and bovids, Susman and Stern's (1982) study on the functional morphology of *Homo habilis*, and Rightmire's (1980) description of hominin cranial, dental, and mandibular remains. The most comprehensive geological study of Olduvai was carried out by Richard Hay who first visited the paleoanthropological complex in 1962 and later published a seminal volume (Hay 1976). Hay (1976) demonstrated that a saline alkaline paleolake existed during Bed I which fluctuated to a smaller size during Bed II. By Bed III, the paleolake disappeared and gave way to small braided streams draining into a playa lake. Bed IV was characterised by major meandering streams and small ponds with the drainage sump slowly shifting southeast. One of Hay's key contributions was to correlate Olduvai's sedimentary units and layers which proved a difficult task considering the gorge had undergone faulting and erosion. In so doing, it allowed Hay to contextualise lithic assemblages with their paleogeographical discard locations. Hay (1976) found that Oldowan-bearing sites were usually situated near the paleolake while Acheulean-bearing sites were situated near fluvial channels, a paleogeographic correlation that continues to guide current paleoanthropological research (Domínguez-Rodrigo et al. 2014).

In 1971 and 1972, James O'Neil conducted $^{18}O/^{16}O$ isotope studies on chert nodules from Bed I and II, as well as from other nearby localities (O'Neil and Hay 1973) based on a corpus of earlier publications (Eugster 1967, 1969; Hay 1968) seeking to determine the petrogenesis of chert. Daniel Stiles later conducted similar analyses on chert artifacts from Geolocality 88a, a site that

was originally excavated by Marie-Louise Harms following its discovery in July 1968 (Stiles et al. 1974).

Paleomagnetic studies were also undertaken at Olduvai to bracket polarity events and further contextualise paleoanthropological studies. Within this framework, it was found that the normal polarity Olduvai Event occurred between approximately 1.9-1.6 Ma (Grommé and Hay 1963) with a later study refining its vertical stratigraphic extent (Brock and Hay 1976). In 1972, Allen Cox initiated a focused search to locate the Matuyama-Brunhes Boundary, dated to 0.78 Ma (Spell and McDougall 1992), as previous studies suggested that it correlated with the interval between Bed III and IV (Brock et al. 1972; Brock and Hay 1976).

By the late 1970s, Mary Leakey shifted her focus on Laetoli, a paleoanthropological complex approximately 40 km southwest of Olduvai. There, her team unearthed a series of bipedal hominin footprints preserved in 3.6 Ma volcanic ash believed to have erupted from Sadiman (Leakey and Harris 1987; but see Zaitsev et al. 2011). In 1977, the Pan-African Congress of Prehistory was once again taken on a similar tour as in 1947 but this time led by Mary Leakey and comprised of stop-overs at both Olduvai and Laetoli (Leakey 1984). In 1984, the proprietary of Mary Leakey's camp at Olduvai was formally handed over to Tanzania's Division of Antiquities to serve the same function for new incoming research teams.

From 1985 to 1988, research at Olduvai was led by Donald Johanson where he discovered a partial *Homo habilis* skeleton at Dik Dik Hill, approximately 250 m southeast from the find spot of *Paranthropus boisei* (Johanson et al. 1987). In 1989, Robert Blumenschine and Fidelis Masao initiated OLAPP with its stated goals to further paleoanthropology's understanding of Oldowan hominin behaviour using an ecological-landscape approach (Blumenschine et al. 2012a). OLAPP conducted fieldwork annually apart from a government-imposed moratorium which lasted from

1990 to 1993 and excavated approximately 20,000 lithics, 25,000 vertebrate fossils, and led to the discovery of nine hominin remains (CODI 2017). In 2006, the still active OGAP was initiated seeking to understand Bed II's paleoenvironmental context for hominin biological and technological evolution during which there is a transition from Oldowan to Acheulean technology associated with the emergence of *Homo erectus*. In 2006, the still active TOPPP was also initiated at which point its members undertook taphonomic studies on fossil collections that were excavated by the Leakeys. Their studies showed that the only site whose faunal remains had been almost exclusively the by-product of hominin agency was where the *Paranthropus boisei* remains were discovered while faunal remains from other sites were primarily carnivore accumulations, background scatters, and palimpsests (Domínguez-Rodrigo et al. 2007). In 2010, the still active OVPP was launched with its stated goal to systematically recover fossils which resulted in the discovery of new hominin remains (Reiner et al. 2017). OVPP has also developed and launched an online platform (CODI) that contains metadata on fossil and artifact collections from Olduvai. In 2014, a team led by Julio Mercader initiated a new research programme at Olduvai and conducted excavations under a mobile cleanroom at Bed I and II sites. In 2017, Julio Mercader initiated the multi-disciplinary SDS project with its stated goals to elucidate the relationships between paleoenvironments, lithic technologies, dietary trends, and hominin sociality. Based on this history of research spanning over a century, Olduvai constitutes as one of the best studied paleoanthropological complexes on the entire African continent and will certainly continue to yield important information about our distinctly hominin past for years to come.

Chapter 4.2

Sedimentary Sequence and Geochronology

Olduvai Gorge was an endorheic basin that once hosted a saline alkaline lake fed by stream networks draining the NVH and characterised by abrupt metamorphic inselbergs (Hay 1976). Sedimentation was interrupted by two major faulting events occurring at 1.6 and 1.2 Ma imprinted onto an earlier episode, with the latter of the two causing a reversal in the drainage direction from east to west, to west to east (Hay 1976; Stollhofen and Stanistreet 2012). The second localised faulting event at Olduvai is correlated to the regional faulting of the Natron-Manyara half-graben (Dawson 2008; Hay 1976). Olduvai's faults trend northeast-southwest following the same direction as the Eyasi-Wembere half-graben (Dawson 2008). Erosional activity from the watercourses draining into the Olbalbal Graben over the last 400 Ka incised the two branches that make up Olduvai Gorge.

The Main Gorge is approximately 46 km long and extends from west to east, while the Side Gorge is approximately 18 km long extends from the southwest to the northeast (Figure 4.2.1). The seasonal Olduvai River flows eastward through the Main Gorge from its source in Lake Masek and Ndutu. The confluence between the Main and Side Gorges occurs between the FLK and Second Faults where the Side Gorge's seasonal Enjoroi stream connects with the seasonal Olduvai River approximately 10 km prior to draining in the Olbalbal Graben. In the western Main Gorge, the sedimentary units are underlain by the Neoproterozoic Mozambique Belt while to the east, they are underlain by igneous rocks primarily from Ngorongoro (Hay 1976; Mollel and Swisher 2012). In the eastern Main Gorge, the exposed Ngorongoro basalt reaches a maximum thickness of approximately 15 m between Geolocality 40 and 41 (Hay 1976).

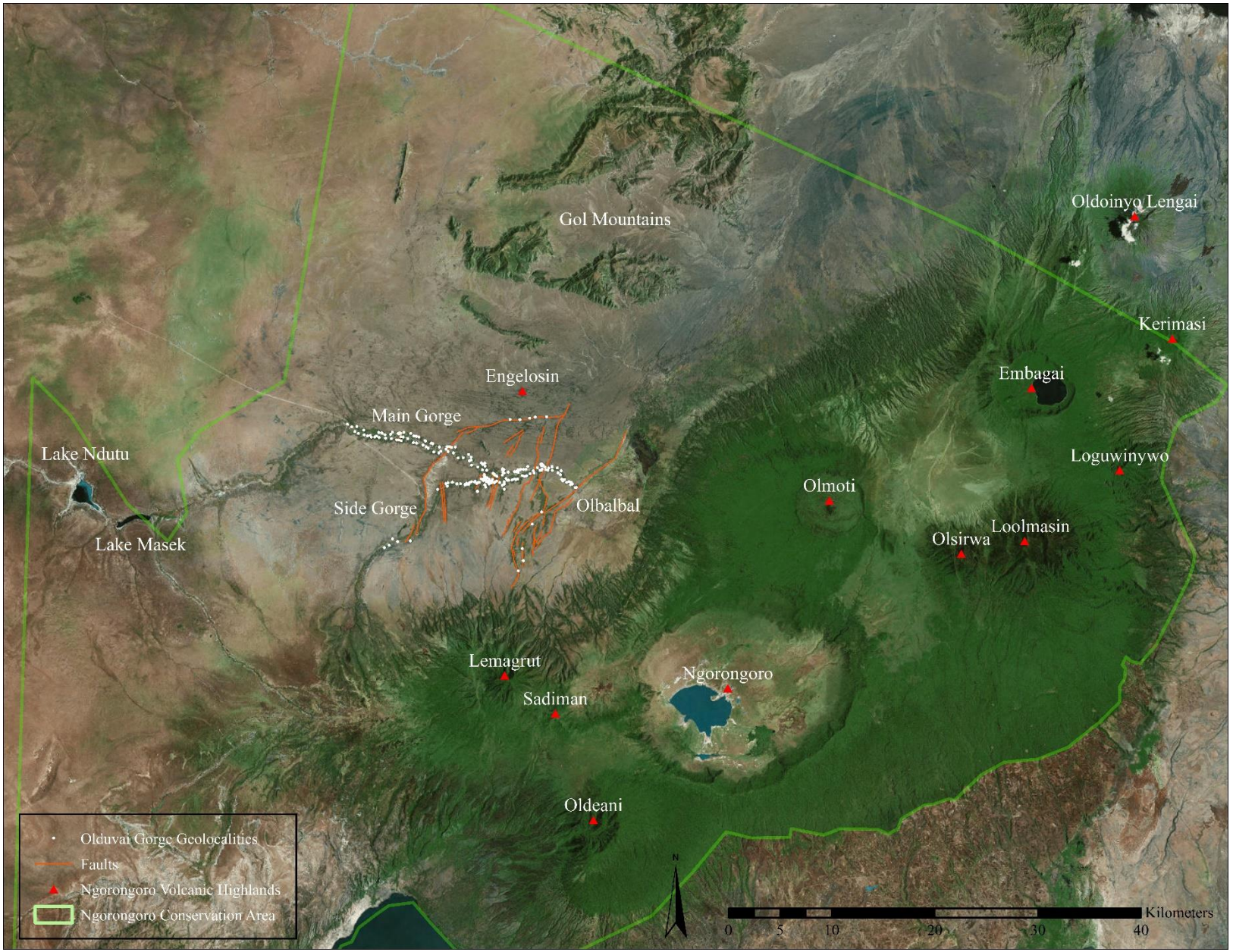

Figure 4.2.1. The greater Olduvai Gorge region. Geolocalities and faults after Hay (1976). Basemap source: Esri, DigitalGlobe, GeoEye, Earthstar Geographics, CNES/Airbus DS, USDA, USGS, AeroGRID, IGN, and the GIS User Community.

The sedimentary sequence from oldest to youngest includes Bed I (>2.038-1.803 Ma), Bed II (<1.803-1.338 Ma), Bed III (1.33-0.8 Ma), Bed IV (0.8-0.6 Ma), the Masek Beds (0.6-0.4 Ma), the Ndutu Beds (0.4-0.032 Ma), the Naisiusiu Beds (22-10 Ka), and Holocene deposits (Table 4.2.1) (Deino 2012; Habermann et al. 2016; Hay 1976).

Bed I (>2.038-1.803 Ma) includes all stratigraphic units from the Orkeri Ignimbrite to Tuff IF (Habermann et al. 2016; Hay 1976:29-54). Bed I sediments are sub-divided into five main lithofacies including lava flows, lake deposits, lake margin deposits, alluvial fan deposits, and alluvial plain deposits (Hay 1976). Bed I contains the lowermost extent of the Olduvai Subchron, a period of normal polarity within the Matuyama Reversed Polarity Chron (Brock and Hay 1976; Grommé and Hay 1963; Tamrat et al. 1995). During Bed I, the saline alkaline paleolake was its biggest occupying an area between a fault near Geolocality 56 and the FLK Fault. The paleolake was fed by networks of streams principally originating from the NVH to the southeast.

Bed II (<1.803-1.338 Ma) includes all stratigraphic units from the Twiglet Tuff to Tuff IID and are inter-stratified by the Lemuta Member, the Augitic Sandstone, and the Bird Print Tuff (Hay 1976:55-114). Lower Bed II includes all units below the Lemuta Member and is characterised by major faulting events. These sediments are sub-divided into lake deposits, lake margin deposits, alluvial fan deposits, and aeolian deposits (Hay 1976). The uppermost extent of the Olduvai Subchron lies below the Lemuta Member (Brock and Hay 1976; Grommé and Hay 1963; Tamrat et al. 1995). Middle and Upper Bed II overlie the faulting disconformity and their sediments are both sub-divided into lake deposits, eastern and western fluvial-lacustrine deposits, and fluvial deposits. During Bed II, the extent of Olduvai's paleolake fluctuated to a gradually smaller size.

Bed III (1.33-0.8 Ma) includes all stratigraphic units from Tuff 1 to 4 (Hay 1976:115-132). The sediments mainly consist of characteristic red volcanic detritus from the southeast deposited

on an alluvial plain. These are sub-divided into eastern fluvial deposits, western fluvial deposits, and fluvial-lacustrine deposits (Hay 1976). During the early deposition of Bed III approximately 1.2 Ma, Olduvai's paleolake disappeared and gave way to small braided streams draining into a playa lake located northeast of Bed I and II's paleolake. The Matuyama-Brunhes Boundary is dated to 0.78 Ma and marks the transition from a reversed polarity chron to a normal polarity chron, and approximately coincides with the Bed III and IV interval (Brock et al. 1972; Brock and Hay 1976; Spell and McDougall 1992).

Bed IV (0.8-0.6 Ma) includes all stratigraphic units above Tuff 4 (Bed III) and below the Lower Unit (Masek Beds) and contains two marker tuffs known as Tuff IVA and IVB (Hay 1976:115-132). Bed IV principally consists of metamorphic sediments from the north and west as well as volcanic detritus from the southeast. The sediments are sub-divided into eastern fluvial deposits, western fluvial deposits, and fluvial-lacustrine deposits (Hay 1976). Major meandering streams and small ponds characterised Bed IV while the drainage sump progressively shifted southeast due to regional tilting (Dawson 2008: Hay 1976; Mees et al. 2007).

The Masek Beds (0.6-0.4 Ma) are sub-divided into a Lower Unit with two marker tuffs and an Upper Unit alternatively named the Norkilili Member (Hay 1976:133-145). The lowermost unit primarily consists of aeolian tuff and detritus that are sub-divided into eastern fluvial deposits, western fluvial deposits, and aeolian deposits (Hay 1976). The Norkilili Member's sediments mainly consist of aeolian tuff (Hay 1976). The Masek Beds were the last sedimentary units deposited prior to the incision of the gorge's two branches after approximately 400 Ka. These units also bear evidence of regional faulting evidenced by unconformable stratigraphy. The paleoenvironment likely resembled that of Bed III and IV.

The Ndutu Beds (0.4-0.032 Ma) are sub-divided into a Lower and Upper Unit each containing a single marker tuff (Hay 1976:146-159). The Lower Unit consists of sandstone, conglomerates, and tuff while the Upper Unit primarily consists of aeolian tuff (Hay 1976). During the deposition of both units, aeolian, fluvial, and colluvial sediments were complexly inter-fingered as the gorge underwent faulting and erosion. The climate was semi-arid, and the Olduvai River flowed seasonally but more continuously than the present day.

The Naisiusiu Beds (22-10 Ka) consist of aeolian tuff and one thin calcareous horizon (Hay 1976:160-165). The Olduvai River continued to flow during the deposition of these beds and the climate was wetter and cooler than the present day.

During the Holocene, the gorge underwent erosion and fluvial sedimentation (Hay 1976:166-174). In the present day, Holocene and Pleistocene sediments are being eroded and transported into the modern drainage sump known as the Olbalbal Graben. The uppermost Holocene sequence contains a stratigraphic marker known as the Namorod Ash that erupted from Oldoinyo Lengai and is dated to approximately 1,250 years BP (Hay 1976). In the present day, the Olduvai River is seasonal, and the climate is semi-arid.

Table 4.2.1 Stratigraphy and Geochronology of Olduvai Gorge							
Epoch	**Sedimentary Units**	**Sub-divisons**	**Marker**	**Marker Dates**	**Bracketing and Other Dates**	**Polarity Event[2]**	**Polarity Epoch[2]**
Holocene			Namorod Ash	1,250 BP	17,550 ± 1,000 - 10,400 ± 600 Ka	C1n 0.78 Ma	Brunhes (C1n)
Pleistocene	Naisiusiu Beds		Unnamed marker tuff		22,000 - 15,000 Ka		
	Ndutu Beds	Upper Unit	Unnamed marker tuff		60,000 - 32,000 Ka		
		Lower Unit	Unnamed marker tuff	129,000 ± 4,000*y* Ka	400,000 - 60,000 Ka		
	Masek Beds	Norkilili Member			0.6 - 0.4 Ma		
		Lower Unit	Unnamed marker tuff				
			Unnamed marker tuff				
	Bed IV		Tuff IVB	0.7~ Ma	0.8 - 0.6 Ma	C1r.1r	Matuyama
			Tuff IVA				
	Bed III		Tuff 4		1.33 - 0.8 Ma		
			Tuff 3			Jaramillo (C1r.1n) 1.07 - 0.99 Ma	
			Tuff 2			C1r.2r	
			Tuff 1	1.33 ± 0.06§ Ma		Cobb (C1r.2n) 1.20 Ma	
	Bed II	Upper Bed II	Tuff IID	1.48 ± 0.05 Ma; 1.338 ± 0.024 Ma	<1.803 - 1.338 Ma	C1r.3r	
		Middle Bed II	Tuff IIC				
			Upper Augitic Sandstone				
			Bird Print Tuff				
			Middle Augitic Sandstone				
			Tuff IIB				
		Lower Bed II	Upper Lemuta				
			Tuff FLK W B	1.664 ± 0.019 Ma			
			Lower Augitic Sandstone				
			Tuff FLK W A	1.698 ± 0.015 Ma			
			Tuff IIA	1.74 ± 0.03 Ma			
			Lower Lemuta				
			Twiglet Tuff				

Table 4.2.1 (continued) Stratigraphy and Geochronology of Olduvai Gorge							
Epoch	**Sedimentary Units**	**Sub-divisions**	**Marker**	**Marker Dates**	**Bracketing and Other Dates**	**Polarity Event²**	**Polarity Epoch²**
Pleisto-cene	Bed I	Upper Bed I	Tuff IF	1.803 ± 0.002 Ma	>2.038 - 1.803 Ma	Olduvai (C2n) 1.95 - 1.77 Ma	
			Tuffs between tuffs IE and IF	1.828 ± 0.005 Ma			
			Tuffs between tuffs IE and IF	1.836 ± 0.015 Ma			
			Tuffs between tuffs IE and IF	1.833 ± 0.005 Ma			
			Tuffs between tuffs IE and IF	1.831 ± 0.006 Ma			
			Kidogo Tuff				
			Ng'eju Tuff	1.818 ± 0.006 Ma			
			Tuff IE	1.831 ± 0.004 Ma			
			Tuff IE Vitric	1.837 ± 0.006 Ma			
			Tuff ID (Plagioclase)	1.854 ± 0.011* Ma			
			Tuff IC	1.832 ± 0.003 Ma; 1.848 ± 0.008* Ma			
			Chapati Tuff				
			Tuff IB	1.848 ± 0.003 Ma			
		Lower Bed I	Bed I Lavas	1.911 ± 0.016 Ma; 1.891 ± 0.010† Ma			
			Tuff above IA	2.060 ± 0.018* Ma			
			Mafic Tuff III			C2r.1r	
			Mafic Tuff II				
			Tuff IA	1.88 ± 0.05 Ma			
			Coarse Feldspar Crystal Tuff (CFCT)	2.015 ± 0.006 Ma			
			Tuff between Naabi Ignimbrite and CFCT‡	2.005 ± 0.007 Ma			
			Mafic Tuff I				
			Naabi Ignimbrite	2.038 ± 0.005 Ma			
			Orkeri Ignimbrite				

Dashed borders indicate uncertain stratigraphic division; ²=Dark grey infill indicates normal polarity, white indicates reversed polarity; ɤ=Estimate by Mehlman (1987) based on a uranium series date post-dating a tuff at Laetoli correlated with this unnamed marker tuff in the Lower Unit of the Ndutu Beds; ~=Estimate by R.L. Hay in Leakey and Roe (1994); §=Manega (1993) refers to Tuff IIIA which is presumed to represent Tuff 1 of Bed III; *=Provisional dates according to Deino (2012); †=Treatment with 7% hydrofluoric acid according to Deino (2012); ǂ=Nomenclature from Deino (2012) even though recent research has shown other inter-stratified tuff deposits; Polarity time scale and magnetic reversals based on Cande and Kent (1995); Stratigraphic units and dates compiled from Deino (2012), Diez-Martín et al. (2015), Domínguez-Rodrigo et al. (2013), Habermann et al. (2016), Hay (1976), Leakey and Roe (1994), Leakey et al. (1972), Manega (1993), and Mehlman (1987).

Chapter 4.3

Geological Setting

Tanzania is bordered by Uganda and Kenya to the north, by the Indian Ocean to the east, by Mozambique, Malawi, and Zambia to the south, and by the Democratic Republic of the Congo, Burundi, and Rwanda to the west. Tanzania has a landmass of over 945,000 km^2 and varies altitudinally from littoral zones at and below sea level to Mount Kilimanjaro rising nearly 6,000 m.a.s.l. and is acclaimed as Africa's tallest mountain. The African continent is underlain by the African Plate which is bound by the Eurasian Plate to the north, by the Arabian and Indian Plates to the northeast, by the Australian Plate to the east, by the Antarctic Plate to the south, and by the South American and North American Plates to the west. The EARS is an active intra-continental extension zone whereby the African Plate is in the process of splitting into two separate plates (i.e. Nubian and Somalian) which together with the Arabian Plate forms the Triple Junction. Rifting commenced between 45-30 Ma and formed three principal branches, namely the Ethiopian, Albertine, and Gregory Rifts (Scoon 2018). The EARS flanks the Tanzania Craton with an Eastern and Western Branch that were coeval in initial rifting (Figure 4.3.1) (Roberts et al. 2012). In this region, the Eastern Branch is alternatively known as the Gregory Rift and splays into a diffuse network of three separate segments to form a tectonic depression known as the NTDZ (Figure 4.3.1) (Baker et al. 1972; Dawson 1992). From east to west, it comprises of the Pangani graben, the Natron-Manyara-Balangida half-graben, and the Eyasi-Wembere half-graben (Foster et al. 1997). These rift structures are imprinted onto Tanzania's five main tectono-stratigraphic units comprising of Archaean cratonic rocks, Proterozoic sedimentary covers and metamorphic terranes, Neoproterozoic metamorphic rocks, Phanerozoic sedimentary basins, and Neogene volcanic rocks (Kasanzu et al. 2008), all but the penultimate are described in the following paragraphs.

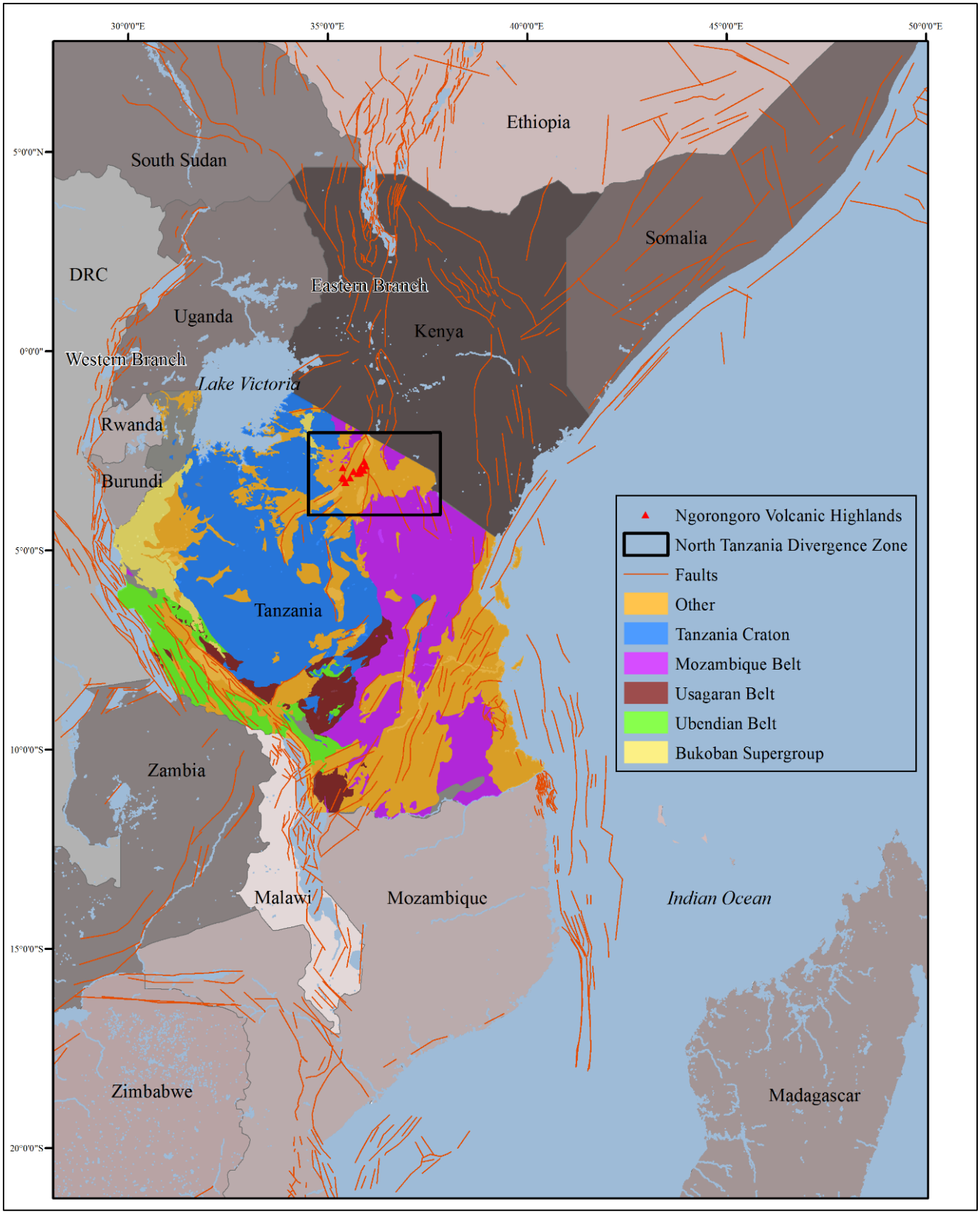

Figure 4.3.1. The East African Rift System superimposed over the Tanzania Craton, the Bukoban Supergroup, orogenic belts, and other units. Geospatial data from Fritz et al. (2013) and Macgregor (2015). See Kabete et al. (2012:Figure 5) for a detailed geological map of Tanzania. See Scoon (2018:Figure 2.2) for a simplified stratigraphic column of East Africa.

The Late Archaean Tanzania Craton is a stable continental crust consisting primarily of granitic rocks and greenstone belts. The craton is sub-divided into three main units, namely the southernmost Dodoman Belt, and the central Nyanzian and northernmost Kavirondian Supergroups (Cahen and Snelling 1966; Cahen et al. 1984; Kasanzu et al. 2008). The lowermost Dodoman Belt is characterised by a granite-migmatite terrain with high- and low-grade supracrustal metamorphic rocks and thin greenstone formations (Cahen et al. 1984; Kabete et al. 2012; Sanislav et al. 2014). The Nyanzian Supergroup is characterised by six east-west trending greenstone belts that are stratigraphically sub-divided in two lithological units. The lowermost unit is composed of metamorphic and igneous rocks while the upper unit is composed of banded ironstone and metamorphic rocks (Sanislav et al. 2014). The Kavirondian Supergroup unconformably overlies the Nyanzian Supergroup and consists of sedimentary and metamorphic rocks (Sanislav et al. 2014). The Neoproterozoic Ikorongo Group is composed of metamorphic and clastic sedimentary rocks that unconformably overly the Nyanzian Supergroup of the Tanzania Craton (Kasanzu et al. 2008). The Ikorongo Group is sub-divided into four lithological units (i.e. Makobo, Kinenge, Sumuji, and Masati) and is correlated to Bukoban Supergroup to the west (Kasanzu et al. 2008). West of the Gol Mountains in the Serengeti National Park, the meta-sedimentary Soit Ayai Group is correlated to the Ikorongo Group (Macfarlane 1969).

The Tanzania Craton is bordered by younger mobile belts, namely the Kibaran Belt to the west, the Ubendian Belt to the southwest, the Usagaran Belt to the south, and the Mozambique Belt to the east (Figure 4.3.1). The north-south trending Neoproterozoic Mozambique Belt was formed by the collision of East and West Gondwana as part of the Pan-African Orogeny between 850-550 Ma (Cahen et al. 1984; Fritz et al. 2013; Hepworth 1972; Holmes 1951; Kröner and Stern 2005). The Mozambique Belt was later uplifted starting approximately 180 Ma as a result of the

breakup of the supercontinent Gondwana (Scoon 2018). Most of the belt's folds are oriented east-west analogous to the greenstone belts of the Tanzania Craton (Hepworth 1972). Forming a portion of the Mozambique Belt, the Kenya-Tanzania Province latitudinally extends from 3° North to 10° South and is sub-divided in two lithological units. The lowermost unit consists of gneisses while the upper unit consists of limestones, schists, gneisses, quartzites, and migmatites (Cahen and Snelling 1966). The Gol Mountains in north-central Tanzania belong to the Mozambique Belt (Cahen et al. 1984; Dawson 2008; Scoon 2018), as do the metamorphic inselbergs and outcroppings to their south adjacent to Olduvai Gorge (Hay 1976).

The formation of igneous provinces in the EARS result from upwells of material from the African Superplume to the base of the lithosphere (Ebinger and Sleep 1998; George et al. 1998; Latin et al. 1993; Nyblade et al. 2000). Lithospheric drip magmatism is also known to contribute to the formation of flood basalts in the northern sector of the EARS (Furman et al. 2016). Recent studies of the central EARS's lithospheric geometry and thermo-rheological structure suggest that the juxtaposed amagmatic Western Branch and magmatic Eastern Branch results from the cratonic keel preferentially channelling plume material up the latter from a deep heterogenous mantle source while also being exposed to greater far-field tectonic stress (Koptev et al. 2016). Rift-associated volcanism initiated in Ethiopia between approximately 45-37 Ma after which strain propagation and plume material progressively migrated southwards towards Tanzania where the latter would begin to erupt approximately 8 Ma (Dawson 2008; George et al. 1998). Most of the EARS's volcanic belts are between 50-60 km wide while in the NTDZ, the Ngorongoro-Kilimanjaro transverse volcanic belt is over 200 km wide. This belt's volcanic centres are spatially aligned along four axes, namely the north-south trending Natron axis, the northeast-southwest trending Eyasi axis, the east-west trending Meru axis, and the northwest-southeast trending Chyulu

Hills axis (Le Gall et al. 2008). The NTDZ's volcanism and rift propagation occurred in five stages. Stage 1 occurred in central Kenya between 8-6 Ma, stage 2 spanned from central Kenya to Essimingor between 6-5 Ma, stage 3 spanned from the NVH to Manyara between 5-2.5 Ma, stage 4 spanned from the end of the Eyasi Trend to east of Essimingor between 2.5-1.5 Ma, and stage 5 occurred at the end of the Eyasi Trend from 1.5 Ma to the present (Le Gall et al. 2008). The splaying of the Eastern Branch occurred in a two-part diachronic event rather than as a synchronic event. The westernmost Eyasi-Wembere and Natron-Manyara-Balangida half-grabens, which are together known as the Mbulu faulted domain, formed earlier than the easternmost Pangani graben which correlates with an eastward migration of magmatism (Le Gall et al. 2008). The northeast-southwest trending Eyasi-Wembere half-graben extends from Lake Eyasi and ends against the Tanzania Craton. The north-south trending Natron-Manyara-Balangida half-graben extends from Lake Natron to the Balangida Basin, and is characterised by a 500 m-high escarpment at Lake Manyara while fading in its southern extension (Ring et al. 2005). Southeast of Kilimanjaro, the volcano-infilled Pangani graben extends from the Pangani Range in the north to the Indian Ocean (Dawson 2008; Le Gall et al. 2008). In central Tanzania, south of the NTDZ is the Manyara-Dodoma Rift segment, an active deformation zone that was heavily faulted during the latter half of a two-stage rifting model proposed for the NTDZ (Macheveki et al. 2008). Further afield, the Mikumi-Kilombero Rift represents the southern extension of the Eastern Branch where it either reconnects with the amagmatic Western Branch or continues to the Mikumi and Kilombero Depressions (Macheveki et al. 2008).

The earliest volcanic activity in the Gregory Rift is associated with the Essimingor volcano (2,165 m.a.s.l.) which was active between 8.1-3.22 Ma (Dawson 2008). To its west are the NVH, a mostly inactive group of volcanoes centred around the Ngorongoro Caldera (2.25-2.01 Ma;

1,700-2,380 m.a.s.l.) that is estimated to have been as high as 5,000-6,000 m.a.s.l. prior to collapse (Dawson 2008; Hay 1976). The NVH are bordered by the Salei Plains to the north, the Natron-Manyara-Balangida half-graben to the east, the Mbulu Plateau to the south, the Eyasi-Wembere half-graben to the southwest, and the Serengeti Plains to the west. The NVH are comprised of other major volcanoes, namely Sadiman (4.63-3.5 Ma; 2,870 m.a.s.l.), Lemagrut (2.4-2.2 Ma; 3,135 m.a.s.l.), Olmoti (2.01-1.80 Ma; 3,101 m.a.s.l.), Oldeani (1.61-1.52 Ma; 3,219 m.a.s.l.), Loolmasin (1.4-1.3 Ma; 3,648 m.a.s.l.), Olsirwa (1.4-1.3 Ma; 3,150 m.a.s.l.), Embagai (1.52-0.5 Ma; 3,235 m.a.s.l.), Kerimasi (1.10-0.08 Ma; 2,607 m.a.s.l.), Oldoinyo Lengai (150 Ka-present; 2,890 m.a.s.l.) which is the world's only active carbonatite volcano, and Loguwinywo (?-? Ma; 2,624 m.a.s.l.) (Dawson 2008; Greenwood 2014; Mollel and Swisher 2012). The isolated Engelosin (3-2.7 Ma; 1,648 m.a.s.l.) volcanic neck is geologically related to the NVH but is situated approximately 30 km northwest of Ngorongoro (Mollel and Swisher 2012).

Olduvai Gorge is bordered by the Gol Mountains to the north, the NVH to the southeast, and the Serengeti Plains to the west. Olduvai was an endorheic basin formed by uplift in the NVH that in its earliest sedimentary phase, hosted a saline alkaline lake (Hay 1976). Throughout its sedimentary history, Olduvai was principally fed by aeolian, fluvial, mass wasting, and pyroclastic material originating from the NVH (Hay 1976). Only five volcanic centres of the NVH drained into the Olduvai paleobasin (McHenry and de la Torre 2018), namely Sadiman (foidite, ijolite, nephelinite, phonolite, phonolitic tuff, and tephrite) (Hay 1976; Mollel and Swisher 2012; Zaitsev et al. 2012), Engelosin (phonolite and phonolitic breccia) (Hay 1976; Mollel and Swisher 2012), Lemagrut (basalt, benmorite, hawaiite, ignimbrite, and mugearite) (Mollel and Swisher 2012), Ngorongoro (agglomerate, basalt, ignimbrite, rhyolite, trachyandesite, trachydacite, and trachyte) (McHenry et al. 2008; Mollel 2002; Mollel et al. 2008; Mollel and Swisher 2012; Pickering 1965),

and Olmoti (basalt, ignimbrite, trachyandesite, and trachyte) (Hay 1976; Manega 1993; McHenry et al. 2008; Mollel 2002; Mollel et al. 2009; Mollel and Swisher 2012; Pickering 1964, 1965).

Chapter 4.4

Geological Outcrops

Outcrops in the greater Olduvai region are displayed in Figure 4.4.1, and many are named after Maasai toponyms, albeit with slightly different spellings (e.g. Engelosin versus Engilusui) (Table 4.4.1). Prior to sampling in 2017, outcrop locations and lithologies were determined based on a literature review (Table 4.4.2). The following paragraphs describe the structural geology and lithology of outcrops in alphabetical order based on field observations in 2017 and 2018.

Table 4.4.1 Place Names in the Greater Olduvai Gorge Region

English Spelling	Maa Spelling	Maa Etymology
Alamirakini Suaten	Alamirakini Suaten	A place to take fat bulls
Endonyo Okule	Endonyo Ekule	Hill of milk
Eng'amata Enqii	Eng'amata Enqii	Mountain pass
Engejuu Enquitock	Engejuu Enquitock	Where lions attack women korongo
Engejuu Ng'iro	Engejuu Ng'iro	Brown korongo
Engelosin	Engilusui	Hill that stands alone
Esinoni	Esinoni	nd (local plant?)
Gol	Gol	Hard mountains
Granite Falls	Nagolong'o	No way to pass
Irikaa	Irikaa	Dangerous place
Isilale Aratum	Isilale Aratum	Forty trees
Kelogi	Kiloki	Enjoroi stream
Kesile	Kesile	Indebted people
Koonge	Koonge	nd
Lemagrut	Makaroti	Big mountain
Lemuta	Lemuta	A place of food preparation for journey
Naabi	Naabi	One steep slope
Naibatat Hill	Naibatat Hill	Two breasts
Namorod	Namoroth	Many small stones
Ngorongoro	El Nkoronkoro	nd (gift of life (?); cattle bells (?))
Noondekei	Noondekei	Aeroplane mountain
Oittii	Oittii	Wait wait plants
Olbalbal	Olbalbal	Depression
Oldeani	Oldeni	nd (local *Acacia* plant?)
Oldoinyo Ng'ro	Oldoinyo Ng'ro	Brown cattle
Olmoti	Olmoti	Small pot
Olongojoo	Olongojoo	Better land for cattle to give birth
Orukurushashi	Orukurushashi	Plant consumed by cattle
Sadiman	Satiman	Small range for bulls
Soit Nasera	Soit Nasera	nd (may refer to prominent black stains on the inselberg or to rock art within the rockshelter (Mehlman 1977))

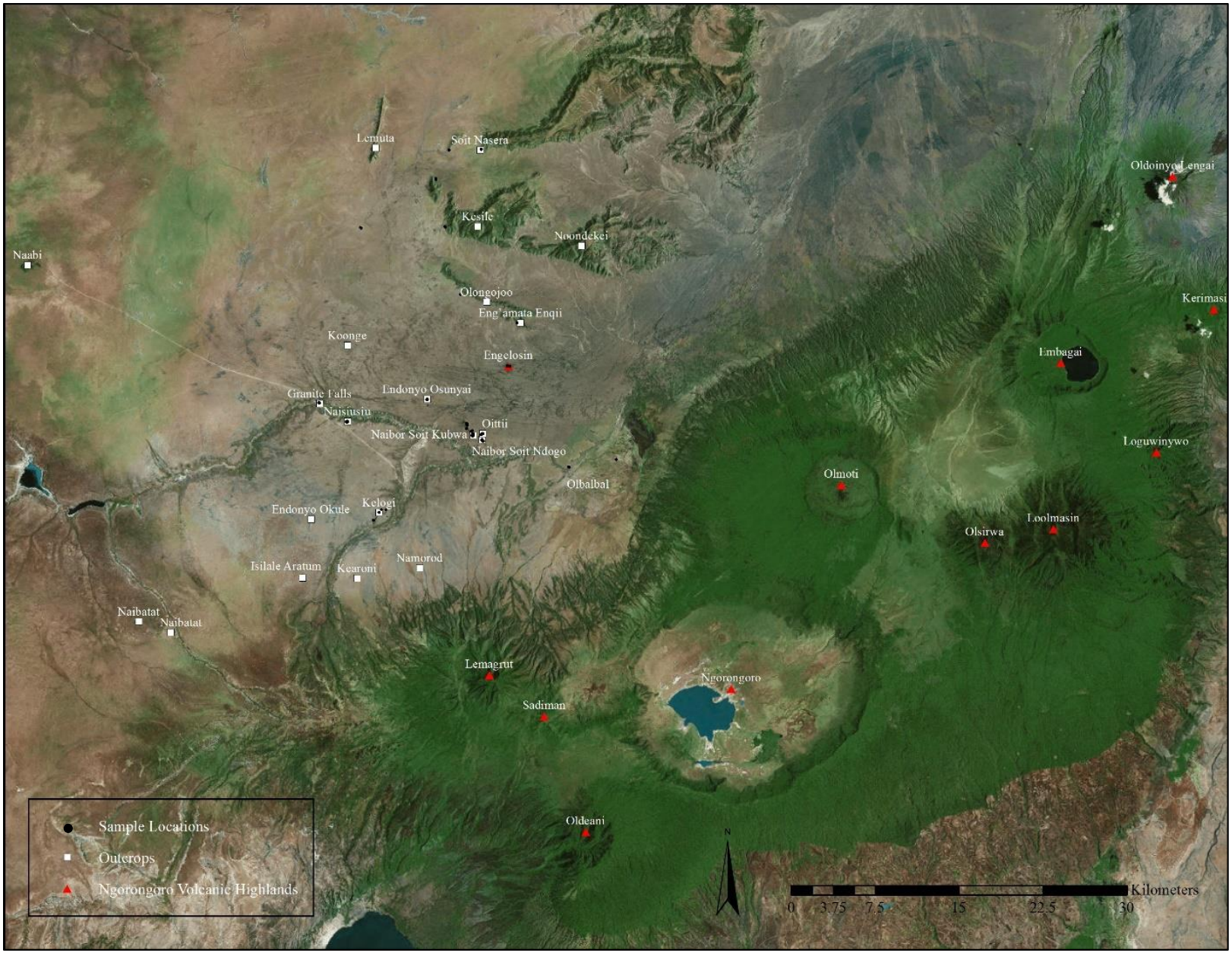

Figure 4.4.1. Geological outcrops in the greater Olduvai Gorge region and locations of samples analysed in this study. Basemap source: Esri, DigitalGlobe, GeoEye, Earthstar Geographics, CNES/Airbus DS, USDA, USGS, AeroGRID, IGN, and the GIS User Community.

Table 4.4.2 Sources/Outcrops in the Greater Olduvai Gorge Region			
Rock Type	**Source/Outcrop**	**Rock**	**Primary and Secondary References**
Igneous	Embagai	Foidite; nephelinite; phonolite; vitric lava	Greenwood 2014; Mollel 2007; Mollel and Swisher 2012
	Engelosin	Phonolite; breccia	Hay 1976; Jones 1979, 1981, 1994; Kyara 1999; Mollel and Swisher 2012; Stiles 1998
	First Stream	Detrital igneous rocks (Lemagrut)	Kyara 1999
	Kerimasi	Agglomerate; limestone; pyroclast	Dawson 1962; Hay 1976, 1983; Mollel and Swisher 2012
	Lemagrut	Basalt; benmorite; hawaiite; ignimbrite; mugearite	Hay 1976; Jones 1994; Kyara 1999; Mollel and Swisher 2012; Stiles 1998
	Namorod	Scoria	Hay 1976
	Ngorongoro	Agglomerate; basalt; ignimbrite; rhyolite; trachyte; trachyandesite; trachydacite	Kyara 1999; McHenry et al. 2008; Mollel 2002; Mollel et al. 2008; Mollel and Swisher 2012; Pickering 1965; Stiles 1998
	Oldeani	Basalt; trachyandesite	Mollel et al. 2011; Mollel and Swisher 2012; Pickering 1964, 1965
	Olmoti	Basalt; ignimbrite; trachyte; trachyandesite	Hay 1973, 1976; Jones 1994; Kyara 1999; Manega 1993; McHenry et al. 2008; Mollel 2002; Mollel et al. 2009; Mollel and Swisher 2012; Pickering 1964, 1965
	Sadiman	Foidite; ijolite; nephelinite; phonolite; tephrite	Hay 1976; Jones 1994; Kyara 1999; Mollel and Swisher 2012; Plummer 2004; Stiles 1998; Zaitsev et al. 2012
	Second Stream	Detrital igneous rocks (basalt; trachyandesite)	Kyara 1999
	Tanzania Craton	Gabbro	Hay 1976; Mollel 2002; Stiles 1991
	Third Stream	Detrital igneous rocks (basalt; phonolite; trachyandesite)	Kyara 1999
Metamorphic	Endonyo Okule	Quartzite	Hay 1976; Kyara 1999
	Endonyo Osunyai	Gneiss; quartzite	Hay 1976; Kyara 1999
	Granite Falls	Granite gneiss; detrital igneous and metamorphic rocks	Hay 1976; Kyara 1999; Tactikos 2005
	Isilale Aratum	Amphibolite; quartzite	Hay 1976
	Kearoni	Granite gneiss	Hay 1976; Kyara 1999
	Kelogi	Granite gneiss	Blumenschine et al. 2008; Hay 1976; Jones 1994; Kyara 1999; Leakey 1971; McHenry and de la Torre 2018; Plummer 2004; Santonja et al. 2014; Stiles 1991, 1998; Tactikos 2005
	Koonge	Quartzite	Hay 1976
	Naibor Soit Kubwa	Gneiss; quartzite	Blumenschine et al. 2008, 2012b; Hay 1976; Jones 1994; Kyara 1999; Leakey 1965; Santonja et al. 2014; Stiles 1998; Tactikos 2005
	Naibor Soit Ndogo	Quartzite	Jones 1994; Kyara 1999; Leakey 1965; Santonja et al. 2014; Stiles 1998
	Naisiusiu	Granite gneiss; mica schist; quartzite	Blumenschine et al. 2008; Hay 1976; Kyara 1999; McHenry and de la Torre 2018; Tactikos 2005
	Oittii	Mica schist; quartzite	Jones 1994; Kyara 1999; Leakey 1965
	Olongojoo	Quartzite	Blumenschine et al. 2008; Hay 1976; Reti 2013
	Inselberg near Eng'amata Enqii	Quartzite	Blumenschine et al. 2008; Reti 2013
Sedimentary	Fifth Fault	Chert	Hay 1976; Kyara 1999; Stiles 1998
	Geolocality 42b	Chert	Hay 1976; McHenry and de la Torre 2018; Uribelarrea et al. 2017
	Geolocality 43	Chert	Hay 1976; Kimura 1997; Kyara 1999; Leakey 1971; Stiles 1991, 1998; Stiles et al. 1974; Uribelarrea et al. 2017
	Geolocality 43a	Chert	Hay 1976
	Geolocality 45	Chert	Hay 1976; Leakey 1971
	Geolocality 78b	Chert	Hay 1976
	Geolocality 80	Chert	Berry 2012; Hay 1976; Hay and Kyser 2001; O'Neil and Hay 1973
	Geolocality 82	Chert	Hay 1976; O'Neil and Hay 1973
	Geolocality 82a	Chert	Hay 1976
	Geolocality 85	Chert	Hay 1976; O'Neil and Hay 1973

Table 4.4.2 (continued) Sources/Outcrops in the Greater Olduvai Gorge Region			
Rock Type	**Source/Outcrop**	**Rock**	**Primary and Secondary References**
Sedimentary	Geolocality 88	Chert	Hay 1976; Kimura 1997; Kyara 1999; Leakey 1971; O'Neil and Hay 1973; Proffitt 2018; Stiles 1991, 1998; Stiles et al. 1974
	Geolocality 88a	Chert	Hay 1976; Stiles et al. 1974
	Geolocality 88b	Chert	Hay 1976; Kyara 1999; Leakey 1971; Stiles et al. 1974
	Geolocality 89	Chert	Hay 1976; Kyara 1999; Leakey 1971; Stiles et al. 1974
	Geolocality 91	Chert	Hay 1976; Stiles 1998
	Geolocality 201	Chert	Hay 1976; Stiles 1998
	Geolocality 202	Chert	Hay 1976; Stiles 1998
	Olbalbal	Detrital igneous, metamorphic, and sedimentary rocks	Dawson 2008; Foster et al. 1997; Hay 1976; Mollel 2002
	Olduvai River	Detrital igneous, metamorphic, and sedimentary rocks	Hay 1976; Tactikos 2005

Endonyo Osunyai is a 100 m-long poorly exposed quartzitic and gneissic outcrop <500 m northeast of Shifting Sands (Figure 4.4.2). Most of the outcrop's quartzites dip south with some exceptions (Figure 4.4.3). The outcrop's northwestern sector bears fractured gneiss outcroppings with mostly horizontal bedding planes, and one asymmetrical fold with harmonic folding (Figure 4.4.3). Three of five samples collected from Endonyo Osunyai in 2017 were analysed for this study and whose locations are displayed in Figure 4.4.2.

Engelosin is a 150 m-high weathered and oxidised phonolitic volcanic neck >6 km north of Oittii (Figure 4.4.1). It belongs to the NVH and was active between 3-2.7 Ma (Mollel and Swisher 2012). Engelosin clasts and detritus drained into the Olduvai paleobasin in combination with sedimentary input from other volcanic centres of the NVH (Dawson 2008; Hay 1976; Mollel and Swisher 2012). Engelosin phonolite has a green to grey colour, is fine- to medium-grained, and contains a wide array of porphyritic and vesicular textures (Figure 4.4.4). In alphabetical order, this phonolite is mineralogically composed of aegirine, alkali feldspar (anorthoclase, sanidine), analcime, apatite, augite, nepheline, and titanite (Dawson 2008; Hay 1976; Manega 1993; Mollel 2007; Mollel and Swisher 2012). From the Pliocene onwards, talus accumulations along its slopes resulted in the petrogenesis of phonolitic breccia cemented by calcrete (Figure 4.4.4). Four of

twelve samples collected from Engelosin in 2017 were analysed for this study and whose locations are displayed in Figure 4.4.5.

The Gol Mountains refers to a series of primarily metamorphic inselbergs that transition northwards into a mountain range. These inselbergs begin to outcrop approximately 4 km north of Engelosin (Figure 4.4.1 and 4.4.6) and belong to the Neoproterozoic Mozambique Belt. The Mozambique Belt was orogenised between 850-550 Ma by westward thrusting against and across the Tanzania Craton resulting in a general eastward dip (Fritz et al. 2013; Hepworth 1972). These mountains were uplifted during the breakup of Gondwana starting approximately 180 Ma and this process continued into the Paleocene resulting in a highly deformed complex with vertical exposures that are typical of mobile belts (Scoon 2018). The Gol Mountains have local community-acknowledged toponyms (Table 4.4.1) and lithologically consist primarily of limestones, schists, gneisses, quartzites, and migmatites (Cahen and Snelling 1966), all of which are occasionally oxidised and capped by calcretes. During the wet season, many inselbergs are drained by streams that can transport clasts up to several kilometres away depending on gradient. The dirt roads that are next to inselbergs and bisect streams are sometimes shouldered by lustrous phyllite which originates from a northern source (personal communication, Lekaai Kisota 2018). Nine of twenty-two samples from the Gol Mountains collected in 2017 were analysed for this study and whose locations are displayed in Figure 4.4.6.

One of the most iconic inselbergs of the Gol Mountains is Soit Nasera (Figure 4.4.7), a 350 m-high quartz-feldspathic monolith (Scoon 2018) that is complexly deformed, faulted, exfoliated, varnished, and contains quartz veins and feldspar outcroppings (sample OOO1) (Figure 4.4.6). Its weakly foliated bedding planes steeply dip northeast while in some places, they are nearly vertical in a similar fashion to outcrops approximately 250 m north. There is a prominent rockshelter on

the northern face of Soit Nasera that was excavated by Louis Leakey in 1932 (Mehlman 1977), by Michael Mehlman in 1975-1976 (Mehlman 1977), and by a team led by José-Manuel Maíllo-Fernández in 2018 (personal communication, David Martín-Perea 2018). Upon sampling, faint panels of rock art were still discernible within the rockshelter along with markings from tourists since the area is a popular safari campsite (personal communication, Reuben Ngwali 2018). Southwest of Soit Nasera is an unnamed >2 km-long northeast-southwest trending quartzitic inselberg (sample PPP1) (Figure 4.4.6). Northwest of Kesile is an unnamed >2.5 km-long northwest-southeast trending quartzitic inselberg (samples RRR1 and SSS1) (Figure 4.4.6). An unnamed metamorphosed granitic inselberg west of Kesile bears partly exfoliated, faulted, and varnished outcroppings while the preserved bedding planes dip east (sample JJJ1) (Figure 4.4.6 and 4.4.7). Northwest of Olongojoo are unnamed low-lying poorly consolidated vertical meta-granitic outcrops with massive quartz surrounded by gently rolling hills (samples TTT1 and UUU1) (Figure 4.4.6 and 4.4.7). Approximately 30 km to their southwest is the Serengeti National Park whose entrance gate is located at the Naabi granitic pluton (Figure 4.4.1) (Scoon 2018).

Granite Falls is an extensive metamorphosed granitic outcrop of the Neoproterozoic Mozambique Belt and underlies Olduvai's sedimentary units in the western Olduvai paleobasin (Hay 1976). The outcroppings are partly exfoliated, faulted, and varnished while the preserved bedding planes are vertical and trend east-west (Figure 4.4.8). In alphabetical order, this meta-granite is mineralogically composed of biotite, microcline, muscovite, plagioclase, and quartz (Hay 1976). Since the Olduvai River flows through Granite Falls during the wet season, the riverbed also contains igneous and metamorphic clasts such as nephelinite (sample Granite Falls 3A/B) originating from Sadiman and quartzite (sample Granite Falls 4A/B) of unknown origin (Figure 4.4.8) (but see Tactikos 2005:70, 114). On the northern bank of the Olduvai River near

Granite Falls, there are granite gneiss outcroppings overlain by thick calcareous rocks. All four samples collected from Granite Falls in 2017 were analysed for this study and whose locations are displayed in Figure 4.4.9.

Kelogi refers to a series of northeast-southwest trending granite gneiss inselbergs east of the Side Gorge (Figure 4.4.10). The outcroppings are distributed over <2 km distance and are complexly deformed, faulted, exfoliated, varnished, and contain quartz and mafic veins occasionally oriented perpendicular to weak foliation planes (Figure 4.4.11). In alphabetical order, this granite gneiss is mineralogically composed of aegirine, albite, biotite, feldspar, garnet, hornblende, orthoclase, and quartz (Hay 1976; Kyara 1999). Kelogi clasts and detritus contributed to sedimentary infill of the Olduvai paleobasin during the Pleistocene (Hay 1976). Upon sampling, obsidian and chert surface artifacts were encountered at the southernmost inselberg near a collapsed rockshelter containing brightly-coloured panels of Maasai rock art (personal communication, Sumat Olenjorio 2017). Three of ten samples collected from Kelogi in 2017 were analysed for this study and whose locations are displayed in Figure 4.4.10.

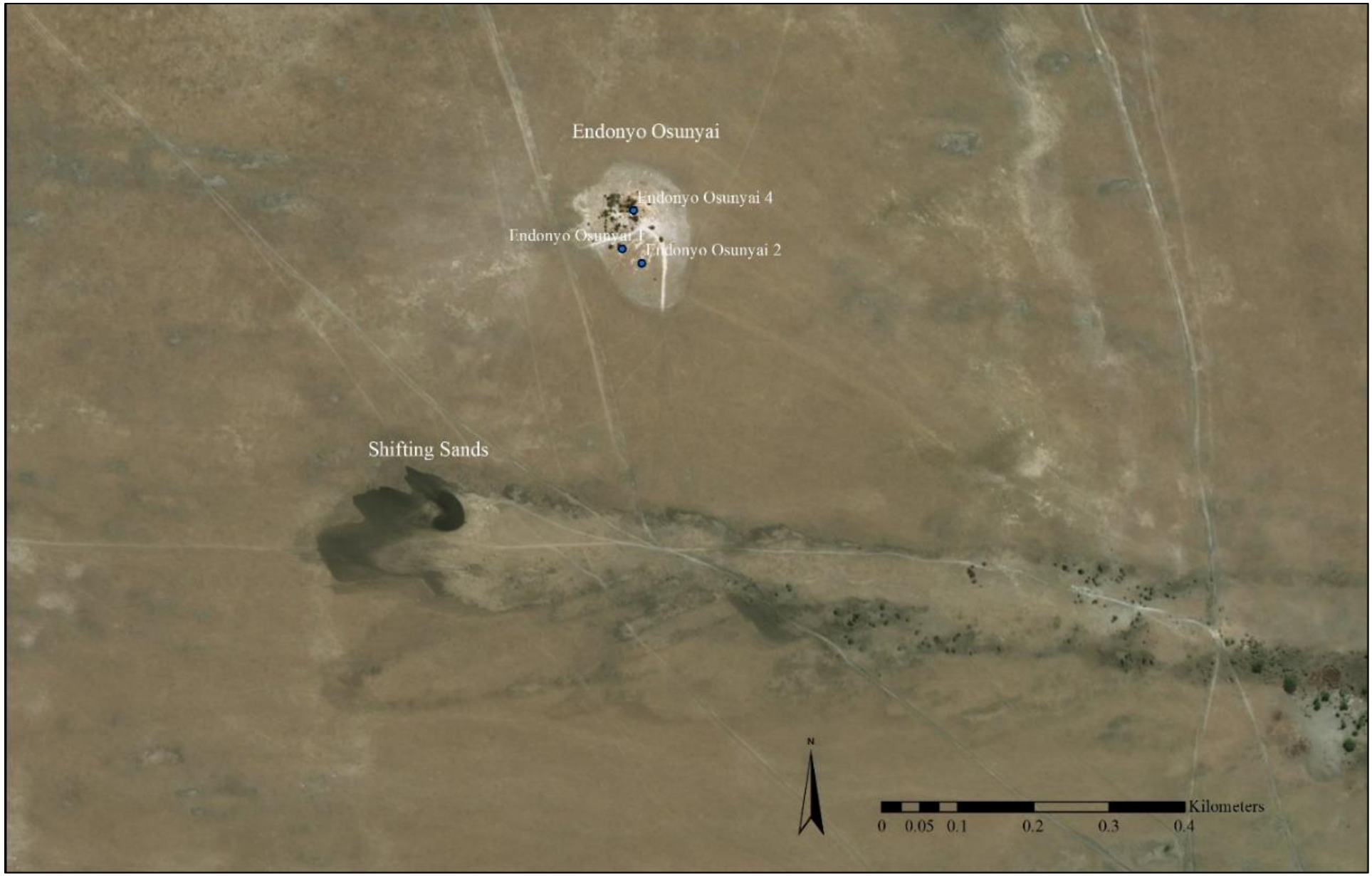

Figure 4.4.2. Endonyo Osunyai sample locations. See Figure 4.4.1 for spatial reference.

Figure 4.4.3. Endonyo Osunyai: (a) quartzites with bedding planes dipping south; (b) poorly exposed quartzitic outcroppings; (c) view south towards Shifting Sands; (d) fractured gneiss outcroppings with horizontal bedding planes and one asymmetrical fold with harmonic folding.

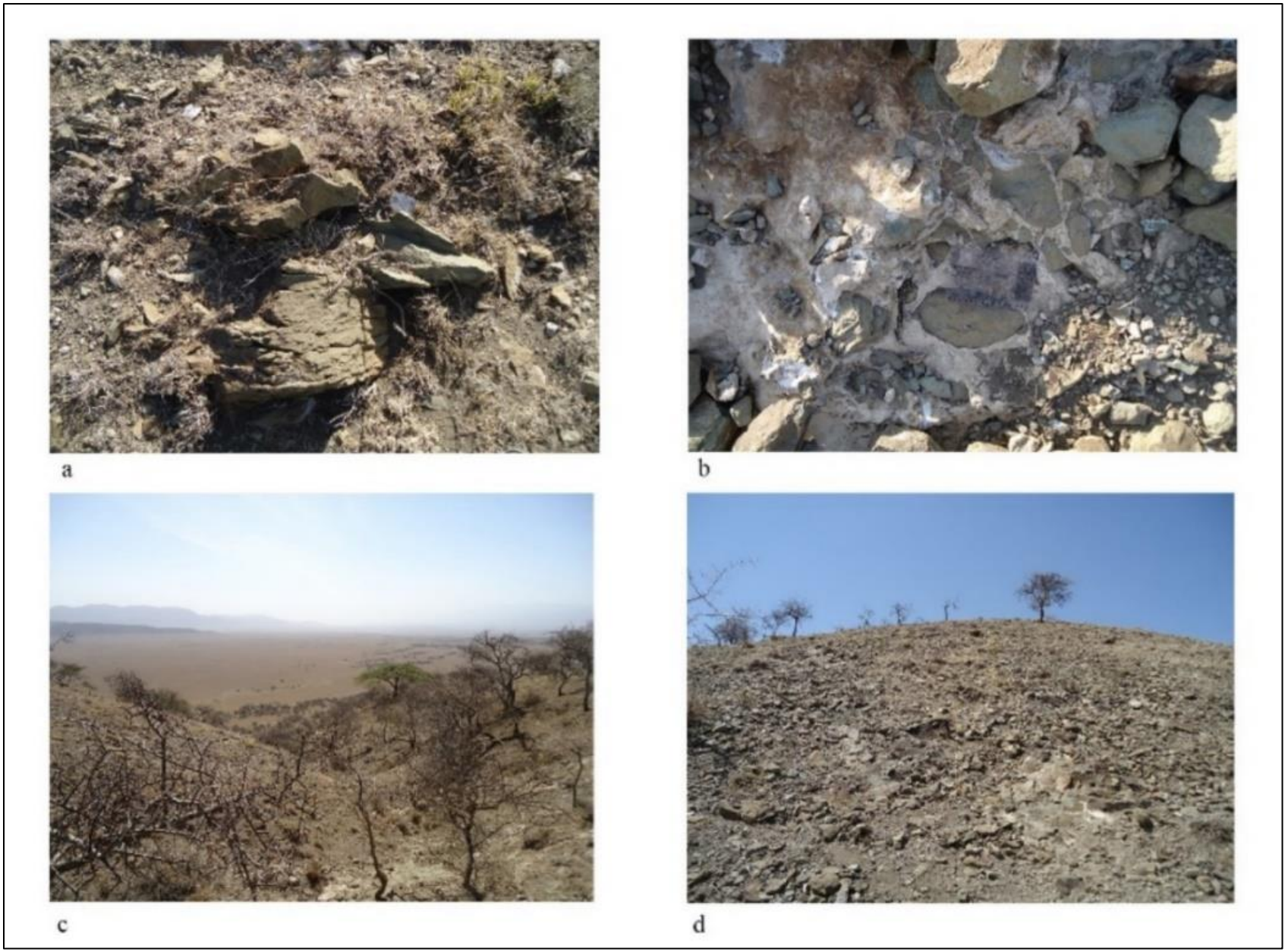

Figure 4.4.4. Engelosin: (a) weathered, oxidised, and fractured phonolite outcroppings; (b) talus accumulations of phonolitic breccia cemented by calcrete; (c) view northeast showing erosion-resistant structure of the original feeder tube; (d) dislodged phonolite blocks on the western slope.

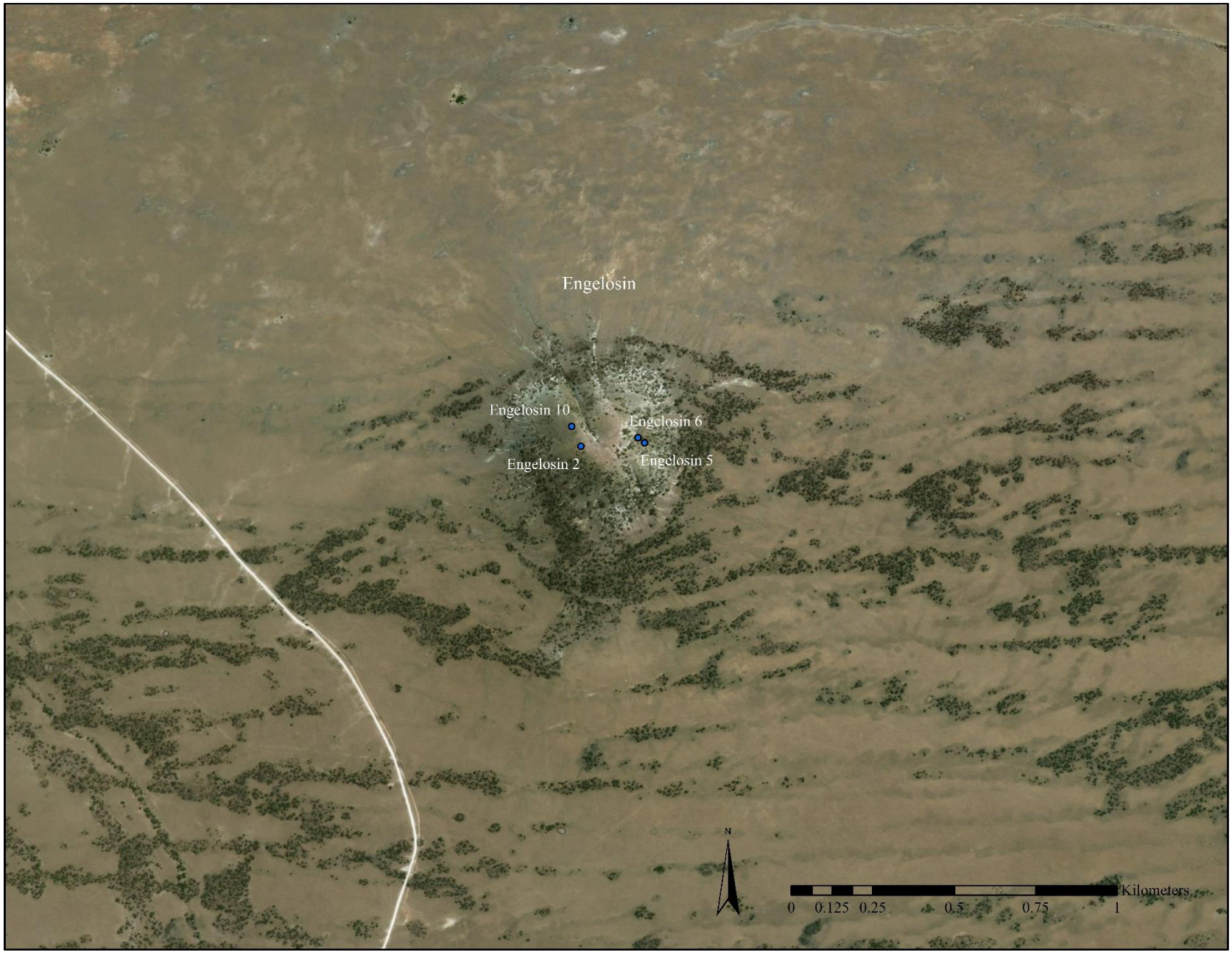

Figure 4.4.5. Engelosin sample locations. See Figure 4.4.1 for spatial reference.

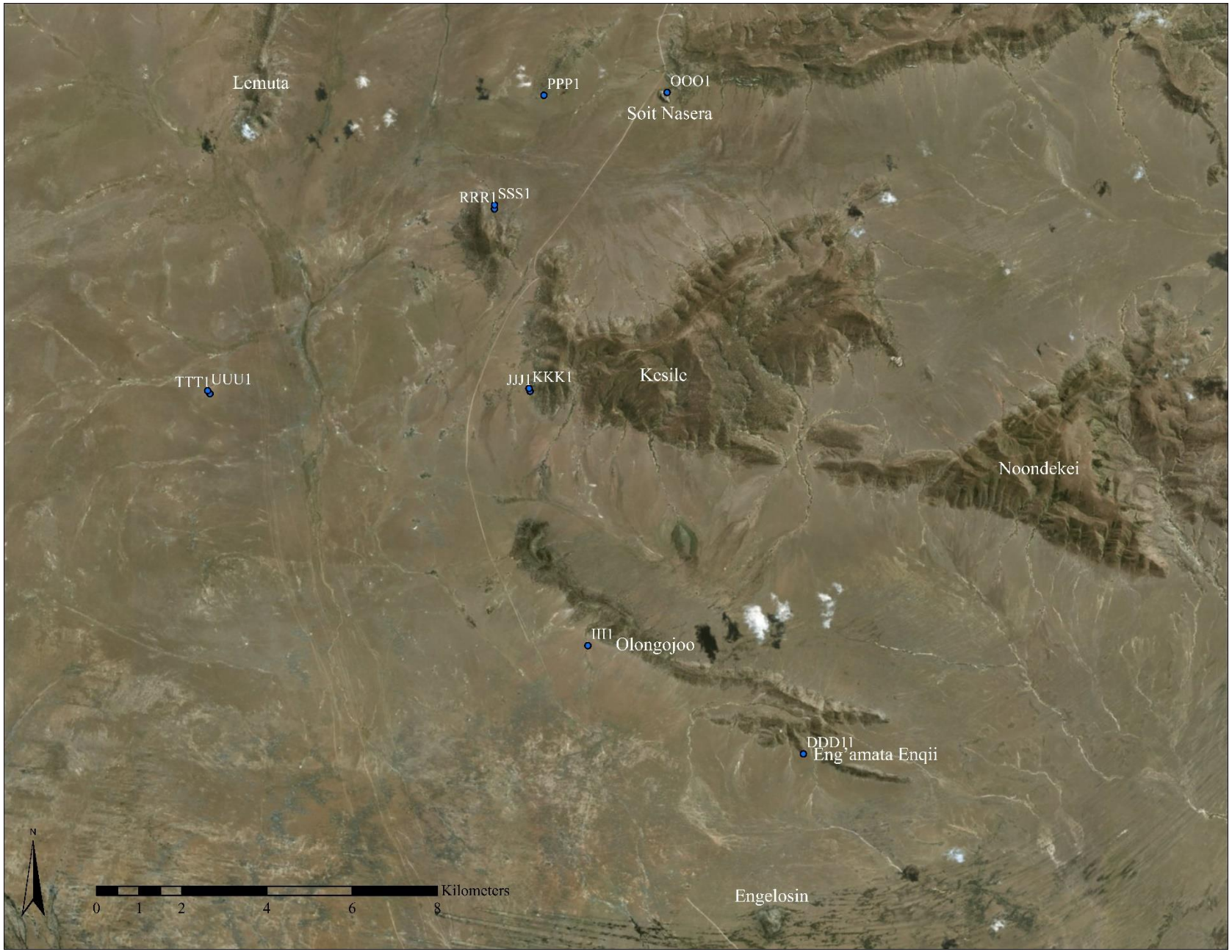

Figure 4.4.6. Gol Mountains sample locations. See Figure 4.4.1 for spatial reference.

Figure 4.4.7. Gol Mountains: (a) seasonal channel draining Olongojoo containing quartz-rich sediment and metamorphic clasts; (b) view southeast towards Eng'amata Enqii from Olongojoo; (c) west of Kesile, complexly deformed and exfoliated north-south trending granite gneiss with nearly vertical bedding planes; (d) view south towards the rockshelter at Soit Nasera which is a quartz-feldspathic monolith; (e) west of Kesile, low-lying poorly consolidated vertical granitic outcroppings; (f) west of Kesile, low-lying eroded granitic outcrop.

Figure 4.4.8. Granite Falls: (a) view east showing vertical granite gneiss forming the riverbed of the seasonal Olduvai River; (b) view west showing partly exfoliated and varnished granite gneiss outcroppings; (c) nephelinite boulder naturally deposited in the riverbed; (d) flaked quartzite in the riverbed.

Figure 4.4.9. Granite Falls sample locations. See Figure 4.4.1 for spatial reference.

Figure 4.4.10. Kelogi sample locations. See Figure 4.4.1 for spatial reference.

Figure 4.4.11. Kelogi: (a) complexly deformed, exfoliated (weathering pits), and varnished granite gneiss; (b) view southeast towards the Side Gorge, Namorod, and Lemagrut; (c) quartz and mafic vein oriented perpendicular to weak foliation planes; (d) close-up of a quartz and mafic vein; (e) view northwest showing massive granite gneiss boulders eroded from the inselberg; (f) view southwest towards the Side Gorge from the top of the southernmost inselberg.

Naibor Soit Kubwa is a <1.8 km-long northwest-southeast trending quartzitic and gneissic inselberg <700 m west of Naibor Soit Ndogo (Figure 4.4.12). Most of the low-grade metamorphic rocks dip northwest, west, or southwest (Figure 4.4.13). The outcrop principally consists of coarse- to medium-grained varieties of white, grey, orange, pink, red, and green quartzites that are occasionally oxidised, stained by organic detritus, and capped by calcretes (Figure 4.4.13). In alphabetical order, this quartzite is mineralogically composed of muscovite and quartz (Hay 1976; Kyara 1999; McHenry and de la Torre 2018; Tactikos 2005). The inselberg's clasts and detritus contributed to sedimentary infill of the Olduvai paleobasin during the Pleistocene (Hay 1976). Protruding through the quartzitic and gneissic outcroppings in the northwestern sector is a prominent amphibolite dyke with sub-parallel quartz veins (Figure 4.4.13). The northern and eastern sides of the outcrop bear sand deposits. The northern deposits are aeolian and originate from nearby barchan (mafic) sand dunes that travel westward according to prevailing winds (e.g. Shifting Sands) (Hay 1976). The eastern deposits are a combination of mafic sands and felsic erosional by-products from the outcrop. Upon sampling, one obsidian surface artifact was encountered on the eastern side of the inselberg. Sixteen of thirty-seven samples collected from Naibor Soit Kubwa between 2015-2017 were analysed for this study and whose locations are displayed in Figure 4.4.12.

Naibor Soit Ndogo is a <1 km-long northwest-southeast trending quartzitic inselberg <700 m east of Naibor Soit Kubwa (Figure 4.4.12). The westernmost quartzites steeply dip south and southwest while the easternmost quartzites steeply dip southwest and west (Figure 4.4.14). The outcrop principally consists of coarse- to medium-grained varieties of white, orange, pink, and green quartzites that are occasionally oxidised and stained by organic detritus (Figure 4.4.14). The easternmost outcroppings bear evidence of heat-induced staining. Based on structural projections,

this outcrop may have been as close as 750 m north of TK in Bed II (Santonja et al. 2014). Five of sixteen samples collected from Naibor Soit Ndogo in 2017 were analysed for this study and whose locations are displayed in Figure 4.4.12.

Naisiusiu is a low-lying <200 m-long east-west trending quartzitic, schistic, and meta-granitic outcrop approximately 3 km southeast of Granite Falls (Figure 4.4.1). The metamorphosed rocks dip southeast (Figure 4.4.15). The top and northern sides of the outcrop host higher numbers of outcroppings than the southern and eastern sides while the western side bears traces of mining activities (Figure 4.4.15). The outcrop principally consists of medium-grained varieties of white, grey, red, and purple quartzites, mica schist, and meta-granitic rocks (Figure 4.4.15). In alphabetical order, these rocks are mineralogically composed of aegirine, alkali feldspar (microcline), amphibole (hornblende), biotite, garnet, kyanite, microcline, muscovite, plagioclase, quartz, staurolite, and titanite (Hay 1976; Kyara 1999; McHenry and de la Torre 2018; Tactikos 2005). Upon sampling, one obsidian surface artifact was encountered on the southern side of the outcrop. Seven of fourteen samples collected from Naisiusiu in 2017 were analysed for this study and whose locations are displayed in Figure 4.4.16.

Namorod is a >350 m-long north-south trending scoriac eruptive fissure on the northwestern slopes of Lemagrut (Figure 4.4.1). This edifice was formed by a volcanic eruption in which dissolved gases were released within molten rock and led to the petrogenesis of agglutinated, poorly consolidated, highly oxidised, phenocryst-rich, vesicular scoria (Figure 4.4.17). The top and western sides of the edifice host higher numbers of spatter deposits than the eastern side and these are occasionally capped by calcretes (Figure 4.4.17). Upon sampling, one obsidian surface artifact was encountered on the western side. No samples collected from Namorod

in 2017 were analysed for this study since there are no recorded instances for the use of scoria in artifact production in the Olduvai paleobasin (Leakey 1971; Leakey and Roe 1994).

Oittii is a low-lying <150 m-wide quartzitic and schistic outcrop >400 m north of Naibor Soit Ndogo (Figure 4.4.12). The complexly metamorphosed outcrop contains east-west trending quartzites dipping north, north-south trending vertical quartzites, and east-west trending vertical mica schist with harmonic folding (Figure 4.4.18). The outcrop principally consists of coarse-grained grey quartzites that are highly oxidised along with mica schist. Four of five samples collected from Oittii in 2017 were analysed for this study and whose locations are displayed in Figure 4.4.12.

Olbalbal is a fault graben located at the base of the Ngorongoro Caldera and Olmoti (Figure 4.4.1 and 4.4.19) and was formed between 1.3-0.6 Ma (Hay 1976; Mollel and Swisher 2012). Since Olbalbal is the modern drainage sump of the Olduvai River and the northwestern NVH, it is an important secondary source of igneous and metamorphic rocks, as well as sediment. Igneous rocks can be sourced to the NVH (Sadiman, Lemagrut, Ngorongoro, and Olmoti), metamorphic rocks can be sourced to nearby inselbergs, and sediments can be sourced to exposed units in the Olduvai paleobasin. Four of ten samples collected from Olbalbal in 2017 were analysed for this study and whose locations are displayed in Figure 4.4.20.

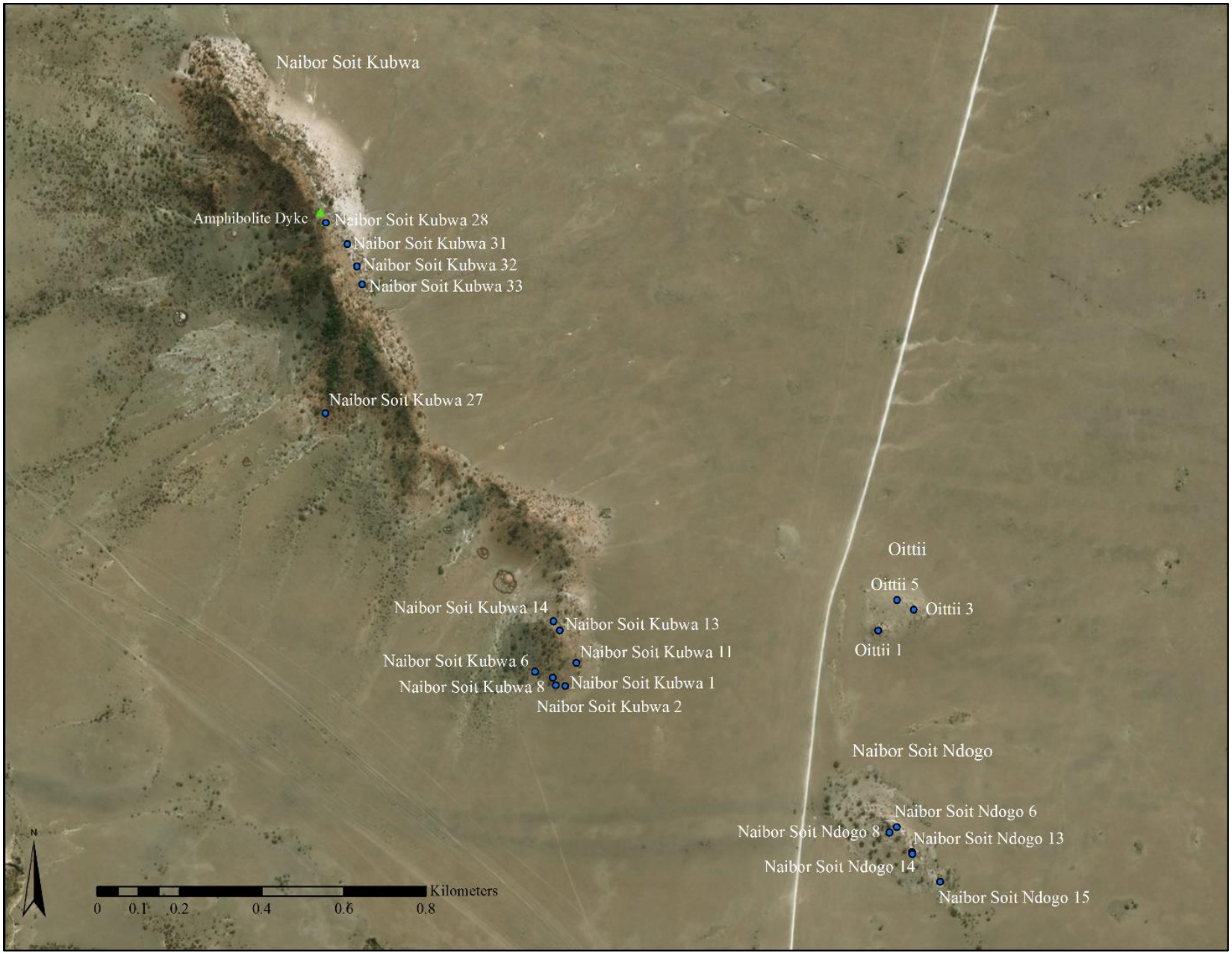

Figure 4.4.12. Naibor Soit Kubwa, Naibor Soit Ndogo, and Oittii sample locations. See Figure 4.4.1 for spatial reference.

Figure 4.4.13. Naibor Soit Kubwa: (a) gneiss with bedding planes dipping northwest; (b) quartzite with bedding planes dipping west overlain by gneissic beds; (c) magnetite-rich quartzite on the eastern side of the inselberg; (d) poorly consolidated quartzite capped by calcrete; (e) portion of the amphibolite dyke with sub-parallel quartz veins protruding through the top of the inselberg; (f) portion of the same amphibolite dyke as in (e).

Figure 4.4.14. Naibor Soit Ndogo: (a) view west towards Naibor Soit Kubwa showing quartzite with bedding planes steeply dipping south; (b) view southeast towards Ngorongoro showing quartzite with bedding planes steeply dipping southwest; (c) fuchsite-bearing quartzite on the southern side of the inselberg; (d) easternmost quartzite outcroppings with heat-induced staining.

Figure 4.4.15. Naisiusiu: (a) view west showing active mining pits on the western side of the outcrop; (b) view east showing meta-granitic outcroppings with bedding planes dipping southeast; (c) quartzitic outcroppings on the northern side of the outcrop; (d) mica schist with bedding planes dipping southeast; (e) mica schist overlain by quartzite indicative of stratic metamorphism with bedding planes dipping southeast; (f) close-up of (e).

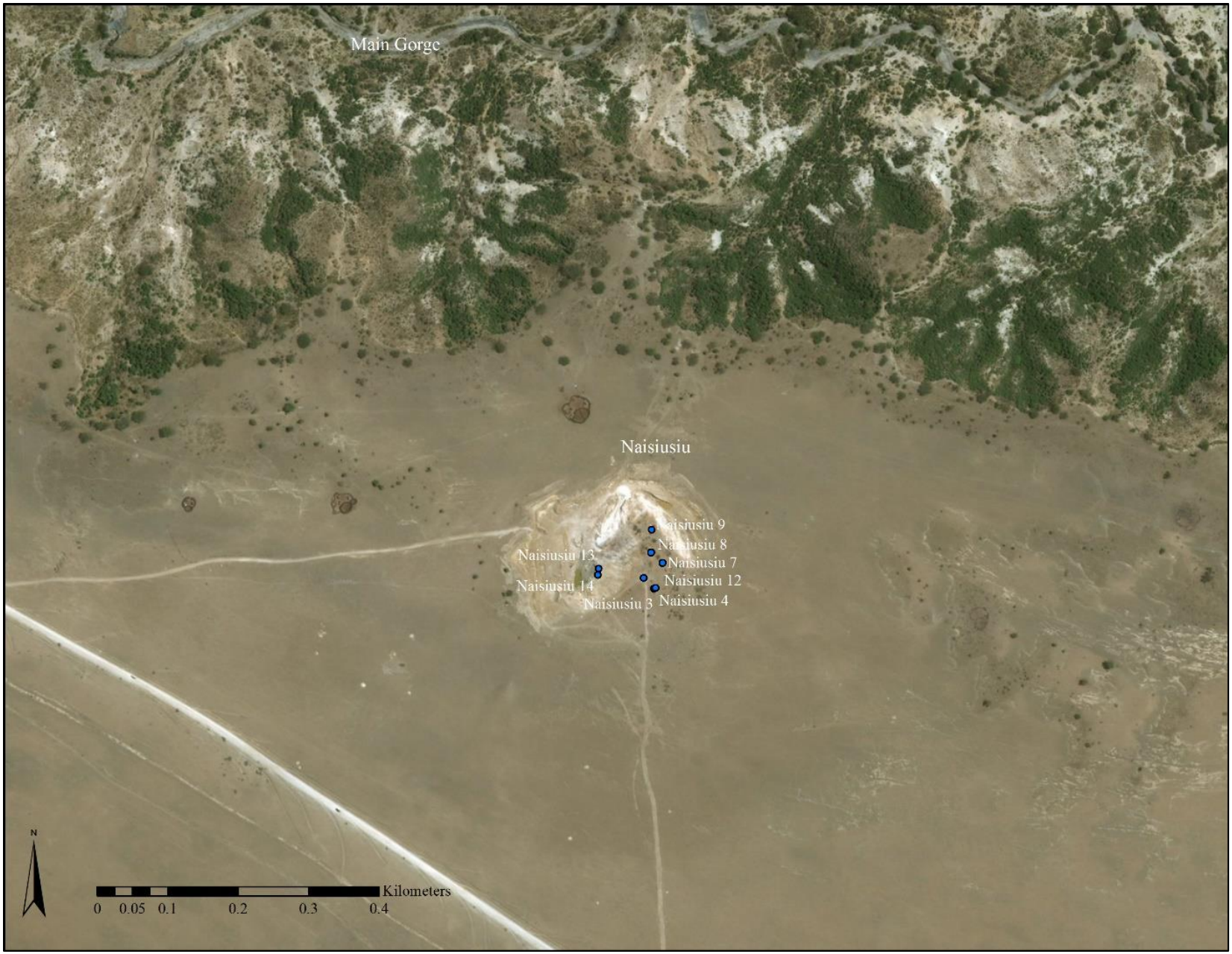

Figure 4.4.16. Naisiusiu sample locations. See Figure 4.4.1 for spatial reference.

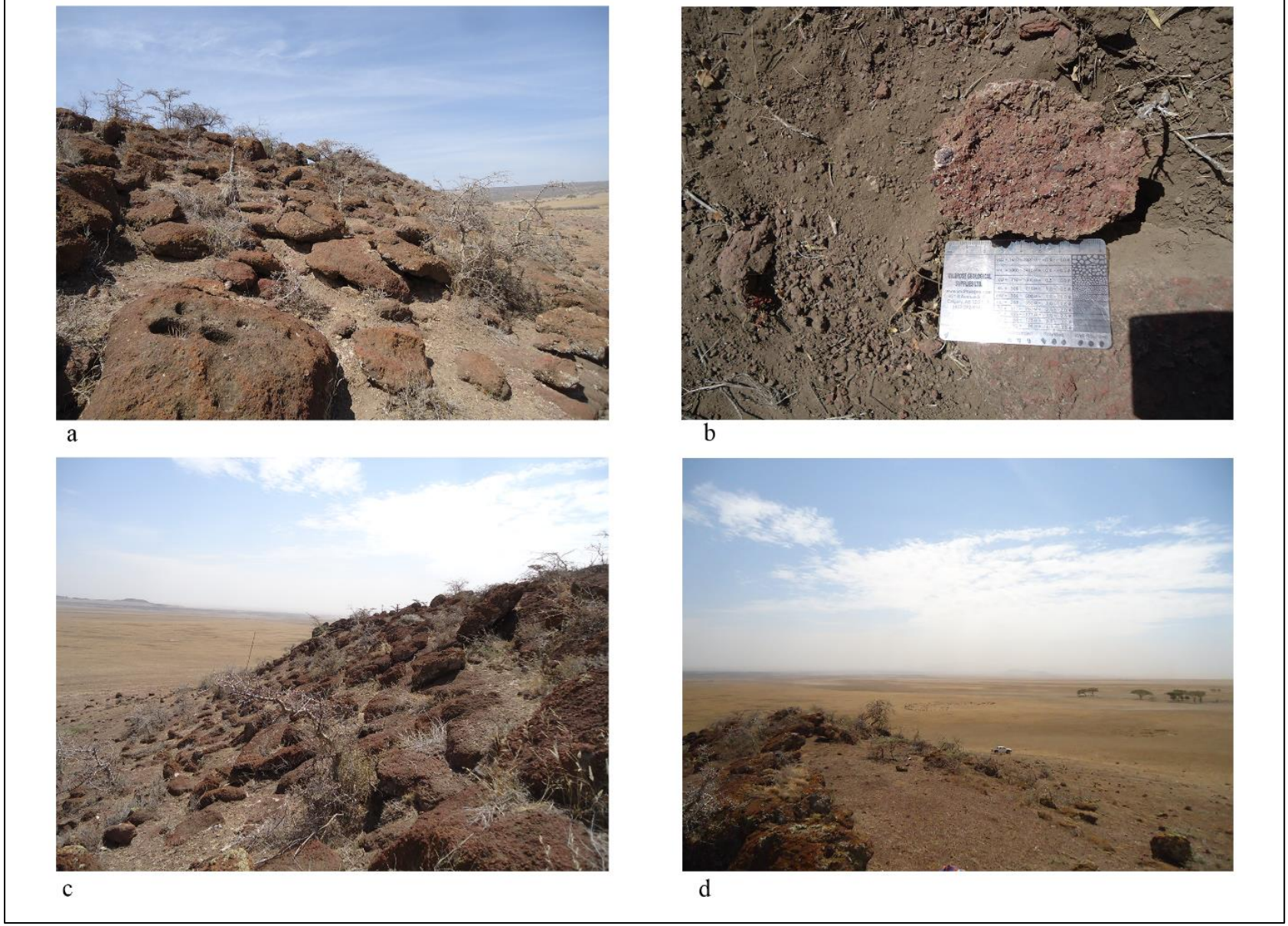

Figure 4.4.17. Namorod: (a) poorly consolidated, highly oxidised, vesicular scoria; (b) vesicular phenocryst-rich scoria; (c) view north towards Kelogi showing high numbers of outcroppings on the western side; (d) view north showing contrast between the number of outcroppings on the western and eastern sides.

Figure 4.4.18. Oittii: (a) view south towards Naibor Soit Ndogo; (b) view west towards Naibor Soit Kubwa showing quartzite with bedding planes dipping north; (c) east-west trending vertical mica schist with harmonic folding; (d) north-south trending vertical quartzite.

Figure 4.4.19. Olbalbal: (a) view east towards Olmoti overlooking extensive clay deposits that contain few volcanic clasts; (b) northeastern swamp margin in 2018; (c) panoramic view northwest towards the First Fault; (d) panoramic view east and south towards the Ngorongoro Volcanic Highlands.

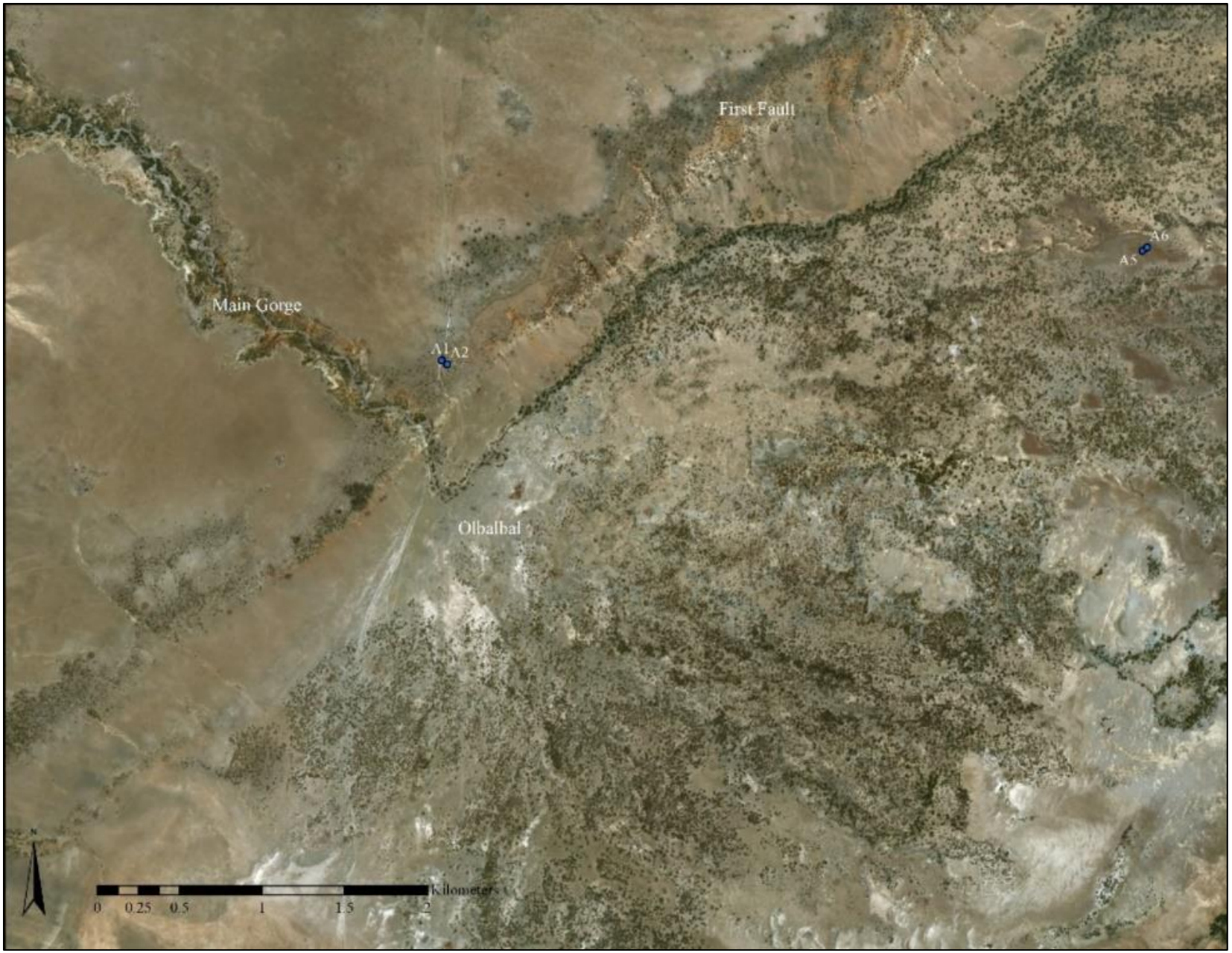

Figure 4.4.20. Olbalbal sample locations. See Figure 4.4.1 for spatial reference.

The metamorphic outcrops described above (i.e. Endonyo Osunyai, Gol Mountains, Granite Falls, Kelogi, Naibor Soit Kubwa, Naibor Soit Ndogo, Naisiusiu, and Oittii) all belong to the Neoproterozoic Mozambique Belt. Some of the outcrops closest to Olduvai, namely Endonyo Osunyai, Naibor Soit Kubwa, Naibor Soit Ndogo, Naisiusiu, and Oittii display atypical dipping planes for the Mozambique Belt (e.g. Hepworth 1972; Scoon 2018). These structural anomalies are best explained of having been exposed to Neogene tectono-magmatic stress and associated mountain-building events imprinted onto an orogenised, highly deformed, and eroded complex. Based on these results, it is hypothesised that un-sampled metamorphic outcrops proximal to the NVH such as Isilale Aratum, Kearoni, and Endonyo Okule (Table 4.4.2) (Figure 4.4.1) may have similarly complex structural geologies while those further north such as Koonge and Olongojoo (Table 4.4.2) (Figure 4.4.1) may align more so with what is commonly expected for the Mozambique Belt.

Chapter 5

Materials and Methods

Geological samples were collected in primary and secondary positions within the greater Olduvai Gorge region by SDS between 2015-2018. At the University of Calgary, selected samples were thin sectioned, analysed, described, and interpreted. Comparative analyses on quartzite and meta-granitic samples were undertaken to determine if there were geographically discrete occurrences of rocks with specific mineral assemblages. The following three sub-chapters provide additional information on the materials and methods of this study.

Chapter 5.1

Field Sampling

In 2017, the author sampled outcrops accessible on the modern landscape according to assumed prehistoric importance, distance to archaeological sites, and whose locations were initially determined based on a literature review (Berry 2012; Blumenschine et al. 2008, 2012b; Hay 1973, 1976; Hay and Kyser 2001; Jones 1979, 1981, 1994; Kimura 1997; Kyara 1999; Leakey 1965; Leakey 1971; Manega 1993; McHenry et al. 2008; Mollel 2002, 2007; Mollel et al. 2008, 2011; Mollel and Swisher 2012; O'Neil and Hay 1973; Plummer 2004; Santonja et al. 2014; Stiles 1991, 1998; Stiles et al. 1974; Tactikos 2005; Zaitsev et al. 2012). Previously unrecorded outcrops were also sampled which is a reminder of the value of non-discriminatory surveying. The primary extents of Endonyo Osunyai, Engelosin, Granite Falls, Kelogi, Naibor Soit Kubwa, Naibor Soit Ndogo, Naisiusiu, Namorod, and Oittii were systematically sampled to capture intra-outcrop variation (Table 5.1.1). Igneous, metamorphic, and sedimentary rocks in primary and secondary positions were also collected at the Gol Mountains, Granite Falls, Kelogi, Naisiusiu, and Olbalbal (Table 5.1.1).

A geological hammer was used to break off a sample from an outcrop and to split a rock in secondary position to obtain a fresh surface. Samples were photographed using a Sony DSLR-A100 and initially identified based on macroscopic and microscopic traits using a hand lens. GPS coordinates were recorded using a Garmin eTrex 10. Structural and lithological characteristics for each sample's outcrop were recorded using a compass (see Chapter 4.4).

With proper authorisation from the Assistant Commissioner for Minerals (Northern Zone) and the Tanzania Commission for Science and Technology, samples were shipped directly to the University of Calgary for further study.

Table 5.1.1 Samples Collected in Primary and Secondary Positions According to Source/Outcrop

Source/Outcrop	Primary Position	Secondary Position
Endonyo Osunyai	x	
Engelosin	x	
Gol Mountains	x	x
Granite Falls	x	x
Kelogi	x	x
Naibor Soit Kubwa	x	
Naibor Soit Ndogo	x	
Naisiusiu	x	x
Namorod	x	
Oittii	x	
Olbalbal		x

Chapter 5.2

Thin Sectioning

Fifty-three samples (Table 5.2.1) in primary position were selected for thin sectioning based on macroscopic variation (i.e. grain size, texture, mineral composition, gloss, transparency, and Munsell colour) in order to obtain a sample population representative of intra-outcrop variation. Nine samples (Table 5.2.1) in secondary position were also selected for thin sectioning based on their macroscopic similarities to samples in primary position, their uniqueness, and/or their assumed importance in artifact production. Ten thin sections analysed for this study were independently prepared in the Geoscience Research Laboratory (University of Calgary) to fast-

track the commencement of microscopic analyses. The remaining samples were thin sectioned in the Tropical Archaeology Lab (University of Calgary) abiding by the following protocol:

1. Sample is cut using a Trim Saw (TS10; Lortone Inc.);
2. Sample is cut using an IsoMet 4000 Linear Precision Saw;
3. Sample is mounted on an unfrosted slide (27x46 mm) with a 1:0.33 solution of EpoFix Resin and Hardener;
4. Sample is cut and ground using a PetroThin Thin Sectioning System;
5. Sample is mounted in a Cast N' Vac 1000 Castable Vacuum System on a frosted slide (27x46 mm) with a 1:0.33 solution of EpoFix Resin and Hardener;
6. Sample is cut and ground using a PetroThin Thin Sectioning System;
7. Sample is ground using a Metaserv 2000 Grinder Polisher to a thickness of ~30-35 μm;
8. Sample is polished using a Metaserv 2000 Grinder Polisher with <3 mL of DiaDuo-2 diamond suspension;
9. Sample is left uncovered, amenable for further study using other analytical techniques.

Table 5.2.1 Sample Position, Outcrop/Source, ID, Rock Type, and Number of Thin Sections Per Sample

Position	Outcrop/Source	Sample ID	Rock Type	Thin Sections, n
Primary	Endonyo Osunyai	Endonyo Osunyai 1	Quartzite	1
		Endonyo Osunyai 2	Quartzite	1
		Endonyo Osunyai 4A/B	Quartzite	2
	Engelosin	Engelosin 2	Phonolite	1
		Engelosin 5A/B	Phonolite	2
		Engelosin 6A/B	Phonolite	2
		Engelosin 10A/B	Phonolite	2
	Gol Mountains	DDD1	Quartzite	1
		JJJ1	Meta-monzo-granite	1
		KKK1	Meta-quartz-rich granitoid	1
		OOO1	Feldspar	1
		PPP1	Quartzite	1
		RRR1	Quartzite	1
		SSS1	Quartzite	1
		TTT1	Meta-quartz-rich granitoid	1
		UUU1	Meta-quartz-rich granitoid	1
	Granite Falls	Granite Falls 1A/B	Granite gneiss	2
		Granite Falls 2	Granite gneiss	1

Table 5.2.1 (continued) Sample Position, Outcrop/Source, ID, Rock Type, and Number of Thin Sections Per Sample				
Position	**Outcrop/Source**	**Sample ID**	**Rock Type**	**Thin Sections, n**
Primary	Kelogi	Kelogi 1	Granite gneiss	1
		Kelogi 3	Granite gneiss	1
		Kelogi 10	Granite gneiss	1
	Naibor Soit Kubwa	Naibor Soit Kubwa N042	Quartzite	1
		Naibor Soit Kubwa E039	Quartzite	1
		Naibor Soit Kubwa S06	Quartzite	1
		Naibor Soit Kubwa 1	Quartzite	1
		Naibor Soit Kubwa 2	Quartzite	1
		Naibor Soit Kubwa 6	Quartzite	1
		Naibor Soit Kubwa 8	Quartzite	1
		Naibor Soit Kubwa 11	Quartzite	1
		Naibor Soit Kubwa 13	Quartzite	1
		Naibor Soit Kubwa 14	Quartzite	1
		Naibor Soit Kubwa 24	Quartzite	1
		Naibor Soit Kubwa 27	Quartzite	1
		Naibor Soit Kubwa 28	Quartz amphibolite	1
		Naibor Soit Kubwa 31	Quartzite	1
		Naibor Soit Kubwa 32	Quartzite	1
		Naibor Soit Kubwa 33	Quartzite	1
	Naibor Soit Ndogo	Naibor Soit Ndogo 6A/B	Quartzite	2
		Naibor Soit Ndogo 8	Quartzite	1
		Naibor Soit Ndogo 13	Quartzite	1
		Naibor Soit Ndogo 14	Quartzite	1
		Naibor Soit Ndogo 15	Quartzite	1
	Naisiusiu	Naisiusiu 3	Meta-syeno-granite	1
		Naisiusiu 4	Quartzite	1
		Naisiusiu 7	Quartzite	1
		Naisiusiu 8	Mica schist	1
		Naisiusiu 9	Quartzite	1
		Naisiusiu 13	Quartzite	1
		Naisiusiu 14	Quartzite	1
	Oittii	Oittii 1A/B	Quartzite	2
		Oittii 3	Quartzite	1
		Oittii 4	Quartzite	1
		Oittii 5A/B	Quartzite	2
Secondary	Gol Mountains	III1	Hornblende granofels	1
	Granite Falls	Granite Falls 3A/B	Nephelinite	2
		Granite Falls 4A/B	Quartzite	2
	Kelogi	Kelogi 9	Quartzite	1
	Naisiusiu	Naisiusiu 12	Nephelinite	1
	Olbalbal	A1A/B	Nephelinite	2
		A2	Basalt (?)	1
		A5A/B	Basalt (?)	2
		A6	Trachyandesite/basalt	1

Chapter 5.3

Thin Section Analysis

Minerals are inorganic, naturally-occurring, and have both a crystalline structure and a well-defined chemical composition (Jones 1987). The majority of naturally-occurring minerals are formed by the combination of elements in solid solution that are joined together by six bond types, namely ionic, covalent, metallic, van der Waals, hydrogen, and dative, with the first three being the most common (Perkins 1998). An individual mineral crystal can be assigned to one of thirty-two classes within seven crystallographic systems (i.e. isometric, tetragonal, orthorhombic, monoclinic, triclinic, hexagonal, and trigonal) defined by their axes' lengths and angles in relation to each other (Cairncross and McCarthy 2015).

Under transmitted light microscopy, a specially-prepared 30-35 μm thin section can help to identify a sample's rock type based on its texture and non-opaque mineralogical composition which together may reveal critical information about its petrogenesis, tectonic setting, nature of metamorphism, cement and events, hydrothermal alteration, diagenesis, and weathering profile (Bucher and Grapes 2011; Gill 2010; Perkins 1998). A total of seventy-four thin sections were analysed for this study using a Leitz HM-POL petrographic microscope (2.5 x, 4 x, 10 x, 40 x). Mineral characteristics such as opacity, size, shape, cleavage angles, colour, and pleochroism were observed under PPL with orthoscopic illumination. Other characteristics such as isotropy, sign of elongation, extinction angle, zoning, twinning, exsolution, and inclusions were determined under XP with orthoscopic illumination and the accessory plate in. Under XP with conoscopic illumination and the Bertrand lens in, characteristics such as uniaxial or biaxial interference figures, optic signs, and approximate 2*V* values were occasionally determined to confirm mineral identification. Observation under PPL and XP using orthoscopic illumination allowed for mineral

identification which was compared with published petrological and mineralogical studies in the greater Olduvai Gorge region (Table 5.3.1). Photomicrographs were taken using a Nikon ECLIPSE 50i POL microscope (2 x, 4 x, 10 x, 40 x) equipped with a Moticam 2500 (Motic Images Plus 2.0).

Table 5.3.1 Published Petrological and Mineralogical Studies in the Greater Olduvai Gorge Region

Rock Type	Source/Outcrop	Rock	Mineralogy	References
Igneous	Embagai	Foidite; nephelinite; phonolite; vitric lava	Nepheline; augite; andradite; titanite; melilite; apatite; titanomagnetite; amphibole; garnet; perovskite; potassium feldspar; calcite; phillipsite; chabazite	Greenwood 2014; Mollel 2007; Mollel and Swisher 2012
	Engelosin	Phonolite; breccia	Alkali feldspar (anorthoclase, sanidine); augite; nepheline; aegirine; analcime; titanite; apatite	Hay 1976; Kyara 1999; Mollel and Swisher 2012
	First Stream	Detrital igneous rocks (Lemagrut)	nd	Kyara 1999
	Kerimasi	Agglomerate; limestone; pyroclast	Nyerereite; apatite; magnetite; olivine; biotite; nepheline; melilite; augite; perovskite; melanite; ilmenite; titanite	Dawson 1962; Hay 1976, 1983; Mollel and Swisher 2012
	Lemagrut	Basalt; benmorite; hawaiite; ignimbrite; mugearite	Augite; plagioclase; anorthoclase; titanomagnetite; amphibole; olivine; biotite; fluoroapatite	Hay 1976; Kyara 1999; Mollel and Swisher 2012
	Namorod	Scoria	nd	Hay 1976
	Ngorongoro	Agglomerate; basalt; ignimbrite; rhyolite; trachyte; trachyandesite; trachydacite	Olivine; augite; plagioclase; anorthoclase; titanomagnetite; amphibole; biotite; quartz; aenigmatite; ilmenite; fayalite	McHenry et al. 2008; Mollel 2002; Mollel et al. 2008; Mollel and Swisher 2012
	Oldeani	Basalt; trachyandesite	Plagioclase; augite; olivine; titanomagnetite; amphibole; biotite	Mollel et al. 2011; Mollel and Swisher 2012; Pickering 1964, 1965
	Olmoti	Basalt; ignimbrite; trachyte; trachyandesite	Augite; feldspar; aenigmatite; amphibole; ilmenite; titanomagnetite; biotite; olivine; apatite; sodalite	Hay 1976; Kyara 1999; Manega 1993; McHenry et al. 2008; Mollel 2002; Mollel et al. 2009; Mollel and Swisher 2012; Pickering 1964, 1965
	Sadiman	Foidite; ijolite; nephelinite; phonolite; tephrite	Nepheline; clinopyroxene (augite); garnet; perovskite; andradite; titanite; titanomagnetite; olivine; apatite; sanidine; wollastonite	Hay 1976; Jones 1994; Kyara 1999; Mollel and Swisher 2012; Zaitsev et al. 2012
	Second Stream	Detrital igneous rocks (basalt; trachyandesite)	nd	Kyara 1999
	Tanzania Craton	Gabbro	nd	Hay 1976
	Third Stream	Detrital igneous rocks (basalt; phonolite; trachyandesite)	nd	Kyara 1999
Metamorphic	Endonyo Okule	Quartzite	Quartz; muscovite; kyanite; biotite; feldspar	Hay 1976; Kyara 1999
	Endonyo Osunyai	Gneiss; quartzite	nd	Hay 1976; Kyara 1999
	Granite Falls	Granite gneiss; detrital igneous and metamorphic rocks	Quartz; microcline; plagioclase; biotite; muscovite	Hay 1976
	Isilale Aratum	Amphibolite; quartzite	Quartz; feldspar; muscovite; biotite	Hay 1976
	Kearoni	Granite gneiss	Quartz; feldspar; biotite; hornblende; garnet[1]	Hay 1976; Kyara 1999
	Kelogi	Granite gneiss	Quartz; orthoclase; albite; aegirine; amphibole (hornblende); biotite; garnet[1]	Hay 1976; Kyara 1999

Table 5.3.1 (continued) Published Petrological and Mineralogical Studies in the Greater Olduvai Gorge Region				
Rock Type	**Source/Outcrop**	**Rock**	**Mineralogy**	**References**
Metamorphic	Koonge	Quartzite	nd	Hay 1976
	Naibor Soit Kubwa	Gneiss; quartzite	Quartz; muscovite	Hay 1976; Kyara 1999; McHenry and de la Torre 2018; Tactikos 2005
	Naibor Soit Ndogo	Quartzite	nd	Kyara 1999; Leakey 1965; Santonja et al. 2014
	Naisiusiu	Granite gneiss; quartzite	Quartz; microcline; plagioclase; aegirine; hornblende; titanite; biotite; muscovite; garnet; kyanite; staurolite[1]	Hay 1976; Kyara 1999; McHenry and de la Torre 2018; Tactikos 2005
	Oittii	Mica schist; quartzite	nd	Jones 1994; Kyara 1999; Leakey 1965
	Olongojoo	Quartzite	nd	Blumenschine et al. 2008; Hay 1976
	Inselberg near Eng'amata Enqii	Quartzite	nd	Blumenschine et al. 2008; Reti 2013
Sedimentary	Fifth Fault	Chert	Quartz	Hay 1976; Kyara 1999; Stiles 1998
	Geolocality 42b	Chert	Quartz	Hay 1976
	Geolocality 43	Chert	Quartz	Hay 1976; Kimura 1997; Kyara 1999; Leakey 1971; Stiles 1991, 1998; Stiles et al. 1974
	Geolocality 43a	Chert	Quartz	Hay 1976
	Geolocality 45	Chert	Quartz	Hay 1976; Leakey 1971
	Geolocality 78b	Chert	Quartz	Hay 1976
	Geolocality 80	Chert	Quartz	Berry 2012; Hay 1976; Hay and Kyser 2001; O'Neil and Hay 1973
	Geolocality 82	Chert	Quartz	Hay 1976; O'Neil and Hay 1973
	Geolocality 82a	Chert	Quartz	Hay 1976
	Geolocality 85	Chert	Quartz	Hay 1976; O'Neil and Hay 1973
	Geolocality 88	Chert	Quartz	Hay 1976; O'Neil and Hay 1973; Stiles et al. 1974
	Geolocality 88a	Chert	Quartz	Hay 1976; Stiles et al. 1974
	Geolocality 88b	Chert	Quartz	Hay 1976; Kyara 1999; Leakey 1971; Stiles et al. 1974
	Geolocality 89	Chert	Quartz	Hay 1976; Kyara 1999; Leakey 1971; Stiles et al. 1974
	Geolocality 91	Chert	Quartz	Hay 1976; Stiles 1998
	Geolocality 201	Chert	Quartz	Hay 1976; Stiles 1998
	Geolocality 202	Chert	Quartz	Hay 1976; Stiles 1998
	Olbalbal	Detrital igneous, metamorphic, and sedimentary rocks	na	Hay 1976
	Olduvai River	Detrital igneous, metamorphic, and sedimentary rocks	na	Hay 1976; Tactikos 2005

[1]=Kyara (1999) notes the presence of quartz, feldspar, biotite, hornblende, and garnet but unclear if in reference to Kearoni, Kelogi, or Naisiusiu.

Magmatic rocks were classified according to their essential, type, accessory, and post-magmatic minerals (*sensu* Gill 2010) although satisfactory identification was occasionally hindered by non-diagnostic mineral assemblages. Lowly metamorphosed plutonic rocks were classified by referencing the Quartz-Alkali Feldspar-Plagioclase-Feldspathoid double ternary diagram (Figure 5.3.1). Metamorphic rocks were classified according to their texture and mineral

composition, and index minerals allowed for the interpretation of metamorphic grade. However, isograds were not mapped since there are large geographic gaps between outcrops as these are of basement origin and are not well-exposed over extended distances. No sedimentary rocks were analysed as part of this study. Textural characteristics such as crystal habit, morphology, replacement textures, intergrowths, foliation, and qualitative grain sizes were noted depending on sample rock type (Fettes and Desmons 2007; Gill 2010). Quantitative grain sizes were not recorded since many samples were of metamorphic lithology, and some were texturally immature considering their sedimentary origin. Furthermore, quantitative grain size analyses on quartzite artifacts undertaken in a recent study have found this to be of little value to identify varieties other than to determine the extent to which a sample was metamorphosed (Prieto et al. 2019).

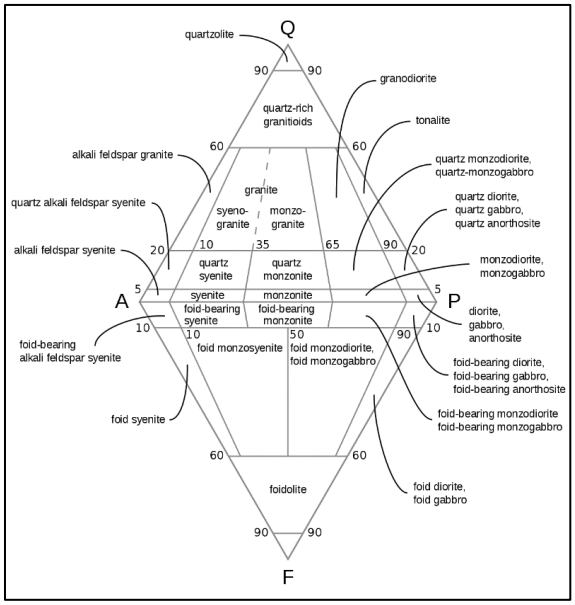

Figure 5.3.1. Quartz-Alkali Feldspar-Plagioclase-Feldspathoid double ternary diagram (after Streckeisen 1976).

Each thin section's modal abundances were visually estimated using a percentage estimation chart (Figure 5.3.2). A comparison between visually estimated modes with point-counted modes tabulated secondarily on two granite gneiss samples revealed comparable results that did not alter rock type assignment (Table 5.3.2). Two samples (Kelogi 10 and Naibor Soit

Kubwa 28) with stark differences in mafic and felsic minerals were also quantitatively analysed in ImageJ by converting a non-representative photomicrograph under PPL to an 8-bit greyscale image to determine their modal abundances and test this methodology (Klein and Philpotts 2017).

Once all thin sections were analysed and described, sample data were tabulated and subject to petrologic interpretations. Certain samples analysed for this study were also previously analysed by way of energy dispersive X-ray spectroscopy using a Thermo Scientific *ARL Quant'X* EDXRF unit (Abtosway 2018). Therefore, an effort was made to correlate specific minerals with elemental data. Comparative analyses of quartzite and meta-granitic samples were undertaken to determine whether the sampled outcrops had unique mineral compositions conducive for artifact sourcing.

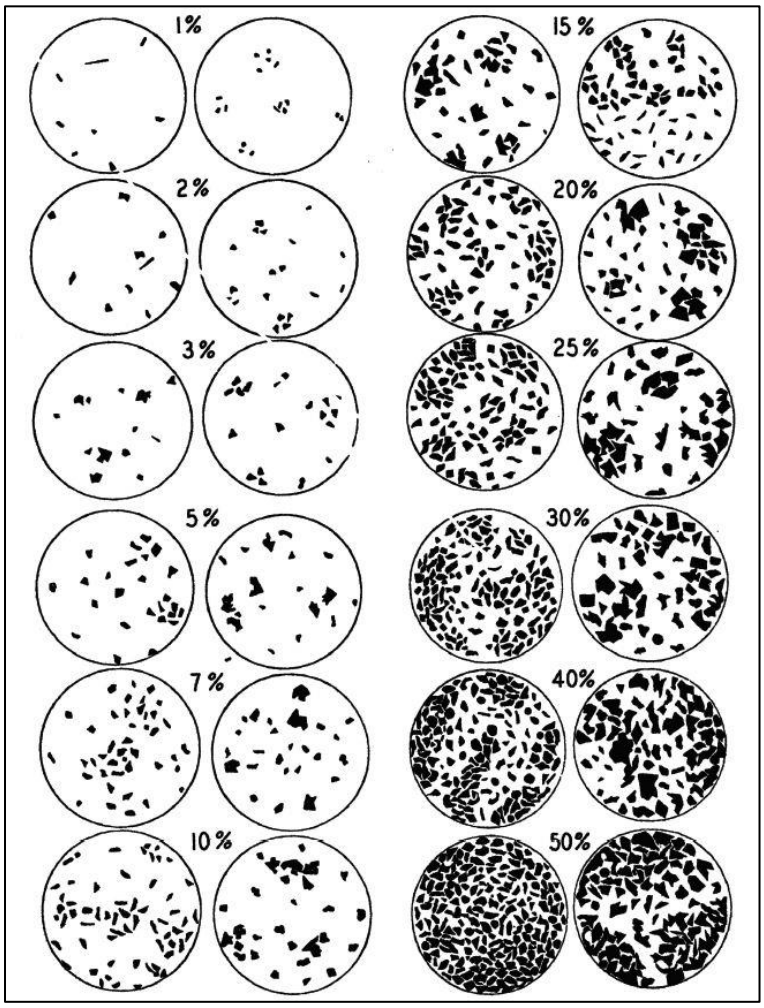

Figure 5.3.2. Modal visual estimation chart (Terry and Chillingar 1955).

Table 5.3.2 Comparison Between Visually Estimated and Point-Counted Modal Percentages Tabulated Secondarily														
Method	**Sample ID**	**Total Points Counted**	**Quartz**		**Aegirine**		**Plagioclase**		**Alkali feldspar**		**Hornblende**		**Hematite**	
			n	**%**	**n**	**%**	**n**	**%**	**n**	**%**	**n**	**%**	**n**	**%**
Point Counts	**Kelogi 1**	435	170	39.1	82	18.9	71	16.3	69	15.9	43	9.9	nd	nd
	Kelogi 3	660	300	45.5	130	19.7	77	11.7	17	2.6	80	12.1	56	8.5
Visual Estimates	**Kelogi 1**	na	na	45	na	15	na	15	na	15	na	10	na	nd
	Kelogi 3	na	na	50	na	20	na	10	na	5	na	10	na	5

Chapter 6

Results

A total of seventy-four thin sections of sixty-two geological samples in primary and secondary positions were analysed for this study. The following sub-chapters are organised alphabetically by source/outcrop and include reviews of prior studies and their results, descriptions of identified rock types and varieties based on textural and mineralogical data, as well as petrologic interpretations. Chapter 6.11 and 6.12 include comparative analyses of quartzites and meta-granites, respectively.

Chapter 6.1

Endonyo Osunyai

Prior studies have identified gneiss and quartzite at this outcrop although no corresponding petrographic analyses have been undertaken (Hay 1976; Kyara 1999). In this study, six minerals have been identified in three quartzite samples, all of which were previously unrecognised. Quartzite is coarse-grained and primarily composed of quartz along with smaller crystals of alkali feldspar, muscovite, hematite, opaque, and rutile. Muscovite is an index mineral for low-grade metamorphism and occurs as platy crystals that are either embedded in quartz or interstitial, and generally have a sub-parallel lineation as a result of bidirectional pressure. Muscovite is responsible for weak foliation in one sample. Alkali feldspar and rutile are common detrital minerals, and together with hematite and quartz are representative of a sandstone protolith that was metamorphosed although no relict sedimentary textures were observed. Based on textural and mineralogical differences between three samples, there are as a minimum two varieties of quartzite at this outcrop (see Table 6.1.1; Chapter 6.11). The first variety contains, on average, 98% quartz and minor amounts of muscovite, opaque, and rutile. The second variety contains, on average,

78.5% quartz, 12.5% alkali feldspar, 7.5% muscovite, and minor amounts of hematite. The following paragraphs describe each thin section.

Endonyo Osunyai 1 is a non-foliated, heteroblastic, coarse-grained quartzite with a mineral assemblage of quartz (98%), muscovite (2%), opaque (<1%), and rutile (<1%). Quartz crystals have sutured boundaries as a result of dynamic recrystallisation primarily stemming from the formation and rotation of sub-grains and/or grain boundary migration (Stipp et al. 2002). Muscovite crystals are either embedded in quartz or interstitial, and have a sub-parallel lineation.

Endonyo Osunyai 2 is a non-foliated, heteroblastic, coarse-grained quartzite with a mineral assemblage of quartz (98%), muscovite (2%), and opaque (<1%). Quartz crystals have sutured boundaries as a result of dynamic recrystallisation primarily stemming from the formation and rotation of sub-grains and/or grain boundary migration (Stipp et al. 2002). Muscovite crystals are either embedded in quartz or interstitial, and have a sub-parallel lineation (Figure 6.1.1).

Endonyo Osunyai 4A is a weakly foliated, heteroblastic, anhedral coarse-grained quartzite with a mineral assemblage of quartz (79%), alkali feldspar (15%), muscovite (5%), and hematite (1%). Muscovite crystals are either embedded in quartz or interstitial and have a sub-parallel lineation. Alkali feldspar crystals show characteristic tartan twinning.

Endonyo Osunyai 4B is a weakly foliated, heteroblastic, anhedral coarse-grained quartzite with a mineral assemblage of quartz (78%), alkali feldspar (10%), muscovite (10%), and hematite (2%). Muscovite crystals are either embedded in quartz or interstitial and have a sub-parallel lineation. Alkali feldspar crystals show characteristic tartan twinning.

Table 6.1.1 Endonyo Osunyai: Sample Position, ID, Rock Type, and Visually Estimated Modal Percentages			
Position	**Sample ID**	**Rock Type**	**Mineralogy**
Primary	Endonyo Osunyai 1	Quartzite	Quartz (98); muscovite (2); opaque (<1); rutile (<1)
	Endonyo Osunyai 2	Quartzite	Quartz (98); muscovite (2); opaque (<1)
	Endonyo Osunyai 4A	Quartzite	Quartz (79); alkali feldspar (15); muscovite (5); hematite (1)
	Endonyo Osunyai 4B	Quartzite	Quartz (78); alkali feldspar (10); muscovite (10); hematite (2)

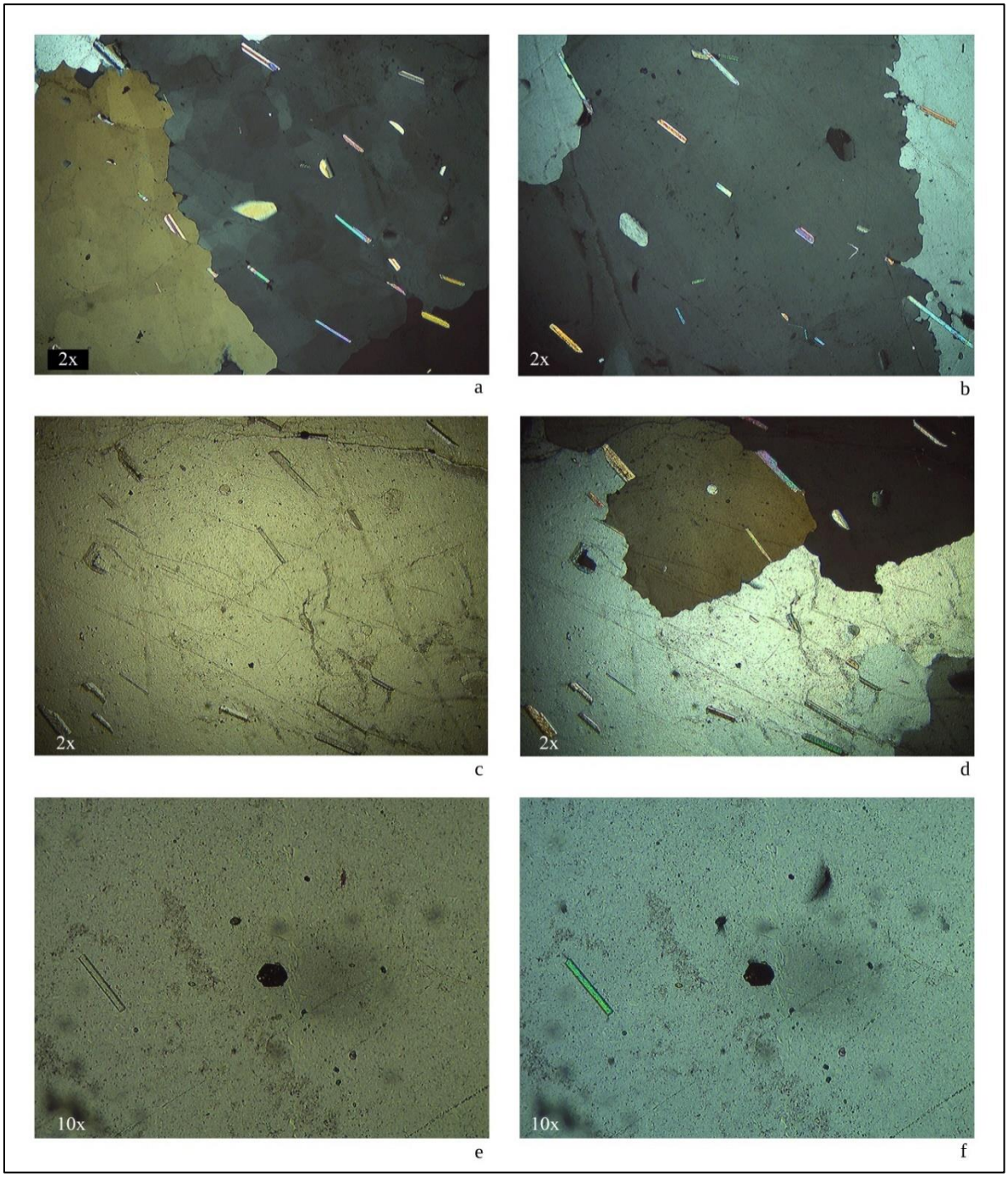

Figure 6.1.1. Endonyo Osunyai 2: (a) sub-parallel muscovite crystals embedded in quartz or interstitial in XP, quartz crystals show undulatory extinction and sutured boundaries; (b) similar to (a) in XP; (c) quartz and muscovite in PPL; (d) same as (c) in XP; (e) idioblastic opaque crystal embedded in quartz in PPL; (f) same as (e) in XP.

Chapter 6.2

Engelosin

Prior studies have identified phonolite and breccia at this outcrop and corresponding petrographic analyses on phonolite, an igneous extrusive intermediate rock, have identified eight minerals, namely alkali feldspar (anorthoclase, sanidine), augite, nepheline, aegirine, analcime, titanite, and apatite (Hay 1976; Kyara 1999; Mollel and Swisher 2012). In this study, five minerals have been identified in phonolite samples, namely sanidine, nepheline, augite, titanite, and sericite (Table 6.2.1). Sericite was previously unrecognised and is an alteration mineral of feldspar. Outcroppings are highly oxidised, and oxides are visible under thin section. Based on textural and mineralogical differences between four samples, there are as a minimum two varieties of phonolite at this outcrop, one flow-aligned variety and a second variety with a felty texture. The following paragraphs describe each thin section.

Engelosin 2 is an inequigranular, flow-aligned microporphyritic phonolite with sanidine (5%), nepheline (1%), titanite (<1%), and sericite (<1%) microphenocrysts embedded in a trachytic light-green groundmass of the same minerals and devitrified glass with minor amounts of oxides (Figure 6.2.1).

Engelosin 5A is a felty, microporphyritic phonolite with sanidine (2%), nepheline (1%), augite (1%), titanite (<1%), and sericite (<1%) microphenocrysts embedded in a felty light-green groundmass of the same minerals and devitrified glass with minor amounts of oxides.

Engelosin 5B is a felty, microporphyritic phonolite with nepheline (1%), sanidine (1%), augite (1%), sericite (<1%), and titanite (<1%) microphenocrysts embedded in a felty light-green groundmass of the same minerals and devitrified glass with minor amounts of oxides.

Engelosin 6A is a flow-aligned, microporphyritic phonolite with sanidine (1%), nepheline (<1%), augite (<1%), sericite (<1%), and titanite (<1%) microphenocrysts embedded in a trachytic light-green groundmass of the same minerals and devitrified glass with minor amounts of oxides.

Engelosin 6B is a flow-aligned, microporphyritic phonolite with nepheline (1%), sanidine (1%), augite (<1%), and sericite (<1%) microphenocrysts embedded in a trachytic light-green groundmass of the same minerals and devitrified glass with minor amounts of oxides.

Engelosin 10A is a flow-aligned, microporphyritic phonolite with sanidine (5%), cumulophyric augite (<1%), titanite (<1%), and nepheline (<1%) microphenocrysts embedded in a trachytic light-grey groundmass of the same minerals and devitrified glass with minor amounts of oxides.

Engelosin 10B is a flow-aligned, microporphyritic phonolite with sanidine (5%), titanite (1%), zoned and cumulophyric augite (1%), and nepheline (<1%) microphenocrysts embedded in a trachytic light-grey groundmass of the same minerals and devitrified glass with minor amounts of oxides.

Table 6.2.1 Engelosin: Sample Position, ID, Rock Type, and Visually Estimated Modal Percentages

Position	Sample ID	Rock Type	Mineralogy
Primary	Engelosin 2	Phonolite	Sanidine (5); nepheline (1); titanite (<1); sericite (<1)
	Engelosin 5A	Phonolite	Sanidine (2); nepheline (1); augite (1); titanite (<1); sericite (<1)
	Engelosin 5B	Phonolite	Nepheline (1); sanidine (1); augite (1); sericite (<1); titanite (<1)
	Engelosin 6A	Phonolite	Sanidine (1); nepheline (<1); augite (<1); sericite (<1); titanite (<1)
	Engelosin 6B	Phonolite	Nepheline (1); sanidine (1); augite (<1); sericite (<1)
	Engelosin 10A	Phonolite	Sanidine (5); augite (<1); titanite (<1); nepheline (<1)
	Engelosin 10B	Phonolite	Sanidine (5); titanite (1); augite (1); nepheline (<1)

Modes for phonolites are for phenocrysts.

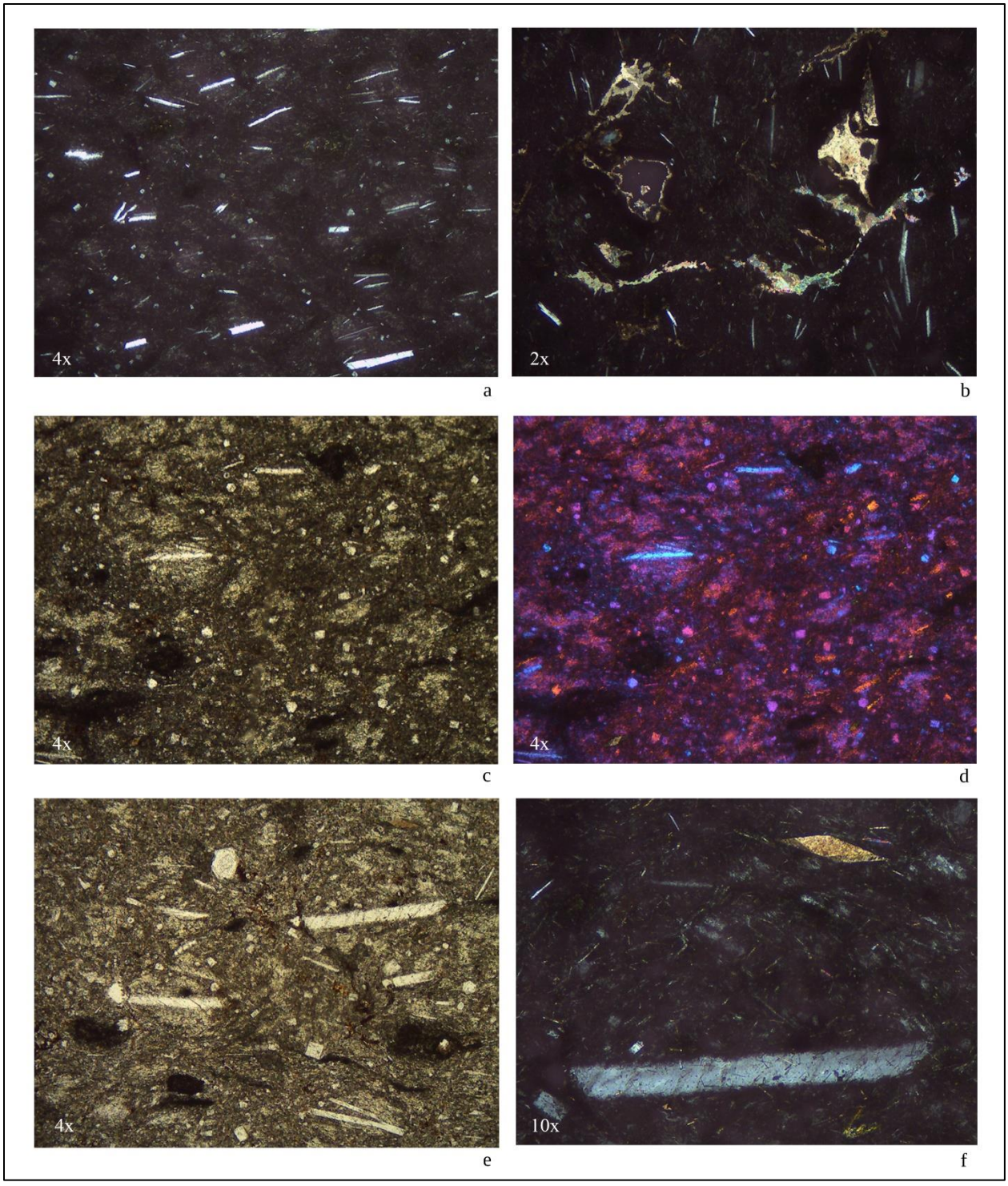

Figure 6.2.1. Engelosin 2: (a) flow-aligned microporphyritic sanidine in XP; (b) sub-parallel sanidine microphenocrysts and fibrous sericite with a silky texture in XP; (c) light-green groundmass in PPL; (d) same as (c) under XP with the accessory plate in, note the similar groundmass' interference colours as the microphenocrysts which suggests that the groundmass is primarily composed of identical minerals; (e) sanidine, nepheline, and titanite microphenocrysts in PPL; (f) sanidine and titanite in XP.

Chapter 6.3

Gol Mountains

Prior studies have identified quartzite at Olongojoo, an inselberg near Eng'amata Enqii, and at inselbergs near Soit Nasera although no corresponding petrographic analyses have been undertaken (Blumenschine et al. 2008; Hay 1976; Mehlman 1977; Reti 2013). In this study, thirteen minerals have been identified in ten samples of various lithologies from different localities in the Gol Mountains ranging from metamorphic to meta-plutonic to plutonic rocks, all of which were previously unrecognised (Table 6.3.1).

Five minerals have been identified in four coarse- and medium-grained quartzite samples, namely quartz, muscovite, alkali feldspar, rutile, and opaque. Muscovite is an index mineral for low-grade metamorphism and occurs as platy crystals that are either embedded in quartz or interstitial, and have either a random or parallel lineation. Alkali feldspar and rutile are rare detrital minerals, and together with quartz are representative of a sandstone protolith that was metamorphosed although no relict sedimentary textures were observed. Two samples have concentrated rutile crystals possibly stemming from localised wave action prior to protolith lithification. Based on textural and mineralogical differences between four samples, there are as a minimum two varieties of quartzite that outcrop in the Gol Mountains (see Chapter 6.11). The first variety contains on average 92.3% quartz, 7.6% muscovite, and minor amounts of rutile and opaque. The second variety has similar modes of quartz and muscovite but is differentiated based on the presence of alkali feldspar.

Eight minerals have been identified four meta-granitic samples, namely quartz, alkali feldspar, biotite, hornblende, plagioclase, rutile, muscovite, and opaque. Biotite, hornblende, and opaque crystals are responsible for the spotted and weakly foliated textures. Based on textural and

mineralogical differences between four samples, there are as a minimum two varieties of meta-granites that outcrop in the Gol Mountains (see Chapter 6.12). These two varieties are differentiated based on the absence and presence of alkali feldspar.

Five minerals have been identified in one feldspar sample, namely microcline, albite, hematite, opaque, and sanidine. This sample was collected from a small outcropping at Soit Nasera which is dominated by quartz-feldspathic gneiss. The microcline was originally crystallised under high-temperature, high-pressure conditions and upon cooling, microcline exsolved into prominent albite lamellae. Similar rock types have been reported near Granite Falls although no mineralogical or textural data are recorded thereby making comparative analyses impossible (Hay 1971, 1976).

Five minerals have been identified in one hornblende granofels sample, namely hornblende, quartz, epidote, opaque, and alkali feldspar. Considering that some hornblende crystals are chloritized, this suggests that the transition phase of the epidote-amphibolite facies where chlorite and epidote react to crystallise into hornblende was not fully reached (Bucher and Grapes 2011). This sample was collected in a seasonal stream channel draining Olongojoo which suggests that in addition to quartzite (Hay 1976), there are granofelsic outcroppings at this inselberg that may grade into amphibolites similarly to Naibor Soit Kubwa (see Chapter 6.6) and Isilale Aratum (Hay 1976). Quartzites, amphibolites, and hornblendic granofels are common rock types in metamorphosed orogenic belts (Bucher and Grapes 2011). The following paragraphs describe each thin section starting with quartzite, meta-granite, feldspar, and hornblende granofels.

DDD1 is a weakly foliated, heteroblastic, coarse-grained quartzite with a mineral assemblage of quartz (90%), muscovite (10%), and alkali feldspar (<1%). Muscovite crystals are either embedded in quartz or interstitial, have a wide grain size variation, and have a random

lineation. Muscovite crystals are responsible for the weak foliation. Alkali feldspar crystals show characteristic tartan twinning.

PPP1 is a non-foliated, heteroblastic, medium-grained quartzite with a mineral assemblage of quartz (95%), muscovite (5%), rutile (<1%), and opaque (<1%). Quartz crystals have sutured boundaries as a result of dynamic recrystallisation primarily stemming from the formation and rotation of sub-grains and/or grain boundary migration (Stipp et al. 2002). Muscovite crystals are either embedded in quartz or interstitial, and have a random lineation. High-relief rutile crystals are concentrated.

RRR1 is a non-foliated, heteroblastic, anhedral coarse-grained quartzite with a mineral assemblage of quartz (90%), muscovite (10%), and rutile (<1%). Quartz crystals have sutured boundaries as a result of dynamic recrystallisation primarily stemming from the formation and rotation of sub-grains and/or grain boundary migration (Stipp et al. 2002). Muscovite crystals are either embedded in quartz or interstitial, and have a parallel lineation. High-relief rutile crystals are concentrated.

SSS1 is a weakly foliated, heteroblastic, anhedral coarse- to medium-grained quartzite with a mineral assemblage of quartz (92%), muscovite (8%), and rutile (<1%). Quartz crystals have sutured boundaries as a result of dynamic recrystallisation primarily stemming from the formation and rotation of sub-grains and/or grain boundary migration (Stipp et al. 2002). Elongate platy muscovite crystals are either embedded in quartz or interstitial, have a parallel lineation, and have a mylonitic foliation. High-relief rutile crystals are not concentrated.

JJJ1 is a spotted, medium-grained meta-monzo-granite with a hypidiomorphic texture and a mineral assemblage of quartz (45%), alkali feldspar (40%), biotite (15%), plagioclase (<1%),

and rutile (<1%). Quartz crystals are primarily monocrystalline and show mild undulatory extinction. Biotite crystals are responsible for the spotted texture.

KKK1 is a weakly foliated, medium- to fine-grained meta-quartz-rich granitoid with a hypidiomorphic texture and a mineral assemblage of quartz (60%), alkali feldspar (20%), biotite (12%), hornblende (6%), and plagioclase (2%). Quartz crystals are primarily monocrystalline and show mild undulatory extinction. Several alkali feldspar crystals have granophyric quartz intergrowths as a result of simultaneous crystal growth. Biotite and hornblende crystals are responsible for the weak foliation.

TTT1 is a spotted (by biotite), fine-grained meta-quartz-rich granitoid with a hypidiomorphic texture and a mineral assemblage of quartz (70%), biotite (10%), plagioclase (10%), alkali feldspar (8%), and opaque (2%). Quartz crystals are primarily monocrystalline and show mild undulatory extinction.

UUU1 is a weakly foliated, medium- to fine-grained meta-quartz-rich granitoid with a hypidiomorphic texture and a mineral assemblage of quartz (70%), biotite (10%), alkali feldspar (10%), plagioclase (5%), opaque (3%), and muscovite (2%). Quartz crystals are primarily monocrystalline, show mild undulatory extinction, and have a primarily granoblastic texture. Biotite and opaque crystals are responsible for the weak foliation.

OOO1 is a fine-grained leucocratic feldspar with a perthitic texture and a mineral assemblage of microcline (73%), albite (25%), hematite (1%), opaque (1%), and sanidine (<1%). Perthitic exsolution lamellae of sodic feldspar exsolved from potassic feldspar are well-defined and visible in hand sample.

III1 is a homeoblastic, fine-grained hornblende granofels with a mineral assemblage of hornblende (50%), quartz (28%), epidote (20%), opaque (2%), and alkali feldspar (<1%) with high

amounts of oxides. This sample lacks a schistose or gneissose texture hence the term granofels (Goldsmith 1959). Some hornblende crystals are chloritized. Quartz crystals are generally euhedral with a granoblastic texture, and minor amounts are slightly deformed.

Table 6.3.1 Gol Mountains: Sample Position, ID, Rock Type, and Visually Estimated Modal Percentages			
Position	**Sample ID**	**Rock Type**	**Mineralogy**
Primary	DDD1	Quartzite	Quartz (90); muscovite (10); alkali feldspar (<1)
	JJJ1	Meta-monzo-granite	Quartz (45); alkali feldspar (40); biotite (15); plagioclase (<1); rutile (<1)
	KKK1	Meta-quartz-rich granitoid	Quartz (60); alkali feldspar (20); biotite (12); hornblende (6); plagioclase (2)
	OOO1	Feldspar	Microcline (73); albite (25); hematite (1); opaque (1); sanidine (<1)
	PPP1	Quartzite	Quartz (95); muscovite (5); rutile (<1); opaque (<1)
	RRR1	Quartzite	Quartz (90); muscovite (10); rutile (<1)
	SSS1	Quartzite	Quartz (92); muscovite (8); rutile (<1)
	TTT1	Meta-quartz-rich granitoid	Quartz (70); biotite (10); plagioclase (10); alkali feldspar (8); opaque (2)
	UUU1	Meta-quartz-rich granitoid	Quartz (70); biotite (10); alkali feldspar (10); plagioclase (5); opaque (3); muscovite (2)
Secondary	III1	Hornblende granofels	Hornblende (50); quartz (28); epidote (20); opaque (2); alkali feldspar (<1)

Chapter 6.4

Granite Falls

Prior studies have identified granite gneiss at this outcrop along with detrital igneous and metamorphic rocks (Hay 1976; Tactikos 2005). Petrographic analyses on granite gneiss have identified five minerals, namely quartz, microcline, plagioclase, biotite, and muscovite (Hay 1976). In this study, five minerals have been identified in granite gneiss samples which correlates with previous studies (Table 6.4.1). Granite gneiss is primarily composed of quartz, alkali feldspar, biotite, muscovite, and plagioclase. Muscovite is an index mineral for low-grade metamorphism and occurs as platy crystals that are either embedded in other crystals or interstitial, and occasionally as microveins within quartz. Biotite is an index mineral for low- to medium-grade metamorphism and is the defining foliation mineral. These two minerals suggest that Granite Falls hosts metamorphosed granitic protoliths of low- to medium-grade. A single variety of granite gneiss is present at Granite Falls which contains between 5-8% muscovite (see Chapter 6.12). The

following paragraphs describe each thin section starting with granite gneiss, nephelinite, and concluding with quartzite.

Granite Falls 1A is a foliated, medium- to fine-grained granite gneiss with a gneissic texture and a mineral assemblage of quartz (50%), alkali feldspar (30%), biotite (15%), muscovite (5%), and plagioclase (<1%). Some quartz crystals are granoblastic and others are highly deformed. Biotite crystals are responsible for the foliation.

Granite Falls 1B is a foliated, medium- to fine-grained granite gneiss with a gneissic texture and a mineral assemblage of quartz (60%), alkali feldspar (20%), biotite (10%), muscovite (8%), and plagioclase (2%). Some quartz crystals are granoblastic and others are highly deformed. Certain deformed quartz crystals have a crack-seal structure filled by muscovite microveins attributed to aseismic and anelastic rock deformation processes. Biotite crystals are responsible for the foliation.

Granite Falls 2 is a weakly foliated, medium- to fine-grained granite gneiss with a gneissic texture and a mineral assemblage of quartz (69%), alkali feldspar (15%), plagioclase (10%), muscovite (5%), and biotite (1%). Some quartz crystals are granoblastic and others are highly deformed. Muscovite crystals are either embedded in other minerals or interstitial and have a wide grain size variation. Biotite crystals are responsible for the weak foliation.

Granite Falls 3A is an inequigranular, weakly aligned, microporphyritic nephelinite with nepheline (5%), opaque (3%), aegirine-augite (<1%), and sanidine (<1%) microphenocrysts embedded in a flow-aligned light-brown groundmass. This sample originates from Sadiman based on mineralogical similarities (Zaitsev et al. 2012).

Granite Falls 3B is an inequigranular, weakly aligned, microporphyritic nephelinite with nepheline (5%), opaque (3%), aegirine-augite (<1%), and sanidine (<1%) microphenocrysts

embedded in a flow-aligned light-brown groundmass. This sample originates from Sadiman based on mineralogical similarities (Zaitsev et al. 2012).

Granite Falls 4A is a weakly foliated, heteroblastic, anhedral medium- to fine-grained quartzite with a mineral assemblage of quartz (95%) and muscovite (5%). Quartz crystals have sutured boundaries as a result of dynamic recrystallisation primarily stemming from the formation and rotation of sub-grains and/or grain boundary migration (Stipp et al. 2002). Muscovite crystals are either embedded in quartz or interstitial, have a parallel lineation, and have a mylonitic foliation evidenced by lozenge-shaped crystals and trails of muscovite fragments. This sample is of unknown provenance.

Granite Falls 4B is a weakly foliated, heteroblastic, anhedral medium- to fine-grained quartzite with a mineral assemblage of quartz (95%) and muscovite (5%). Quartz crystals have sutured boundaries as a result of dynamic recrystallisation primarily stemming from the formation and rotation of sub-grains and/or grain boundary migration (Stipp et al. 2002). Muscovite crystals are either embedded in quartz or interstitial, have a parallel lineation, and have a mylonitic foliation evidenced by lozenge-shaped crystals and trails of muscovite fragments. This sample is of unknown provenance.

Table 6.4.1 Granite Falls: Sample Position, ID, Rock Type, and Visually Estimated Modal Percentages

Position	Sample ID	Rock Type	Mineralogy
Primary	Granite Falls 1A	Granite gneiss	Quartz (50); alkali feldspar (30); biotite (15); muscovite (5); plagioclase (<1)
	Granite Falls 1B	Granite gneiss	Quartz (60); alkali feldspar (20); biotite (10); muscovite (8); plagioclase (2)
	Granite Falls 2	Granite gneiss	Quartz (69); alkali feldspar (15); plagioclase (10); muscovite (5); biotite (1)
Secondary	Granite Falls 3A	Nephelinite	Nepheline (5); opaque (3); aegirine-augite (<1); sanidine (<1)
	Granite Falls 3B	Nephelinite	Nepheline (5); opaque (3); aegirine-augite (<1); sanidine (<1)
	Granite Falls 4A	Quartzite	Quartz (95); muscovite (5)
	Granite Falls 4B	Quartzite	Quartz (95); muscovite (5)

Modes for nephelinites are for phenocrysts.

Chapter 6.5

Kelogi

Prior studies have identified granite gneiss at this outcrop and corresponding petrographic analyses have identified seven minerals, namely quartz, orthoclase, albite, aegirine, amphibole (hornblende), biotite, and garnet (Hay 1976; Kyara 1999). In this study, eight minerals have been identified in granite gneiss, namely quartz, aegirine, plagioclase, hornblende, alkali feldspar, hematite, titanite, and biotite (Table 6.5.1). Titanite was previously unrecognised and is a common accessory mineral in igneous rocks. Quartz crystals commonly show undulatory extinction. Hornblende and aegirine are the defining foliation minerals that are responsible for the gneissose texture. Present in one sample, biotite is an index mineral for low- to medium-grade metamorphism. The mineral and textural data suggest that Kelogi hosts metamorphosed granitic protoliths. Based on textural and mineralogical differences between three samples in primary position, there are as a minimum two varieties of granite gneiss, one quartz-rich variety and a second foliated quartz-poor variety (see Chapter 6.12). The following paragraphs describe each thin section starting with granite gneiss and concluding with quartzite.

Kelogi 1 is a spotted, medium-grained granite gneiss with a mineral assemblage of quartz (40%), aegirine (20%), plagioclase (15%), alkali feldspar (15%), and hornblende (10%) with low amounts of oxides. The oxides are concentrated near the cortical surface indicative of weathering processes. Quartz crystals are anhedral and show undulatory extinction. Aegirine and hornblende crystals are responsible for the spotted texture.

Kelogi 3 is a weakly foliated, medium-grained granite gneiss with a mineral assemblage of quartz (45%), aegirine (20%), hornblende (12%), plagioclase (12%), alkali feldspar (3%), and

hematite (8%). Quartz crystals are anhedral and show undulatory extinction. Aegirine and hornblende crystals are responsible for the weak foliation.

Kelogi 10 is a foliated, medium- to fine-grained gneissose granite gneiss with a mineral assemblage of plagioclase (25%), quartz (25%), hornblende (20%), aegirine (20%), alkali feldspar (10%), titanite (<1%), and biotite (<1%). Quartz crystals are anhedral and show undulatory extinction (Figure 6.5.1). Hornblende crystals are responsible for the foliated texture. Since this sample contains stark differences in felsic and mafic minerals, a non-representative photomicrograph was taken under PPL and converted to an 8-bit greyscale image and quantitatively analysed for its mode in ImageJ (Figure 6.5.2). Under PPL, plagioclase and quartz are colourless, and hornblende and aegirine appear yellow/brown/green due to intense pleochroism. By selecting greyscale values between 0-61, the mode for hornblende and aegirine is 23.34% while the mode for plagioclase and quartz is 76.66%. By comparing the visually estimated modes with the automated ones, the values obtained for felsic and mafic minerals are highly inaccurate. The major issue that was encountered with this automated technique is that 8-bit values are not fully exclusive as certain minerals are highly pleochroic, particularly hornblende and aegirine, thereby making this technique of limited use to accurately and precisely determine modal abundances without testing different parameters.

Kelogi 9 is a mylonitised, fine-grained quartzite with a mineral assemblage quartz (86%), biotite (8%), muscovite (5%), and opaque (1%). Quartz crystals are anhedral and show undulatory extinction. Muscovite crystals are either embedded in quartz or interstitial and have a parallel lineation. Muscovite and biotite are together indicative of a low- to medium-grade metamorphosed sandstone. This sample originates from Endonyo Okule based on mineralogical similarities (Hay 1976:Table 6).

Table 6.5.1 Kelogi: Sample Position, ID, Rock Type, and Visually Estimated Modal Percentages			
Position	**Sample ID**	**Rock Type**	**Mineralogy**
Primary	Kelogi 1	Granite gneiss	Quartz (40); aegirine (20); plagioclase (15); alkali feldspar (15); hornblende (10)
	Kelogi 3	Granite gneiss	Quartz (45); aegirine (20); hornblende (12); plagioclase (12); hematite (8); alkali feldspar (3)
	Kelogi 10	Granite gneiss	Plagioclase (25); quartz (25); hornblende (20); aegirine (20); alkali feldspar (10); titanite (<1); biotite (<1)
Secondary	Kelogi 9	Quartzite	Quartz (86); biotite (8); muscovite (5); opaque (1)

Modes for Kelogi 1 and 3 are based on point counts instead of visual estimates (see Table 5.3.2).

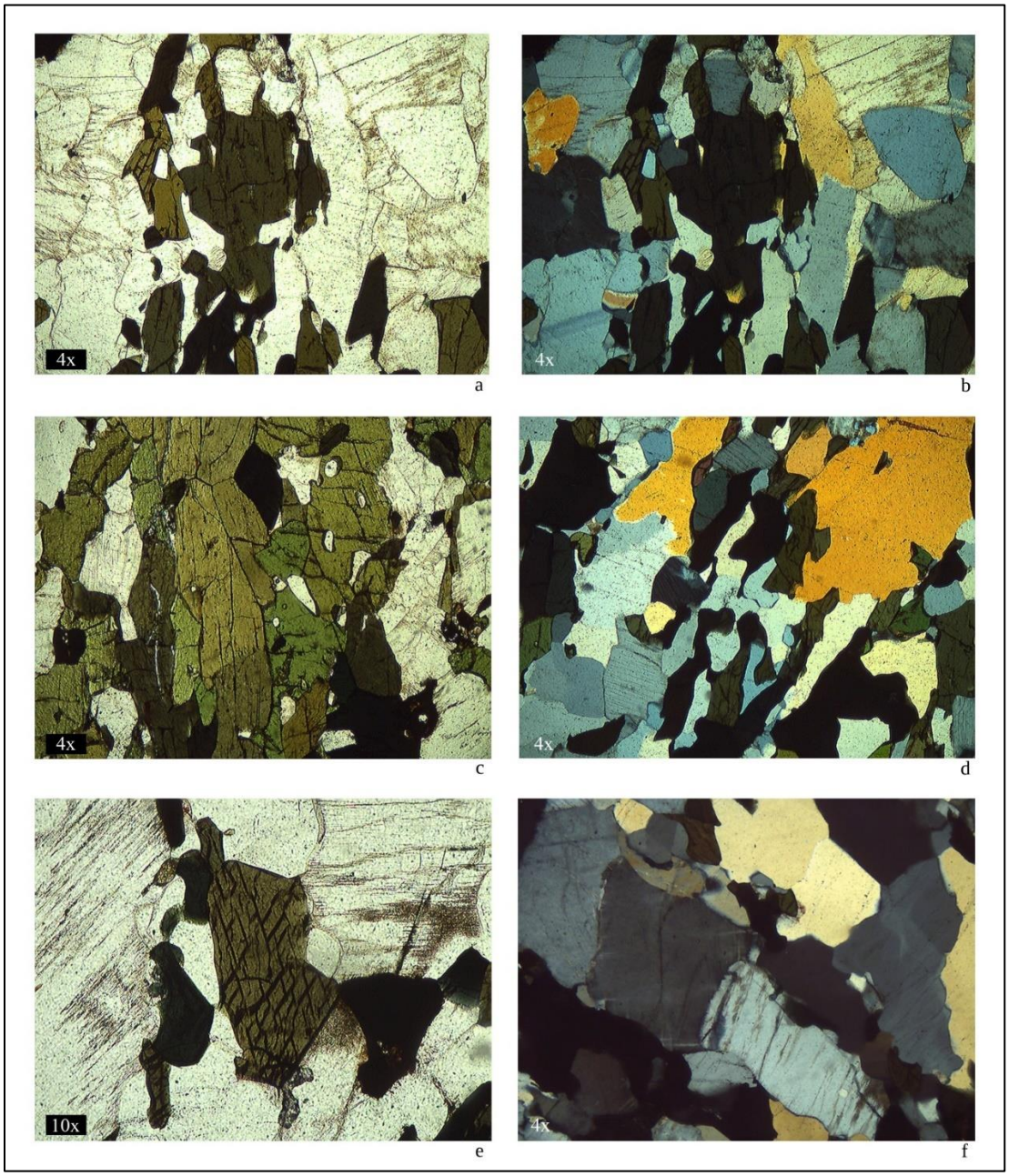

Figure 6.5.1. Kelogi 10: (a) foliation defined by hornblende in PPL; (b) same as (a) in XP, plagioclase and quartz are also visible; (c) hornblende and aegirine in PPL; (d) plagioclase, quartz, hornblende, and aegirine in XP; (e) hornblende with characteristic 56° and 124° cleavage angles in PPL; (f) alkali feldspar with characteristic tartan twinning in XP.

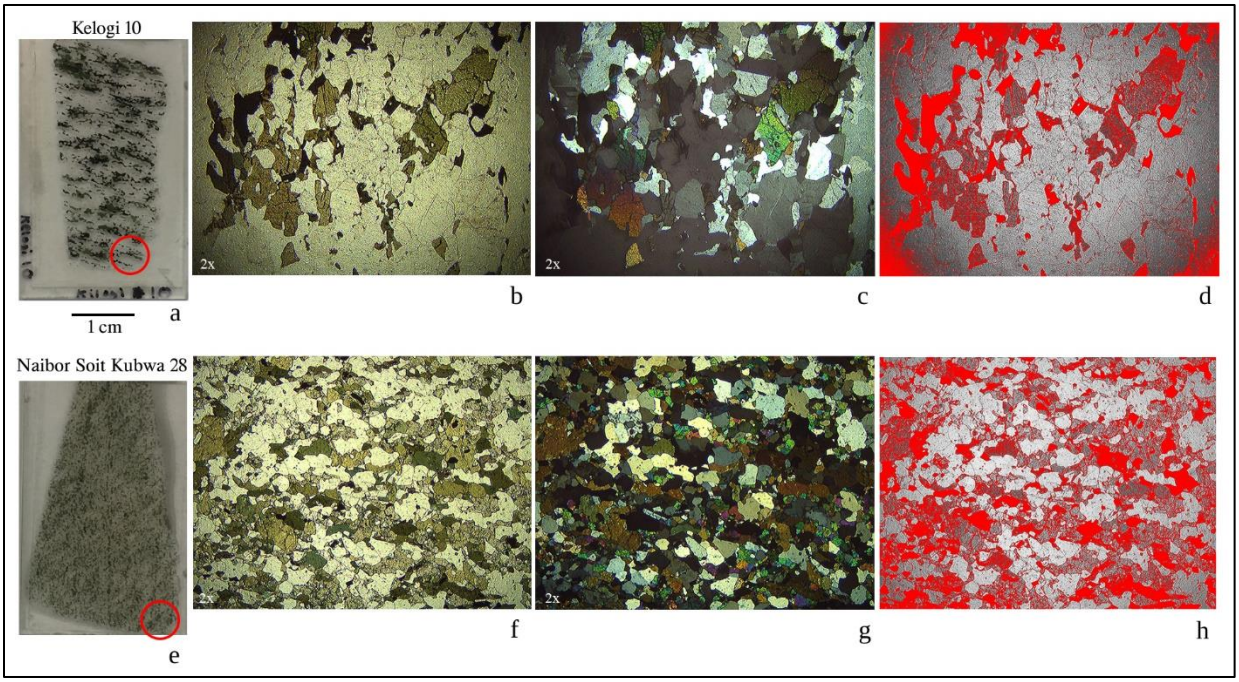

Figure 6.5.2. (a) Kelogi 10, red circle represents the area of the photomicrograph in (b); (b) PPL photomicrograph; (c) same as (b) in XP; (d) greyscale photomicrograph in PPL of Kelogi 10, hornblende and aegirine are in red, poor shading on contours turned quartz to red; (e) Naibor Soit Kubwa 28, red circle represents the of the photomicrograph in (f); (f) PPL photomicrograph; (g) same as (f) in XP; (h) greyscale photomicrograph in PPL of Naibor Soit Kubwa 28, hornblende and epidote are in red since greyscale values are not fully discriminatory.

Chapter 6.6

Naibor Soit Kubwa

Prior studies have identified gneiss and quartzite at this outcrop and corresponding petrographic analyses on coarse-grained quartzite have identified two minerals, namely quartz and muscovite (Hay 1976; Kyara 1999; McHenry and de la Torre 2018; Tactikos 2005). In this study, seven minerals have been identified in fifteen quartzite samples (Table 6.6.1) that are predominantly coarse-grained (Table 6.11.1). Quartzite is primarily composed of quartz along with smaller crystals of muscovite and rutile, and rare occurrences of hematite, opaque, fuchsite, and magnetite. Muscovite is an index mineral for low-grade metamorphism and occurs as crystals that are either embedded in quartz or interstitial. Muscovite crystals primarily have a parallel to sub-

parallel lineation as a result of bidirectional pressure and rarely have a random lineation. Rare occurrences of fuchsite, a chromium-rich variety of muscovite, occur as small crystals that are either embedded in quartz or interstitial. Rutile is a common detrital mineral in many quartzite samples. Hematite generally occurs interstitial to quartz and predominantly formed by the infiltration of oxides between inter-granular pores and foliation planes. Hematite was also likely formed, in part, by the weathering of magnetite, the latter having originally replaced hematite during prograde regional metamorphism. Altogether, the mineral assemblages of quartzite suggest that its petrogenesis was the result of low-grade metamorphism of a sandstone protolith although no relict sedimentary textures were observed, apart from one sample (Naibor Soit Kubwa 24). Based on textural and mineralogical differences between fifteen samples, there are as a minimum two varieties of quartzite at this outcrop (see Chapter 6.11). The first variety contains, on average, 95% quartz, 5% muscovite, and a presence or absence of accessory minerals such as rutile, opaque, fuchsite, hematite, and magnetite. The second variety contains, on average, 80% quartz, 20% muscovite, and a presence or absence of accessory minerals such as rutile, fuchsite, and hematite.

Six minerals have been identified in one quartz amphibolite sample obtained from a previously unrecorded meta-basitic dyke protruding through the top of the quartzite-dominated inselberg. The mineral assemblage of hornblende, epidote, quartz, opaque, plagioclase, and calcite are indexical of the epidote-amphibolite facies in which a basaltic protolith metamorphosed into amphibolite. Metamorphic processes may have impacted surrounding quartz-rich lithologies which may explain the high proportion of quartz and the presence of foliation-parallel quartz veins in hand sample. The following paragraphs describe each thin section starting with quartzite and concluding with quartz amphibolite.

Naibor Soit Kubwa N042 is a weakly foliated, heteroblastic, coarse-grained quartzite with a mineral assemblage of quartz (85%), muscovite (15%), and hematite (<1%). Muscovite crystals are either embedded in quartz or interstitial, have a parallel lineation, and are responsible for the weak foliation. Hematite crystals are interstitial to quartz.

Naibor Soit Kubwa E039 is a weakly foliated, heteroblastic, coarse-grained quartzite with a mineral assemblage of quartz (92%) and muscovite (8%). Quartz crystals have sutured boundaries as a result of dynamic recrystallisation primarily stemming from the formation and rotation of sub-grains and/or grain boundary migration (Stipp et al. 2002). Muscovite crystals are either embedded in quartz or interstitial, have a parallel lineation, and are responsible for the weak foliation.

Naibor Soit Kubwa S06 is a non-foliated, heteroblastic, coarse-grained quartzite with a mineral assemblage of quartz (95%) and muscovite (5%). Quartz crystals have sutured boundaries as a result of dynamic recrystallisation primarily stemming from the formation and rotation of sub-grains and/or grain boundary migration (Stipp et al. 2002). Muscovite crystals are either embedded in quartz or interstitial, and have a sub-parallel lineation.

Naibor Soit Kubwa 1 is a non-foliated, heteroblastic, anhedral medium-grained quartzite with a mineral assemblage of quartz (93%), muscovite (5%), hematite (1%), and rutile (1%). Muscovite crystals are either embedded in quartz or interstitial, and have a parallel lineation. High-relief rutile crystals are embedded in quartz and not concentrated. Hematite crystals are interstitial to quartz. Based on energy dispersive X-ray spectroscopic data (Abtosway 2018), the value of one major element (TiO_2=0.014) measured as oxides in weight % is likely, in part, attributable to the presence of rutile (TiO_2).

Naibor Soit Kubwa 2 is a weakly foliated, heteroblastic, anhedral medium-grained quartzite with a mineral assemblage of quartz (95%), muscovite (5%), rutile (<1%), and opaque (<1%). Quartz crystals have sutured boundaries as a result of dynamic recrystallisation primarily stemming from the formation and rotation of sub-grains and/or grain boundary migration (Stipp et al. 2002). Muscovite crystals are either embedded in quartz or interstitial, have a parallel lineation, and are responsible for the weak foliation. High-relief rutile crystals are embedded in quartz and not concentrated.

Naibor Soit Kubwa 6 is a weakly foliated, heteroblastic, anhedral medium-grained quartzite with a mineral assemblage of quartz (92%), muscovite (5%), rutile (1%), opaque (1%), and fuchsite (1%). Quartz crystals have sutured boundaries as a result of dynamic recrystallisation primarily stemming from the formation and rotation of sub-grains and/or grain boundary migration (Stipp et al. 2002). Muscovite crystals are either embedded in quartz or interstitial, have a parallel lineation, and are responsible for the weak foliation. Fuchsite crystals are either embedded in quartz or interstitial, and have a parallel lineation. High-relief rutile crystals are embedded in quartz and not concentrated.

Naibor Soit Kubwa 8 is a non-foliated, heteroblastic, anhedral coarse-grained quartzite with a mineral assemblage of quartz (94%), muscovite (6%), opaque (<1%), and rutile (<1%). Quartz crystals have sutured boundaries as a result of dynamic recrystallisation primarily stemming from the formation and rotation of sub-grains and/or grain boundary migration (Stipp et al. 2002). Muscovite crystals are either embedded in quartz or interstitial, and have a parallel lineation. A single high-relief rutile crystal is embedded in quartz.

Naibor Soit Kubwa 11 is a non-foliated, heteroblastic, anhedral coarse-grained quartzite with a mineral assemblage of quartz (98%), muscovite (2%), and rutile (<1%). Muscovite crystals

are either embedded in quartz or interstitial, and have a random lineation. A single high-relief rutile crystal is embedded in quartz.

Naibor Soit Kubwa 13 is a non-foliated, heteroblastic, anhedral coarse-grained quartzite with a mineral assemblage of quartz (92%), muscovite (8%), and rutile (<1%). Muscovite crystals are either embedded in quartz or interstitial, have a sub-parallel lineation, and have a larger grain size than all other quartzite samples. Based on energy dispersive X-ray spectroscopic data (Abtosway 2018), values for certain major elements (Al_2O_3=3.303; K_2O=0.007) measured as oxides in weight % are likely, in part, attributable to the high modal abundance of muscovite ($KAl_2(Si_3AlO_{10})(OH)_2$).

Naibor Soit Kubwa 14 is a non-foliated, heteroblastic, anhedral coarse-grained quartzite with a mineral assemblage of quartz (92%) and muscovite (8%). Platy muscovite crystals are either embedded in quartz or interstitial, and have a parallel lineation.

Naibor Soit Kubwa 24 is a non-foliated, heteroblastic, anhedral coarse- to fine-grained quartzite with a mineral assemblage of quartz (99%), muscovite (1%), and opaque (<1%). Quartz crystals are granoblastic in the fine-grained sector. Muscovite crystals are either embedded in quartz or interstitial, and have a parallel lineation. Muscovite crystals are also are concentrated in the coarse-grained quartz sector where the latter show undulatory extinction. Therefore, the muscovite-poor fine-grained sector may be a protolith relict texture.

Naibor Soit Kubwa 27 is a foliated, heteroblastic, micaceous coarse- to fine-grained quartzite with a mineral assemblage of quartz (70%) and muscovite (30%). Variably sized quartz crystals indicate a textural immaturity likely the result of the metamorphism of a poorly sorted protolith. Platy muscovite crystals are either embedded in quartz or interstitial, have a parallel lineation, and are responsible for the foliated texture. Based on energy dispersive X-ray

spectroscopic data (Abtosway 2018), relatively elevated values for certain major elements (Al_2O_3=4.752; K_2O=0.291) measured as oxides in weight % are likely, in part, attributable to the high modal abundance of muscovite ($KAl_2(Si_3AlO_{10})(OH)_2$).

Naibor Soit Kubwa 31 is a weakly foliated, heteroblastic, anhedral coarse-grained quartzite with a mineral assemblage of quartz (92%) and muscovite (8%). Quartz crystals have sutured boundaries as a result of dynamic recrystallisation primarily stemming from the formation and rotation of sub-grains and/or grain boundary migration (Stipp et al. 2002). Muscovite crystals are either embedded in quartz or interstitial, have a parallel lineation, and are responsible for the weak foliation.

Naibor Soit Kubwa 32 is a non-foliated, heteroblastic, anhedral coarse- to medium-grained quartzite with a mineral assemblage of quartz (85%), muscovite (14%), rutile (1%), and fuchsite (<1%) with low amounts of oxides. Quartz crystals have sutured boundaries as a result of dynamic recrystallisation primarily stemming from the formation and rotation of sub-grains and/or grain boundary migration (Stipp et al. 2002). Platy and plumose muscovite crystals are either embedded in quartz or interstitial, and have a sub-parallel lineation. Plumose and acicular muscovite crystals superficially resemble sillimanite and rutile crystals. Platy fuchsite crystals are embedded in quartz, and have a sub-parallel lineation (Figure 6.6.1). Based on energy dispersive X-ray spectroscopic data (Abtosway 2018), relatively elevated values for certain major elements (Al_2O_3=3.472; K_2O=0.029) measured as oxides in weight % are likely, in part, attributable to the high modal abundance of muscovite ($KAl_2(Si_3AlO_{10})(OH)_2$). The value of one major element (TiO_2=0.036) is likely, in part, attributable to the presence of rutile (TiO_2).

Naibor Soit Kubwa 33 is a weakly foliated, homeoblastic, anhedral coarse-grained quartzite with a mineral assemblage of quartz (97%), muscovite (3%), and magnetite (<1%). Small fine-

grained quartz intergrowths are also present. Quartz crystals have sutured boundaries as a result of dynamic recrystallisation primarily stemming from the formation and rotation of sub-grains and/or grain boundary migration (Stipp et al. 2002). Muscovite crystals are either embedded in quartz or interstitial, have a sub-parallel lineation, and are responsible for the weak foliation. Magnetite crystals are interstitial to quartz (Figure 6.6.2).

Naibor Soit Kubwa 28 is a foliated, fine-grained gneissose quartz amphibolite with a mineral assemblage of hornblende (40%), epidote (32%), quartz (24%), opaque (3%), plagioclase (1%), and calcite (<1%). Hornblende crystals are responsible for the foliated texture, are highly pleochroic, and display characteristic 56° and 124° cleavage angles (Figure 6.6.3). Since this sample contains stark differences in felsic and mafic minerals, a non-representative photomicrograph was taken under PPL and converted to an 8-bit greyscale image and quantitatively analysed for its mode in ImageJ (Figure 6.5.2). Under PPL, quartz and plagioclase are colourless, epidote crystals are cloudy, hornblende crystals are green/yellow due to intense pleochroism, and opaque minerals are black. By selecting greyscale values between 0-84, the mode for hornblende and opaque minerals is 33.56% while the mode for epidote, quartz, and plagioclase is 66.44%. By comparing the visually-estimated modes with the automated ones, the values obtained for felsic minerals are relatively comparable. However, the values obtained for mafic minerals are not accurate. The major issue that was encountered with this automated technique is that 8-bit values are not fully exclusive as certain minerals are highly pleochroic, particularly hornblende, thereby making this technique of limited use to accurately and precisely determine modal abundances without testing different parameters.

Table 6.6.1 Naibor Soit Kubwa: Sample Position, ID, Rock Type, and Visually Estimated Modal Percentages			
Position	**Sample ID**	**Rock Type**	**Mineralogy**
Primary	Naibor Soit Kubwa N042	Quartzite	Quartz (85); muscovite (15); hematite (<1)
	Naibor Soit Kubwa E039	Quartzite	Quartz (92); muscovite (8)
	Naibor Soit Kubwa S06	Quartzite	Quartz (95); muscovite (5)
	Naibor Soit Kubwa 1	Quartzite	Quartz (93); muscovite (5); hematite (1); rutile (1)
	Naibor Soit Kubwa 2	Quartzite	Quartz (95); muscovite (5); rutile (<1); opaque (<1)
	Naibor Soit Kubwa 6	Quartzite	Quartz (92); muscovite (5); rutile (1); opaque (1); fuchsite (1)
	Naibor Soit Kubwa 8	Quartzite	Quartz (94); muscovite (6); opaque (<1); rutile (<1)
	Naibor Soit Kubwa 11	Quartzite	Quartz (98); muscovite (2); rutile (<1)
	Naibor Soit Kubwa 13	Quartzite	Quartz (92); muscovite (8); rutile (<1)
	Naibor Soit Kubwa 14	Quartzite	Quartz (92); muscovite (8)
	Naibor Soit Kubwa 24	Quartzite	Quartz (99); muscovite (1); opaque (<1)
	Naibor Soit Kubwa 27	Quartzite	Quartz (70); muscovite (30)
	Naibor Soit Kubwa 28	Quartz amphibolite	Hornblende (40); epidote (32); quartz (24); opaque (3); plagioclase (1); calcite (<1)
	Naibor Soit Kubwa 31	Quartzite	Quartz (92); muscovite (8)
	Naibor Soit Kubwa 32	Quartzite	Quartz (85); muscovite (14); rutile (1); fuchsite (<1)
	Naibor Soit Kubwa 33	Quartzite	Quartz (97); muscovite (3); magnetite (<1)

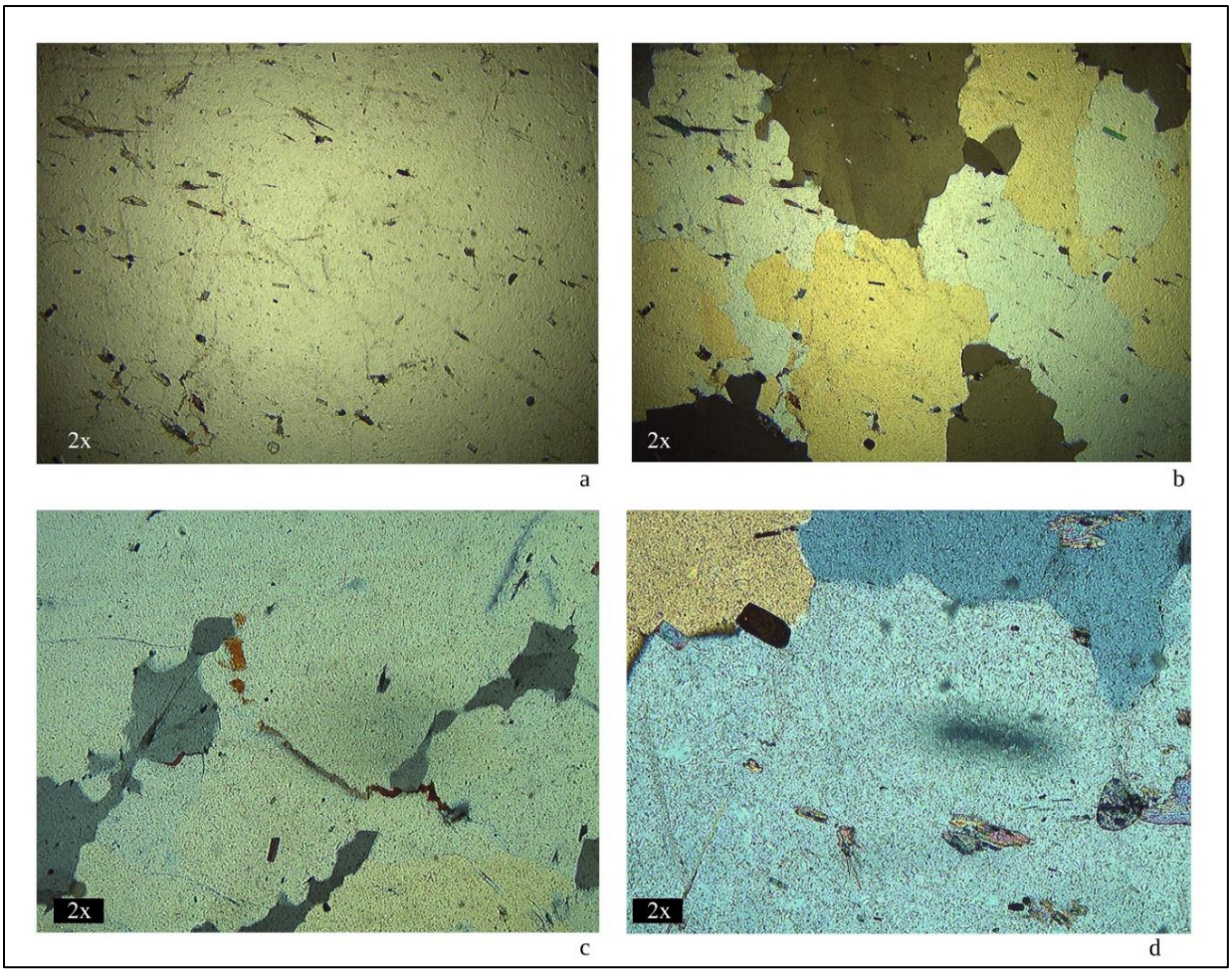

Figure 6.6.1. Naibor Soit Kubwa 32: (a) sub-parallel muscovite crystals with a plumose and acicular habit in PPL; (b) same as (a) in XP, quartz crystals show undulatory extinction and sutured boundaries; (c) rutile crystals in XP; (d) idioblastic rutile crystal in XP.

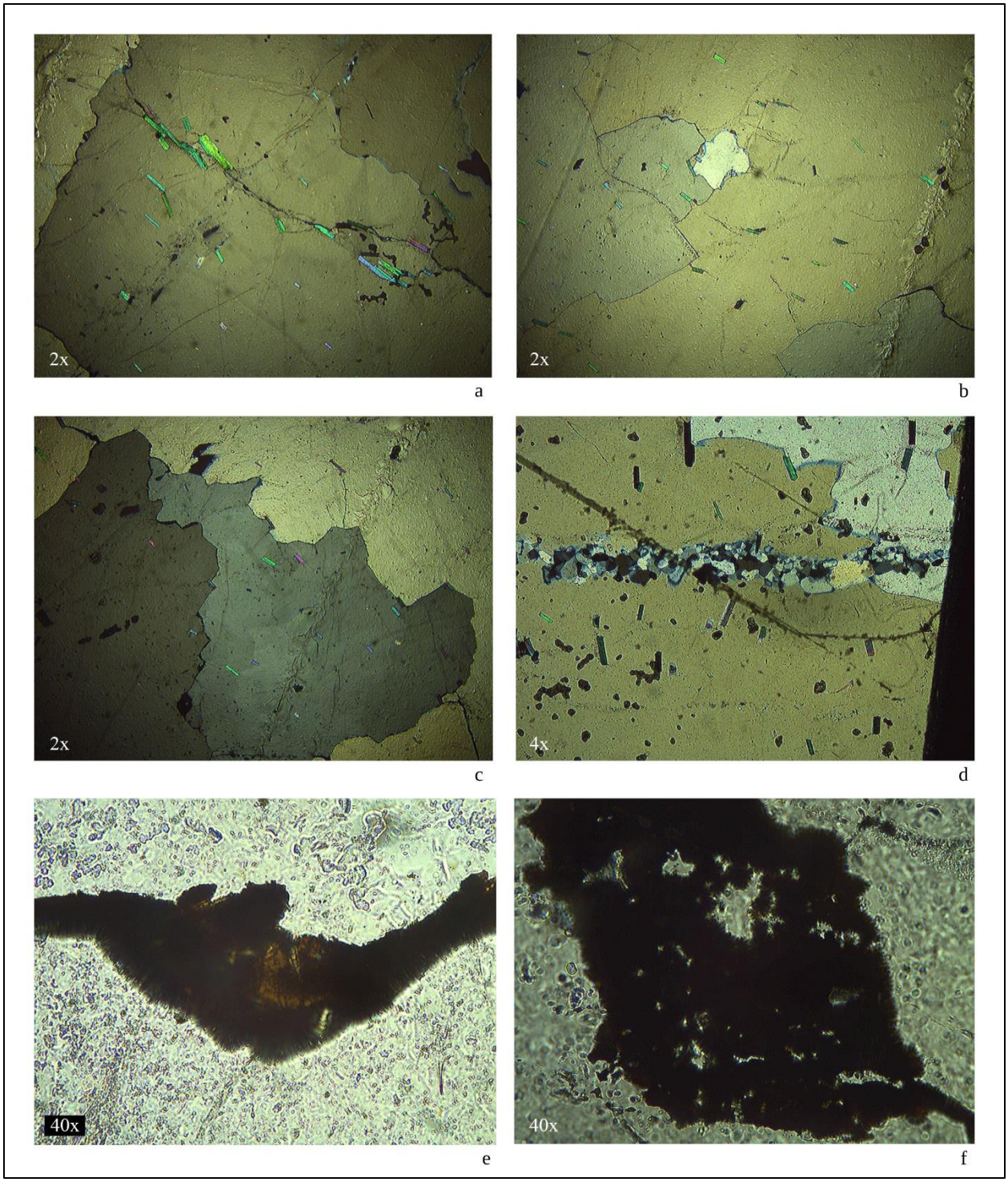

Figure 6.6.2. Naibor Soit Kubwa 33: (a) sub-parallel muscovite crystals embedded in quartz or interstitial in XP; (b) similar to (a) in XP; (c) quartz crystals show undulatory extinction and sutured boundaries in XP; (d) fine-grained quartz intergrowth in XP; (e) magnetite crystal with dark metallic lustre and a dendritic habit in PPL; (f) similar to (e) in PPL.

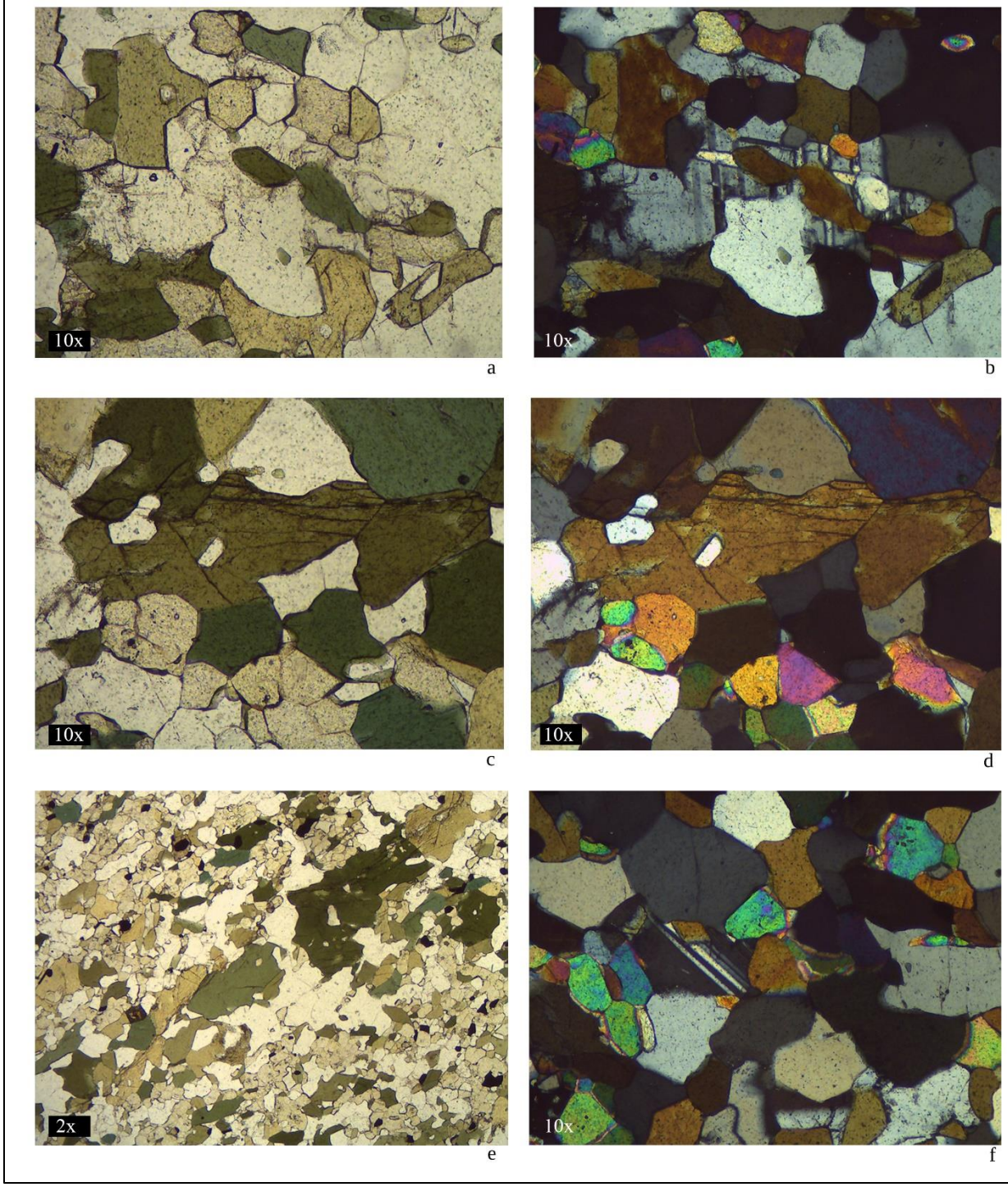

Figure 6.6.3. Naibor Soit Kubwa 28: (a) calcite crystal surrounded by pleochroic hornblende, cloudy epidote, and colourless quartz in PPL; (b) same as (a) in XP, note calcite's twin planes parallel to its long axis; (c) hornblende with characteristic 56° and 124° cleavage angles in PPL; (d) same as (c) in XP, note the high interference colours for epidote crystals; (e) foliation defined by hornblende in PPL; (f) plagioclase crystal with characteristic polysynthetic twinning in XP.

Chapter 6.7

Naibor Soit Ndogo

Prior studies have identified quartzite at this outcrop although no corresponding petrographic analyses have been undertaken (Hay 1976; Kyara 1999; Leakey 1965; Santonja et al. 2014). In this study, six minerals have been identified in five quartzite samples, all of which were previously unrecognised (Table 6.7.1). Quartzite is coarse-grained and primarily composed of quartz along with smaller crystals of muscovite, and rare occurrences of fuchsite, opaque, rutile, and hematite. Muscovite is an index mineral for low-grade metamorphism and occurs as platy crystals that are either embedded in quartz or interstitial. Muscovite crystals generally have a parallel to sub-parallel lineation as a result of bidirectional pressure. Rare occurrences of fuchsite, a chromium-rich variety of muscovite, occur as small crystals that are either embedded in quartz or interstitial. Rutile is a rare accessory mineral and hematite generally occurs interstitial to quartz. Altogether, the mineral assemblages of quartzite suggest that its petrogenesis was the result of low-grade metamorphism of a sandstone protolith although no relict sedimentary textures were observed. Based on textural and mineralogical differences between five samples, there are as a minimum two varieties of quartzite at this outcrop (see Chapter 6.11), one fuchsite-bearing variety and a second variety that contains no fuchsite. The following paragraphs describe each thin section.

Naibor Soit Ndogo 6A is a non-foliated, heteroblastic, coarse-grained quartzite with a mineral assemblage of quartz (95%) and muscovite (5%). Quartz crystals have sutured boundaries as a result of dynamic recrystallisation primarily stemming from the formation and rotation of sub-grains and/or grain boundary migration (Stipp et al. 2002). Platy muscovite crystals are either embedded in quartz or interstitial, and have a sub-parallel lineation. Muscovite crystals are occasionally lozenge-shaped, and show fragmented trails.

Naibor Soit Ndogo 6B is a non-foliated, heteroblastic, coarse-grained quartzite with a mineral assemblage of quartz (95%) and muscovite (5%). Quartz crystals have sutured boundaries as a result of dynamic recrystallisation primarily stemming from the formation and rotation of sub-grains and/or grain boundary migration (Stipp et al. 2002). Platy muscovite crystals are either embedded in quartz or interstitial, and have a sub-parallel lineation. Muscovite crystals are occasionally lozenge-shaped, show fragmented trails, and form bookshelf-sliding microstructures.

Naibor Soit Ndogo 8 is a weakly foliated, heteroblastic, coarse-grained quartzite with a mineral assemblage of quartz (98%) and muscovite (2%). Quartz crystals have sutured boundaries as a result of dynamic recrystallisation primarily stemming from the formation and rotation of sub-grains and/or grain boundary migration (Stipp et al. 2002). Platy muscovite crystals are either embedded in quartz or interstitial, have a parallel lineation, and are responsible for the weak foliation.

Naibor Soit Ndogo 13 is a weakly foliated, heteroblastic, coarse-grained quartzite with a mineral assemblage of quartz (96%), muscovite (3%), fuchsite (1%), rutile (<1%), and opaque (<1%). Quartz crystals have sutured boundaries as a result of dynamic recrystallisation primarily stemming from the formation and rotation of sub-grains and/or grain boundary migration (Stipp et al. 2002). Platy muscovite and fuchsite crystals are either embedded in quartz or interstitial, have a parallel lineation, and are responsible for the weak foliation (Figure 6.7.1). Based on energy dispersive X-ray spectroscopic data (Abtosway 2018), the value of one major element (TiO_2=0.015) measured as oxides in weight % is likely, in part, attributable to the presence of rutile (TiO_2).

Naibor Soit Ndogo 14 is a weakly foliated, homeoblastic, anhedral coarse-grained quartzite with a mineral assemblage of quartz (98%), muscovite (2%), and fuchsite (<1%). Platy muscovite

and fuchsite crystals are either embedded in quartz or interstitial, have a parallel lineation, and are responsible for the weak foliation (Figure 6.7.2).

Naibor Soit Ndogo 15 is a weakly foliated, heteroblastic, coarse-grained quartzite with a mineral assemblage of quartz (95%), muscovite (5%), opaque (<1%), hematite (<1%), and rutile (<1%). Quartz crystals have sutured boundaries as a result of dynamic recrystallisation primarily stemming from the formation and rotation of sub-grains and/or grain boundary migration (Stipp et al. 2002). Platy muscovite crystals are either embedded in quartz or interstitial, have a parallel lineation, and are responsible for the weak foliation. Muscovite crystals are occasionally lozenge-shaped, and show fragmented trails. Based on energy dispersive X-ray spectroscopic data (Abtosway 2018), the value of one major element (TiO_2=0.015) measured as oxides in weight % is likely, in part, attributable to the presence of rutile (TiO_2).

Table 6.7.1 Naibor Soit Ndogo: Sample Position, ID, Rock Type, and Visually Estimated Modal Percentages

Position	Sample ID	Rock Type	Mineralogy
Primary	Naibor Soit Ndogo 6A	Quartzite	Quartz (95); muscovite (5)
	Naibor Soit Ndogo 6B	Quartzite	Quartz (95); muscovite (5)
	Naibor Soit Ndogo 8	Quartzite	Quartz (98); muscovite (2)
	Naibor Soit Ndogo 13	Quartzite	Quartz (96); muscovite (3); fuchsite (1); rutile (<1); opaque (<1)
	Naibor Soit Ndogo 14	Quartzite	Quartz (98); muscovite (2); fuchsite (<1)
	Naibor Soit Ndogo 15	Quartzite	Quartz (95); muscovite (5); opaque (<1); hematite (<1); rutile (<1)

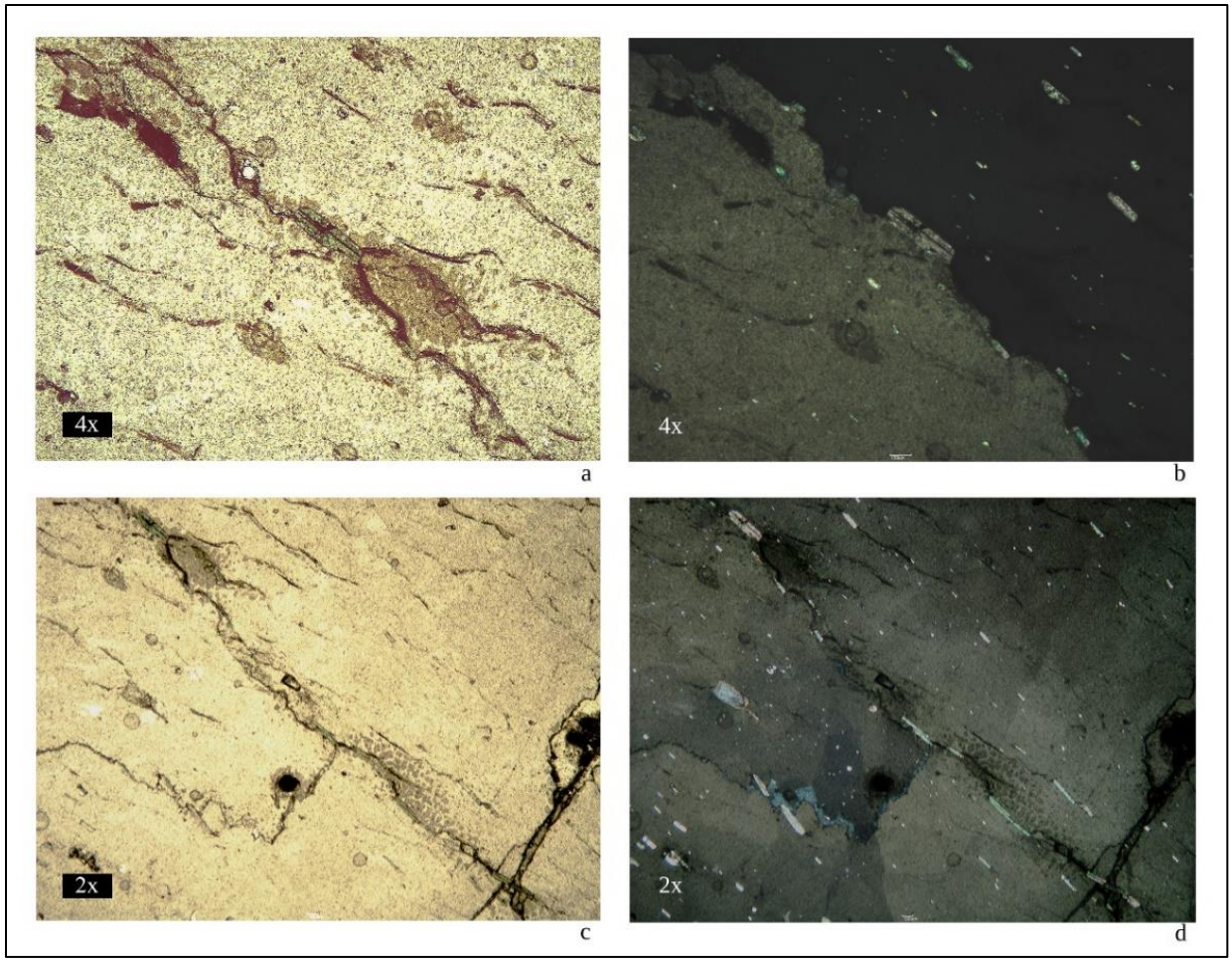

Figure 6.7.1. Naibor Soit Ndogo 13 (thin section was damaged while processing hence the cracks and uneven surface): (a) green fuchsite crystal in centre under PPL; (b) same as (a) in XP; (c) pale green fuchsite crystals and colourless muscovite embedded in quartz and interstitial in PPL; (d) same as (c) in XP.

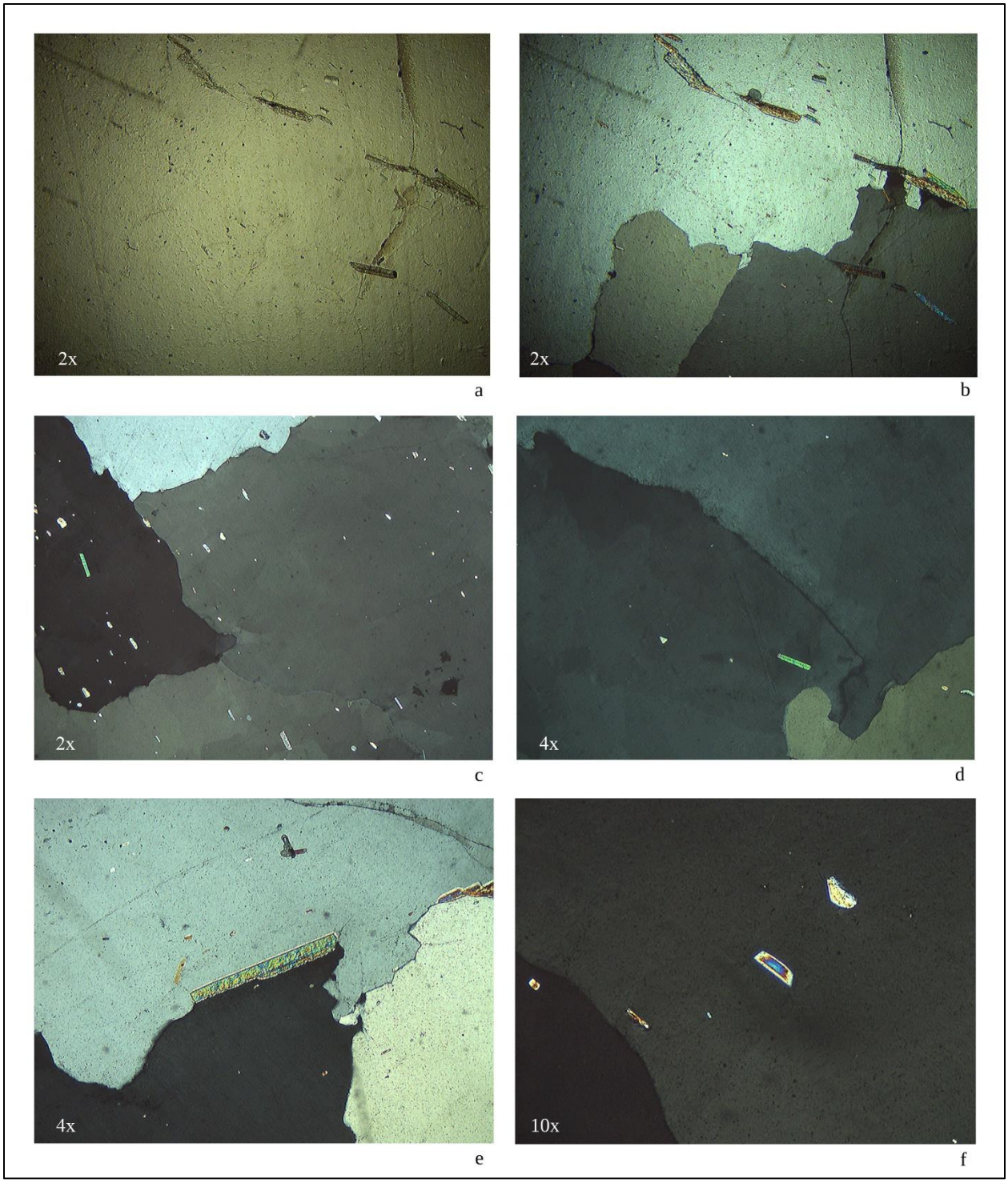

Figure 6.7.2. Naibor Soit Ndogo 14: (a) sub-parallel muscovite crystals embedded in quartz or interstitial in PPL; (b) same as (a) in XP; (c) quartz crystals show undulatory extinction in XP; (d) similar to (c) in XP; (e) interstitial muscovite crystal in XP; (f) zoned muscovite crystal in XP.

Chapter 6.8

Naisiusiu

Prior studies have identified granite gneiss and quartzite at this outcrop. Corresponding petrographic analyses on quartzite have identified six minerals, namely quartz, microcline, muscovite, garnet, kyanite, and staurolite (Hay 1976; Kyara 1999; McHenry and de la Torre 2018; Tactikos 2005). In this study, seven minerals have been identified in five quartzite samples that generally have bimodal grain sizes. Mineralogically, these samples are composed of quartz, chloritized biotite, muscovite, chlorite, opaque, hematite, and calcite (Table 6.8.1). Muscovite is an index mineral for low-grade metamorphism and occurs as platy crystals that are either embedded in quartz or interstitial, and have a parallel to random lineation while chloritized biotite is indicative of retrograde metamorphism. Variably sized quartz grains indicate a textural immaturity and together with quartz overgrowths and interstitial cement, suggest that the quartzite at Naisiusiu is a metamorphosed, poorly-sorted, sandstone protolith. Based on textural and mineralogical differences between five samples, there are as a minimum two varieties of quartzite at this outcrop (see Chapter 6.11). The first variety contains, on average, 90% quartz along with minor amounts of chloritized biotite, chlorite, muscovite, opaque, and calcite. The second variety contains, on average, 95% quartz, 4% muscovite, and a presence or absence of accessory minerals such as hematite and opaque.

Prior studies on granite gneiss have identified seven minerals, namely quartz, microcline, plagioclase, aegirine, hornblende, titanite, and biotite (Hay 1976; Kyara 1999). Six minerals have been identified in one metamorphosed syeno-granite sample, namely quartz, alkali feldspar, plagioclase, opaque, biotite, and hornblende. Opaque crystals are responsible for this sample's spotted texture. Based on textural and mineralogical differences between one sample and

previously published data, there are as a minimum two varieties of meta-granites that outcrop at Naisiusiu, a meta-syeno-granite variety and a granite gneiss variety (see Chapter 6.12).

Four minerals have been identified in one mica schist sample, a previously unrecognised rock type, namely muscovite, quartz, biotite, and plagioclase. The following paragraphs describe each thin section starting with quartzite, meta-syeno-granite, mica schist, and concluding with nephelinite.

Naisiusiu 4 is a weakly foliated, heteroblastic, medium- to fine-grained quartzite with a mineral assemblage of quartz (85%), chloritized biotite (13%), muscovite (1%), opaque (1%), chlorite (<1%), and calcite (<1%) with minor amounts of oxides. Quartz crystals show undulatory extinction, and have sutured boundaries as a result of dynamic recrystallisation primarily stemming from the formation and rotation of sub-grains and/or grain boundary migration (Stipp et al. 2002). Chloritized biotite crystals are responsible for the weak foliation, occur as platy yellow aggregates under PPL, and show high-order colours under XP.

Naisiusiu 7 is a weakly foliated, heteroblastic, coarse- to fine-grained quartzite with a mineral assemblage of quartz (94%), chlorite (4%), muscovite (1%), and opaque (1%) with minor amounts of oxides. Quartz crystals have sutured boundaries as a result of dynamic recrystallisation primarily stemming from the formation and rotation of sub-grains and/or grain boundary migration (Stipp et al. 2002). Quartz crystals also show undulatory extinction, and their variable sizes indicate a textural immaturity likely the result of the metamorphism of a poorly sorted protolith. Chlorite crystals are responsible for the weak foliation.

Naisiusiu 9 is a non-foliated, heteroblastic, anhedral medium-grained quartzite with a mineral assemblage of quartz (95%) and muscovite (5%). Quartz crystals have sutured boundaries as a result of dynamic recrystallisation primarily stemming from the formation and rotation of sub-

grains and/or grain boundary migration (Stipp et al. 2002). Quartz crystals are also occasionally cemented and overgrown. Platy muscovite crystals are either embedded in quartz or interstitial, and have a sub-parallel lineation.

Naisiusiu 13 is a non-foliated, heteroblastic, anhedral coarse- to medium-grained quartzite with a mineral assemblage of quartz (97%), muscovite (2%), hematite (1%), and opaque (<1%). Quartz crystals have sutured boundaries as a result of dynamic recrystallisation primarily stemming from the formation and rotation of sub-grains and/or grain boundary migration (Stipp et al. 2002). Platy muscovite crystals are either embedded in quartz or interstitial, and have a random lineation. Hematite is interstitial to quartz crystals.

Naisiusiu 14 is a non-foliated, heteroblastic, anhedral coarse- to fine-grained quartzite with a mineral assemblage of quartz (94%), muscovite (5%), and opaque (1%). Quartz crystals have sutured boundaries as a result of dynamic recrystallisation primarily stemming from the formation and rotation of sub-grains and/or grain boundary migration (Stipp et al. 2002). Platy muscovite crystals are either embedded in quartz or interstitial, and have a parallel lineation.

Naisiusiu 3 is a spotted, medium- to fine-grained meta-syeno-granite with a hypidiomorphic texture and a mineral assemblage of quartz (45%), alkali feldspar (35%), plagioclase (10%), opaque (7%), biotite (2%), and hornblende (1%) with minor amounts of oxides. Quartz crystals are anhedral and show undulatory extinction. Opaque crystals are responsible for the spotted texture.

Naisiusiu 8 is a foliated, medium- to fine-grained partly decussate but primarily lepidoblastic mica schist with a mineral assemblage of muscovite (75%), quartz (15%), biotite (10%), and plagioclase (<1%). Muscovite crystals are responsible for foliated texture. A single plagioclase crystal shows characteristic polysynthetic twinning.

Naisiusiu 12 is a flow-aligned, microporphyritic allotriomorphic nephelinite with nepheline (3%), aegirine-augite (<1%), sanidine (<1%), hornblende (<1%), and opaque (<1%) microphenocrysts embedded in a flow-aligned brown-grey groundmass with devitrified glass and minor amounts of oxides. Two hornblende crystals are present and display characteristic 56° and 124° cleavage angles. This sample originates from Sadiman based on mineralogical similarities (Zaitsev et al. 2012).

Table 6.8.1 Naisiusiu: Sample Position, ID, Rock Type, and Visually Estimated Modal Percentages

Position	Sample ID	Rock Type	Mineralogy
Primary	Naisiusiu 3	Meta-syeno-granite	Quartz (45); alkali feldspar (35); plagioclase (10); opaque (7); biotite (2); hornblende (1)
	Naisiusiu 4	Quartzite	Quartz (85); chloritized biotite (13); muscovite (1); opaque (1); chlorite (<1); calcite (<1)
	Naisiusiu 7	Quartzite	Quartz (94); chlorite (4); muscovite (1); opaque (1)
	Naisiusiu 8	Mica schist	Muscovite (75); quartz (15); biotite (10); plagioclase (<1)
	Naisiusiu 9	Quartzite	Quartz (95); muscovite (5)
	Naisiusiu 13	Quartzite	Quartz (97); muscovite (2); hematite (1); opaque (<1)
	Naisiusiu 14	Quartzite	Quartz (94); muscovite (5); opaque (1)
Secondary	Naisiusiu 12	Nephelinite	Nepheline (3); aegirine-augite (<1); sanidine (<1); hornblende (<1); opaque (<1)

Mode for nephelinite is for phenocrysts.

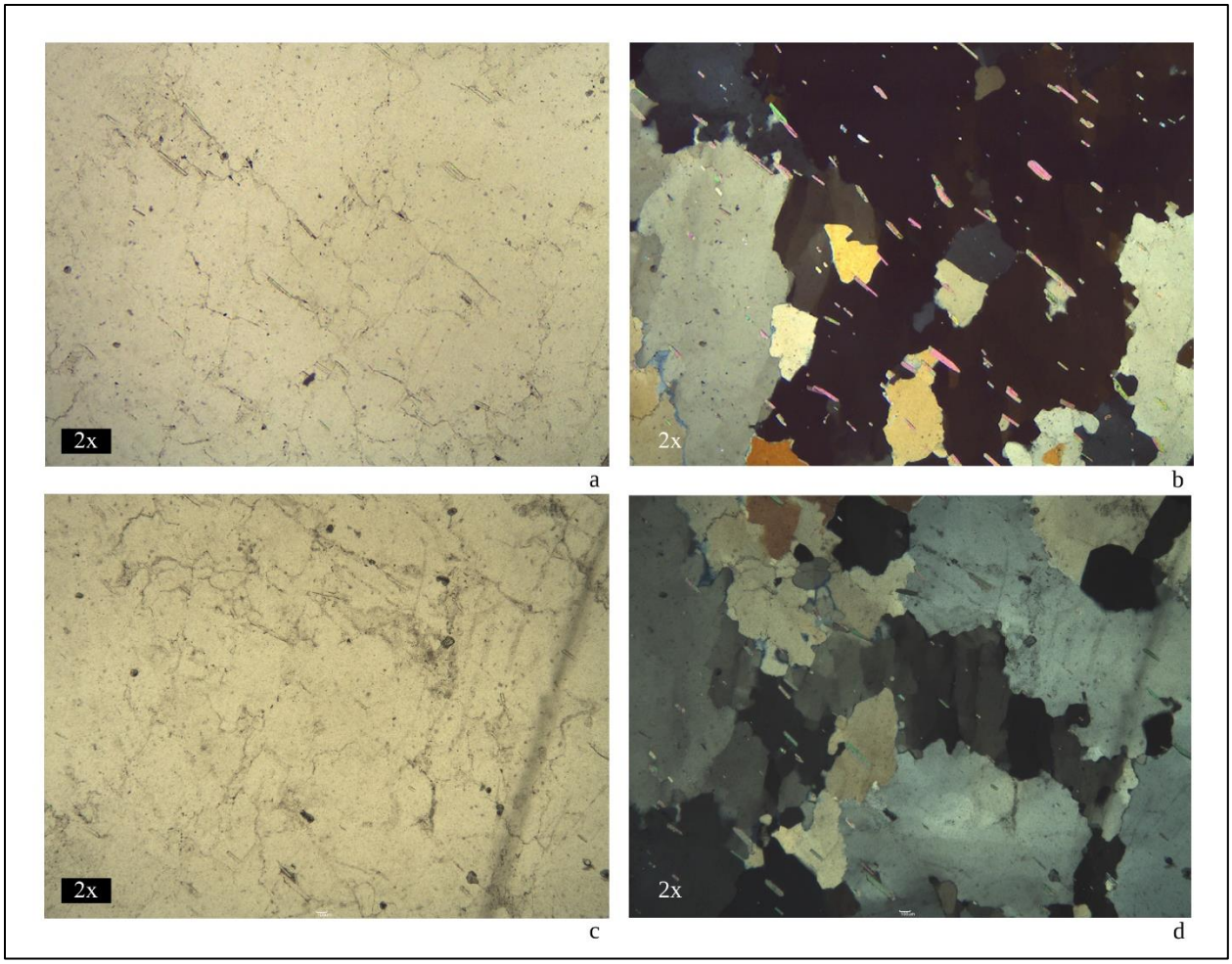

Figure 6.8.1. Naisiusiu 14: (a) Quartz and muscovite in PPL; (b) Same as (a) in XP, quartz crystals show undulatory extinction and sutured boundaries; (c) similar to (a) in PPL; (d) same as (c) in XP, quartz crystal in centre shows intensive undulatory extinction.

Chapter 6.9

Oittii

Prior studies have identified mica schist and quartzite at this outcrop although no corresponding petrographic analyses have been undertaken (Jones 1994; Kyara 1999; Leakey 1965). In this study, six minerals have been identified in four quartzite samples, all of which were previously unrecognised (Table 6.9.1). Quartzite is primarily medium-grained and composed of quartz along with smaller crystals of muscovite, alkali feldspar, hematite, rutile, and plagioclase. Muscovite is an index mineral for low-grade metamorphism and occurs as platy crystals that are

either embedded in quartz or interstitial, and have a sub-parallel to random lineation. Alkali feldspar, plagioclase, and rutile are common detrital minerals, and together with hematite and quartz are representative of a sandstone protolith that was metamorphosed although no relict sedimentary textures were observed. Based on textural and mineralogical differences between four samples, there are as a minimum two varieties of quartzite at this outcrop (see Chapter 6.11). The first variety contains, on average, 94% quartz and minor amounts of muscovite, hematite, and rutile. The second variety contains, on average, 85% quartz, 13% muscovite, and minor amounts of alkali feldspar and plagioclase. The following paragraphs describe each thin section.

Oittii 1A is a non-foliated, heteroblastic, anhedral, granular medium-grained quartzite with a mineral assemblage of quartz (93%), muscovite (3%), hematite (3%), and rutile (1%). Quartz crystals have sutured boundaries as a result of dynamic recrystallisation primarily stemming from the formation and rotation of sub-grains and/or grain boundary migration (Stipp et al. 2002). Xenoblastic muscovite crystals are either embedded in quartz or interstitial, and have a random lineation (Figure 6.9.1).

Oittii 1B is a non-foliated, heteroblastic, anhedral, granular medium-grained quartzite with a mineral assemblage of quartz (93%), muscovite (3%), hematite (3%), and rutile (1%). Quartz crystals have sutured boundaries as a result of dynamic recrystallisation primarily stemming from the formation and rotation of sub-grains and/or grain boundary migration (Stipp et al. 2002). Xenoblastic muscovite crystals are either embedded in quartz or interstitial, and have a random lineation.

Oittii 3 is a non-foliated, heteroblastic, anhedral, granular coarse- to medium-grained quartzite with a mineral assemblage of quartz (85%), muscovite (10%), alkali feldspar (5%), and plagioclase (<1%). Large platy muscovite crystals are either embedded in quartz or interstitial, and

have a sub-parallel lineation. Alkali feldspar crystals show characteristic tartan twinning. Based on energy dispersive X-ray spectroscopic data (Abtosway 2018), relatively elevated values for two major elements (Al_2O_3=5.199; K_2O=0.905) measured as oxides in weight % are likely, in part, attributable to the high modal abundance of muscovite ($KAl_2(Si_3AlO_{10})(OH)_2$).

Oittii 4 is a non-foliated, heteroblastic, anhedral, granular coarse- to fine-grained quartzite with a mineral assemblage of quartz (96%), muscovite (2%), hematite (1%), and rutile (1%). Platy muscovite crystals are either embedded in quartz or interstitial, and have a sub-parallel lineation. Hematite crystals are interstitial to quartz.

Oittii 5A is a non-foliated, heteroblastic, anhedral, granular medium-grained quartzite with a mineral assemblage of quartz (85%), muscovite (15%), and alkali felspar (<1%). Platy muscovite crystals are either embedded in quartz or interstitial, and have a sub-parallel lineation. Alkali feldspar crystals show characteristic tartan twinning.

Oittii 5B is a non-foliated, heteroblastic, anhedral, granular medium-grained quartzite with a mineral assemblage of quartz (85%), muscovite (15%), and alkali felspar (<1%). Platy muscovite crystals are either embedded in quartz or interstitial, and have a sub-parallel lineation. Alkali feldspar crystals show characteristic tartan twinning.

Table 6.9.1 Oittii: Sample Position, ID, Rock Type, and Visually Estimated Modal Percentages

Position	Sample ID	Rock Type	Mineralogy
Primary	Oittii 1A	Quartzite	Quartz (93); muscovite (3); hematite (3); rutile (1)
	Oittii 1B	Quartzite	Quartz (93); muscovite (3); hematite (3); rutile (1)
	Oittii 3	Quartzite	Quartz (85); muscovite (10); alkali feldspar (5); plagioclase (<1)
	Oittii 4	Quartzite	Quartz (96); muscovite (2); hematite (1); rutile (1)
	Oittii 5A	Quartzite	Quartz (85); muscovite (15); alkali feldspar (<1)
	Oittii 5B	Quartzite	Quartz (85); muscovite (15); alkali feldspar (<1)

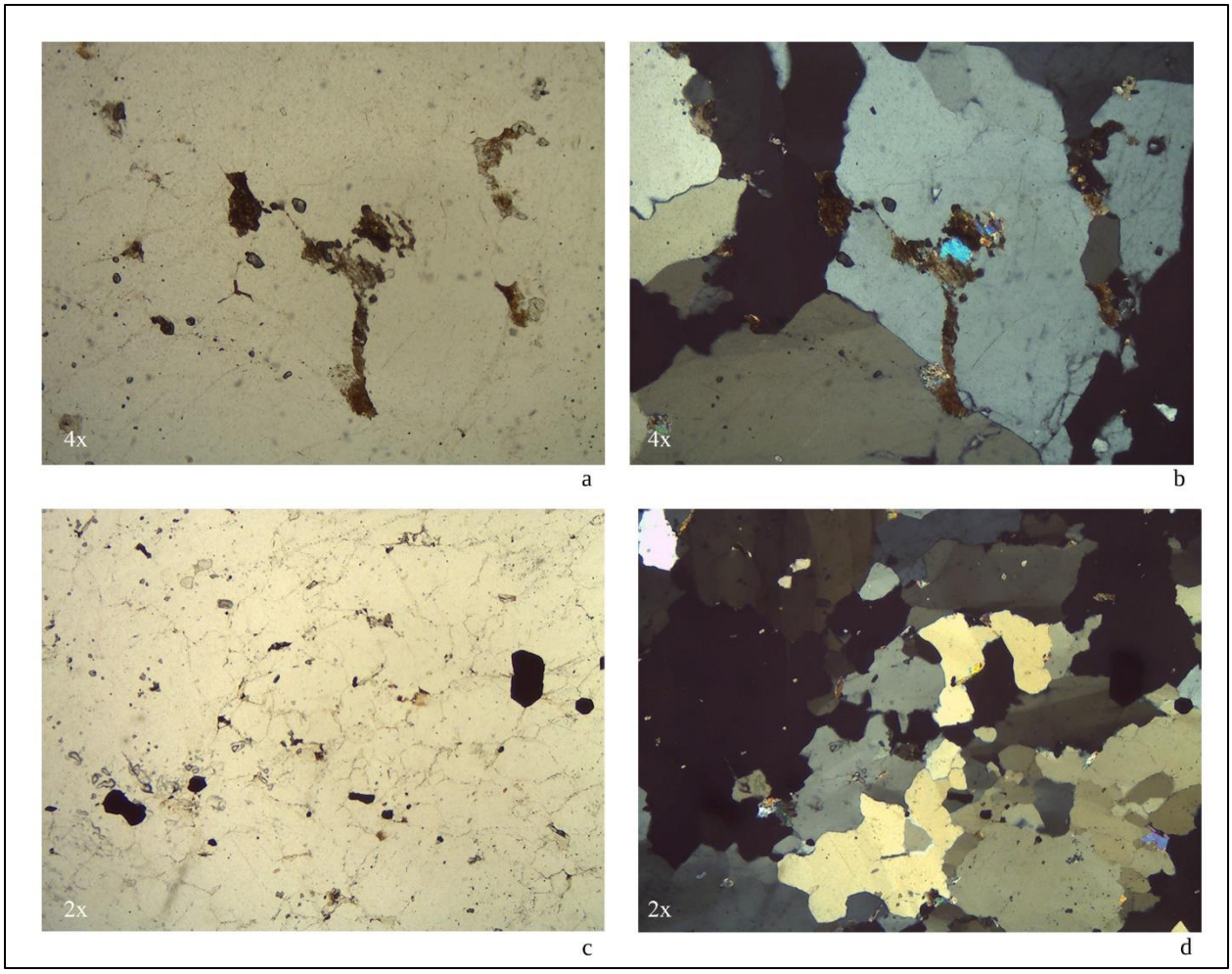

Figure 6.9.1. Oittii 1A: (a) xenoblastic hematite crystals in PPL; (b) same as (a) in XP; (c) large idioblastic rutile crystals in PPL; (d) same as (c) in XP, quartz crystals show undulatory extinction, and muscovite crystals are fragmented, and have a random lineation.

Chapter 6.10

Olbalbal

Since Olbalbal is the drainage sump of the Olduvai River and the northwestern NVH, it is a secondary source of igneous rocks drained from nearby volcanic centres, namely Sadiman, Lemagrut, Ngorongoro, and Olmoti (Dawson 2008; Foster et al. 1997; Hay 1976; Mollel 2002). In this study, nine minerals have been identified in four igneous samples, namely plagioclase, augite, opaque, olivine, kaersutite, nepheline, titanite, as well as secondary hematite and

carbonates (Table 6.10.1). Nephelinite contains predominantly nepheline phenocrysts and lesser amounts of aegirine-augite, hornblende, and titanite and is ultimately sourced to Sadiman (Zaitsev et al. 2012). The non-diagnostic mineral assemblages hindered satisfactory identification for the remaining three samples (A2, A5, and A6). However, sample A6 was identified as a trachyandesite/basalt from Olmoti in reference to previously published mineralogical data (see Table 5.3.1; Mollel 2002; Mollel et al. 2009). Oxides were common under thin section in these three samples, and together with the presence of secondary carbonate crystals, are in part, indicative of seasonal exposure to variable inundation regimes. Based on textural and mineralogical differences between four samples, there are as a minimum four varieties of igneous rocks that can be found at Olbalbal. These include a phenocryst-rich nephelinite variety from Sadiman, two basaltic (?) varieties with differing amounts of plagioclase phenocrysts, and a kaersutite-bearing trachyandesite/basalt variety from Olmoti. The following paragraphs describe each thin section starting with nephelinite, basalt (?), and concluding with trachyandesite/basalt.

A1A is an inequigranular, porphyritic nephelinite with nepheline (65%), aegirine-augite (10%), hornblende (1%), and titanite (<1%) phenocrysts embedded in a dark-brown groundmass. The phenocrysts and groundmass are both weakly aligned. Nepheline phenocrysts are euhedral while aegirine-augite and hornblende phenocrysts are anhedral. Hornblende phenocrysts display characteristic 56° and 124° cleavage angles. Titanite phenocrysts are wedge-shaped. This sample originates from Sadiman based on mineralogical similarities (Zaitsev et al. 2012).

A1B is an inequigranular, porphyritic nephelinite with nepheline (65%), aegirine-augite (10%), hornblende (1%), and titanite (<1%) phenocrysts embedded in a dark-brown groundmass. The phenocrysts and groundmass are both weakly aligned. Nepheline phenocrysts are euhedral while aegirine-augite and hornblende phenocrysts are anhedral. Aegirine-augite phenocrysts are

occasionally zoned. Hornblende phenocrysts display characteristic 56° and 124° cleavage angles. Titanite phenocrysts are wedge-shaped. This sample originates from Sadiman based on mineralogical similarities (Zaitsev et al. 2012).

A2 is an inequigranular, flow-aligned, porphyritic basalt (?) with plagioclase (20%), opaque (1%), augite (1%), and olivine (1%) phenocrysts embedded in a trachytic light-grey plagioclase-rich groundmass with minor amounts of oxides. Plagioclase phenocrysts show characteristic polysynthetic twinning and occasionally combined Carlsbad-polysynthetic twins. Plagioclase phenocrysts are occasionally zoned and have a glomerophyric texture. Prismatic augite phenocrysts show characteristic octagonal cross-sections. Olivine phenocrysts are occasionally altered evidenced by internal cracks filled with opaque material.

A5A is a flow-aligned, porphyritic basalt (?) with plagioclase (1%) and augite (<1%) phenocrysts embedded in a trachytic light-grey plagioclase-rich groundmass with high amounts of secondary hematite. Vesicles are occasionally filled with secondary micritic carbonate crystals that precipitated from seasonal standing water rather than having crystallised from molten-carbonate magma.

A5B is a flow-aligned, porphyritic basalt (?) with plagioclase (1%) and augite (<1%) phenocrysts embedded in a trachytic light-grey plagioclase-rich groundmass with high amounts of secondary hematite. Vesicles are occasionally filled with secondary micritic carbonate crystals that precipitated from seasonal standing water rather than having crystallised from molten-carbonate magma.

A6 is a vesicular, felty, microporphyritic trachyandesite/basalt with plagioclase (1%), kaersutite (1%), and augite (<1%) microphenocrysts embedded in a felty light-grey groundmass. Kaersutite crystals are occasionally prismatic although they are not pleochroic which is typical of

the amphibole group. Kaersutite crystals have been recorded from trachyandesite/basalt samples from Olmoti (Mollel 2002; Mollel et al. 2009), and considering that this mineral was not present in other samples, this together with the mineral assemblage suggests that A6 is a trachyandesite/basalt from Olmoti.

Table 6.10.1 Olbalbal: Sample Position, ID, Rock Type, and Visually Estimated Modal Percentages			
Position	**Sample ID**	**Rock Type**	**Mineralogy**
Secondary	A1A	Nephelinite	Nepheline (65); aegirine-augite (10); hornblende (1); titanite (<1)
	A1B	Nephelinite	Nepheline (65); aegirine-augite (10); hornblende (1); titanite (<1)
	A2	Basalt (?)	Plagioclase (20); opaque (1); augite (1); olivine (1)
	A5A	Basalt (?)	Plagioclase (1); augite (<1)
	A5B	Basalt (?)	Plagioclase (1); augite (<1)
	A6	Trachyandesite/basalt	Plagioclase (1); kaersutite (1); augite (<1)

Modes for igneous rocks are for phenocrysts.

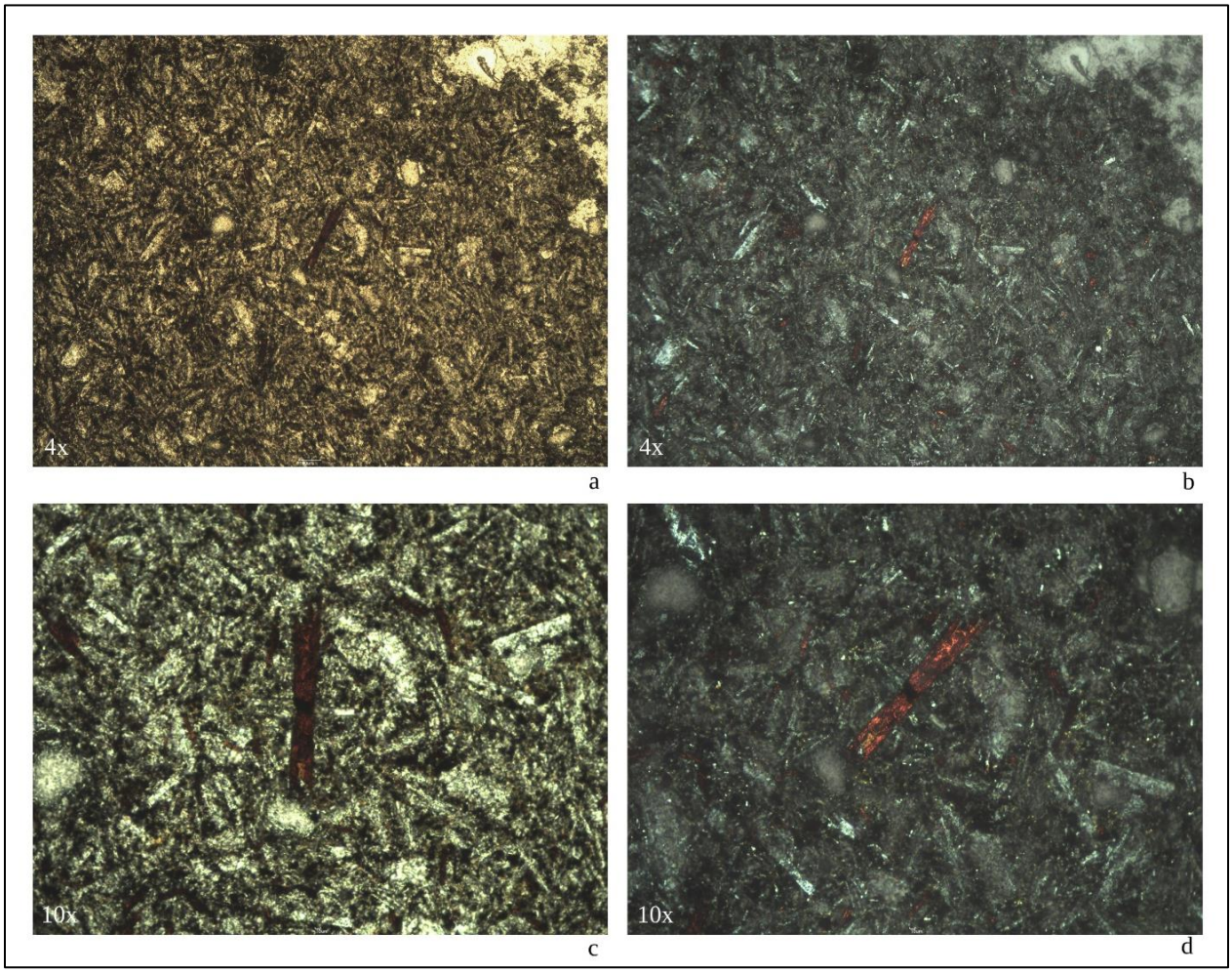

Figure 6.10.1. A6: (a) red kaersutite crystals embedded in a felty groundmass in PPL; (b) same as (a) in XP; (c) prismatic kaersutite crystal in PPL; (d) same as (c) in XP.

Chapter 6.11

Quartzites: A Comparative Analysis

Quartzites were one of the most highly utilised raw materials by early hominins at Olduvai Gorge (Leakey 1971; Leakey and Roe 1994). Therefore, a preliminary comparative analysis was devised to determine if quartzite-bearing outcrops show discriminatory differences in mineral assemblages to establish the prospects of sourcing this raw material type by thin section petrography. Other than relative grain size, textural data for each sample were not considered as there was overlap between outcrops resulting from relatively homogenous metamorphic conditions and protolith grain sizes. The primary form of data utilised for this comparative analysis are visually estimated modal abundances with the understanding that while these constitute as qualitative in nature and may not be entirely accurate, they are internally precise. Each sample was classified according to its identification code and outcrop. Samples were grouped into a total of fourteen varieties based on mineral assemblages, and occasionally on the presence of individual minerals (Table 6.11.1). The following paragraphs describe the degree to which quartzite varieties are unique to individual outcrops, and concludes by summarising what are deemed as significant results.

Variety 1 (Qtz-Ms-Op-Rt) from Endonyo Osunyai is polymineralic and coarse-grained. Mineralogically, it is distinguishable to Variety 2, 4, 5, 9, 12, and 14 but undistinguishable to Variety 3, 6, 7, 8, 10, 11, and 13.

Variety 2 (Qtz-Afs-Ms-Hem) from Endonyo Osunyai is polymineralic and coarse-grained. Mineralogically, it is distinguishable to all other quartzite varieties based on the modal abundances of quartz and alkali feldspar.

Variety 3 (Qtz-Ms-Rt-Op) from the Gol Mountains is polymineralic and coarse- to medium-grained. Mineralogically, it is distinguishable to Variety 2, 4, 5, 8, 9, 12, and 14 but undistinguishable to Variety 1, 6, 7, 10, 11, and 13.

Variety 4 (Qtz-Ms-Afs) from the Gol Mountains is trimineralic and coarse-grained. Mineralogically, it is distinguishable to all quartzite varieties except for Variety 12 (Oittii) as they both have comparable modal abundances of quartz, muscovite, and alkali feldspar.

Variety 5 (Qtz-Ms-Rt-Fu-Hem) from Naibor Soit Kubwa is polymineralic and coarse- to fine-grained. Mineralogically, it is distinguishable to all quartzite varieties based on the modal abundances of quartz and muscovite. The absence of alkali feldspar distinguishes Variety 5 from Variety 12 (Endonyo Osunyai).

Variety 6 (Qtz-Ms-Rt-Op-Fu-Hem-Mag) from Naibor Soit Kubwa is polymineralic and coarse- to fine-grained. Mineralogically, it is distinguishable to Variety 2, 4, 5, 9, 12, and 14 but undistinguishable to Variety 1, 3, 7, 8, 10, 11, and 13. One magnetite-bearing sample (Naibor Soit Kubwa 33) may be classified within a separate variety although magnetite may have weathered into hematite which is present in another sample in Variety 6 (Naibor Soit Kubwa 1) (see Figure 4.4.13; Chapter 6.6; Table 6.11.1). Regardless of classification, magnetite has only been observed in quartzite from Naibor Soit Kubwa which may be used to source an artifact to this outcrop.

Variety 7 (Qtz-Ms-Op-Hem-Rt) from Naibor Soit Ndogo is polymineralic and coarse-grained. Mineralogically, it is distinguishable to Variety 2, 4, 5, 8, 9, 12, and 14 but undistinguishable to Variety 1, 3, 6, 10, 11, and 13.

Variety 8 (Qtz-Ms-Fu-Rt-Op) from Naibor Soit Ndogo is polymineralic and coarse-grained. Mineralogically, it is distinguishable to all quartzite varieties except for Variety 6 (Naibor

Soit Kubwa) as they both have comparable modal abundances of quartz and muscovite, and contain fuchsite.

Variety 9 (Qtz-Chloritized Bt-Chl-Ms-Op-Cal) from Naisiusiu is polymineralic and coarse- to fine-grained. Mineralogically, it is distinguishable to all quartzite varieties based on the presence of chloritized biotite and chlorite.

Variety 10 (Qtz-Ms-Hem-Op) from Naisiusiu is polymineralic and coarse- to fine-grained. Mineralogically, it is distinguishable to Variety 2, 4, 5, 8, 9, 12, and 14 but undistinguishable to Variety 1, 3, 6, 7, 11, and 13.

Variety 11 (Qtz-Ms-Hem-Rt) from Oittii is polymineralic and coarse- to fine-grained. Mineralogically, it is distinguishable to Variety 2, 4, 5, 8, 9, 12, and 14 but undistinguishable to Variety 1, 3, 6, 7, 10, and 13.

Variety 12 (Qtz-Ms-Afs-Pl) from Oittii is polymineralic and coarse- to medium-grained. Mineralogically, it is distinguishable to all quartzite varieties except for Variety 4 (Gol Mountains) as they both have comparable modal abundances of quartz, muscovite, and alkali feldspar.

Variety 13 (Qtz-Ms) from Granite Falls is bimineralic and medium- to fine-grained. Mineralogically, it is distinguishable to Variety 2, 4, 5, 8, 9, 12, and 14 but undistinguishable from Variety 1, 3, 6, 7, 10, and 11.

Variety 14 (Qtz-Bt-Ms-Op) from Kelogi but sourced to Endonyo Okule is polymineralic and fine-grained. Mineralogically, it is distinguishable to all quartzite varieties based on the presence of biotite.

From the fourteen varieties described above, there are two that co-occur at two outcrops. Variety 8 from Naibor Soit Ndogo is a coarse-grained fuchsite-bearing quartzite, and similar modal abundances of quartz, muscovite, fuchsite, rutile, and opaque can also be found at Naibor Soit

Kubwa in Variety 6. The presence of fuchsite at both outcrops is unique compared to all sampled outcrops in the Olduvai paleobasin, while the presence of magnetite is unique to quartzite from Naibor Soit Kubwa. Variety 12 from Oittii is a coarse- to medium-grained alkali feldspar-bearing quartzite, and similar modal abundances of quartz, muscovite, and alkali feldspar can also be found in the Gol Mountains in Variety 4.

From the fourteen varieties, there are four that uniquely occur at an individual outcrop. Variety 2 is a coarse-grained alkali feldspar-bearing quartzite from Endonyo Osunyai, and the modal abundances of quartz and alkali feldspar are unique to this outcrop. Variety 5 is a coarse- to fine-grained muscovite-rich quartzite from Naibor Soit Kubwa, and the modal abundances of quartz and muscovite are unique to this outcrop. Variety 9 is a coarse- to fine-grained chloritized biotite-bearing quartzite from Naisiusiu, and is unique compared to all sampled outcrops. Variety 14 is a fine-grained biotite-bearing quartzite that was obtained in secondary position at Kelogi, and is unique to all sampled outcrops. Based on published mineralogical data (Hay 1976:Table 6), it may be inferred that this sample was transported in recent times from Endonyo Okule and discarded at Kelogi. Although quartzitic outcrops in the Olduvai paleobasin have similar mineral facies, the results of this comparative analysis reveal that four outcrops bear quartzites with unique mineral assemblages, and two pairs of outcrops share similar mineral assemblages and modes unlike all other outcrops. Therefore, these results demonstrate it is feasible to source some quartzite lithics from Olduvai Gorge using thin section petrography.

Table 6.11.1 Quartzite Varieties			
Source/Outcrop	**Sample ID**	**Mineralogy**	**Grain Size**
Endonyo Osunyai	Endonyo Osunyai 1	Quartz (98); muscovite (2); opaque (<1); rutile (<1)	Coarse
	Endonyo Osunyai 2	Quartz (98); muscovite (2); opaque (<1)	Coarse
	Endonyo Osunyai 4A	Quartz (79); alkali feldspar (15); muscovite (5); hematite (1)	Coarse
	Endonyo Osunyai 4B	Quartz (78); alkali feldspar (10); muscovite (10); hematite (2)	Coarse
Gol Mountains	PPP1	Quartz (95); muscovite (5); rutile (<1); opaque (<1)	Medium
	RRR1	Quartz (90); muscovite (10); rutile (<1)	Coarse
	SSS1	Quartz (92); muscovite (8); rutile (<1)	Coarse-medium
	DDD1	Quartz (90); muscovite (10); alkali feldspar (<1)	Coarse
Naibor Soit Kubwa	Naibor Soit Kubwa N042	Quartz (85); muscovite (15); hematite (<1)	Coarse
	Naibor Soit Kubwa 27	Quartz (70); muscovite (30)	Coarse-fine
	Naibor Soit Kubwa 32	Quartz (85); muscovite (14); rutile (1); fuchsite (<1)	Coarse-medium
	Naibor Soit Kubwa E039	Quartz (92); muscovite (8)	Coarse
	Naibor Soit Kubwa S06	Quartz (95); muscovite (5)	Coarse
	Naibor Soit Kubwa 1	Quartz (93); muscovite (5); hematite (1); rutile (1)	Medium
	Naibor Soit Kubwa 2	Quartz (95); muscovite (5); rutile (<1); opaque (<1)	Medium
	Naibor Soit Kubwa 6	Quartz (92); muscovite (5); rutile (1); opaque (1); fuchsite (1)	Medium
	Naibor Soit Kubwa 8	Quartz (94); muscovite (6); opaque (<1); rutile (<1)	Coarse
	Naibor Soit Kubwa 11	Quartz (98); muscovite (2); rutile (<1)	Coarse
	Naibor Soit Kubwa 13	Quartz (92); muscovite (8); rutile (<1)	Coarse
	Naibor Soit Kubwa 14	Quartz (92); muscovite (8)	Coarse
	Naibor Soit Kubwa 24	Quartz (99); muscovite (1); opaque (<1)	Coarse-fine
	Naibor Soit Kubwa 31	Quartz (92); muscovite (8)	Coarse
	Naibor Soit Kubwa 33	Quartz (97); muscovite (3); magnetite (<1)	Coarse
Naibor Soit Ndogo	Naibor Soit Ndogo 6A	Quartz (95); muscovite (5)	Coarse
	Naibor Soit Ndogo 6B	Quartz (95); muscovite (5)	Coarse
	Naibor Soit Ndogo 8	Quartz (98); muscovite (2)	Coarse
	Naibor Soit Ndogo 15	Quartz (95); muscovite (5); opaque (<1); hematite (<1); rutile (<1)	Coarse
	Naibor Soit Ndogo 13	Quartz (96); muscovite (3); fuchsite (1); rutile (<1); opaque (<1)	Coarse
	Naibor Soit Ndogo 14	Quartz (98); muscovite (2); fuchsite (<1)	Coarse
Naisiusiu	Naisiusiu 4	Quartz (85); chloritized biotite (13); muscovite (1); opaque (1); chlorite (<1); calcite (<1)	Medium-fine
	Naisiusiu 7	Quartz (94); chlorite (4); muscovite (1); opaque (1)	Coarse-fine
	Naisiusiu 9	Quartz (95); muscovite (5)	Medium
	Naisiusiu 13	Quartz (97); muscovite (2); hematite (1); opaque (<1)	Coarse-medium
	Naisiusiu 14	Quartz (94); muscovite (5); opaque (1)	Coarse-fine
Oittii	Oittii 1A	Quartz (93); muscovite (3); hematite (3); rutile (1)	Medium
	Oittii 1B	Quartz (93); muscovite (3); hematite (3); rutile (1)	Medium
	Oittii 4	Quartz (96); muscovite (2); hematite (1); rutile (1)	Coarse-fine
	Oittii 3	Quartz (85); muscovite (10); alkali feldspar (5); plagioclase (<1)	Coarse-medium
	Oittii 5A	Quartz (85); muscovite (15); alkali feldspar (<1)	Medium
	Oittii 5B	Quartz (85); muscovite (15); alkali feldspar (<1)	Medium
Granite Falls	Granite Falls 4A	Quartz (95); muscovite (5)	Medium-fine
	Granite Falls 4B	Quartz (95); muscovite (5)	Medium-fine
Kelogi	Kelogi 9	Quartz (86); biotite (8); muscovite (5); opaque (1)	Fine

Varieties
1
2
3
4
5
6
7
8
9
10
11
12
13
14

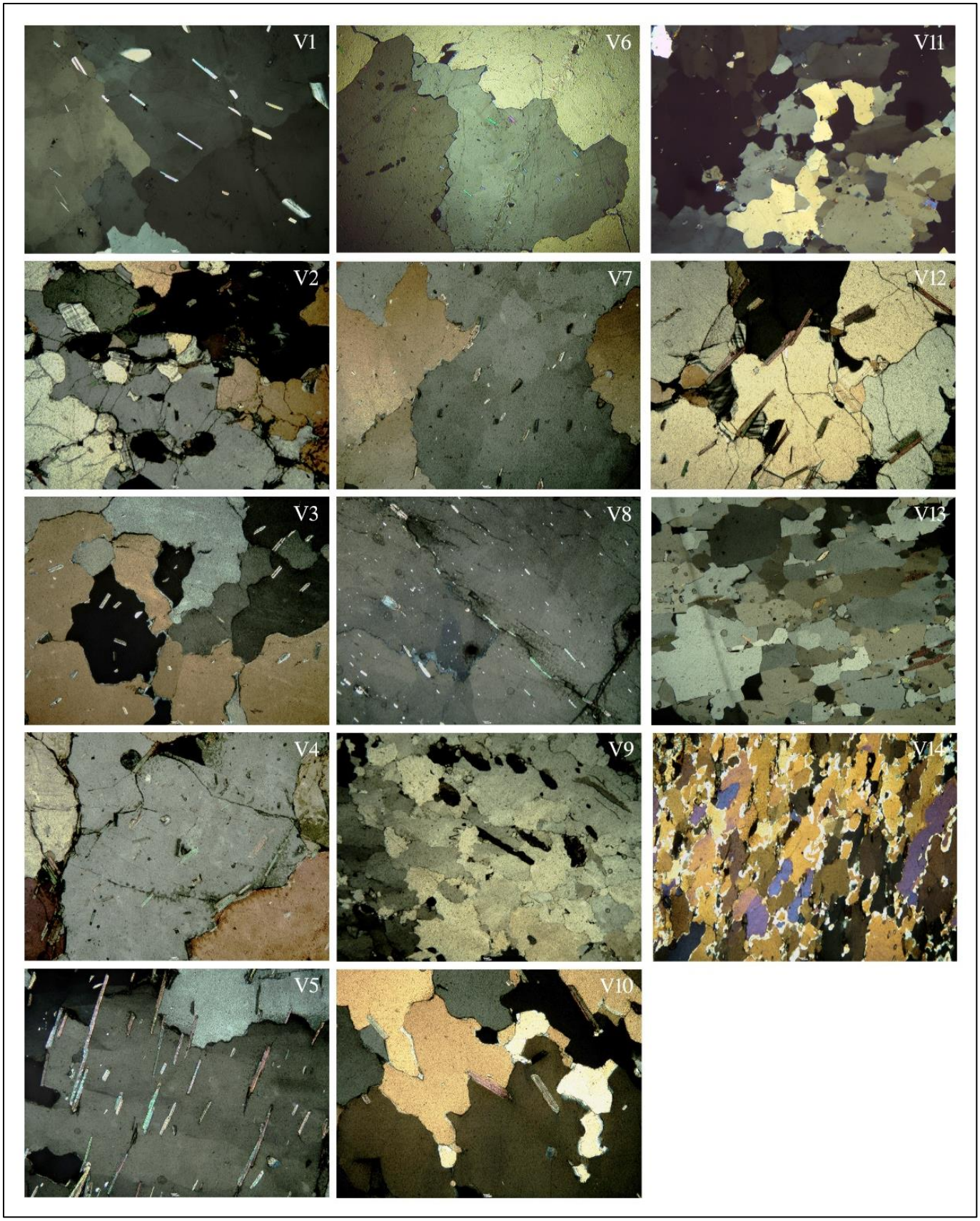

Figure 6.11.1. Quartzite Varieties: (V1) Endonyo Osunyai; (V2) Endonyo Osunyai; (V3) Gol Mountains; (V4) Gol Mountains; (V5) Naibor Soit Kubwa; (V6) Naibor Soit Kubwa; (V7) Naibor Soit Ndogo; (V8) Naibor Soit Ndogo; (V9) Naisiusiu; (V10) Naisiusiu; (V11) Oittii; (V12) Oittii; (V13) Granite Falls; (V14) Kelogi.

Chapter 6.12

Meta-Granites: A Comparative Analysis

Meta-granites were sporadically utilised raw materials by early hominins at Olduvai Gorge (Leakey 1971; Leakey and Roe 1994). Nevertheless, a preliminary comparative analysis was devised to determine if meta-granitic outcrops show discriminatory differences in mineral composition to establish the prospects of sourcing this raw material type by thin section petrography. Textural data were not considered for this analysis since there was overlap between outcrops resulting from relatively homogenous protolith grain sizes and metamorphic conditions. As in Chapter 6.11, the primary form of data utilised for this comparative analysis are visually estimated modal abundances (except for two samples, see Table 5.3.2) with the understanding that while these may not be entirely accurate, they are internally precise. Each sample was classified according to its identification code and outcrop, and grouped into a total of six varieties based on mineral composition (Table 6.12.1). The following paragraphs describe the degree to which meta-granitic varieties are unique to individual outcrops, and concludes by summarising what are deemed as significant results.

Variety 1 (Qtz-Afs-Bt-Hbl-Pl-Rt) from the Gol Mountains is polymineralic and medium- to fine-grained. Mineralogically, it is distinguishable to all meta-granitic varieties including Variety 2 based on the modal abundances of quartz, alkali feldspar, and plagioclase.

Variety 2 (Qtz-Bt-Afs-Pl-Op-Ms) from the Gol Mountains is polymineralic and medium- to fine-grained. Mineralogically, it is distinguishable to all meta-granitic varieties based on the modal abundances of quartz.

Variety 3 (Qtz-Afs-Bt-Ms-Pl) from Granite Falls is polymineralic and medium- to fine-grained. Mineralogically, it is distinguishable to all meta-granitic varieties based on the modal abundances of muscovite.

Variety 4 (Qtz-Aeg-Pl-Hbl-Afs-Hem) from Kelogi is polymineralic and medium-grained. Mineralogically, it is distinguishable to all meta-granitic varieties based on the presence of aegirine.

Variety 5 (Pl-Qtz-Hbl-Aeg-Afs-Ttn-Bt) from Kelogi is polymineralic and medium- to fine-grained. Mineralogically, it is distinguishable to all meta-granitic varieties based on the modal abundances of plagioclase and quartz, and the presence of titanite.

Variety 6 (Qtz-Afs-Pl-Op-Bt-Hbl) from Naisiusiu is polymineralic and medium- to fine-grained. Mineralogically, it is distinguishable to all meta-granitic varieties based on the modal abundances of biotite versus Variety 1 and 2, of opaque crystals versus all other varieties, and of hornblende versus all other varieties.

From the six varieties described above, there are two that co-occur at two outcrops. Variety 1 from the Gol Mountains comprises a meta-monzo-granite (JJJ1) and a meta-quartz-rich granitoid (KKK1), and Variety 2 from the Gol Mountains includes two meta-quartz-rich granitoids (TTT1 and UUU1). From the six varieties, four of them are unique to individual outcrops. Variety 3 is a medium- to fine-grained muscovite-bearing granite gneiss from Granite Falls whose modal abundance of muscovite allows its differentiation from other outcrops. Variety 4 is a medium-grained aegirine-bearing granite gneiss from Kelogi whose modal abundances of aegirine together with plagioclase serves to differentiate it from Variety 5, also from Kelogi, and from all other varieties. The relative proportions of biotite, opaque crystals, and hornblende allow the identification of Variety 6 from Naisiusiu and its differentiation from all other sampled outcrops.

The results of this comparative analysis reveal that three outcrops bear four varieties of meta-granites with unique mineral assemblages, and two pairs of outcrops share similar mineral assemblages and modes unlike all other outcrops. Therefore, these results demonstrate it is feasible to source meta-granitic lithics from Olduvai Gorge using thin section petrography.

Table 6.12.1 Meta-Granite Varieties

Source/ Outcrop	Sample ID	Mineralogy	Grain Size
Gol Mountains	JJJ1	Quartz (45); alkali feldspar (40); biotite (15); plagioclase (<1); rutile (<1)	Medium
	KKK1	Quartz (60); alkali feldspar (20); biotite (12); hornblende (6); plagioclase (2)	Medium-fine
	TTT1	Quartz (70); biotite (10); plagioclase (10); alkali feldspar (8); opaque (2)	Fine
	UUU1	Quartz (70); biotite (10); alkali feldspar (10); plagioclase (5); opaque (3); muscovite (2)	Medium-fine
Granite Falls	Granite Falls 1A	Quartz (50); alkali feldspar (30); biotite (15); muscovite (5); plagioclase (<1)	Medium-fine
	Granite Falls 1B	Quartz (60); alkali feldspar (20); biotite (10); muscovite (8); plagioclase (2)	Medium-fine
	Granite Falls 2	Quartz (69); alkali feldspar (15); plagioclase (10); muscovite (5); biotite (1)	Medium-fine
Kelogi	Kelogi 1	Quartz (40); aegirine (20); plagioclase (15); alkali feldspar (15); hornblende (10)	Medium
	Kelogi 3	Quartz (45); aegirine (20); hornblende (12); plagioclase (12); hematite (8); alkali feldspar (3)	Medium
	Kelogi 10	Plagioclase (25); quartz (25); hornblende (20); aegirine (20); alkali feldspar (10); titanite (<1); biotite (<1)	Medium-fine
Naisiusiu	Naisiusiu 3	Quartz (45); alkali feldspar (35); plagioclase (10); opaque (7); biotite (2); hornblende (1)	Medium-fine

Modes for Kelogi 1 and 3 are based on point counts instead of visual estimates (see Table 5.3.2).

Varieties	
	1
	2
	3
	4
	5
	6

Chapter 7

Discussion

This study has characterised a significant portion of the fundamental rock reservoir available for hominin exploitation at Olduvai Gorge. Certainly, not all rock types characterised in this study were utilised by Pleistocene hominins (e.g. mica schist) considering their inferior mechanical and/or morphological properties for knapping. Nevertheless, by characterising varied lithologies, irrespective of mechanical and morphological traits, this will allow future researchers to identify complementary research avenues that may even lie beyond the scope of paleoanthropology. The objectives of the following sub-chapters are to summarise the results of this thesis, contextualise the results by referencing topics and case studies addressed in earlier chapters, apply them, where applicable, to Olduvai's archaeological record, discuss methodological considerations, and future research opportunities and outstanding questions.

Chapter 7.1

Summary of Results

The comparative analysis between quartzite samples in Chapter 6.11 show that four outcrops have unique mineral assemblages, and two pairs of outcrops share unique mineral assemblages and modes. Grain size was not an important variable as different outcrops share similar grain sizes. One sample recovered in secondary position at Kelogi is a mylonitised quartzite with a mineral assemblage of quartz, biotite, muscovite, and opaque. This sample's unique mineralogy is unlike any other quartzite sample analysed in this study, and matches published data for Endonyo Okule (Hay 1976:Table 6) meaning that this rock was transported in recent times over a distance of approximately 5.5 km. Therefore, the prospects of provenancing quartzite lithics from Olduvai using thin section petrography are clearly not futile, nor is it the case with other rock

types. The results of the comparative analysis between meta-granite samples in Chapter 6.12 reveal that three outcrops have unique mineral compositions, and two pairs of outcrops share similar mineral assemblages and modes. Although this study has been primarily focused on characterising metamorphic lithologies, magmatic samples were also collected in primary position at Engelosin, and in secondary position at Granite Falls, Naisiusiu, and Olbalbal. These samples include phonolite, nephelinite, and basaltic rocks that are all differentiable from each other based on mineral composition and texture, and those in secondary position may be sourced to their volcanic centre by referencing published data (see Table 5.3.1).

Altogether, the results of this thesis demonstrate it is possible to provenance certain varieties of quartzites, meta-granites, phonolites, nephelinites, and occasionally, basalts to their primary source of origin using thin section petrography. Importantly, this implies that it is feasible to source lithic artifacts on these raw materials by way of optical mineralogy. Therefore, it is no longer appropriate to largely assume from which outcrop hominins obtained raw materials, particularly quartzite (e.g. Blumenschine et al. 2008). This thesis also contributes to the growing body of work which shows that quartzitic outcrops in a variety of geological settings are differentiable from each other despite their assumed homogeneity (e.g. Blomme et al. 2012; Cnudde et al. 2013; Dalpra and Pitblado 2016; Pitblado et al. 2008, 2013; Soto et al. forthcoming; Veldeman et al. 2012).

Chapter 7.2

Methodological Considerations: A Look Ahead

Certainly, a greater number of samples will help to validate the results of this thesis and potentially establish a greater number of lithological varieties. Future characterisation studies will also require representative sample collections from other outcrops to determine whether these

unsampled outcrops host rock types that are different or similar at the mineralogical level to the varieties identified herein (see Table 4.4.2 and 5.3.1). This raises one important point, that is, while not every recorded outcrop in the Olduvai paleobasin was sampled or characterised, there is great value in non-*a priori* sampling. For example, this study has revealed that there are additional outcrops that have not been previously recorded (see Figure 4.4.1), and even those that have played a central role in discussions on hominin behaviour and raw material exploitation at Olduvai are poorly characterised (e.g. Naibor Soit Kubwa) (Blumenschine et al. 2008). Future studies should also seek to measure outcrop features such as the orientation of geological planes and dipping angles which would greatly enhance the geological and paleoecological reconstruction of the Olduvai paleobasin.

The automated modal analyses for samples were not entirely precise nor accurate since some pleochroic minerals have overlapping greyscale values with felsic minerals depending on stage orientation (see Chapter 6.5 and 6.6). Therefore, without testing different parameters, this technique was of limited use to accomplish the objectives of this study.

It is recommended that future studies rely on point-counted modal data rather than visual estimates, not because this affected sample classification (see Chapter 5.3), but because this would allow one to employ multivariate statistics to quantitively establish rock type varieties. If one is to continue using visually estimated modal abundances, it is recommended that blind tests be carried out in order to determine inter-analyst variation, if applicable.

Grain size for quartzites was generally not a useful variable to identify varieties as many samples were metamorphic, and had intra-sample grain size distributions since their sedimentary protoliths were texturally immature (see Table 6.11.1). Although generally, quartzites from Naisiusiu (Variety 9 and 10), Granite Falls (Variety 13), and Kelogi (Endonyo Osunyai) (Variety

14) are finer-grained and weakly foliated compared with quartzite-bearing outcrops in the eastern Olduvai paleobasin (see Figure 6.11.1). The quantification of textural data could potentially be used to create dendrograms to better understand the relationships between textures and minerals (e.g. Prieto et al. 2019). Further research will be required to determine whether textural characteristics may be used as sourcing criterion for quartzites.

Based on SDS' ongoing quartzite characterisation studies at Olduvai Gorge using macroscopic, petrographic, and geochemical techniques (Soto et al. forthcoming), such an approach offers the strongest ability to differentiate between the lithologies of different outcrops that no singular technique alone accomplishes on a satisfactory basis (see also Hermes et al. 2001). This approach also lends itself useful for archaeological purposes at Olduvai since the macroscopic and geochemical components can be non-destructive, and permit restrictions generally bar destructive analyses of artifacts (personal communication, Godwin Mollel 2017; Mollel 2002:22; but see Stiles et al. 1974; Santonja et al. 2014). However, further research will require one to establish stronger links between geochemical and mineralogical data. In this study, an effort was made to associate elemental data with mineralogical observations, yet not all muscovite-rich quartzites had the highest Al_2O_3 and K_2O values (see Abtosway 2018). The majority of thin sections analysed for this study were left uncovered. This will facilitate future joint scanning electron microscopy and energy dispersive X-ray spectroscopy to confirm and complement visual observations, as well as to determine the individual elemental composition of certain minerals which will be instrumental to interpret non-destructive X-ray spectroscopic data without direct observation by way thin section petrography.

In this study, two basaltic (?) samples collected from Olbalbal were identified on a preliminary basis. However, under thin section these samples did not contain diagnostic mineral

assemblages as low amounts of plagioclase, augite, and olivine phenocrysts may be found in different magmatic rocks (Gill 2010). Since the NVH to the south and east of Olduvai are geologically well-studied, geochemical testing would facilitate the identification of igneous rocks so as to easily determine from which volcanic centre these originate from based on published data (see Table 4.4.2 and 5.3.1).

Chapter 7.3

Archaeological and Geological Applications of Results

While not all known igneous, metamorphic, nor sedimentary sources/outcrops have been characterised as part of this study (see Table 4.4.2 and 5.3.1), inferences may be drawn concerning hominin raw material transport at Olduvai. In Chapter 3.1, Mary Leakey's findings at JK W in Bed III's fine-grained ferruginous sands were recapitulated, in part, because she noted the occurrence of a single double-edged heavy-duty scraper on green quartzite (Leakey 1994a). Based on the findings from this thesis, it can be inferred that the hominin/s who manufactured this artifact procured fuchsitic tabular quartzite directly from either Naibor Soit Kubwa and/or Naibor Soit Ndogo since no other known quartzitic outcrops contain fuchsite which gives quartzite a green colouration. According to tabulated data in McHenry and de la Torre (2018:Table 5), it can be also inferred that hominins responsible for Bed II's HWK EE and EF-HR lithic assemblages obtained fuchsitic quartzite from either Naibor Soit Kubwa and/or Naibor Soit Ndogo since these sites have yielded three (55.8 g) and two (13.2 g) lithics, respectively, of this rock type. These inferences imply that both fuchsite-bearing outcrops were accessible at the time of site occupation which correlates with basin-wide paleogeographic trends for Bed II and III (see Chapter 4.2). Furthermore, it can be said that both Oldowan (HWK EE) and Acheulean (JK W and EF-HR) tool-making hominins, of possibly different taxa, exploited the same outcrops for raw materials.

This study has identified a hornblende granofels sample that was recovered in secondary position south of Olongojoo. This discovery is of high significance as it implies that there are unmapped granofelsic outcroppings that may grade into the epidote-amphibolite facies in a similar fashion to Naibor Soit Kubwa (see Chapter 6.6) and Isilale Aratum (Hay 1976). This finding relates to Olduvai's archaeology as gabbroic rocks can metamorphose into hornblendic granofels (Bucher and Grapes 2011) thereby meaning that the single "altered but unmetamorphosed" gabbro artifact recovered from HWK in Lower Bed II may have been sourced from the Gol Mountains that are geographically much closer to HWK than the Tanzania Craton (Hay 1976:185).

The weathering profiles of igneous rock types pose an analytical challenge in terms of macroscopic identification. In fact, McHenry and de la Torre (2018) noted the contrasting results for macroscopic and geochemical identification of fine-grained rocks with a reddened cortex. Archaeologically, this particular colour is of interest since Mary Leakey (1994b) discovered two large cutting tools at HEB W with a red colouration and suggested that these materials were from an unknown, and possibly distant source (see Chapter 3.1). Alternatively, these artifacts may be interpreted as weathered implements from a known source (see McHenry and de la Torre 2018).

Based on field observations in 2018, forming the riverbed of the Olduvai River near Geolocality 63 in the western Main Gorge are darkly weathered porphyritic and microporphyritic nephelinitic/phonolitic flows and dislodged blocks of uncertain provenance that superficially appear like basalt based on their cortical colour. The closest source of phonolite is Engelosin which was active between 3-2.7 Ma while the closest source of nephelinite is Sadiman which was active between 4.63-3.5 Ma (Mollel and Swisher 2012). Determining the provenance and radiometric age of this rock type would be of immense help to reconstruct the early geological history of the western Olduvai paleobasin. Furthermore, this would help to shed light on the local raw material

availability since during Bed I and Lower Bed II, hominins preferentially utilised nephelinite in artifact production whose dense homogenous texture may have been a selective factor (Hay 1976). Moreover, Mollel (2002) identified phonolite and phonolitic nephelinite cobbles from paleoconglomerates at HWK, MCK, and PEK. Therefore, it may be suggested that the secondary source for these rock types are the nephelinitic/phonolitic flows and blocks near Geolocality 63 that may have been re-deposited closer to archaeological sites in the eastern paleobasin where they may have been flaked for suitability and later transported on-site (see also Leakey 1971; Santonja et al. 2014). If proven as nephelinite, it may be that the nephelinite sample recovered in secondary position at Naisiusiu (see Table 6.8.1) was transported in recent times from this portion of the Olduvai riverbed.

In Chapter 3.1, Jones' (1979, 1994) experimental studies were reviewed, in part, because he noted that Olduvai hominins utilised non-flow-banded Engelosin phonolite. This rock type would have been ideal in artifact production since it would not have dictated flaking planes as opposed to flow-banded phonolite. Jones (1979, 1994) asserts that non-flow-banded lithologies are non-existent at Engelosin since these were fully exhausted by hominin agency, thereby creating a discordant reference collection. However, based on the findings from this study, Engelosin still yields non-flow-banded phonolite evidenced by one variety with a felty texture (see Chapter 6.2).

East of the rockshelter on the northern face of Soit Nasera, there are previously unreported perthitic feldspar outcroppings. Similar lithologies occur as basement rocks in the western Olduvai paleobasin near Granite Falls (Hay 1971, 1976), and artifactual feldspar is recorded at HWK EE and EF-HR (McHenry and de la Torre 2018), along with other sites (Leakey 1971). However, no mineralogical or textural data are reported for geological and artifactual feldspar. Therefore, additional characterisation studies are required in order to determine whether it is feasible to

discriminate between feldspar outcroppings in the greater Olduvai region prior to archaeological testing.

Finally, as Naibor Soit Kubwa and Naibor Soit Ndogo exclusively yield quartzite, not quartz, it is highly recommended for future studies to use the proper terminology when referencing raw materials from these inselbergs. This is worthy of note as previous techno-typological analyses and experimental studies use the term quartz or quartzite, or interchangeably use both terms to denote material from these inselbergs (e.g. Byrne et al. 2016; de la Torre et al. 2013; Diez-Martín et al. 2009, 2010, 2011; Gurtov and Eren 2014; Leakey 1971; Yustos et al. 2015). The use of the term quartz to denote material from these two inselbergs is presumably based on its mechanical properties while acknowledging that it is of metamorphic origin (Diez-Martín et al. 2011). As a related note, and to avoid future confusion of place names, Engitati has been incorrectly used in reference to a quartzitic inselberg near Eng'amata Enqii in the Gol Mountains (personal communication, Lucas Zebedayo 2018) (see Blumenschine et al. 2008:80; Reti 2013:101-102). For both the local Maasai communities and most scientific researchers, the proper designation of Engitati is in reference to a cinder cone in the Ngorongoro Caldera (Dawson 2008:44; Hay 1976:13; Kyara 1999:64; Mollel 2002:14) rather than an inselberg in the Gol Mountains.

Chapter 7.4

Future Research Opportunities and Outstanding Questions

Soit Nasera is an important rockshelter well-known for its MSA and LSA deposits (Mehlman 1977). The site is located >25 km north of Olduvai within the Gol Mountains and is surrounded by towering metamorphic inselbergs, including some of quartzitic lithology. Considering that this thesis has characterised quartzites from said inselbergs (see Figure 4.4.1), one of which was found to have a unique mineral composition (see Chapter 6.3 and 6.11),

additional characterisation studies could serve as a referential framework in comparison with artifactual quartzite from Soit Nasera. This would allow one to understand the localised procurement of quartzite and further nuance our understanding of the site's MSA and LSA inhabitants whom are known to have had complex ecological and/or social links evidenced by long-distance obsidian procurement (Merrick et al. 1994). As such, the results of this thesis are not only of importance to the archaeological context of Olduvai, but also for the region. While some of Soit Nasera's nearby inselbergs yield mineralogically unique quartzites, most are mineralogically similar to those nearest to Olduvai Gorge (see Chapter 6.3; Hay 1976). This mineralogical similarity on a regional scale raises a series of open-ended questions. If different outcrops bear raw materials of identical rock type and mineral composition to artifacts, may it be assumed that the outcrop closest to where an artifact was discarded be inferred as its source? Can and/or should researchers impose an arbitrary geographic limit from where raw materials may have been obtained? Would doing so improve the prospects of sourcing lithic artifacts at Olduvai and elsewhere? Addressing these theoretical and methodological questions lie beyond the scope of this thesis but are worthy to note since these are applicable to nearly to any lithology, and in fact, to nearly any raw material exploited prehistorically and in the context of the modern globalised world.

Overall, it is difficult to discern whether igneous artifacts from Olduvai, and elsewhere, were manufactured from fluvial clasts or from material directly obtained from a volcanic centre. Presumably, early hominins implemented a least-effort strategy by manufacturing such artifacts from river-fed boulders, cobbles, and pebbles which were more proximal to known sites (see Goldman-Neuman and Hovers 2012). A traditional approach to overcome this difficulty is by studying an artifact's size, roundness and/or morphology, and cortex in combination with site

formation processes (e.g. Fernandes 2012). Considering there are discriminatory differences between modern stream channels and paleoconglomerates (see Table 4.4.2; Kyara 1999; Mollel 2002), one proposed strategy to overcome this difficulty is to excavate along presumed courses of paleoconglomerates (Kyara 1999). However, this poses significant logistical difficulties considering that the Olduvai sedimentary sequence can be as thick as 100 m at some localities within the gorge (Hay 1976). Alternatively, remote-sensing and geophysical techniques may allow the detection of paleochannels, and potentially of different rock types, although it is unclear how well such techniques would perform considering the thickness of Olduvai's sedimentary sequence and the fact that it is characterised by tuffaceous and clay-rich units (see Chapter 4.2) that would likely interfere with frequency bands. Future studies specifically-dealing with provenancing igneous artifacts will require novel approaches considering the limited exposures in the Olduvai paleobasin that may or may not attest to the presence of river-fed igneous rocks (see Chapter 2).

Based on the findings from this study, Naibor Soit Kubwa hosts an amphibolite dyke whose mineral assemblage suggests it is a metamorphosed basaltic protolith (see Chapter 6.6). In hand sample, weathered amphibolite superficially resembles basaltic lithologies which could potentially lead to mis-identification similarly to reddened fine-grained igneous rocks (see Chapter 7.3). Overlooking its mechanical and morphological properties, this could explain why there are no recorded instances of hominin amphibolite utilisation at Olduvai. Isilale Aratum is located approximately 20 km southwest of Naibor Soit Kubwa and hosts amphibolite outcroppings (Hay 1976). Therefore, irrespective of whether this rock type was prehistorically utilised, it would be desirable for future studies to characterise amphibolite from Isilale Aratum to determine if there are discriminatory features with that of Naibor Soit Kubwa, and with possible outcroppings at Olongojoo (see Chapter 7.3).

Obsidian has been reported from Oldowan contexts at Olduvai's HWK E and HWK EE sites (Leakey 1971:89; McHenry and de la Torre 2018:Table 4) which is of great significance since it would imply that early hominins obtained some of their lithic raw materials from sources tens to hundreds of kilometres away which would suggest an earlier origin for long-distance obsidian transport (see Blegen 2017). Artifactual obsidian of this age is exceptional considering that most artifacts dating to the Early Pleistocene at Olduvai are manufactured on coarser-grained rocks with relatively good tool-making properties (Leakey 1971; see Chapter 3.2.1). However, these early occurrences of obsidian may be alternatively interpreted as geofacts since clasts of this material are found in conglomeratic alluvial fan deposits in Bed I, and in tuffaceous deposits alongside mafic vitroclasts in Bed II (Hay 1973, 1976). Not to mention, these two sites were positioned at their time of deposition well-within the central depozone stemming from the southeastern NVH during Bed I and II (Hay 1976). Furthermore, obsidian has a Mohs's hardness value of 5.5 which may lend itself to false positive scars that could appear artifactual. Hence, there is a great need to resolve whether these early occurrences of obsidian at Olduvai are artifactual or geofactual.

Since this study has petrographically characterised lithic raw materials in the Olduvai paleobasin, this may serve as a stepping-stone for other types of research beyond the traditional bounds of provenance studies. More specifically, this study may allow future researchers to determine the knappability of lithic raw materials per outcrop by studying their mechanical and physical characteristics to shed light on the selective criteria that may have been considered by hominins (see Wadley and Kempson 2011).

Future studies may also explore the correlation/s between different rock types and technological strategies. In a similar fashion to organic residue analysis, one may attempt to spatially plot, extract, and analyse, not organics, but rather ingrained minerals from a stone tool

atypical of its rock type, all the while accounting for several variables such as post-depositional processes (Peacock 1989). Scanning electron microscopy could be used to characterise the microtopography of an "exotic" mineral as well as to differentiate between microdebitage and a site's sediments (Susino 2007). Since scanning electron microscopes are commonly fitted with an energy dispersive X-ray detective system, the latter could be utilised to obtain characteristic spectra for the elemental determination of production-based inorganic residues (Byrne et al. 2006). Such lines of evidence in combination with a techno-functional and refit analysis could potentially allow one to identify whether a given artifact was an active or an objective piece (Peacock 1989), and/or even identify its function (e.g. Sorensen et al. 2018). For example, if one were to analyse a quartzite spheroid in such a manner, one could potentially identify ingrained within the artifact a mineral indexical of an igneous rock type which could suggest that the spheroid was used as a hammerstone or was alternatively flaked with an igneous hammerstone (see Jones 1994). Prior to testing this methodology, it is recommended that experiments be conducted to determine its feasibility (see Byrne et al. 2006) on raw materials from Olduvai, and the microtopographical features or microtextures typical of mineral residues, if feasible, experimental microdebitage, and sedimentary grains.

Chapter 8

Conclusions

Olduvai Gorge is situated within a designated UNESCO World Heritage Site in northern Tanzania along the EARS and is widely considered as Africa's most iconic paleoanthropological complex. Olduvai's sedimentary record displays a long sequence of hominin and faunal remains found alongside increasingly complex hominin lithic technologies. While diachronic technological change is detectable, one aspect that remained largely unchanged through time was the totality of locally available rock types. This very fact makes local provenance studies of high value to understand the way in which hominins of different taxa with different technological repertoires interacted with their immediate, and always changing, ecological surroundings. As such, this study was designed with these premises in mind while also adhering to disciplinary standards for source characterisation and provenance studies. Overall, this thesis constitutes Olduvai Gorge's first systematic survey and characterisation of source lithologies using thin section petrography. The objectives of this thesis were to establish the range of available lithic raw materials, petrographically characterise these, and determine if there were unique inter-outcrop petrographic signatures to determine whether sourcing lithic artifacts is feasible at the mineralogical level.

A comparative analysis between quartzite samples revealed that four outcrops have unique mineral assemblages, and two pairs of outcrops share unique mineral assemblages and modes. It is shown that the presence and/or abundances of accessory minerals such as alkali feldspar, biotite, chloritized biotite, chlorite, fuchsite, magnetite, muscovite, and rutile are only found in certain varieties of quartzite from specific outcrops. A comparative analysis between meta-granite samples revealed that three outcrops have unique mineral compositions, and two pairs of outcrops share unique mineral assemblages and modes. Magmatic samples such as phonolite, nephelinite,

and basalt (?) collected in both primary and secondary position are differentiable from each other based on mineral composition and texture, and those in secondary position can be sourced to their volcanic centre. For example, at Olbalbal, there are as a minimum four varieties of igneous rock types that can be found in the present day. This includes two basaltic (?) varieties, a kaersutite-bearing trachyandesite/basalt variety from Olmoti, and a phenocryst-rich nephelinite variety from Sadiman. Altogether, the results of this thesis reveal it is possible to establish the provenance of certain varieties of quartzites, as well as meta-granites, phonolites, nephelinites, and occasionally, basalts to their primary source. Therefore, it is possible to source lithic artifacts from Olduvai Gorge by way of optical mineralogy. The results of this study also contribute to the growing body of literature which shows that quartzite-bearing outcrops can be differentiated from each other despite their assumed homogeneity on a regional scale (e.g. Blomme et al. 2012; Cnudde et al. 2013; Dalpra and Pitblado 2016; Pitblado et al. 2008, 2013; Soto et al. forthcoming; Veldeman et al. 2012).

Considering that thousands of artifacts are excavated every field season at Olduvai, that there are collections curated at multiple institutions throughout the world, and that this thesis has validated the feasibility of sourcing lithic artifacts at the mineralogical level, perhaps policy reforms may allow for partially destructive petrographic analyses. However, the heritage value of these archaeological collections for some communities usually inhibits destructive testing (but see Stiles et al. 1974; Santonja et al. 2014).

While acknowledging that not every recorded outcrop in the Olduvai paleobasin was sampled or characterised for this study, there is great value in non-*a priori* sampling. Nevertheless, additional characterisation studies of all regional outcroppings are required to further refine the results of this study. Built upon generations of research in the Olduvai region, this thesis along

with future characterisation studies will serve as important stepping-stones for future researchers to ultimately determine the provenance of lithic artifacts at Olduvai Gorge, and gain new insights into hominin ecology and sociality.

Bibliography

Abtosway, M.

2018 Geochemical Source Analysis: Preliminaries and Potential at Olduvai Gorge, Tanzania. Master's Thesis, University of Calgary.

Adelsberger, K.A., Wirth, K.R., Mabulla, A.Z.P., Bowman, D.C.

2011 Geochemical and Mineralogic Characterization of Middle Stone Age Tools of Laetoli, Tanzania, and Comparisons with Possible Source Materials. In *Paleontology and Geology of Laetoli*, edited by Harrison, T., pp. 143-165. Springer, Dordrecht.

Agha-Aligol, D., Lamehi-Rachti, M., Oliaiy, P., Shokouhi, F., Farahani, M.F., Moradi, M., Jalali, F.F.

2015 Characterization of Iranian Obsidian Artifacts by PIXE and Multivariate Statistical Analysis. *Geoarchaeology* 30, 261-270.

Archer, W., Braun, D.R.

2010 Variability in bifacial technology at Elandsfontein, Western cape, South Africa: a geometric morphometric approach. *Journal of Archaeological Science* 37, 201-209.

Baker, B.H., Mohr, P.A., Williams, L.A.J.

1972 Geology of the Eastern Rift System of Africa. *Geological Society of America Special Papers* 136, 1-68.

Balzeau, A., Buck, L.T., Albessard, L., Becam, G., Grimaud-Hervé, D., Rae, T.C., Stringer, C.B.

2017 The Internal Cranial Anatomy of the Middle Pleistocene Broken Hill 1 Cranium. *PaleoAnthropology* 2017, 107-138.

Barut, S.

1994 Middle and Later Stone Age Lithic Technology and Land Use in East African Savannas. *The African Archaeological Review* 12, 43-72.

Berger, L.R., Hawks, J., de Ruiter, D.J., Churchill, S.E., Schmid, P., Delezene, L.K., Kivell, T.L., Garvin, H.M., Williams, S.A., DeSilva, J.M., Skinner, M.M., Musiba, C.M., Cameron, N., Holliday, T.W., Harcourt-Smith, W., Ackermann, R.R., Bastir, M., Bogin, B., Bolter, D., Brophy, J., Cofran, Z.D., Congdon, K.A., Deane, A.S., Dembo, M., Drapeau, M., Elliott, M.C., Feuerriegel, E.M., Garcia-Martinez, D., Green, D.J., Gurtov, A., Irish, J.D., Kruger, A., Laird, M.F., Marchi, D., Meyer, M.R., Nalla, S., Negash, E.W., Orr, C.M., Radovcic, D., Schroeder, L., Scott, J.E., Throckmorton, Z., Tocheri, M.W., VanSickle, C., Walker, C.S., Wei, P., Zipfel, B.,

2015 Homo naledi, a new species of the genus Homo from the Dinaledi Chamber, South Africa. *eLife* 4, e09560.

Berry, P.A.

2012 Lake Cycles and Sediments: Locality 80, Olduvai Gorge, Tanzania. MSc Thesis, Georgia State University.

Beyene, Y., Katoh, S., WoldeGabriel, G., Hart, W.K., Uto, K., Sudo, M., Kondo, M., Hyodo, M., Renne, P.R., Suwa, G., Asfaw, B.

2013 The characteristics and chronology of the earliest Acheulean at Konso, Ethiopia. *Proceedings of the National Academy of Sciences of the United States of America* 110, 1584-1591.

Bird, J.R., Ambrose, W.R., Russell, L.H., Scott, M.D.

1981 *The characterisation of Melanesian obsidian sources and artefacts using the proton induced gamma-ray emission (PIGME) technique*. Australian Atomic Energy Commission AA EC/E510, Lucan Heights.

Blegen, N.
2017 The earliest long-distance obsidian transport: Evidence from the ~200 ka Middle Stone Age Sibilo School Road Site, Baringo, Kenya. *Journal of Human Evolution* 103, 1-19.
Blomme, A., Degryse, P., Van Peer, P., Elsen, J.
2012 The characterization of sedimentary quartzite artefacts from Mesolithic sites, Belgium. *Geologica Belgica* 15, 193-199.
Blumenschine, R.J., Masao, F.T., Tactikos, J.C., Ebert, J.I.
2008 Effects of distance from stone source on landscape-scale variation in Oldowan artifact assemblages in the Paleo-Olduvai Basin, Tanzania. *Journal of Archaeological Science* 35, 76-86.
Blumenschine, R.J., Stanistreet, I.G., Masao, F.T.
2012a Olduvai Gorge and the Olduvai Landscape Paleoanthropology Project. *Journal of Human Evolution* 63, 247-250.
Blumenschine, R.J., Masao, F.T., Stollhofen, H., Stanistreet, I.G., Bamford, M.K., Albert, R.M., Njau, J.K., Prassack, K.A.
2012b Landscape distribution of Oldowan stone artifact assemblages across the fault compartments of the eastern Olduvai Lake Basin during early lowermost Bed II times. *Journal of Human Evolution* 63, 384-394.
Bond, G.
1948 Rhodesian Stone Age Man and His Raw Materials. *The South African Archaeological Bulletin* 3, 55-60.
Boswell, P.G.H.
1932 The Oldoway Human Skeleton. *Nature* 130, 237-238.
Braun, D.R., Plummer, T., Ditchfield, P., Ferraro, J.V., Maina, D., Bishop, L.C., Potts, R.
2008 Oldowan behavior and raw material transport: perspectives from the Kanjera Formation. *Journal of Archaeological Science* 35, 2329-2345.
Brock, A., Hay, R.L.
1976 The Olduvai Event at Olduvai Gorge. *Earth and Planetary Science Letters* 29, 126-130.
Brock, A., Hay, R.L., Brown, F.H.
1972 Magnetic stratigraphy of Olduvai Gorge and Ngorongoro, Tanzania. *Geological Society of America Abstracts* 4, 457.
Brooks, A.S., Yellen, J.E., Potts, R., Behrensmeyer, A.K., Deino, A.L., Leslie, D.E., Ambrose, S.H., Ferguson, J.R., d'Errico, F., Zipkin, A.M., Whittaker, S., Post, J., Veatch, E.G., Foecke, K., Clark, J.E.
2018 Long-distance stone transport and pigment use in the earliest Middle Stone Age. *Science* 360, 90-94.
Bucher, K., Grapes, R.
2011 *Petrogenesis of Metamorphic Rocks*. 8th Edition. Springer, Heidelberg.
Byrne, L., Ollé, A., Vergès, J.M.
2006 Under the hammer: residues resulting from production and microwear on experimental stone tools. *Archaeometry* 48, 549-564.
Byrne, F., Proffitt, T., Arroyo, A., de la Torre, I.
2016 A comparative analysis of bipolar and freehand experimental knapping products from Olduvai Gorge, Tanzania. *Quaternary International* 424, 58-68.

Cahen, L., Snelling, N.J.
1966 *The Geochronology of Equatorial Africa*. North-Holland, Amsterdam.
Cahen, L., Snelling, N.J., Delhal, J., Vail, J.R., Bonhomme, M., Ledent, D.
1984 *The geochronology and evolution of Africa*. Clarendon Press, Oxford.
Cairncross, B., McCarthy, T.S.
2015 *Understanding Minerals and Crystals*. Struik Nature, Cape Town.
Caley, E.R.
1948 On the Application of Chemistry to Archaeology. *The Ohio Journal of Science* 48, 1-14.
Cande, S.C., Kent, D.V.
1995 Revised calibration of the geomagnetic polarity timescale for the late Cretaceous and Cenozoic. *Journal of Geophysical Research* 100, 6093-6095.
Cann, J.R., Renfrew, C.
1964 The Characterization of Obsidian and its application to the Mediterranean Region. *Proceedings of the Prehistoric Society* 30, 111-133.
Carter, T.
2014 The contribution of obsidian characterization studies to early prehistoric archaeology. In *Lithic raw material exploitation and circulation in prehistory: a comparative perspective in diverse palaeoenvironments*, edited by Yamada, M., Ono, A., pp. 23-33. ERAUL, Liège.
Clark, G.
1969 *World Prehistory: A New Outline*. Cambridge University Press, Cambridge.
Clark, G.A., Lindly, J.M.
1991 On Paradigmatic Biases and Paleolithic Research Traditions. *Current Anthropology* 32, 577-587.
Cnudde, V., Dewanckele, J., De Kock, T., Boone, M., Baele, J.-M., Crombé, P., Robinson, E.
2013 Preliminary structural and chemical study of two quartzite varieties from the same geological formation: a first step in the sourcing of quartzites utilized during the Mesolithic in northwest Europe. *Geologica Belgica* 16, 27-34.
Cogné, J.E., Giot, P.-R.
1952 Étude pétrographique des haches polies de Bretagne. *Bulletin de la Société préhistorique française* 49, 388-395.
Comprehensive Olduvai Database Initiative (CODI)
2017 https://olduvai-paleo.org/. Electronic document, accessed December 3, 2017.
Curran, J.M., Meighan, I.G., Simpson, D.D.A., Rogers, G., Fallick, A.E.
2001 $^{87}Sr/^{86}Sr$: a New Discriminant for Provenancing Neolithic Porcellanite Artifacts from Ireland. *Journal of Archaeological Science* 28, 713-720.
Dalpra, C.L., Pitblado, B.L.
2016 Discriminating Quartzite Sources Petrographically in the Upper Gunnison Basin, Colorado: Implications for Paleoamerican Lithic-Procurement Studies. *PaleoAmerica* 2, 22-31.
Dawson, J.B.
1992 Neogene tectonics and volcanicity in the North Tanzania sector of the Gregory Rift Valley: contrasts with the Kenya sector. *Tectonophysics* 204, 81-92.
2008 *The Gregory Rift Valley and Neogene–Recent Volcanoes of Northern Tanzania*. Geological Society Memoir No. 33, London.

Day, M.H., Molleson, T.I.
1976 The puzzle from JK2 – A femur and a tibial fragment (O.H.34) from Olduvai Gorge, Tanzania. *Journal of Human Evolution* 5, 455-465.
Deino, A.L.
2012 $^{40}Ar/^{39}Ar$ dating of Bed I, Olduvai Gorge, Tanzania, and the chronology of early Pleistocene climate change. *Journal of Human Evolution* 63, 251-273.
Deino, A.L., Behrensmeyer, A.K., Brooks, A.S., Yellen, J.E., Sharp, W.D., Potts, R.
2018 Chronology of the Acheulean to Middle Stone Age transition in eastern Africa. *Science* 360, 95-98.
de la Torre, I., Mora, R.
2005 Unmodified lithic material at Olduvai Bed I: manuports or ecofacts? *Journal of Archaeological Science* 32, 273-285.
de la Torre, I., Benito-Calvo, A., Arroyo, A., Zupancich, A., Proffitt, T.
2013 Experimental protocols for the study of battered stone anvils from Olduvai Gorge (Tanzania). *Journal of Archaeological Science* 40, 313-332.
Diez-Martín, F., Sanchez, P., Domínguez-Rodrigo, M., Mabulla, A., Barba, R.
2009 Were Olduvai Hominins making Butchering Tools or Battering Tools? Analysis of a Recently Excavated Lithic Assemblage from BK (Bed II, Olduvai Gorge, Tanzania). *Journal of Anthropological Archaeology* 28, 274-289.
Diez-Martín, F., Sanchez Yustos, P., Domínguez-Rodrigo, M., Mabulla, A.Z.P., Bunn, H.T., Ashley, G.M., Barba, R., Baquedano, E.
2010 New insights into hominin lithic activities at FLK North Bed I, Olduvai Gorge, Tanzania. *Quaternary Research* 74, 376-387.
Diez-Martín, F., Yustos, P.S., Domínguez-Rodrigo, M., Prendergast, M.E.
2011 An Experimental Study of Bipolar and Freehand Knapping of Naibor Soit Quartz from Olduvai Gorge (Tanzania). *American Antiquity* 76, 690-708.
Diez-Martín, F., Sánchez Yustos, P., Uribelarrea, D., Baquedano, E., Mark, D.F., Mabulla, A., Fraile, C., Duque, J., Díaz, I., Pérez-González, A., Yravedra, J., Egeland, C.P., Organista, E., Domínguez-Rodrigo, M.
2015 The origin of the Acheulean: the 1.7 million-year-old site of FLK West, Olduvai Gorge (Tanzania). *Scientific Reports* 5, 17839.
Dirks, P.H.G.M., Roberts, E.M., Hilbert-Wolf, H., Kramers, J.D., Hawks, J., Dosseto, A., Duval, M., Elliott, M., Evans, M., Grün, R., Hellstrom, J., Herries, A.I.R., Joannes-Boyau, R., Makhubela, T.V., Placzek, C.J., Robbins, J., Spandler, C., Wiersma, J., Woodhead, J., Berger, L.R.
2017 The age of Homo naledi and associated sediments in the Rising Star Cave, South 308 Africa. *eLife* 6, e24231.
Domínguez-Rodrigo, M., Egido, R.B., Egeland, C.P.
2007 *Deconstructing Olduvai: A Taphonomic Study of the Bed I Sites*. Springer, Dordrecht.
Domínguez-Rodrigo, M., Pickering, T.R., Baquedano, E., Mabulla, A., Mark, D.F., Musiba, C., Bunn, H.T., Uribelarrea, D., Smith, V., Diez-Martín, F., Pérez-González, A., Sánchez, P., Santonja, M., Barboni, D., Gidna, A., Ashley, G., Yravedra, J., Heaton, J.L., Arriaza, M.C.
2013 First partial skeleton of a 1.34-million-year-old Paranthropus boisei from Bed II, Olduvai Gorge, Tanzania. *PLoS ONE* 8, e80347.

Domínguez-Rodrigo, M., Diez-Martín, F., Mabulla, A., Baquedano, E., Bunn, H.T., Musiba, C.
2014 The evolution of hominin behavior during the Oldowan-Acheulean transition: Recent evidence from Olduvai Gorge and Peninj (Tanzania). *Quaternary International* 322-323, 1-6.

Domínguez-Rodrigo, M., Alcalá, L.
2016 3.3-million-year-old stone tools and butchery traces? More evidence needed. *PaleoAnthropology* 2016, 46-53.

Ebinger, C.J., Sleep, N.H.
1998 Cenozoic magmatism throughout east Africa resulting from impact of a single plume. *Nature* 395, 788-791.

Ebright, C.A.
1987 Quartzite Petrography and its Implications for Prehistoric Use Archeological Analysis. *Archaeology of Eastern North America* 15, 29-45.

Eren, M.I., Durant, A.J., Prendergast, M., Mabulla, A.Z.P.
2014 Middle Stone Age archaeology at Olduvai Gorge, Tanzania. *Quaternary International* 322-323, 292-313.

Eugster, H.P.
1967 Hydrous Sodium Silicates from Lake Magadi, Kenya: Precursors of Bedded Chert. *Science* 157, 1177-1180.
1969 Inorganic bedded cherts from the Magadi area, Kenya. *Contributions to Mineralogy and Petrology* 22, 1-31.

Féblot-Augustins, J.
1990 Exploitation des matières premières dans l'Acheuléen d'Afrique: perspectives comportementales. *Paléo* 2, 27-42.

Fernandes, P.
2012 Itinéraires et transformations du silex: une pétroarchéologie refondée, application au Paléolithique moyen. Ph.D. Dissertation, Université de Bordeaux.

Fettes, D., Desmons, J.
2007 *Metamorphic Rocks: A Classification and Glossary of Terms*. Cambridge University Press, Cambridge.

Flannery, K.V.
1976 *The Early Mesoamerican Village*. Academic Press, London.

Foster, A., Ebinger, C., Mbede, E., Rex, D.
1997 Tectonic development of the northern Tanzanian sector of the East African Rift System. *Journal of the Geological Society* 154, 689-700.

Frahm, E.
2012 Evaluation of Archaeological Sourcing Techniques: Reconsidering and Re-Deriving Hughes' Four-Fold Assessment Scheme. *Geoarchaeology* 27, 166-174.

Freestone, I.C., Middleton, A.P.
1987 Mineralogical applications of the analytical SEM in archaeology. *Mineralogical Magazine* 51, 21-31.

Fritz, H., Abdelsalam, M., Ali, K.A., Bingen, B., Collins, A.S., Fowler, A.R., Ghebreab, W., Hauzenberger, C.A., Johnson, P.R., Kusky, T.M., Macey, P., Muhongo, S., Stern, R.J., Viola, G.
2013 Orogen styles in the East African Orogen: A review of the Neoproterozoic to Cambrian tectonic evolution. *Journal of African Earth Sciences* 86, 65-106.

Furman, T., Nelson, W.R., Elkins-Tanton, L.T.
2016 Evolution of the East African rift: Drip magmatism, lithospheric thinning and mafic volcanism. *Geochimica et Cosmochimica Acta* 185, 418-434.
Garrison, E.G.
2003 *Techniques in Archaeological Geology*. Springer, New York.
Gentry, A.W.
1966 Fossil Mammals of Africa No. 20: Fossil Antilopini of East Africa. *Bulletin of the British Museum (Natural History): Geology* 12, 45-106.
1967 Fossil Mammals of Africa No. 22: Pelorovis Oldowayensis Reck, An Extinct Bovid from East Africa. *Bulletin of the British Museum (Natural History): Geology* 14, 245-299.
Gentry, A.W., Gentry, A.
1969 Fossil Camels in Kenya and Tanzania. *Nature* 222, 898.
1978a Fossil bovidae (Mammalia) of Olduvai Gorge, Tanzania, Part I. *Bulletin of the British Museum (Natural History): Geology* 29, 289-446.
1978b Fossil bovidae (Mammalia) of Olduvai Gorge, Tanzania, Part II. *Bulletin of the British Museum (Natural History): Geology* 30, 1-83.
George, R., Rogers, N., Kelley, S.
1998 Earliest magmatism in Ethiopia: Evidence for two mantle plumes in one flood basalt province. *Geology* 26, 923-926.
Gill, R.
2010 *Igneous Rock and Processes: A Practical Guide*. Wiley-Blackwell, Chichester.
Glascock, M.D., Braswell, G., Cobean, R.H.
1998 A Systematic Approach to Obsidian Source Characterization. In *Archaeological Obsidian Studies: Method and Theory*, edited by Shackley, M.S., pp. 15-66. Springer, New York.
Glascock, M.D., Neff, H.
2003 Neutron activation analysis and provenance research in archaeology. *Measurement Science and Technology* 14, 1516-1526.
Goldman-Neuman, T., Hovers, E.
2012 Raw material selectivity in Late Pliocene Oldowan sites in the Makaamitalu Basin, Hadar, Ethiopia. *Journal of Human Evolution* 62, 353-366.
Goldsmith, R.
1959 Granofels, a New Metamorphic Rock Name. *The Journal of Geology* 67, 109-110.
Goodwin, A.J.H., Van Riet Lowe, C.
1929 *The Stone Age Cultures of South Africa*. Annals of the South African Museum, Cape Town.
Greenwood, S.M.
2014 Mineralogy and Geochemistry of Pleistocene Volcanics at Embagai Caldera and Natron Basin, Tanzania: Potential Constraints on the Stratigraphy of Olduvai Gorge. MSc Thesis, The University of Wisconsin-Milwaukee.
Grommé, C.S., Hay, R.L.
1963 Magnetization of Basalt of Bed I, Olduvai Gorge, Tanganyika. *Nature* 200, 560-561.
Gurtov, A.N., Eren, M.I.
2014 Lower Paleolithic bipolar reduction and hominin selection of quartz at Olduvai Gorge, Tanzania: What's the connection? *Quaternary International* 322-323, 285-291.

Habermann, J.M., McHenry, L.J., Stollhofen, H., Tolosana-Delgado, R., Stanistreet, I.G., Deino, A.L.
2016 Discrimination, correlation, and provenance of Bed I tephrostratigraphic markers, Olduvai Gorge, Tanzania, based on multivariate analyses of phenocryst compositions. *Sedimentary Geology* 339, 115-133.
Hall, E.T.
1960 X-ray fluorescent analysis applied to archaeology. *Archaeometry* 3, 29-35.
Harmand, S., Lewis, J.E., Feibel, C.S., Lepre, C.J., Prat, S., Lenoble, A., Boës, X., Quinn, R.L., Brenet, M., Arroyo, A., Taylor, N., Clément, S., Daver, G., Brugal, J.-P., Leakey, L., Mortlock, R.A., Wright, J.D., Lokorodi, S., Kirwa, C., Kent, D.V., Roche, H.
2015 3.3-million-year-old stone tools from Lomekwi 3, West Turkana, Kenya. *Nature* 521, 310-315.
Hay, R.L.
1968 Chert and Its Sodium-Silicate Precursors in Sodium-Carbonate Lakes of East Africa. *Contributions to Mineralogy and Petrology* 17, 255-274.
1971 Geologic Background of Beds I and II: Stratigraphic Summary. In *Olduvai Gorge Vol. 3: Excavations in Beds I and II, 1960-1963*, edited by Leakey, M.D., pp. 9-18. Cambridge University Press, Cambridge.
1973 Lithofacies and Environments of Bed I, Olduvai Gorge, Tanzania. *Quaternary Research* 3, 541-560.
1976 *Geology of the Olduvai Gorge: A Study of Sedimentation in a Semiarid Basin*. University of California Press, Berkeley.
1990 Olduvai Gorge: A case history in the interpretation of hominid paleoenvironments in East Africa. In *Establishment of a Geologic Framework for Paleoanthropology*, edited by Laporte, L.F., pp. 23-37. Geological Society of America Special Paper 242, Boulder.
Hay, R.L., Kyser, T.K.
2001 Chemical sedimentology and paleoenvironmental history of Lake Olduvai, a Pliocene lake in northern Tanzania. *GSA Bulletin* 113, 1505-1521.
Heizer, R.F., Williams, H., Graham, J.A.
1965 Notes on Mesoamerican Obsidians and Their Significance in Archaeological Studies. *Contributions of the University of California Archaeological Research Facility* 1, 94-103.
Henderson, J.
2000 *The Science and Archaeology of Materials: An Investigation of Inorganic Materials*. Routledge, London.
Hepworth, J.V.
1972 The Mozambique orogenic belt and its foreland in northeast Tanzania: a photogeologically-based study. *Journal of the Geological Society* 128, 461-494.
Hermes, O.D., Luedtke, B.E., Ritchie, D.
2001 Melrose Green Rhyolite: Its Geologic Setting and Petrographic and Geochemical Characteristics. *Journal of Archaeological Science* 28, 913-928.
Hodgson, D.L.
2011 *Being Maasai, Becoming Indigenous*. Indiana University Press, Bloomington.
Holmes, A.
1951 The sequence of Precambrian orogenic belts in south and central Africa. *18th International Geological Congress* 14, 254-269.

Hublin, J.-J., Ben-Ncer, A., Bailey, S.E., Freidline, S.E., Neubauer, S., Skinner, M.M., Bergmann, I., Le Cabec, A., Benazzi, S., Harvati, K., Gunz, P.
2017 New fossils from Jebel Irhoud, Morocco and the pan-African origin of Homo sapiens. *Nature* 546, 289-292.
Jack, R.N., Heizer, R.F.
1968 "Finger-Printing" of some Mesoamerican Obsidian Artifacts. *Contributions of the University of California Archaeological Research Facility* 5, 81-100.
Johanson, D.C., White, T.D., Coppens, Y.
1978 A new species of the genus Australopithecus (Primates: Hominidae) from the Pliocene of Eastern Africa. *Kirtlandia* 28, 2-14.
Johanson, D.C., Masao, F.T., Eck, G.G., White, T.D., Walter, R.C., Kimbel, W.H., Asfaw, B., Manega, P., Ndessokia, P., Suwa, G.
1987 New partial skeleton of Homo habilis from Olduvai Gorge, Tanzania. *Nature* 327, 205-209.
Johnson, C.R., McBrearty, S.
2010 500,000 year old blades from the Kapthurin Formation, Kenya. *Journal of Human Evolution* 58, 193-200.
Jones, M.P.
1987 *Applied mineralogy: A quantitative approach*. Graham and Trotman, London.
Jones, P.R.
1979 Effects of Raw Materials on Biface Manufacture. *Science* 204, 835-836.
1981 Experimental Implement Manufacture and Use; A Case Study from Olduvai Gorge, Tanzania. *Philosophical Transactions of the Royal Society of London Series B, Biological Sciences* 292, 189-195.
1994 Results of Experimental Work in Relation to the Stone Industries of Olduvai Gorge. In *Olduvai Gorge Volume 5: Excavations in Beds III, IV and the Masek Beds, 1968-1971*, edited by Leakey, M.D., Roe, D.A., pp. 254-298. Cambridge University Press, Cambridge.
Kabete, J.M., Groves, D.I., McNaughton, N.J., Mruma, A.H.
2012 A new tectonic and temporal framework for the Tanzanian Shield: implications for gold metallogeny and undiscovered endowment. *Ore Geology Reviews* 48, 88-124.
Kasanzu, C., Maboko, M.A.H., Manya, S.
2008 Geochemistry of fine-grained clastic sedimentary rocks of the Neoproterozoic Ikorongo Group, NE Tanzania: Implications for provenance and source rock weathering. *Precambrian Research* 164, 201-213.
Kasztovszky, Z.S., Biró, K.T., Markó, A., Dobosi, V.
2008 Cold neutron prompt gamma activation analysis – a non destructive method for characterisation of high silica content chipped stone tools and raw materials. *Archaeometry* 50, 12-29.
Keiller, A., Piggott, S., Wallis, F.S.
1941 First Report of the Sub-Committee of the South-Western Group of Museums and Art Galleries on the Petrological Identification of Stone Axes. *Proceedings of the Prehistoric Society* 7, 50-72.
Kervyn, M., Ernst, G.G.J., Klaudius, J., Keller, J., Mbede, E., Jacobs, P.
2008 Remote sensing study of sector collapses and debris avalanche deposits at Oldoinyo Lengai and Kerimasi volcanoes, Tanzania. *International Journal of Remote Sensing* 29, 6565-6595.

Kimura, Y.
1997 The MNK Chert Factory Site: The Chert-Using Strategy by Early Hominids at Olduvai Gorge, Tanzania. *African Study Monographs* 18, 1-28.
Klein, C., Philpotts, A.R.
2017 Earth *Materials: Introduction to Mineralogy and Petrology*. 2nd Edition. Cambridge University Press, Cambridge.
Kleindienst, M.R.
1964 Summary report on excavations at site JK 2, Olduvai Gorge, Tanganyika, 1961-1962. *Annual Report of the Antiquities Division of Tanganyika*, Appendix 2, 4-6.
1973 Excavations at Site JK2, Olduvai Gorge, Tanzania, 1961-1962; The Geological Setting. *Quarternia* 17, 145-208.
Kooyman, B.P.
2000 *Understanding Stone Tools and Archaeological Sites*. University of Calgary Press, Calgary.
Koptev, A., Burov, E., Calais, E., Leroy, S., Gerya, T., Guillou-Frottier, L., Cloetingh, S.
2016 Contrasted continental rifting via plume-craton interaction: Applications to Central East African Rift. *Geoscience Frontiers* 7, 221-236.
Kröner, A., Stern, R.J.
2005 Pan-African Orogeny. In *Encyclopedia of Geology*, Vol. 1, pp. 1-12. Elsevier, Amsterdam.
Kyara, O.
1996 Lithic raw materials as an epistemological tool for hominid behavioural reconstruction: a preliminary overview. In *Aspects of African Archaeology: Papers from the Congress of the PanAfrican Association for Prehistory and Related Studies*, edited by Pwiti, G., Soper, R., pp. 111-120. University of Zimbabwe, Harare.
1999 Lithic Raw Materials and their Implications on Assemblage Variation and Hominid Behavior during Bed II, Olduvai Gorge, Tanzania. Ph.D. Dissertation, Rutgers University.
Latin, D., Norry, M.J., Tarzey, R.J.E.
1993 Magmatism in the Gregory Rift, East Africa: Evidence for Melt Generation by a Plume. *Journal of Petrology* 34, 1007-1027.
Leakey, L.S.B.
1959a The Fossil Skull from Olduwai. *British Medical Journal* 2, 635.
1959b A New Fossil Skull from Olduvai. *Nature* 184, 491-493.
1965 *Olduvai Gorge, 1951-1961. Vol. 1: A Preliminary Report on the Geology and Fauna*. Cambridge University Press, Cambridge.
1974 *By the Evidence: Memoirs, 1932-1951*. Harcourt Brace Jovanovich, New York.
Leakey, L.S.B., Hopwood, A.T., Reck, H.
1931 Age of the Oldoway Bone Beds, Tanganyika Territory. *Nature* 128, 724.
Leakey, L.S.B., Reck, H., Boswell, P.G.H., Hopwood, A.T., Solomon, J.D.
1933 The Oldoway Human Skeleton. *Nature* 131, 397-398.
Leakey, L.S.B., Evernden, J.F., Curtis, G.H.
1961 Age of Bed I, Olduvai Gorge, Tanganyika. *Nature* 191, 478-479.
Leakey, L.S.B., Tobias, P.V., Napier, J.R.
1964 A New Species of the Genus Homo from Olduvai Gorge. *Nature* 202, 7-9.

Leakey, M.D.
1971 *Olduvai Gorge Vol. 3: Excavations in Beds I and II, 1960-1963*. Cambridge University Press, Cambridge.
1978 Olduvai Gorge 1911-75: a history of the investigations. *Geological Society* 6, 151-155.
1979 *Olduvai Gorge: My Search for Early Man*. Collins, London.
1984 *Disclosing the Past*. Weidenfeld and Nicolson, London.
1994a Bed III Site JK (Juma's Korongo). In *Olduvai Gorge Vol. 5: Excavations in Beds III, IV and the Masek Beds, 1968-1971*, edited by Leakey, M.D., Roe, D.A., pp. 15-35. Cambridge University Press, Cambridge.
1994b Lower Bed IV HEB East, HEB and HEB West, WK Intermediate Channel. In *Olduvai Gorge Volume 5: Excavations in Beds III, IV and the Masek Beds, 1968-1971*, edited by Leakey, M.D., Roe, D.A., pp. 45-72. Cambridge University Press, Cambridge.
Leakey, M.D., Hay, R.L., Thurber, D.L., Protsch, R., Berger, R.
1972 Stratigraphy, Archaeology, and Age of the Ndutu and Naisiusiu Beds, Olduvai Gorge, Tanzania. *World Archaeology* 3, 328-341.
Leakey, M.D., Harris, J.M.
1987 *Laetoli: A Pliocene Site in Northern Tanzania*. Oxford University Press, Oxford.
Leakey, M.D., Roe, D.A.
1994 *Olduvai Gorge Volume 5: Excavations in Beds III, IV and the Masek Beds, 1968-1971*. Cambridge University Press, Cambridge.
Leakey, M.G., Spoor, F., Brown, F.H., Gathogo, P.N., Kiarie, C., Leakey, L.N., McDougall, I.
2001 New hominin genus from eastern Africa shows diverse middle Pliocene lineages. *Nature* 410, 433-440.
Lebo, S.A., Johnson, K.T.M.
2007 Geochemical sourcing of rock specimens and stone artifacts from Nihoa and Necker Islands, Hawai'i. *Journal of Archaeological Science* 34, 858-871.
Le Gall, B., Nonnotte, P., Rolet, J., Benoit, M., Guillou, H., Mousseau-Nonnotte, M., Albaric, J., Deverchère, J.
2008 Rift propagation at craton margin. Distribution of faulting and volcanism in the North Tanzanian Divergence (East Africa) during Neogene times. *Tectonophysics* 448, 1-19.
Lee, P.
2018 Digging Droughts: Maasai and Palaeoanthropological Knowledge, Subsistence, and Collaboration in Oldupai Gorge, Tanzania. Master's Thesis, University of Calgary.
Lee, P., Koromo, S., Mercader, J., Mather, C.
2019 Scientific facts and oral traditions in Oldupai Gorge, Tanzania: Symmetrically analysing palaeoanthropological and Maasai black boxes. *Social Science Information*, 1-27.
Lepre, C.J., Roche, H., Kent, D.V., Harmand, S., Quinn, R.L., Brugal, J.-P., Texier, P.-J., Lenoble, A., Feibel, C.S.
2011 An earlier origin for the Acheulian. *Nature* 477, 82-85.
Mabulla, A.Z.P.
1990 Preliminary report on an archaeological survey of the Ndutu Beds, Olduvai Gorge, Tanzania. *Nyame Akuma* 33, 20-25.

Macfarlane, A.
1969 Preliminary report on the geology of the Central Serengeti, NE Tanzania. In *13th Annual Report on Scientific Results,* Research Institute of African Geology, University of Leeds, pp. 14-16.
Macheveki, A.S., Delvaux, D., De Batist, M., Mruma, A.
2008 Fault kinematics and tectonic stress in the seismically active Manyara–Dodoma Rift segment in Central Tanzania – Implications for the East African Rift. *Journal of African Earth Sciences* 51, 163-188.
Mallory-Greenough, L.M., Greenough, J.D., Owen, J.V.
1998 New Data For Old Pots: Trace-Element Characterization of Ancient Egyptian Pottery Using ICP-MS. *Journal of Archaeological Science* 25, 85-97.
Mana, S., Furman, T., Carr, M.J., Mollel, G.F., Mortlock, R.A., Feigenson, M.D., Turrin, B.D. Swisher, C.C.
2012 Geochronology and geochemistry of the Essimingor volcano: Melting of metasomatized lithospheric mantle beneath the North Tanzanian Divergence zone (East African Rift). *Lithos* 155, 310-325.
Manega, P.C.
1993 Geochronology, Geochemistry and Isotopic Study of the Plio-Pleistocene Hominid Sites and the Ngorongoro Volcanic Highland in Northern Tanzania. Ph.D. Dissertation, University of Colorado.
Mason, O.K., Aigner, J.S.
1987 Petrographic Analysis of Basalt Artifacts from Three Aleutian Sites. *American Antiquity* 52, 595-607.
Matu, M., Crevecoeur, I., Huchet, J.-B.
2017 Taphonomy and Paleoichnology of Olduvai Hominid 1 (OH1), Tanzania. *International Journal of Osteoarchaeology* 27, 785-800.
McBrearty, S., Brooks, A.S.
2000 The revolution that wasn't: a new interpretation of the origin of modern human behavior. *Journal of Human Evolution* 39, 453-563.
McBrearty, S., Tryon, C.A.
2006 From Acheulean to Middle Stone Age in the Kapthurin Formation, Kenya. In *Transitions Before the Transition: Evolution and Stability in the Middle Paleolithic and Middle Stone Age*, edited by Hovers, E., Kuhn, S.L., pp. 257-277. Springer, New York.
Macgregor, D.
2015 History of the development of the East African Rift System: A series of interpreted maps through time. *Journal of African Earth Sciences* 101, 232-252.
McHenry, L.J., de la Torre, I.
2018 Hominin raw material procurement in the Oldowan-Acheulean transition at Olduvai Gorge. *Journal of Human Evolution* 120, 378-401.
McHenry, L.J., Mollel, G.F., Swisher, C.C.
2008 Compositional and textural correlations between Olduvai Gorge Bed I tephra and volcanic sources in the Ngorongoro Volcanic Highlands, Tanzania. *Quaternary International* 178, 306-319.
Mees, F., Segers, S., Van Ranst, E.
2007 Palaeoenvironmental significance of the clay mineral composition of Olduvai basin deposits, northern Tanzania. *Journal of African Earth Sciences* 47, 39-48.

Mehlman, M.J.
1977 Excavations at Nasera Rock, Tanzania. *Azania* 12, 111-118.
1987 Provenience, Age and Associations of Archaic Homo sapiens Crania from Lake Eyasi, Tanzania. *Journal of Archaeological Science* 14, 133-162.
Mercader, J., Gosse, J.C., Bennett, T., Hidy, A.J., Rood, D.H.
2012 Cosmogenic nuclide age constraints on Middle Stone Age lithics from Niassa, Mozambique. *Quaternary Science Reviews* 47, 116-130.
Merrick, H.V., Brown, F.H.
1984 Obsidian Sources and Patterns of Source Utilization in Kenya and Northern Tanzania: Some Initial Findings. *African Archaeological Review* 2, 129-152.
Merrick, H.V., Brown, F.H., Nash, W.P.
1994 Use and movement of obsidian in the Early and Middle Stone Ages of Kenya and northern Tanzania. In *Society, Culture, and Technology in Africa*, edited by Childs, S.T., pp. 29-44. MASCA Research Papers in Science and Archaeology Vol. 11, Philadelphia.
Mollel, G.F.
2002 Petrology and Geochemistry of the Southeastern Ngorongoro Volcanic Highland; and Contribution to "Sourcing" of Stone Tools at Olduvai Gorge, Tanzania. MSc Thesis, Rutgers University.
2007 Petrochemistry and Geochronology of Ngorongoro Volcanic Highland Complex (NVHC) and its Relationship to Laetoli and Olduvai Gorge, Tanzania. Ph.D. Dissertation, Rutgers University.
Mollel, G.F., Swisher, C.C., Feigenson, M.D., Carr, M.J.
2008 Geochemical evolution of Ngorongoro Caldera, Northern Tanzania: Implications for crust–magma interaction. *Earth and Planetary Science Letters* 271, 337-347.
Mollel, G.F., Swisher, C.C., McHenry, L.J., Feigenson, M.D., Carr, M.J.
2009 Petrogenesis of basalt–trachyte lavas from Olmoti Crater, Tanzania. *Journal of African Earth Sciences* 54, 127-143.
Mollel, G.F., Swisher, C.C.
2012 The Ngorongoro Volcanic Highland and its relationships to volcanic deposits at Olduvai Gorge and East African Rift volcanism. *Journal of Human Evolution* 63, 274-283.
Mora, R., de la Torre, I.
2005 Percussion Tools in Olduvai Beds I and II (Tanzania): Implications for Early Human Activities. *Journal of Anthropological Archaeology* 24, 179-192.
Morell, V.
1995 *Ancestral Passions: The Leakey Family and the Quest for Humankind's Beginnings*. Simon and Schuster, New York.
Nash, D.J., Coulson, S., Staurset, S., Ullyott, J.S., Babutsi, M., Hopkinson, L., Smith, M.P.
2013 Provenancing of silcrete raw materials indicates long-distance transport to Tsodilo Hills, Botswana, during the Middle Stone Age. *Journal of Human Evolution* 64, 280-288.
Neff, H.
2017 Inductively Coupled Plasma-Mass Spectrometry (ICP-MS). In *Encyclopedia of Geoarchaeology*, edited by Gilbert, A.S., pp. 433-449. Springer, Dordrecht.
Negash, A., Shackley, M.S., Alene, M.
2006 Source provenance of obsidian artifacts from the Early Stone Age (ESA) site of Melka Konture, Ethiopia. *Journal of Archaeological Science* 33, 1647-1650.

Negash, A., Brown, F., Nash, B.
2011 Varieties and sources of artefactual obsidian in the middle stone age of the middle Awash, Ethiopia. *Archaeometry* 53, 661-673.
Negash, A., Shackley, M.S.
2006 Geochemical provenance of obsidian artefacts from the MSA site of Porc Epic, Ethiopia. *Archaeometry* 48, 1-12.
Nesse, W.D.
2013 *Introduction to Optical Mineralogy*. 4th Edition. Oxford University Press, Oxford.
Nyblade, A.A., Owens, T.J., Gurrola, H., Ritsema, J., Langston, C.A.
2000 Seismic evidence for a deep upper mantle thermal anomaly beneath east Africa. *Geology* 28, 599-602.
O'Neil, J.R., Hay, R.L.
1973 $^{18}O/^{16}O$ ratios in cherts associated with the saline lake deposits of East Africa. *Earth and Planetary Science Letters* 19, 257-266.
Parish, R.M., Swihart, G.M., Li, Y.S.
2013 Evaluating Fourier Transform Infrared Spectroscopy as a Non-Destructive Chert Sourcing Technique. *Geoarchaeology* 28, 289-307.
Parks, G.A., Tieh, T.T.
1966 Identifying the geographical Source of Artefact Obsidian. *Nature* 211, 289-290.
Peacock, D.P.S.
1967 Romano-British pottery production in the Malvern district of Worcestershire. *Transactions of the Worcestershire Archaeological Society* 1, 15-28.
Peacock, E.
1989 Microdebitage from Cached Pitted Stones. *Mississippi Archaeology* 24, 17-27.
Perkins, D.
1998 *Mineralogy*. Prentice Hall, New Jersey.
Pickering, R.
1958 Oldoinyo Ogol (Serengeti Plain East). Geological Survey of Tanganyika Quarter Degree Sheet 38.
1960 A Preliminary Note on the Quaternary Geology of Tanganyika. In *Joint Meeting, East-Central, West-Central and Southern Regional Committees for Geology*, pp. 77-89.
1964 Endulen. Geological Survey of Tanzania Quarter Degree Sheet 52.
1965 Ngorongoro. Geological Survey of Tanzania Quarter Degree Sheet 53.
Pitblado, B.L., Dehler, C., Neff, H., Nelson, S.T.
2008 Pilot Study Experiments Sourcing Quartzite, Gunnison Basin, Colorado. *Geoarchaeology* 23, 742-778.
Pitblado, B.L., Cannon, M.B., Neff, H., Dehler, C.M., Nelson, S.T.
2013 LA-ICP-MS analysis of quartzite from the Upper Gunnison Basin, Colorado. *Journal of Archaeological Science* 40, 2196-2216.
Plummer, T.
2004 Flaked Stones and Old Bones: Biological and Cultural Evolution at the Dawn of Technology. *American Journal of Physical Anthropology* 47, 118-164.
Pollard, A.M., Bray, P.J., Gosden, C.
2014 Is there something missing in scientific provenance studies of prehistoric artefacts? *Antiquity* 88, 625-631.

Potts, R.
1988 *Early Hominid Activities at Olduvai*. Aldine de Gruyter, New York.
Prieto, A., Yusta, I., Arrizabalaga, A.
2019 Defining and characterizing archaeological quartzite: sedimentary and metamorphic processes in the lithic assemblages of El Habario and El Arteu (Cantabrian Mountains, northern Spain). *Archaeometry* 61, 14-30.
Proffitt, T.
2018 Is there a Developed Oldowan A at Olduvai Gorge? A diachronic analysis of the Oldowan in Bed I and Lower-Middle Bed II at Olduvai Gorge, Tanzania. *Journal of Human Evolution* 120, 92-113.
Protsch, R.
1974 The Age and Stratigraphic Position of Olduvai Hominid I. *Journal of Human Evolution* 3, 379-385.
Redmount, C.A., Morgenstein, M.E.
1996 Major and Trace Element Analysis of Modern Egyptian Pottery. *Journal of Archaeological Science* 23, 741-762.
Reimer, R.
2018 Lithic Sourcing in Canada. *Canadian Journal of Archaeology* 43, 137-143.
Reiner, W.B., Masao, F., Sholts, S.B., Songita, A.V., Stanistreet, I., Stollhofen, H., Taylor, R.E., Hlusko, L.J.
2017 OH 83: A new early modern human fossil cranium from the Ndutu beds of Olduvai Gorge, Tanzania. *Journal of Physical Anthropology* 164, 533-545.
Renfrew, C.
1975 Trade as Action at a Distance. In *Ancient Civilization and Trade*, edited by Sabloff, J.A., Lamberg-Karlovsky, C.C., pp. 3-60. University of New Mexico Press, Albuquerque
Reti, J.S.
2013 Methods for Determining Differential Behaviors in Stone Tool Production and Application to the Oldowan of Olduvai Gorge, Tanzania and Koobi Fora, Kenya. Ph.D. Dissertation, Rutgers University.
Richter, D., Grün, R., Joannes-Boyau, R., Steele, T.E., Amani, F., Rué, M., Fernandes, P., Raynal, J.-P., Geraads, D., Ben-Ncer, A., Hublin, J.-J., McPherron, S.P.
2017 The age of the hominin fossils from Jebel Irhoud, Morocco, and the origins of the Middle Stone Age. *Nature* 546, 293-296.
Rightmire, G.P.
1980 Middle Pleistocene hominids from Olduvai Gorge, Northern Tanzania. American *Journal of Physical Anthropology* 53, 225-242.
Ring, U., Schwartz, H.L., Bromage, T.G., Sanaane, C.
2005 Kinematic and sedimentological evolution of the Manyara Rift in northern Tanzania, East Africa. *Geological Magazine* 142, 355-368.
Roberts, P.
2016 'We have never been behaviourally modern': The implications of Material Engagement Theory and Metaplasticity for understanding the Late Pleistocene record of human behaviour. *Quaternary International* 405, 8-20.

Roberts, E.M., Stevens, N.J., O'Connor, P.M., Dirks, P.H.G.M., Gottfried, M.D., Clyde, W.C., Armstrong, R.A., Kemp, A.I.S., Hemming, S.
2012 Initiation of the western branch of the East African Rift coeval with the eastern branch. *Nature Geoscience* 5, 289-294.
Sanislav, I.V., Wormald, R.J., Dirks, P.H.G.M., Blenkinsop, T.G., Salamba, L., Joseph, D.
2014 Zircon U–Pb ages and Lu–Hf isotope systematics from late-tectonic granites, Geita Greenstone Belt: Implications for crustal growth of the Tanzania Craton. *Precambrian Research* 242, 187-204.
Santonja, M., Panera, J., Rubio-Jara, S., Pérez-González, A., Uribelarrea, D., Domínguez-Rodrigo, M., Mabulla, A.Z.P., Bunn, H.T., Baquedano, E.
2014 Technological strategies and the economy of raw materials in the TK (Thiongo Korongo) lower occupation, Bed II, Olduvai Gorge, Tanzania. *Quaternary International* 322-323, 181-208.
Sayre, E.V., Dodson, R.W.
1957 Neutron Activation Study of Mediterranean Potsherds. *American Journal of Archaeology* 61, 35-41.
Scoon, R.N.
2018 *Geology of National Parks of Central/Southern Kenya and Northern Tanzania*. Springer, Cham.
Semaw, S., Renne, P., Harris, J.W.K., Feibel, C.S., Bernor, R.L., Fesseha, N., Mowbray, K.
1997 2.5-million-year-old stone tools from Gona, Ethiopia. *Nature* 385, 333-336.
Semaw, S., Rogers, M.J., Renne, P.R., Butler, R.F., Dominguez-Rodrigo, M., Stout, D., Hart, W.S., Pickering, T., Simpson, S.W.
2003 2.6-Million-year-old stone tools and associated bones from OGS-6 and OGS-7, Gona, Afar, Ethiopia. *Journal of Human Evolution* 45, 169-177.
Shackley, M.S.
2008 Archaeological petrology and the archaeometry of lithic materials. *Archaeometry* 50, 194-215.
2011 An Introduction to X-Ray Fluorescence (XRF) Analysis in Archaeology. In *X-Ray Fluorescence Spectrometry (XRF) in Geoarchaeology*, edited by Shackley, M.S., pp. 7-44. Springer, New York.
Sheppard, A.O.
1936 Technology of Pecos pottery. In *The Pottery of Pecos*, edited by Kidder, A.V., Shepard, A.O., pp. 389-587. Papers of the Phillips Academy Southwestern Expedition, No. 7. Yale University Press, New Haven.
Shotton, F.W., Hendry, G.L.
1979 The Developing Field of Petrology in Archaeology. *Journal of Archaeological Science* 6, 75-84.
Sidrys, R.V.
1976 Classic Maya Obsidian Trade. *American Antiquity* 41, 449-464.
Sorensen, A.C., Claud, E., Soressi, M.
2018 Neandertal fire-making technology inferred from microwear analysis. *Scientific Reports* 8, 10065.

Soto, M., Favreau, J., Campeau, K., Carter, T., Abtosway, M., Bushozi, P.M., Clarke, S., Durkin, P.R., Hubbard, S.M., Inwood, J., Itambu, M., Koromo, S., Larter, F., Lee, P., Mwambwiga, A., Nair, R., Patalano, R., Tucker, L., Zebedayo, L., Mercader, J.

Forthcoming Fingerprinting of Quartzitic Outcrops at Olduvai Gorge, Tanzania. To be submitted to *Palaeogeography, Palaeoclimatology, Palaeoecology*.

Speakman, R.J., Glascock, M.D.

2007 Acknowledging fifty years of neutron activation analysis in archaeology. *Archaeometry* 49, 179-183.

Spell, T.L., McDougall, I.

1992 Revisions to the age of the Brunhes-Matuyama Boundary and the Pleistocene geomagnetic polarity timescale. *Geophysical Research Letters* 19, 1181-1184.

Stiles, D.

1991 Early Hominid Behaviour and Culture Tradition: Raw Material Studies in Bed II, Olduvai Gorge. *The African Archaeological Review* 9, 1-19.

1998 Raw material as evidence for human behaviour in the Lower Pleistocene: the Olduvai case. In *Early Human Behaviour in Global Context: The Rise and Diversity of the Lower Palaeolithic Record*, edited by Petraglia, M.D., Korisettar, R., pp. 130-145. Routledge, London.

Stiles, D.N., Hay, R.L., O'Neil, J.R.

1974 The MNK Chert Factory Site, Olduvai Gorge, Tanzania. *World Archaeology* 5, 285-308.

Stipp, M., Stünitz, H., Heilbronner, R., Schmid, S.M.

2002 Dynamic recrystallization of quartz: correlation between natural and experimental conditions. In *Deformation Mechanisms, Rheology and Tectonics: Current Status and Future Perspectives*, edited by De Meer, S., Drury, M.R., De Bresser, J.H.P., Pennock, G.M., pp. 171-190. Geological Society, London.

Stollhofen, H., Stanistreet, I.G.

2012 Plio-Pleistocene synsedimentary fault compartments, foundation for the eastern Olduvai Basin paleoenvironmental mosaic, Tanzania. *Journal of Human Evolution* 63, 309-327.

Stoltman, J.B.

1989 A Quantitative Approach to the Petrographic Analysis of Ceramic Thin Sections. *American Antiquity* 54, 147-160.

Stout, D., Quade, J., Semaw, S., Rogers, M.J., Levin, N.E.

2005 Raw material selectivity of the earliest stone toolmakers at Gona, Afar, Ethiopia. *Journal of Human Evolution* 48, 365-380.

Streckeisen, A.

1976 To each plutonic rock its proper name. *Earth Science Reviews* 12, 1-33.

Stross, F.H., Hay, R.L., Asaro, F., Bowman, H.R., Michel, H.V.

1988 Sources of the quartzite of some ancient Egyptian sculptures. *Archaeometry* 30, 109-119.

Sunyer, M.R., Torcal, R.M., Figueroa, J.P., Martínez-Moreno, J., Benito-Calvo, A.

2017 Quartzite selection in fluvial deposits: The N12 level of Roca dels Bous (Middle Palaeolithic, southeastern Pyrenees). *Quaternary International* 435, 49-60.

Susino, G.J.
2007 *Analysis of lithic artefact microdebitage for chronological determination of archaeological sites*. Archaeopress, Oxford.
Susman, R.L., Stern, J.T.
1982 Functional Morphology of Homo habilis. *Science* 217, 931-934.
Tactikos, J.C.
2005 A Landscape Perspective on the Oldowan from Olduvai Gorge, Tanzania. Ph.D. Dissertation, Rutgers University.
Tamrat, E., Thouveny, N., Taïeb, M., Opdyke, N.D.
1995 Revised magnetostratigraphy of the Plio-Pleistocene sedimentary sequence of the Olduvai Formation (Tanzania). *Palaeogeography, Palaeoclimatology, Palaeoecology* 114, 273-283.
Terry, R.D., Chilingar, G.V.
1955 Summary of "Concerning Some Additional Aids in Studying Sedimentary Formations" By M.S. Shvetsov. *Journal of Sedimentary Petrology* 25, 229-234.
Thomas, H.H.
1923 The Source of the Stones of Stonehenge. *The Antiquaries Journal* 3, 239-260.
Toth, N., Schick, K.
2018 An overview of the cognitive implications of the Oldowan Industrial Complex. *Azania* 53, 3-39.
Trigger, B.
2006 *A History of Archaeological Thought*. 2nd Edition. Cambridge University Press, New York.
Tryon, C.A., Faith, J.T.
2013 Variability in the Middle Stone Age of Eastern Africa. *Current Anthropology* 54, S234-S254.
Uribelarrea, D., Martín-Perea, D., Diez-Martín, F., Sánchez-Yustos, P., Domínguez-Rodrigo, M., Baquedano, E., Mabulla, A.
2017 A reconstruction of the paleolandscape during the earliest Acheulian of FLK West: The co-existence of Oldowan and Acheulian industries during lowermost Bed II (Olduvai Gorge, Tanzania). *Palaeogeography, Palaeoclimatology, Palaeoecology* 488, 50-58.
Veldeman, I., Baele, J.-M., Goemaere, E., Deceukelaire, M., Dusar, M., De Doncker, H.W.J.A.
2012 Characterizing the hypersiliceous rocks of Belgium used in (pre-)history: a case study on sourcing sedimentary quartzites. *Journal of Geophysics and Engineering* 9, S118-S128.
Vince, A.
2005 Ceramic Petrology and the Study of Anglo-Saxon and Later Medieval Ceramics. *Medieval Archaeology* 49, 219-245.
Wadley, L.
2001. What is cultural modernity? A general view and a South African perspective from Rose Cottage Cave. *Cambridge Archaeological Journal* 11, 201-221.
Wadley, L., Kempson, H.
2011 A review of rock studies for archaeologists, and an analysis of dolerite and hornfels from the Sibudu area, KwaZulu-Natal. *Southern African Humanities* 23, 87-107.
Weaver, J., Stross, F.
1965 Analysis by x-ray fluorescence of some American obsidians. *Contributions of the University of California Archaeological Research Facility* 1, 89-93.

Weigand, P.C., Harbottle, G., Sayre, E.V.
1977 Turquoise sources and source analysis: Mesoamerica and the Southwestern USA. In *Exchange Systems in Prehistory*, edited by Earle, T.K., Ericson, J.E., pp. 15-34. Academic Press, New York.
Weisler, M.I.
1993 Provenance Studies of Polynesian Basalt Adze Material: A Review and Suggestions for Improving Regional Data Bases Source. *Asian Perspectives* 32, 61-83.
Wilkins, J., Chazan, M.
2012 Blade production ~500 thousand years ago at Kathu Pan 1, South Africa: support for a multiple origins hypothesis for early Middle Pleistocene blade technologies. *Journal of Archaeological Science* 39, 1883-1900.
Wood, B.
2014 Fifty years after Homo habilis. *Nature* 508, 31-33.
Yravedra, J., Maté-González, M.Á., Palomeque-González, J.F., Aramendi, J., Estaca-Gómez, V., San Juan Blazquez, M., García Vargas, E., Organista, E., González-Aguilera, D., Arriaza, M.C.
2017 A new approach to raw material use in the exploitation of animal carcasses at BK (Upper Bed II, Olduvai Gorge, Tanzania): a micro-photogrammetric and geometric morphometric analysis of fossil cut marks. *Boreas* 46, 860-873.
Yustos, P.S., Diez-Martín, F., Díaz, I.M., Duque, J., Fraile, C., Domínguez, M.
2015 Production and use of percussive stone tools in the Early Stone Age: Experimental approach to the lithic record of Olduvai Gorge, Tanzania. *Journal of Archaeological Science: Reports* 2, 367-383.
Zaitsev, A.N., Wenzel, T., Spratt, J., Williams, T.C., Strekopytov, S., Sharygin, V.V., Petrov, S.V., Golovina, T.A., Zaitseva, E.O., Markl, G.
2011 Was Sadiman volcano a source for the Laetoli Footprint Tuff? *Journal of Human Evolution* 61, 121-124.
Zaitsev, A.N., Marks, M.A.W., Wenzel, T., Spratt, J., Sharygin, V.V., Strekopytov, S., Markl, G.
2012 Mineralogy, geochemistry and petrology of the phonolitic to nephelinitic Sadiman volcano, Crater Highlands, Tanzania. *Lithos* 152, 66-83.

Appendix A Coordinates and Elevation Per Sample					
Position	**Outcrop/Source**	**Sample ID**	**Elevation**	**Latitude**	**Longitude**
Primary	Endonyo Osunyai	Endonyo Osunyai 1	1535.359375	-2.94173193	35.31578445
		Endonyo Osunyai 2	1537.794434	-2.941903114	35.31601715
		Endonyo Osunyai 4A/B	1539.992554	-2.941279888	35.31591797
	Engelosin	Engelosin 2	1648.300781	-2.914887905	35.38070679
		Engelosin 5A/B	1627.44812	-2.914793968	35.38246536
		Engelosin 6A/B	1623.505859	-2.914653063	35.38228607
		Engelosin 10A/B	1637.711548	-2.914340019	35.3804512
	Gol Mountains	DDD1	1589.018799	-2.879957914	35.38819504
		JJJ1	1679.474487	-2.803467035	35.33052063
		KKK1	1680.617798	-2.802887917	35.33030319
		OOO1	1823.522461	-2.740452051	35.35943985
		PPP1	1758.585571	-2.741049051	35.33343124
		RRR1	1756.909668	-2.765012026	35.32299805
		SSS1	1751.413208	-2.764199018	35.32303238
		TTT1	1669.74585	-2.80397296	35.2629509
		UUU1	1675.977417	-2.803359032	35.2624855
	Granite Falls	Granite Falls 1A/B	1532.859863	-2.944104195	35.22867584
		Granite Falls 2	1534.00000	-2.944531441	35.22938156
	Kelogi	Kelogi 1	1547.785767	-3.030328035	35.28295135
		Kelogi 3	1570.539917	-3.032514095	35.27731705
		Kelogi 10	1556.505737	-3.030023098	35.27932739
	Naibor Soit Kubwa	Naibor Soit Kubwa N042	1542.00000	-2.966530085	35.35212708
		Naibor Soit Kubwa E039	1526.00000	-2.969201088	35.35315704
		Naibor Soit Kubwa S06	1508.00000	-2.970542908	35.35207748
		Naibor Soit Kubwa 1	1500.893433	-2.970767021	35.35266113
		Naibor Soit Kubwa 2	1499.945923	-2.970746994	35.35244751
		Naibor Soit Kubwa 6	1508.743652	-2.970451117	35.35199356
		Naibor Soit Kubwa 8	1510.912109	-2.970580101	35.35238647
		Naibor Soit Kubwa 11	1518.263428	-2.970252037	35.35290146
		Naibor Soit Kubwa 13	1543.760864	-2.969549894	35.35253525
		Naibor Soit Kubwa 14	1546.023315	-2.969346046	35.35240173
		Naibor Soit Kubwa 24	1546.618652	-2.966960907	35.35132599
		Naibor Soit Kubwa 27	1544.821289	-2.964801073	35.34741211
		Naibor Soit Kubwa 28	1588.950928	-2.96064496	35.34741974
		Naibor Soit Kubwa 31	1582.825928	-2.961110115	35.34789276
		Naibor Soit Kubwa 32	1575.530884	-2.961592913	35.34810257
		Naibor Soit Kubwa 33	1573.38623	-2.961992979	35.34821701
	Naibor Soit Ndogo	Naibor Soit Ndogo 6A/B	1490.372314	-2.973845005	35.35990524
		Naibor Soit Ndogo 8	1491.948975	-2.973954916	35.35974503
		Naibor Soit Ndogo 13	1488.549927	-2.974387884	35.36024094
		Naibor Soit Ndogo 14	1487.340454	-2.974428892	35.36024475
		Naibor Soit Ndogo 15	1474.883301	-2.975039005	35.36085129
	Naisiusiu	Naisiusiu 3	1563.726318	-2.959692001	35.25185013
		Naisiusiu 4	1562.429321	-2.959681988	35.25186539
		Naisiusiu 7	1560.914673	-2.95936203	35.25196075
		Naisiusiu 8	1561.971191	-2.959228039	35.25181198
		Naisiusiu 9	1557.089355	-2.958939075	35.25182343
		Naisiusiu 13	1557.507324	-2.959434986	35.25114441
		Naisiusiu 14	1553.195801	-2.959515095	35.25113678

Appendix A (continued) Coordinates and Elevation Per Sample					
Position	**Outcrop/Source**	**Sample ID**	**Elevation**	**Latitude**	**Longitude**
Primary	Oittii	Oittii 1A/B	1480.81897	-2.969552994	35.35950089
		Oittii 3	1482.421631	-2.969093084	35.3602829
		Oittii 4	1475.302612	-2.969093084	35.36051559
		Oittii 5A/B	1482.475098	-2.968885899	35.3599205
Secondary	Gol Mountains	III1	1598.079224	-2.857125044	35.34272766
	Granite Falls	Granite Falls 3A/B	1533.00000	-2.944388628	35.22921371
		Granite Falls 4A/B	1534.00000	-2.94420433	35.2293396
	Kelogi	Kelogi 9	1554.03894	-3.038587093	35.27263641
	Naisiusiu	Naisiusiu 12	1566.630249	-2.959553003	35.25172043
	Olbalbal	A1A/B	1361.123901	-2.995872974	35.42964554
		A2	1361.256836	-2.996087074	35.42993546
		A5A/B	1290.886841	-2.989922047	35.4677887
		A6	1291.423828	-2.989748001	35.46803284

Appendix B Visually Estimated Modal Percentages Per Sample				
Position	**Outcrop/Source**	**Sample ID**	**Rock Type**	**Mineralogy**
Primary	Endonyo Osunyai	Endonyo Osunyai 1	Quartzite	Quartz (98); muscovite (2); opaque (<1); rutile (<1)
		Endonyo Osunyai 2	Quartzite	Quartz (98); muscovite (2); opaque (<1)
		Endonyo Osunyai 4A	Quartzite	Quartz (79); alkali feldspar (15); muscovite (5); hematite (1)
		Endonyo Osunyai 4B	Quartzite	Quartz (78); alkali feldspar (10); muscovite (10); hematite (2)
	Engelosin	Engelosin 2	Phonolite	Sanidine (5); nepheline (1); titanite (<1); sericite (<1)
		Engelosin 5A	Phonolite	Sanidine (2); nepheline (1); augite (1); titanite (<1); sericite (<1)
		Engelosin 5B	Phonolite	Nepheline (1); sanidine (1); augite (1); sericite (<1); titanite (<1)
		Engelosin 6A	Phonolite	Sanidine (1); nepheline (<1); augite (<1); sericite (<1); titanite (<1)
		Engelosin 6B	Phonolite	Nepheline (1); sanidine (1); augite (<1); sericite (<1)
		Engelosin 10A	Phonolite	Sanidine (5); augite (<1); titanite (<1); nepheline (<1)
		Engelosin 10B	Phonolite	Sanidine (5); titanite (1); augite (1); nepheline (<1)
	Gol Mountains	DDD1	Quartzite	Quartz (90); muscovite (10); alkali feldspar (<1)
		JJJ1	Meta-monzo-granite	Quartz (45); alkali feldspar (40); biotite (15); plagioclase (<1); rutile (<1)
		KKK1	Meta-quartz-rich granitoid	Quartz (60); alkali feldspar (20); biotite (12); hornblende (6); plagioclase (2)
		OOO1	Feldspar	Microcline (73); albite (25); hematite (1); opaque (1); sanidine (<1)
		PPP1	Quartzite	Quartz (95); muscovite (5); rutile (<1); opaque (<1)
		RRR1	Quartzite	Quartz (90); muscovite (10); rutile (<1)
		SSS1	Quartzite	Quartz (92); muscovite (8); rutile (<1)
		TTT1	Meta-quartz-rich granitoid	Quartz (70); biotite (10); plagioclase (10); alkali feldspar (8); opaque (2)
		UUU1	Meta-quartz-rich granitoid	Quartz (70); biotite (10); alkali feldspar (10); plagioclase (5); opaque (3); muscovite (2)
	Granite Falls	Granite Falls 1A	Granite gneiss	Quartz (50); alkali feldspar (30); biotite (15); muscovite (5); plagioclase (<1)
		Granite Falls 1B	Granite gneiss	Quartz (60); alkali feldspar (20); biotite (10); muscovite (8); plagioclase (2)
		Granite Falls 2	Granite gneiss	Quartz (69); alkali feldspar (15); plagioclase (10); muscovite (5); biotite (1)
	Kelogi	Kelogi 1	Granite gneiss	Quartz (40); aegirine (20); plagioclase (15); alkali feldspar (15); hornblende (10)
		Kelogi 3	Granite gneiss	Quartz (45); aegirine (20); hornblende (12); plagioclase (12); hematite (8); alkali feldspar (3)
		Kelogi 10	Granite gneiss	Plagioclase (25); quartz (25); hornblende (20); aegirine (20); alkali feldspar (10); titanite (<1); biotite (<1)
	Naibor Soit Kubwa	Naibor Soit Kubwa N042	Quartzite	Quartz (85); muscovite (15); hematite (<1)
		Naibor Soit Kubwa E039	Quartzite	Quartz (92); muscovite (8)
		Naibor Soit Kubwa S06	Quartzite	Quartz (95); muscovite (5)
		Naibor Soit Kubwa 1	Quartzite	Quartz (93); muscovite (5); hematite (1); rutile (1)
		Naibor Soit Kubwa 2	Quartzite	Quartz (95); muscovite (5); rutile (<1); opaque (<1)
		Naibor Soit Kubwa 6	Quartzite	Quartz (92); muscovite (5); rutile (1); opaque (1); fuchsite (1)
		Naibor Soit Kubwa 8	Quartzite	Quartz (94); muscovite (6); opaque (<1); rutile (<1)
		Naibor Soit Kubwa 11	Quartzite	Quartz (98); muscovite (2); rutile (<1)
		Naibor Soit Kubwa 13	Quartzite	Quartz (92); muscovite (8); rutile (<1)
		Naibor Soit Kubwa 14	Quartzite	Quartz (92); muscovite (8)
		Naibor Soit Kubwa 24	Quartzite	Quartz (99); muscovite (1); opaque (<1)

Appendix B (continued) Visually Estimated Modal Percentages Per Sample				
Position	**Outcrop/Source**	**Sample ID**	**Rock Type**	**Mineralogy**
Primary	Naibor Soit Kubwa	Naibor Soit Kubwa 27	Quartzite	Quartz (70); muscovite (30)
		Naibor Soit Kubwa 28	Quartz amphibolite	Hornblende (40); epidote (32); quartz (24); opaque (3); plagioclase (1); calcite (<1)
		Naibor Soit Kubwa 31	Quartzite	Quartz (92); muscovite (8)
		Naibor Soit Kubwa 32	Quartzite	Quartz (85); muscovite (14); rutile (1); fuchsite (<1)
		Naibor Soit Kubwa 33	Quartzite	Quartz (97); muscovite (3); magnetite (<1)
	Naibor Soit Ndogo	Naibor Soit Ndogo 6A	Quartzite	Quartz (95); muscovite (5)
		Naibor Soit Ndogo 6B	Quartzite	Quartz (95); muscovite (5)
		Naibor Soit Ndogo 8	Quartzite	Quartz (98); muscovite (2)
		Naibor Soit Ndogo 13	Quartzite	Quartz (96); muscovite (3); fuchsite (1); rutile (<1); opaque (<1)
		Naibor Soit Ndogo 14	Quartzite	Quartz (98); muscovite (2); fuchsite (<1)
		Naibor Soit Ndogo 15	Quartzite	Quartz (95); muscovite (5); opaque (<1); hematite (<1); rutile (<1)
	Naisiusiu	Naisiusiu 3	Meta-syeno-granite	Quartz (45); alkali feldspar (35); plagioclase (10); opaque (7); biotite (2); hornblende (1)
		Naisiusiu 4	Quartzite	Quartz (85); chloritized biotite (13); muscovite (1); opaque (1); chlorite (<1); calcite (<1)
		Naisiusiu 7	Quartzite	Quartz (94); chlorite (4); muscovite (1); opaque (1)
		Naisiusiu 8	Mica schist	Muscovite (75); quartz (15); biotite (10); plagioclase (<1)
		Naisiusiu 9	Quartzite	Quartz (95); muscovite (5)
		Naisiusiu 13	Quartzite	Quartz (97); muscovite (2); hematite (1); opaque (<1)
		Naisiusiu 14	Quartzite	Quartz (94); muscovite (5); opaque (1)
	Oittii	Oittii 1A	Quartzite	Quartz (93); muscovite (3); hematite (3); rutile (1)
		Oittii 1B	Quartzite	Quartz (93); muscovite (3); hematite (3); rutile (1)
		Oittii 3	Quartzite	Quartz (85); muscovite (10); alkali feldspar (5); plagioclase (<1)
		Oittii 4	Quartzite	Quartz (96); muscovite (2); hematite (1); rutile (1)
		Oittii 5A	Quartzite	Quartz (85); muscovite (15); alkali feldspar (<1)
		Oittii 5B	Quartzite	Quartz (85); muscovite (15); alkali feldspar (<1)
Secondary	Gol Mountains	III1	Hornblende granofels	Hornblende (50); quartz (28); epidote (20); opaque (2); alkali feldspar (<1)
	Granite Falls	Granite Falls 3A	Nephelinite	Nepheline (5); opaque (3); aegirine-augite (<1); sanidine (<1)
		Granite Falls 3B	Nephelinite	Nepheline (5); opaque (3); aegirine-augite (<1); sanidine (<1)
		Granite Falls 4A	Quartzite	Quartz (95); muscovite (5)
		Granite Falls 4B	Quartzite	Quartz (95); muscovite (5)
	Kelogi	Kelogi 9	Quartzite	Quartz (86); biotite (8); muscovite (5); opaque (1)
	Naisiusiu	Naisiusiu 12	Nephelinite	Nepheline (3); aegirine-augite (<1); sanidine (<1); hornblende (<1); opaque (<1)
	Olbalbal	A1A	Nephelinite	Nepheline (65); aegirine-augite (10); hornblende (1); titanite (<1)
		A1B	Nephelinite	Nepheline (65); aegirine-augite (10); hornblende (1); titanite (<1)
		A2	Basalt (?)	Plagioclase (20); opaque (1); augite (1); olivine (1)
		A5A	Basalt (?)	Plagioclase (1); augite (<1)
		A5B	Basalt (?)	Plagioclase (1); augite (<1)
		A6	Trachyandesite/basalt	Plagioclase (1); kaersutite (1); augite (<1)

Modes for igneous rocks are for phenocrysts. Modes for Kelogi 1 and 3 are based on point counts instead of visual estimates (see Table 5.3.2).

Appendix C Textural Data Per Magmatic Sample					
Sample ID	**Rock Type**	**Porphyry**	**Porphyritic Texture**	**Groundmass**	**Groundmass Texture**
Engelosin 2	Phonolite	Microporphyritic	Flow-aligned	Light-green	Trachytic
Engelosin 5A	Phonolite	Microporphyritic	Felty	Light-green	Felty
Engelosin 5B	Phonolite	Microporphyritic	Felty	Light-green	Felty
Engelosin 6A	Phonolite	Microporphyritic	Flow-aligned	Light-green	Trachytic
Engelosin 6B	Phonolite	Microporphyritic	Flow-aligned	Light-green	Trachytic
Engelosin 10A	Phonolite	Microporphyritic	Flow-aligned	Light-grey	Trachytic
Engelosin 10B	Phonolite	Microporphyritic	Flow-aligned	Light-grey	Trachytic
Granite Falls 3A	Nephelinite	Microporphyritic	Weakly aligned	Light-brown	Flow-aligned
Granite Falls 3B	Nephelinite	Microporphyritic	Weakly aligned	Light-brown	Flow-aligned
Naisiusiu 12	Nephelinite	Microporphyritic	Flow-aligned	Brown-grey	Flow-aligned
A1A	Nephelinite	Porphyritic	Weakly aligned	Dark-brown	Weakly aligned
A1B	Nephelinite	Porphyritic	Weakly aligned	Dark-brown	Weakly aligned
A2	Basalt (?)	Porphyritic	Flow-aligned	Light-grey	Trachytic
A5A	Basalt (?)	Porphyritic	Flow-aligned	Light-grey	Trachytic
A5B	Basalt (?)	Porphyritic	Flow-aligned	Light-grey	Trachytic
A6	Trachyandesite/basalt	Microporphyritic	Felty	Light-grey	Felty

Appendix D Grain Size Per Sample		
Sample ID	**Rock Type**	**Grain Size**
Endonyo Osunyai 1	Quartzite	Coarse
Endonyo Osunyai 2	Quartzite	Coarse
Endonyo Osunyai 4A	Quartzite	Coarse
Endonyo Osunyai 4B	Quartzite	Coarse
Engelosin 2	Phonolite	na
Engelosin 5A	Phonolite	na
Engelosin 5B	Phonolite	na
Engelosin 6A	Phonolite	na
Engelosin 6B	Phonolite	na
Engelosin 10A	Phonolite	na
Engelosin 10B	Phonolite	na
DDD1	Quartzite	Coarse
JJJ1	Meta-monzo-granite	Medium
KKK1	Meta-quartz-rich granitoid	Medium-fine
OOO1	Feldspar	Fine
PPP1	Quartzite	Medium
RRR1	Quartzite	Coarse
SSS1	Quartzite	Coarse-medium
TTT1	Meta-quartz-rich granitoid	Fine
UUU1	Meta-quartz-rich granitoid	Medium-fine
Granite Falls 1A	Granite gneiss	Medium-fine
Granite Falls 1B	Granite gneiss	Medium-fine
Granite Falls 2	Granite gneiss	Medium-fine
Kelogi 1	Granite gneiss	Medium
Kelogi 3	Granite gneiss	Medium
Kelogi 10	Granite gneiss	Medium-fine
Naibor Soit Kubwa N042	Quartzite	Coarse
Naibor Soit Kubwa E039	Quartzite	Coarse
Naibor Soit Kubwa S06	Quartzite	Coarse
Naibor Soit Kubwa 1	Quartzite	Medium
Naibor Soit Kubwa 2	Quartzite	Medium
Naibor Soit Kubwa 6	Quartzite	Medium
Naibor Soit Kubwa 8	Quartzite	Coarse
Naibor Soit Kubwa 11	Quartzite	Coarse
Naibor Soit Kubwa 13	Quartzite	Coarse
Naibor Soit Kubwa 14	Quartzite	Coarse
Naibor Soit Kubwa 24	Quartzite	Coarse-fine
Naibor Soit Kubwa 27	Quartzite	Coarse-fine
Naibor Soit Kubwa 28	Amphibolite	Fine
Naibor Soit Kubwa 31	Quartzite	Coarse
Naibor Soit Kubwa 32	Quartzite	Coarse-medium
Naibor Soit Kubwa 33	Quartzite	Coarse
Naibor Soit Ndogo 6A	Quartzite	Coarse
Naibor Soit Ndogo 6B	Quartzite	Coarse
Naibor Soit Ndogo 8	Quartzite	Coarse
Naibor Soit Ndogo 13	Quartzite	Coarse
Naibor Soit Ndogo 14	Quartzite	Coarse
Naibor Soit Ndogo 15	Quartzite	Coarse
Naisiusiu 3	Meta-syeno-granite	Medium-fine
Naisiusiu 4	Quartzite	Medium-fine
Naisiusiu 7	Quartzite	Coarse-fine
Naisiusiu 8	Mica schist	Medium-fine

Appendix D (continued) Grain Size Per Sample		
Sample ID	**Rock Type**	**Grain Size**
Naisiusiu 9	Quartzite	Medium
Naisiusiu 13	Quartzite	Coarse-medium
Naisiusiu 14	Quartzite	Coarse-fine
Oittii 1A	Quartzite	Medium
Oittii 1B	Quartzite	Medium
Oittii 3	Quartzite	Coarse-medium
Oittii 4	Quartzite	Coarse-fine
Oittii 5A	Quartzite	Medium
Oittii 5B	Quartzite	Medium
III1	Hornblende granofels	Fine
Granite Falls 3A	Nephelinite	na
Granite Falls 3B	Nephelinite	na
Granite Falls 4A	Quartzite	Medium-fine
Granite Falls 4B	Quartzite	Medium-fine
Kelogi 9	Quartzite	Fine
Naisiusiu 12	Nephelinite	na
A1A	Nephelinite	na
A1B	Nephelinite	na
A2	Basalt (?)	na
A5A	Basalt (?)	na
A5B	Basalt (?)	na
A6	Trachyandesite/basalt	na